Contents

Softcopy of this book can be downloaded at conference webpage.

Abstract

The 16th Asian Conference on Electrical Discharge (ACED 2012) Conference will be held at Johor Bahru, Johor, Malaysia, from 10th – 12th December, 2012. Past ACED conferences have been held in Xian, China, (2010), Bandung, Indonesia (2008), Hokkaido, Japan (2006), Shenzhen, China (2004), Seoul, Korea (2002), Kyoto, Japan (2000), Bandung, Indonesia (1998), Bangkok, Thailand (1996), Xian, China (1994), Oita, Japan (1993) and Singapore (1992). The purpose of this conference is to provide a forum for researchers, scientist and engineers to exchange ideas and discuss recent progresses in properties, phenomena and applications of electrical discharges. This book is the conference proceeding of the 16th Asian Conference on Electrical Discharge (ACED 2012). A number of papers have been accepted for oral presentations from different countries mostly from Asia and Australia. In addition keynote speeches will also be presented from renowned researchers in the field of electrical discharges. This conference proceeding contains the extended abstracts of papers presented.

Preface

On behalf of the organizing committee, I am honoured to welcome all colleagues from around the world to attend the 16th Asian Conference on Electrical Discharge (ACED 2012) in Johor Bahru, Malaysia on December 10-12, 2012.

The conference is organized by the Institute of High Voltage and High Current (IVAT), Universiti Teknologi Malaysia. This is the first time the conference is held in Malaysia. The conference will be held at The ZON Regency Hotel, Johor Bahru. It will be an opportunity for the international community, academics, scientists, engineers and researchers to present their original work, exchange ideas, and discuss recent progress in the field of Electrical Discharges in particular, and of High Voltage Technology in general. A total of 84 papers from 9 countries (Iran, Malaysia, Indonesia, Japan, China, India, Australia, Sweden, UAE) have been accepted for the oral presentations. After a further review process, each paper will be published in one of the previously identified journals, namely the International Journal on Electrical Engineering and Informatics, Journal of Science and Technology, Jurnal Teknologi, Jurnal Elektrika, or Elektropika.

Four Invited Talks from distinguished researchers and specialists will be presented in the plenary sessions. The conference presentations have been grouped into the following main topics: Plasma and Discharges, Electrical Insulation, Partial Discharge Phenomena and Measurements, Electromagnetic Fields Measurements, Condition Monitoring and Diagnostics, and Overvoltages and Others.

Johor prouds itself as a state which contains the southern-most tip of Asia, located at Tanjung Piai, Johor. There are numerous attractions and historical sites in Johor Bahru and nearby areas waiting for your visit and discovery. The conference venue is also located a short distance away from Singapore.

As the Chairman of ACED 2012, I would like to extend my warm welcome to all participants to attend ACED 2012.

I wish you a joyous and rewarding stay in Johor Bahru.

Assoc. Prof. Dr. Zulkurnain Abdul-Malek
Chairman of ACED 2012

Committee

International Steering Committee

K. Hidaka (Chairperson, Japan)
Z. C. Guan (Co-Chairperson, China)
J. Y. Koo (Co-Chairperson, Korea)
N. Hayashi (Secretary, Japan)
G. J. Zhang (China)
H-Y. Kim (Korea)
K.H. Lock (Singapore)
R. Mardiana(Indonesia)
S. Sangkasaad (Thailand)
M. Akbar (Pakistan)
Hussein Ahmad (Malaysia)

International Advisory Committee

M. Akazaki (Japan)
T. Takuma (Japan)
M. Hara (Japan)
Y. Sakai (Japan)
Y. Qiu (China)
R. Y. Zhang (China)
J. S. Cho (Korea)
C. H. Park (Korea)
K. T. Sirait (Indonesia)
H. R. Kwak (Korea)

Local Organizing Committee

Ahmad Darus (General Chair 1)
Hussein Ahmad (General Chair 2)
Zulkurnain Abdul-Malek (Chair)
Noor Azlinda Ahmad (Secretary)
Zolkafle Buntat
Mohd. Afendi Mohd. Piah
Mohd. Muhridza Yaacob
Zuraimy Adzis
Nor Asiah Muhamad
Eileen Su Lee Ming
Yanuar Zulardiansyah Arief
Nouruddeen Bashir
Mohd Nazren Mohd Ghazali
Muhammad Abu Bakar Sidik

International Organizing Committee

M. Akazaki(Japan)
T. Takuma(Japan)
M. Hara(Japan)
Y. Sakai(Japan)
Y. Qiu(China)
R. Y. Zhang(China)
J. S. Cho(Korea)
C. H. Park(Korea)
K. T. Sirait(Indonesia)
H. R. Kwak(Korea)
C. Gomes(Malaysia)
Suwarno(Indonesia)
T. Blackburn(Australia)
N. Masayuki(Japan)
H. Masayuki(Japan)
S. Manjang(Indonesia)
Y. M.Li(China)
M. Fernando(Sri Lanka)
Zainuddin Nawawi (Indonesia)
Muhammad 'Irfan Jambak (Indonesia)
M. A. Salam (Brunei)

Publisher

Institute of High Voltage and High Current (IVAT)
Block P06, Faculty of Electrical Engineering
Universiti Teknologi Malaysia
81310 Johor Bahru, Johor, Malaysia

Phone: +60-7-5535263
Fax: +60-7-5578150
E-mail: aced_secretariat@fke.utm.my
Website: aced2012.fke.utm.my

Editorial Board

A003

ELECTRICAL CHARACTERISTICS OF POLYVINYL CHLORIDE WITH WOLLASTONITE FILLER FOR HIGH VOLTAGE OUTDOOR INSULATION MATERIAL

MM Yaacob, A Aman, NA Mazlan, NF Noramat and N Kamaruddin
Institute of High Voltage and High Current
Faculty of Electrical Engineering
Universiti Teknologi Malaysia

Abstract: Outdoor insulation materials are the most important factor that needs to be considered in order to design high voltage equipment such as lightning arrestors, circuit breaker, line isolator, current transformer, capacitive voltage transformer and any other primary equipment at substation. A long time ago, porcelain was used as the bushing insulator for primary equipment and this traditional material has been replaced by polymeric types which have lot of benefits compared to porcelain type. Porcelain has some limitations which are easily broken in handling, heavy weight, and violent failure mode as results of an internal dielectric breakdown, complex geometry and hydrophilic characteristics. Recently, polymer composite material has been widely use as an outdoor insulation material due to its advantages such as low surface energy, light weight, good pollution performance (hydrophobic) and shorter processing time. However, their life expectancy is still unknown since the polymeric insulations are relatively new. Thus, to develop a better insulation, it is important to determine the ageing and electrical properties of the polymeric material. In the past research, it was discovered that by using filler which is added to the polymer will help to increase the arc tracking resistance. In this paper, new filler called Wollastonite (CaSio3) is added to the existing Polyvinyl Chloride (PVC) as a new polymer insulation material. A seashell (CaCO3) and waste glass (SiO2) were selected to produce an artificial wollastonite (calcium silicate-CaSiO3) as reinforcement and PVC is used as a matrix for this composite. The polymer material will undergo ageing process by conducting surface tracking and erosion resistance tests in accordance with BSEN 60587:2007. Electrical properties of the material such as tangent loss, capacitance, insulation resistance and dielectric strength are taken before and after the ageing test. Comparisons are made between the PVC with filler and PVC without filler based on the experimental results. Results from the tests show that the PVC with added filler of wollastonite having better electrical properties after undergoing the aging or contamination process. The development of the new materials can be used in future as high voltage insulation which can slow the ageing process and at the same time increase the efficiency of the insulators. It is hoped that this new material can replace the existing porcelain and silicone rubber. The test set-up and sample preparation are shown in the following figures.

REFERENCE

[1] MM Yaacob and A Aman, "Dielectric Properties of Waste Tyre Dust-Polypropylene (WTD-PP) for High Voltage Application", Australian Journal of Basic and Applied Sciences, 5(9): 1578-1583, 2011.

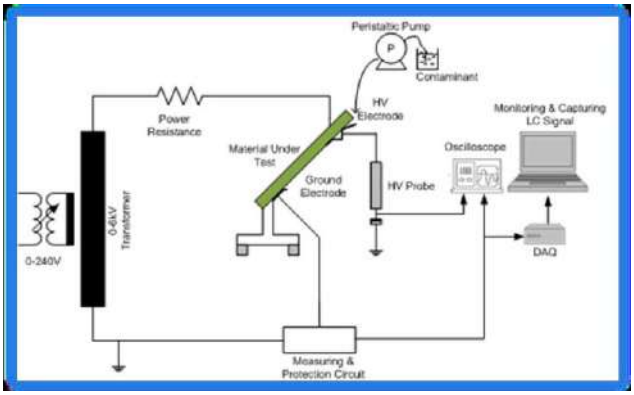

Figure 1. Inclined Plane Test Set-up.

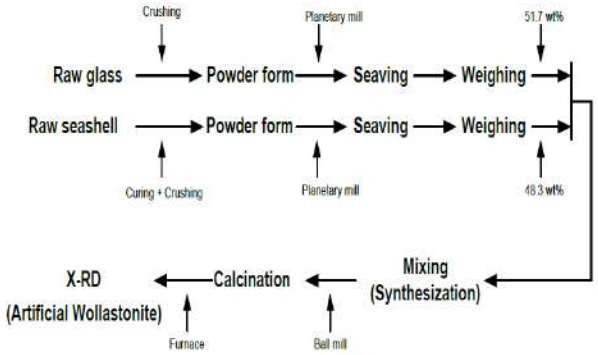

Figure 2. Preparation of artificial wollastonite

Figure 3. Preparation of Test Sample

A004

REVIEW OF PARTIAL DISCHARGE SIGNAL MONITORING IN POWER TRANSFORMER USING CHROMATIC APPROACH

MM Yaacob and MA AlSaedi
Institute of High Voltage and High Current
Faculty of Electrical Engineering
Universiti Teknologi Malaysia

Abstract: High-voltage power equipment is critical and costly components. The failure of this equipment without warning, results in fires and damage to equipment. Insulation breakdown is the main type of power transformer breakdown. Partial discharge (PD) is a main cause of insulation breakdown. PD are electrical discharges that do not completely bridge; they are localized to small area within insulation medium. PD can occur when electric field strength exceed the breakdown strength of insulation after that the insulation is unable to withstand the electrical stress and lead to flashover. Studying and monitoring of PD are done to detect insulation problems. Generally; some approach can be used to detect partial discharges in high-voltage power equipment. Some examples of this method in high-voltage equipment are acoustic method, optical method, electrical method and chemical method. Partial discharge in transformer can lead to corrosion in solid insulating materials and thus cause a breakdown of concerned operating component in the long term. The existing method of PD signal analysis does not give the right indication of the equipment condition due to disturbances and interferences of noise during detection. Therefore it is vital to have a new method of PD signal analysis in order to give the correct value of PD signals. This paper presents the application of new method of PD signal analysis using chromatic technique. In this technique the ultra high frequency (UHF) signals emitted from partial discharge activities in a high voltage transformer are analysed using the chromatic approach. As the frequency band of this UHF sensor was 300~1500MHz, envelope detection technique was used to extract UHF signals excited from PD sources inside the transformer These signals in the UHF identification domain are transformed in the form of chromatic maps. These maps are taken from the polar diagrams of chromatic parameters which are the hue, H (dominant frequency), saturation, S (effect signal bandwidth) and lightness, L (nominal signal strength). The colour science with the algorithms H, S, L helped to process the output from chromatic processors. The results of MATLAB simulations have shown that UHF PD signals can be effectively extracted by this method. Preliminary results also show that PD signals analysed using the chromatic technique give better interpretation as compared to the existing technique. Since this technique will give the optimum PD activities in the transformer thus being able to monitor the condition precisely. The research work will help the power authority in Malaysia in determining the condition of the transformer thus saving costs in maintenance. The chromatic method and preliminary PD signals results are shown in the following figures.

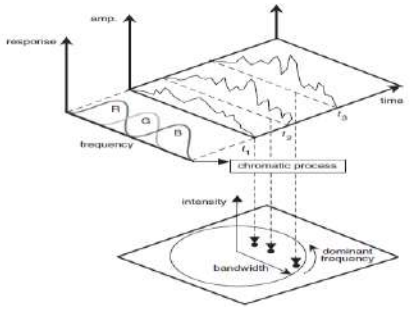

Figure 1. Schematics of chromatic signal processing [1]

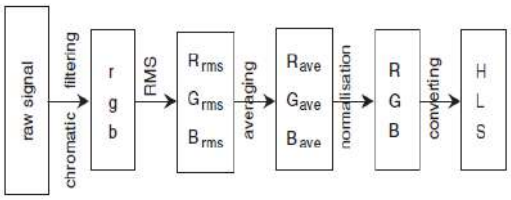

Figure 2. Flow diagram of chromatic processing [1]

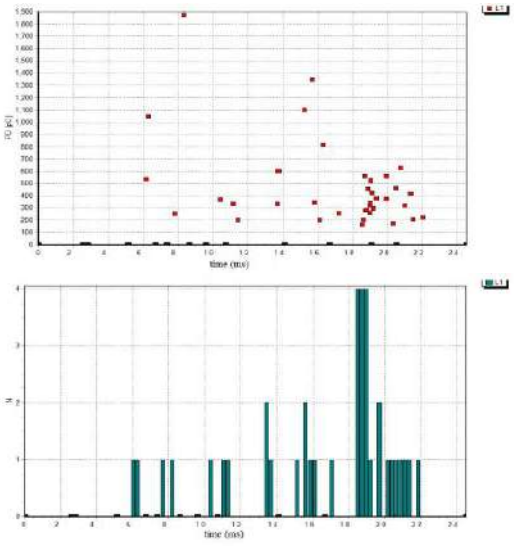

Figure 3. PD signal at transformer at Mutiara Rini Substation No4

REFERENCE

[1] J. Zhang, G.R Jones, J.W. Spencer, P. Jarman, I.J. Kemp, Z. Wang, P.L. Lewin and R.K. Aggarwal, " Chromatic Classification of RF Signals Produced by Electrical Discharges in HV Transformers", IEE Proc-Gener. Transm. Distrb, Vol. 152, No. 5, September 2005.

A005

EFFECT OF HIGH VOLTAGE ELECTRIC FIELD (AC) ON PINEAPPLE

Ali Mohammad Dastgheib*, Zolkafle Buntat[1], S. M. Zafar Iqbal[2]
Faculty of Electrical Engineering, Universiti Teknologi Malaysia,
81310 UTM Skudai, Johor, Malaysia
*Corresponding author: ali_m_Dastgheib@yahoo.com

Keywords: High voltage, Pineapple, food processing, microscope, chemical test, non-thermal technology.

Abstract: The high voltage electric field processing (EFP) is an innovative non-thermal technique that is used for preservation purpose of fruits. The main purpose of high voltage electric field application in food industry is to prolong the time to preserve and to maintain the high quality and natural properties of the food. In this study the high voltage electric field is applied for preservation purpose of pineapple. We have treated the pineapple samples by different strength of Ac high voltage of 0.67 kV/cm, 1.33 kV/cm and 2.0 kV/cm for 3 hours in each test. During the test, all samples were kept in normal condition for seven days. Before and after test observations were recorded for all samples by visual inspection of color, odors, cover hardness and taste. The pH value, conductivity and salinity of all samples were also recorded before and after the test. Based on the visual inspection results, it was observed that the injection of AC electric field of 2.0 kV/cm has produced the best effect on the pineapple characteristics as compared to 0.67 kV/cm and 1.33 kV/cm applied AC electric field. The experimental results are encouraging and supportive for the application of the technique in fruit preservation.

1. INTRODUCTION

Nonthermal food preservation methods have generated considerable interest in food industry for their potential to offer an alternative to the traditional thermal processing methods. One of these nonthermal methods is pulses electric field (PEF) method. It involves the application of pulse of high voltage to our samples, placed between two electrodes at room temperature. The applied high voltage results in an electric field that causes microbial inactivation. The electric field may be applied in the form of exponentially decaying, square wave, bipolar, or oscillatory pulses and at ambient, sub-ambient, or slightly above-ambient temperature [2]. The PEF technique is a non-thermal method of food preservation that uses short bursts of electricity for microbial inactivation and causes minimal or no detrimental effect on food quality attributes. The PEF technique is an emerging electro-food processing technology that has become a suitable method for long time food preservation. The main advantage of this emerging technology is that it is a dry process and the retention of fresh quality attributes are well proven during the preservation process of fruit. However, in the food industry, non-thermal pasteurization like PEF is a new technology which processes the food in such a manner that it retains fresh physical, chemical, and nutritional characteristics. Since it preserves food without using heat, so food treated in this way retain their fresh aroma, taste, and appearance. After the treatment, the food is packaged aseptically and stored under refrigeration. [2].

Moreover, PEF technique could also be used for processing of liquid, semi-liquid food products and also for solid like pineapple fruit. PEF processing technique offers dry processing which is capable to retain high quality of food with excellent flavor, nutritional value, and shelf-life. The processed food also possesses a satisfactory shelf life at ambient temperature [1]. In some cases, PEF pasteurized products currently store food using refrigeration technique (for example, milk), this is necessary for safety (to prevent the growth of spores in low-acid foods). For acid foods, refrigeration is not necessary for microbial stability, but is used to preserve flavor quality for extended periods of time.

2. METHODOLOGY

The present study was focused on the six parameters i.e. (i) life time of pineapple which is the duration related to pineapple spoiled processes (ii) the beginning of high voltage impulse test (iii) the value of high voltage impulse (iv) pH value of a sample before and after experiment (v) salinity taste and odors (vi) microscopic examination.

The schematic diagram of experimental setup is shown in Fig. 1. The pineapple samples were placed in a glass chamber where three types of pulse electric field 0.67, 1.33 and 2 kV/cm were applied for 20 times in each test. During the test all samples were kept in normal condition for seven days and the observations were recorded. In the Impulse test the best results were observed under the applied voltage of 2kV/cm. Before and after test all samples were preformed visual inspection of color, odors, cover hardness and taste. The pH value, conductivity and salinity of all samples were also recorded before and after the test.

The see the micro -detail of change in color and squeezed parts microscope (SZM) was used and photographs were recorded for comparison.

The power supply (Messwardler Bau Gmbh Bamberg) made in Japan was used which was capable to induce 120 KV/ 50 Hz. In this experiment the transformer was able to generate pulse electric field with the rate 230V /100 KV, so in primary and secondary sides the rates of voltages are 230V and 100000V. Also it must be notice that currents rate in this transformer is 21.7/0.05 A. Two metal parallel plates were used with 15cm distance and pineapples were placed in between them.

Finally, the results were compared & analyzed for measured values of pH, conductivity and salinity which are discussed here.

2.4 AC test on Pineapple

In this test like DC test the study installed the AC circuit by the aims of applying the AC voltage and observing the effectiveness of AC high voltage on pineapple, also it tried to keep pineapples during the longitudinal process. Ac test contains of different ranges of voltages like 10, 20 and 30 KV. In this test for the purpose of installing the AC circuit at lab, used two resistors in 375Ωand 60W and 100KV, 100 ρf capacitor also used. The temperature in lab was 25.5 c and humidity was 53%.

3. RESULTS AND DISCUSSION

3.2 AC high voltage result

During this process three levels of AC high voltages applied to nine samples. Each three of pineapples used for 10 KV, 20 KV and 30 KV in AC high voltages separately. It must be mentioned that the period of process was three hours, and the same in three voltages.

3.2.1 Effect of 10 KVAC

The study applied 10 KV AC on three pineapples in duration of three hours. The average of temperature at the lab was 25.5 c; also the humidity was 53%. After seven days it is obvious in figure 4.1 the samples is not so fresh and the colors of pineapples are changed. In addition, the bottom of pineapples completely spoiled and mashed. So all the characteristics checked by the microscope, and compared with other samples. A s it shown in figure 4.3, the spoiled parts of pineapple during 10 KVAC is obvious.

3.2.2 Effect of 20 KVAC

This section is related to 20 KV which the study applied on three pineapples in period of three hours. The average of temperature in this location was 25 c and humidity was 63%. After seven days, the study observed that the samples under 20 KVAC has better condition than the samples under 10 KVAC. As it is obvious in blow figure the sample in dark, but not so much, also there are not black dots on surface of sample only a little changing on color and squeezing on sample after 20 KVAC test. The microscope picture illustrates that the edge of the sample is darker than center, why the high voltage has effected on the edge rather than the center of pineapple.

3.2.3 Effect of 30 KVAC

The last test is related to 30 KVAC which applied on three pineapples in a period of three hours. The temperature in the test time was 25.5 c and humidity was 64%. After seven days, while observing the results, it found that in 30 KVAC test all samples are so fresh. The figure shown a little spoiled on bottom side of the sample is observed. The present picture is taken under the microscope after seven days, so it shows completely the freshness, and stable color of pineapple. Comparing the test makes it possible to get that the samples relate to 30 KVAC are more freshness than the others tests.

4. CONCLUSIONS

In this study high voltage field treatment is successfully applied to pineapple samples to check the preservation characteristics. The results are convincing and show that the technique is feasible and has potential of its application for other fruits. The experimental results also prove that fruits like pineapples could be preserved for longtime by this technique.

In this experiment the best results were obtained while using 2 kV/cm impulses as compare to other applied high voltage test. It was deduced that after spending seven days the color and taste were changed and the samples show squeezed and spoiled parts were so small than the other tests. The chemical tests performed about the measurement of conductivity, salinity and pH show that the 2 kV/cm impulses have better effect on pineapple as compare to without high voltage stress fresh samples of pineapple.

It was also explored in this study that the pineapple become spoil after the period of seven days and high voltage does not have any good effects on spoiled pineapple samples.

REFERENCES

[1] A.J.Castro, G.V.Barbosa - Canovas and .G.Swanson, "Microbial Inactivation of Foods by Pulsed Electric Fields", J.Food Proc. Pres., Vol.17, pp.47-73, IEEE (1993).

[2] M.M. Go´ ngora-Nieto, D.R.Se pu´ lveda, G.V.Bar bosa-Ca´novas ―Food Processing by Pulsed Electric Fields: Treatment Delivery, Inactivation Level, and Regulatory Aspects Washington State University, Biological Systems Engineering Department, Pullman, WA (U.S.A.), (2002).

A006

INFLUENCE OF VERY FAST VOLTAGE-OSCILLATION WITH POLARITY REVERSAL ON PARTIAL DISCHARGE INCEPTION VOLTAGE FOR TWISTED ENAMELED-WIRES

Kazunori Kadowaki*, Yujiro Takemura
Ehime University
Graduate School of Science and Engineering, Bunkyo-cho 3, Matsuyama, Ehime, 790-8577, Japan

Keywords: modified-inverter-surge, partial discharge, polarity-reversed pulse, twisted-pair, pulse width

Abstract: This paper deals with partial discharge characteristics of twisted enameled wires subjected to a modified inverter-surge. In order to obtain repetitive partial discharge inception voltage (RPDIV) in a statistically optimum method, we develop an automatic RPDIV measurement system for the twisted enamelled wires subjected to the repetitive pulses with step-by-step changing in the voltage heights. Two kinds of voltage waveforms, very fast polarity-reversed pulse with damped oscillation of the order of 100 ns and an impulse-like pulses with exponential tail of the order of 100 μs[4], are used. In the test for the impulse-like voltage, RPDIV decreases with increasing the pulse width. This results agree with that in previous reports. However, RPDIV for the polarity-reversed pulse with higher frequency oscillation becomes lower than that for the same pulse with lower frequency oscillation. The difference in the RPDIV characteristics between the voltage waveforms will be discussed on the basis of charge dynamics on the wire surfaces.

I. INTRODUCTION

It is very important to improve the reliability and safety of power drive systems of hybrid and electric vehicles from the practical point of view. One of problems is the degradation of motor coil insulation under high voltage pulse with high repetition rate. Enameled wires in inverter-fed motors are subjected to repetitive transient voltage oscillation on the front of square voltage from PWM-inverter-circuit, so called inverter-surges. In the last decade, partial discharge phenomena caused by modified inverter surges were studied by many researchers. Impulse-like voltages or squre-like voltages are used as a modified inverter surge in many cases [1]-[3]. However, actual voltage waveform of the inverter surge is not a simple impulse but a very fast damped oscillation with changing its polarity. In this study, repetitive partial discharge inception voltages (RPDIV) are evaluated by an automatic measurement system for two kinds of modified inverter surges, very fast polarity-reversed pulse with damped oscillation of the order from 10 ns to 100 ns and an impulse-like pulses with exponential tail of the order from 1 μs to 100 μs [4].

II. EXPERIMENTAL PROCEDURE

Twisted-pairs made with Polyamide-imide enamelled magnet wire (AIW, Sumitomo Wintec Co.) of 0.82 mm in conductor diameter are used as test samples. The twistedpare sample is suspended in a desicator filled with dry air. Typical waveforms of the applied voltages are shown in Fig.1(a) for the impulse-like pulse and in Fig.1(b) for the very fast polarity-reversed pulse with damped oscillation.

Statistical data of the partial discharge is automatically stored in a computer in RPDIV measurement system shown in Fig.2. To determine RPDIV, the voltage pulses with various heights are repeatedly applied to the twisted pare sample with a constant interval in one cycle of the test. The sequence of repetitive application is equivalent to round-robin test on PDIV measurement by six laboratories in Japan since 2008 to 2010 [5].

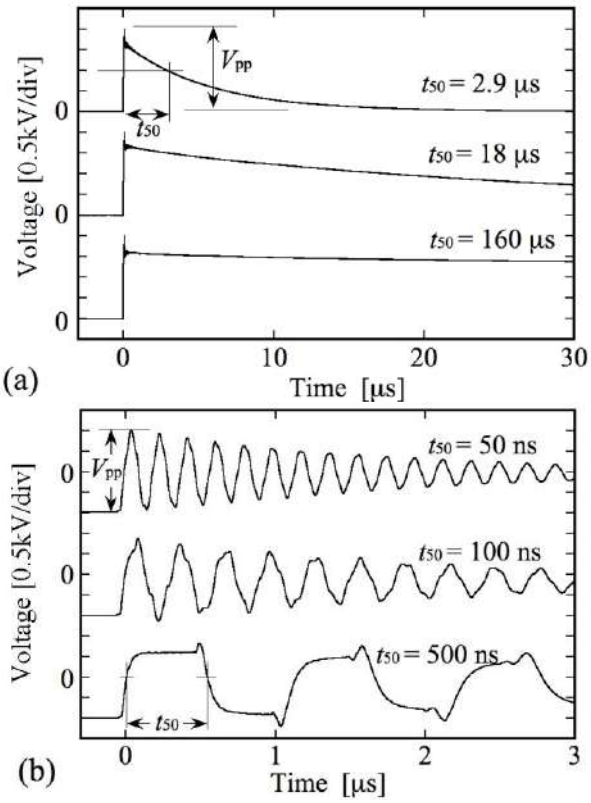

Figure 1. Voltage waveforms for (a) impulse-like pulse and for (b) very fast polarity-reversal pulse.

III. RESULTS AND DISCUSSION

Relationships between applied voltage *V*pp and inception probability of partial discharges are shown in Fig.3(a) for impulselike pulse and in Fig.3(b) for very fast polarity-reversal pulse. PD inception probability at a certain applied voltage for one sample is calculated with data of 100 repetitive measurements. In this experiment, 10 samples are prepared for each test, so that each plot in Figs.3(a) and 3(b) corresponds to statistical value with 1000 measurements. RPDIV is defined as a critical voltage that PD inception probability exceeds 50 % during the stepwise increase of the voltage height. RPDIV for the impulse-like pulse is 2270 V for *t*50=2.9 μs, 2090 V for *t*50=18 μs and 1920 V for *t*50=160 μs respectively. Results in Fig.3(a) indicate that RPDIV decreases with increasing the pulse width [6]. The reason for the decrease in RPDIV for the longer

*E-mail : kadowaki.kazunori.mc@ehime-u.ac.jp,Tel : +81-89-927-9797, Fax : +81-89-927-9790

pulse can be explained as follows. Probability of the initial electron emission per unit time is constant because this phenomenon is based on stochastic mechanism. Therefore, propagation probability of an avalanche produced by the initial electron must be increased with increasing the pulse width. It should be noted, however, RPDIV for the shorter voltage pulse with $t50$=50 ns is lower than those for the other longer voltage pulses for the case of the very fast polarity reversal as shown in Fig.3(b). RPDIV is 1800 V for $t50$=50 ns, 1950 V for $t50$=100 ns and 1950 V for $t50$=500 ns respectively. The reason why RPDIV for the shorter pulse is lower than those of the others can be explained as follows. We statistically measured the time lag distribution of the partial discharge. Regardless of the pulse width, most partial discharges occurred when the applied voltage attained the overshoot point after the first polarity reversal. For the case of the 50ns pulse, the overshoot is observed just after the polarity reversal is completed. Therefore, most part of surface residual charges produced by the dc pre-stress still remain on the enamel surface, so that field strength must by enhanced by the residual charges. On the other hand, the first polarity reversal is followed by a plateau for the longer pulse, so that the delay time from the polarity reversal to the overshoot becomes long. Some part of the surface charges produced by the dc pre-stress must be neutralized during the delay time. Therefore, RPDIV for the longer pulse tends to be higher than those for the shorter pulse.

The authors wish to thank Mr. Susumu Kiyohara (Nitto Denko Co.) for supplying the samples.

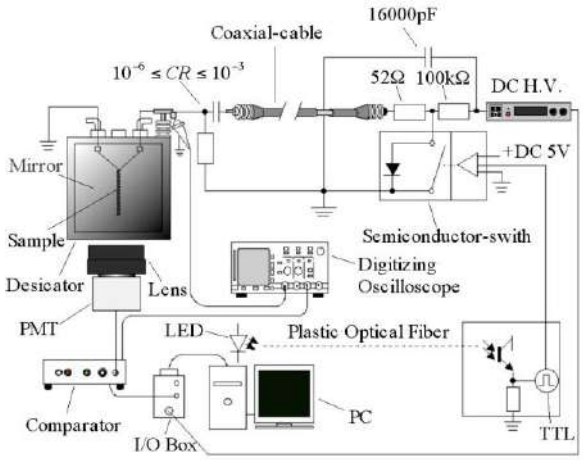

Figure 2. Schematic view of RPDIV measurement system.

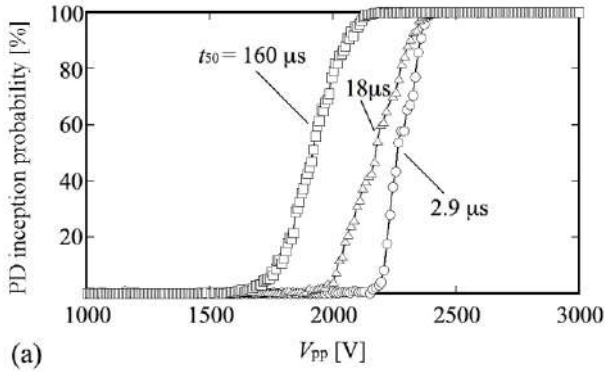

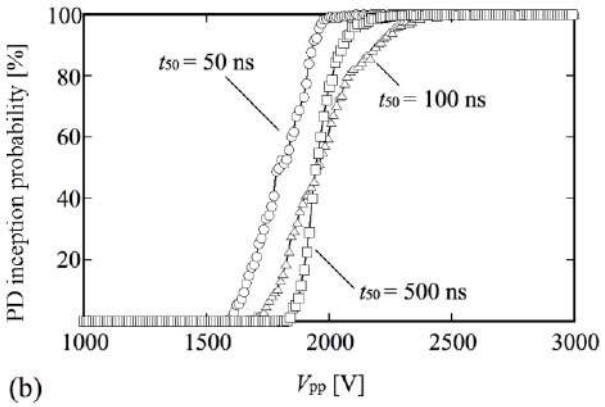

Figure 3. Relationships between applied voltage Vpp and inception probability of partial discharges for (a)impulse-like pulse and for (b) very fast polarity-reversal pulse.

REFERENCES

[1] N. Hayakawa and H. Okubo, "Partial Discharge Characteristics of Inverter-fed Motor Coil Samples under ac and Surge Voltage Conditions", IEEE Elect. Insul. Mag. , Vol. 21, No.1, pp. 5-10, 2005.

[2] D. Fabiani, G.C. Montanari, A. Cavallini and G. Mazzanti, "Relation between Space Charge Accumulation and Partial Discharge Activity in Enameled Wires under PWM-like Voltage Waveforms", IEEE Trans. on Diele. and Electr. Insul., Vol.11, No.5, pp.393-405, 2004.

[3] R. Busch, F. Pohlmann and K. Mueller, "Insulating Systems for Three-Phase Current Low-Voltage Motors Controlled by PWM Inverters: State of Development and Application Aspects", Proc. Of INSUCON 2002, Vol. 1, pp. 341-345, 2002.

[4] K. Kadowaki, K. Arita, J. Etsuda, T. Ohta, S. Kiyohara and S. Mitsuya, "Degradation Mechanism of Epoxy-Based Composite Sheet Subjected to Repetitive Voltage Pulses under High Temperature", Proc. of 2010 IEEE Int'l Conf. on Solid Diele., Vol. 1, pp. 95-98, 2010

[5] K.Kimura, M. Hikita, N. Hayakawa, M. Nagata, K. Kadowaki and Y. Murakami, "Round-Robin Test on Repetitive PD Inception Voltage of Twisted-Pairs", Proc. of 2010 IEEE Int'l Conf. on Elect. Insul. and Diele. Phenomena, Vol. 1, pp. 489-492, 2010.

[6] K. Wada, K. Tsuji, H. Muto and S. Mizoguchi, "Partial Discharge Inception Characteristics and *V-t* Characteristics of Sheath Material of Cables for High Voltage Inverter Systems", IEEJ Trans. FM, Vol. 127 No.2, pp. 71-77, 2010 (in Japanese).

A007

OPTICAL MEASUREMENT OF SPACE CHARGE DISTRIBUTION IN A DIELECTRIC LIQUID

Haruo Ihori*, Hayato Nakao, Masaharu Fujii
Faculty of Engineering, Ehime University
3, Bunkyo-cho, Matsuyama, Ehime, 790-8577, Japan
Phone : +81-89-927-9893 , FAX : +81-89-927-9893
ihori@eng.ehime-u.ac.jp

Keywords : Space charge, Dielectric liquid, Kerr effect

We have investigated the measurement of electric field distribution in liquids using an optical method. In this paper, the time series measurement of the electric field distribution in a parallel plane electrode system in a liquid containing space charges, was carried out at intervals of 1 ms. Using our optical measumerement system as shown in Fig.1, we measured the light intensity changing by the applied voltage. From the obtained light intensity, the electric field strength was calculated on the basis of Kerr electrooptical method. The cell was filled with propylene carbonate. Propylene carbonate is used as good solvent for the electrolytic liquid. In the cell, the parallel plane electrode system with gap of 10 mm, was setup. The field strength between the gap was measured every 0.8mm.

When the voltage pulse of width of 800 ms and the height of -10 kV was applied to the electrode system, the change of the light intensity was measured at each measured position. The measurement carried out 60 times at an interval of 1ms.

Figure 2 shows the electric field distribution between the gap. Time t is the elapsed time since the start of the applied voltage. Fitting curves were calculated by an interpolation operator. The electric field was small as increasing t because the applied voltage was also small with time. This cause would be lack of capacity of the power source. In positions near the upper electrode, the electric field strength changed specifically. Those were clearly smaller than the strength in a static field. Moreover, the position that the strength was smallest shifted as increasing t. We considered that a layer of charge might be formed in its position.

From the results of Fig. 2, we considered that a layer of charge might be formed in its position and that the layer might have a density gradient of space charge. If roughly,

$$\frac{dE(L)}{dL} = \frac{\rho(L)}{\varepsilon}$$

holds, the differential of E would be proportional to space charge density. So, Fig.3 shows differential of E that was calculated by applying a difference method to these curves in Fig. 3. As shown in Fig. 3, in position near the upper electrode, the space charge density was gradually larger with time. And then, the charge layer seemed to move toward the lower electrode.

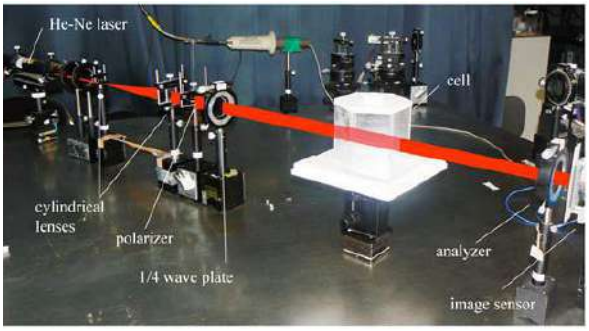

Figure 1. Optical measurement system

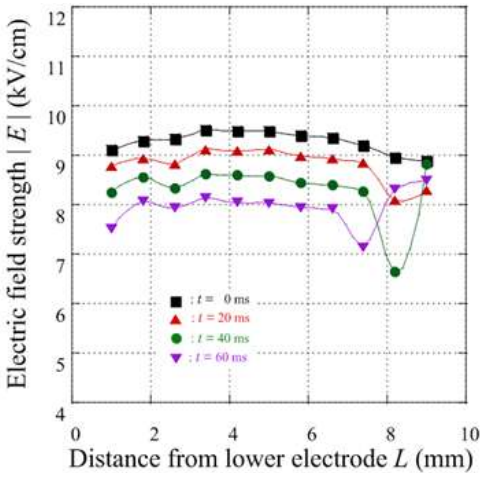

Figure 2. Electric field distribution

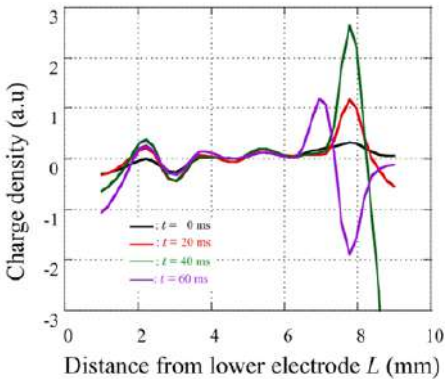

Figure 3. Space charge distribution.

A008

ORGANO-MONMORILLONITE AS A NEW ORGANIC FILLER FOR ELECTRICAL TREE INHIBITION

A. A. A. Jamil*[1], M. H. Ahmad[2], M. Kamarol[1], Y. Z. Arief [2], M. Mariatti[3], M. U. Wahit[4]
[1]School of Electrical and Electronics Engineering, Universiti Sains Malaysia, 14300 Nibong Tebal, Penang, Malaysia.
[2]Institute of High Voltage and High Current, Faculty of Electrical Engineering, Universiti Teknologi Malaysia, 81310, UTM Johor Bahru, Johor Darul Ta'azim, Malaysia.
[3]School of Material and Mineral Resources Engineering Engineering Campus,Universiti Sains Malaysia, 14300 Nibong Tebal, Penang, Malaysia.
[4]Department of Polymer, Faculty of Chemical Engineering, Universiti Teknologi Malaysia, 81310, UTM Johor Bahru, Johor Darul Ta'azim, Malaysia.
abdulazimabdjamil@gmail.com, mohdhafizi@fke.utm.my, eekamarol@eng.usm.my, yzarief@fke.utm.my, mariatti@eng.usm.my, mat.uzir@cheme.utm.my

Keywords: Electrical treeing, silicone rubber, organo-montmorillonite, tree inception voltage

Abstract: Electrical treeing is an electric breakdown process of considerable technological importance to the electrical power industry. It is a complex phenomenon involving several processes which depend upon many factors. Electrical treeing involves electrical, chemical and mechanical processes. To avoid electrical treeing occur, nanofiller are employed to be electrical tree inhibitors in polymeric insulating material. Recently, silicone rubber (SiR) widely used as insulating material because of its high of insulation resistance, thermal conductivity, hydrophobic, better gaseous and vapor permeability. To enhance the electrical and mechanical properties, it is usually mixed with appropriate filler. Polymer composite with addition of nano-sized filler attracts much attention compare to polymer composite with addition micro-sized filler because they are expected to have improved properties. Recently, material researcher found Organo-Montmorillonite (OMMT) which is modified version Montmorillonite (MMT) as new organic filler. This paper discussed potential OMMT/SiR to be a retardant to the initiation and growth of electrical treeing occurring in polymeric materials for high voltage application. Effect of electrical treeing on OMMT/SiR are the main subject to be discussed in this paper.

I. INTRODUCTION

Electrical tree is one of the main reasons for failure of polymeric materials used in high voltage applications. Treeing is observed to originate at points where impurities, voids, defects, or conducting projections causing excessive electrical field stress within small regions of the dielectric. Therefore, nanofillers are employed as electrical tree inhibitor in polymeric insulating material.

Nowadays, silicone rubber (SiR) is widely used as an insulation material in many electrical apparatuses because of its hydrophobic, excellent electrical and manufacture characteristics.

It is blended with filler to enhance the resistance to tracking and erosion as well as to provide improved mechanical and thermal performance[1-2].

In this research, a new organic nanofiller will be introduced which would increase the hardness of polymer and would inhibit the initiation and propagation of electrical treeing.The organic nanofiller that will be employed in this research is organo-montmorillonite (OMMT) which is a new modified nanoclay.Previously, microfillers have given wide attentions to fundamental material researchers but recently nanofillers have found to be better than microfillers in terms of surface area and interaction of polymer matrices [3]. Hitherto, the studies of mechanical and thermal properties of polymer nanocomposites using OMMT as nanofiller are widely conducted, but the research on electrical properties due to treeing of this nanocomposites is considered new [4-6].

Therefore, effects of organic nanofiller on the initiation and propagation of electrical treeing will be investigated. Test samples will be prepared in form of leaf-like specimen [7-9]. The tree parameters such as growth rate, tree length, tree inception voltage (TIV) will be investigated and measured for OMMT/SiR nanocomposites. Thus, this research will discover a new material of nanocomposites which can be used in the future as a new tree retardant insulating material.

II. MATERIALS AND METHODS

The silicone rubber that will be used in this study is Sylgard 184 Silicone Elastomer with dielectric strength is 24kV/mm and tensile strength is 6.2 MPa. Tear strength is 2.7kN/m and it is low viscosity liquid. The curing agent to be mixed is a 10:1 ratio by weight or volume. This material is supplied by Farnell/ Element 14. The OMMT (Nanomer 1.42E OMMT) is supplied by NanocorInc, USA. The OMMT is montmorillonite clay modified with ammonium ions. The OMMT particle surface dimensions generally range from 300 to more than 600 nm, length/thickness ratio is 200-300 and specific surface area is 750 m2g.

III. RESULTS AND DISCUSSION

TABLE 1. Tree inception voltage for silicone rubber with 1 % wt OMMT

No of Sample	Silicone Rubber + 1% OMMT TIV (kV)
1	8.5
2	8.5
3	9.5
4	10
5	10.5
6	11
7	11.5
8	12
9	12.5
10	13

* A.A.A Jamil, School of Electrical and Electronics Engineering, Universiti Sains Malaysia, 14300 Nibong Tebal, Penang, Malaysia.
abdulazimabdjamil@gmail.com

Table 1 shows the tree inception voltage for non-filled silicone rubber and filled silicone rubber with 1wt % OMMT nanofiller.

REFERENCES

[1] L. Yang, Y. Hu, H. Lu, L. Song, "Morphology, Thermal, and Mechanical Properties of Flame- Retardant Silicone Rubber/ Motmorillonite Nanocomposites", Journal of Applied Polymer Science, Vol. 99, pp. 3275-3280, 2006.

[2] Q. Mu, S. Feng, "Thermal conductivity of Graphite/ Silicone Rubber Prepared by Solution Intercalation", Thermochimica Acta 462, pp. 70-75, 2007.

[3] K. Y. Lau, M. A. M. Piah, "Polymer Nanocomposites in High Voltage Electrical Insulation Perspective: A Review", Malaysian Polymer Journal, Vol. 6, No. 1, pp. 58-69, 2011.

[4] W. S. Chow, "Water Absorption of Epoxy/Glass Fiber/ Organo-Montmorillonite Nanocomposites", eXPRESS Polymer Letter Vol. 1, No. 2, pp 104-108, 2007.

[5] C. H. Shyang, N. H. M. Zulfli, " Flexural And Morphological Properties Of Epoxy/ Glas Fibre / Silane-Treated Organo-Montmorillonite Composites, Journal Of Physical Science, Vol. 21(2), Pp. 41-50, 2010.

[6] W. S. Chow, S. R. Lim, "Characterization of Optical and Flammability Properties of Epoxy/ Organo-Montmorillonite Nanocomposites", Malaysian Polymer Journal, Vol. 5, No. 2, pp. 99-107, 2010.

[7] M. H. Ahmad, A. A. A. Jamil, H. Ahmad, A. Darus, Y. Z. Arief, " Experimental Investigation On Tree Inception Voltage Of EFB/SiR Leaf-Like Specimen", Jurnal Teknologi 56 (Sains) Keluaran Khas, 2011.

[8] M. H. Ahmad, H. Ahmad, Y. Z. Arief, R. Kurnianto, " Effects of Oil Palm Shell Filler on Inception and Propagation of Electrical Treeing in Silicone Rubber Composite Material Under AC Voltage", International Review on Modeling and Simulations (IREMOS), Vol. 4, No. 2, pp. 653-660, 2011.

[9] M. H. Ahmad, A. A. A. Jamil, H. Ahmad, M. A. M. Piah, A. Darus, Y. Z. Arief, N. Bashir, " Oil Palm Empty Fruit Bunch as A new Organic Filler for Electrical Tree Inhibition", International Conference on Electrical, Computer, Electronics and Communication Engineering, Kuala Lumpur, 19-21 February, pp. 1-6, 2012.

A009

THERMAL IMAGE AND LEAKAGE CURRENT AS TOOLS FOR TESTING AND CONDITION MONITORING OF ZNO SURGE ARRESTERS

Novizon[1, 2], Zulkurnain Abdul-Malek[1], Nouruddeen Bashir Umar[1], Nur Asilah Abdul Ghafar[1]
[1]Universiti Teknologi Malaysia (UTM), Malaysia
[2]University of Andalas (UNAND), Indonesia

Keywords : Zinc oxide arrester; leakage current, thermal image, artificial neural network, intelligent system.

Abstract: A new method to assess the condition of metal-oxide surge arresters is presented. The thermal image and third harmonic leakage current is used as an indicator. The linear relationship between the leakage current and temperature of arrester is processed using neural network. The temperature profile of arrester, ambient temperature and humadity as input to neural network and the peak value of the third harmonic resistive current as target. Results are presented the training of neural network close to the target and testing result is 98% successfully.

I. INTRODUCTION

There are a variable of technique and method to evaluate the condition of zinc oxide (ZnO) surge arrester. The assessment technique using leakage current was done by some researcher [1-14]. According to some papers, the leakage current of surge arrester, especially the third harmonic of total leakage current is the good indicator of aging or failure surge arresters [3,8,9, 15]. Another assessment technique to monitor ZnO arrester degradation based on the thermal temperature arises on the arrester body. The thermal behaviour of ZnO arrester is an important application consideration. Thermal capability of a design takes advantage of overvoltage protection capability. The thermal capability of ZnO arrester depends on the assembly structure of the arrester. If heat generated from the ZnO elements due to continuous operating voltages and surges is more than the thermal power dissipation of the housing, the elements will severe in an aged condition and fail of performing their protective function.

The thermal change curve of the ZnO arrester shown in figure.1. In the region below the temperature limit, t1, the level of heat generation of the ZnO arrester block is lower than the level of heat dissipation. The temperature decreases gradually, finally reaching a stable condition as shown in curve B. On the contrary, when the temperature of the ZnO arrester block reaches a level of higher than the temperature limit t2, the level of heat generation becomes higher than the level of heat dissipation and degradation occurs as shown by curve A at the end, ultimately resulting in thermal runaway [16].

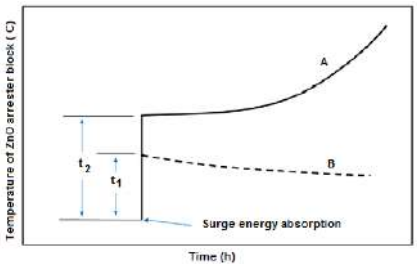

Figure 1. Thermal runaway phenomenon on ZnO surge arrester

The monitoring of surge arrester using thermal image technique and analyzed hot spot have conducted by several researchers [2, 4, 10, 17, 18]. The methodology to extract information to enable the detection and diagnosis of faults in surge arresters uses a digital image processing algorithm [4]. Most study just using the hotpot temperature of arrester and based of this hotspot the condition of arrester is known.

This paper proposes ZnO surge arrester condition based monitoring (CBM) using correlation between the third harmonic resistive leakage current and thermal image. The main idea of CBM of ZnO surge arrester is to predict and prevent a ZnO surge arrester from failure or damage in order to minimize maintenance cost.

II. RESEARCH METHODOLOGY

In this study artificial neural network (ANN) back propagation (BP) type is used. The BP algorithm is a kind of supervised learning algorithm. The BPNN contains three layers. These are input, hidden, and output layers as shown in figure 2. During the training phase, the training data such as humidity, ambient temperature, maximum and minimum temperature of arrester and temperature whole body of arrester are fed into to the input layer. The data is propagated to the hidden layer and then to the output layer. This system has one output layer that is third harmonic of resistive leakage current. This is called the forward pass of the back propagation algorithm. In forward pass, each node in hidden layer gets input from all the nodes from input layer, which are multiplied with appropriate weights and then summed. The output of the hidden node is the non-linear transformation of this resulting sum. Similarly each node in output layer gets input from all the nodes from hidden layer, which are multiplied with appropriate weights and then summed. The output of this node is the non-linear transformation of the resulting sum.

The output values of the output layer are compared with the target output values. The target output values are those that attempt to teach the network. The error between actual output values and target output values is calculated and propagated back toward hidden layer. This is called the backward pass of the back propagation algorithm. The error is used to update the connection strengths between nodes, weight matrices between input-hidden layers and hidden-output layers are updated. During the testing phase, no learning takes place, meaning all weight matrices are not changed. Each test vector is fed into the input layer. The feed forward of the testing data is similar to the feed forward of the training data.

In this study, the input data of neural network is designed for more than one thousand data set. The computer ability for running huge data became a problem.

*Zulkurnain Abdul Malek, IVAT FKE UTM, zulk@fke.utm.my

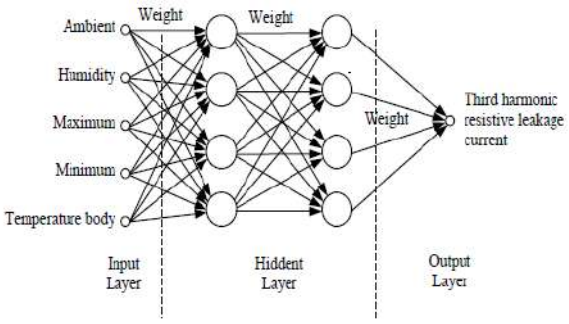

Figure2. Back Propagation Neural Network Configuration

III. RESULTS AND DISCUSSION

Neural network was running using about 500 set of data. The data consist of temperature along arrester body which obtains from arrester thermal profile. The result is shown in figure 3 presented the training of neural network close to the target and testing result is 98% successfully.

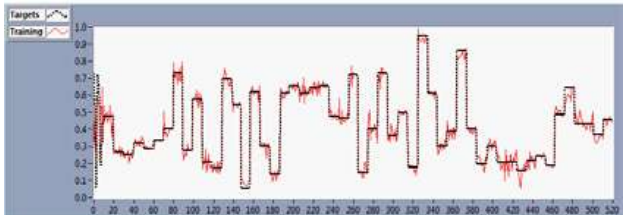

Figure 3. Training and testing result of some set of arrester data

REFERENCES

[1] T. Tada, *et al.*, "A diagnosis of remaining life characteristics of ZnO type surge arresters (1st stage) for 275 kV power systems," in *Transmission and Distribution Conference and Exhibition 2002: Asia Pacific. IEEE/PES*, 2002, pp. 2233-2238 vol.3.

[2] X. Chen, *et al.*, "Research of Infrared Diagnosed of Faults of Arrester," in *High Voltage Engineering and Application, 2008. ICHVE 2008. International Conference on*, 2008, pp. 637-640.

[3] C. A. Christodoulou, *et al.*, "Measurement of the resistive leakage current in surge arresters under artificial rain test and impulse voltage subjection," *Science, Measurement & Technology, IET*, vol. 3, pp. 256-262, 2009.

[4] C. A. Laurentys Almeida, *et al.*, "Intelligent Thermographic Diagnostic Applied to Surge Arresters: A New Approach," *Power Delivery, IEEE Transactions on*, vol. 24, pp. 751-757, 2009.

[5] J. Jun and W. Yu, "Research on online monitoring of arrester," in *2010 China International Conference on Electricity Distribution, CICED 2010, September 13, 2010 - September 16, 2010*, Nanjing, China, 2010.

[6] C. Srisukkhom and P. Jirapong, "Analysis of electrical and thermal characteristics of gapless metal oxide arresters using thermal images," in *Electrical Engineering/Electronics, Computer, Telecommunications and Information Technology (ECTI-CON), 2011 8th International Conference on*, 2011, pp. 677-680.

[7] E. T. Wanderley Neto, *et al.*, "Monitoring and Diagnosis of ZnO Arresters," *Latin America Transactions, IEEE (Revista IEEE America Latina)*, vol. 4, pp. 170-176, 2006.

[8] Z. Abdul-Malek, *et al.*, "A new method to extract the resistive component of the metal oxide surge arrester leakage current," in *Power and Energy Conference, 2008. PECon 2008. IEEE 2nd International*, 2008, pp. 399-402.

[9] B.-H. Lee and S.-M. Kang, "A new on-line leakage current monitoring system of ZnO surge arresters," *Materials Science and Engineering B*, vol. 119, pp. 13-18, 2005.

[10] E. T. W. Neto, *et al.*, "Electro-thermal simulation of ZnO arresters for diagnosis using thermal analysis," in *Transmission and Distribution Conference and Exposition: Latin America, 2004 IEEE/PES*, 2004, pp. 338-343.

[11] K. L. Wong, *et al.*, "Emission-based condition monitoring technique for ZnO surge arrester," in *Proceedings of the Seventh IASTED International Conference on Power and Energy Systems, November 28, 2004 - December 1, 2004*, Clearwater Beach, FL, United states, 2004, pp. 234-237.

[12] C. Karawita and M. R. Raghuveer, "Onsite MOSA condition Assessment-a new approach," *Power Delivery, IEEE Transactions on*, vol. 21, pp. 1273-1277, 2006.

[13] E. T. W. Neto, *et al.*, "Failure Analysis in ZnO Arresters Using Thermal Images," in *Transmission & Distribution Conference and Exposition: Latin America, 2006. TDC '06. IEEE/PES*, 2006, pp. 1-5.

[14] W. Zhou, *et al.*, "Design of on-line monitoring device for MOA used in 10kV distribution network," in *Condition Monitoring and Diagnosis, 2008. CMD 2008. International Conference on*, 2008, pp. 407-411.

[15] J. Lundquist, *et al.*, "New method for measurement of the resistive leakage currents of metal-oxide surge arresters in service," *Power Delivery, IEEE Transactions on*, vol. 5, pp. 1811-1822, 1990.

[16] S.-B. Lee, *et al.*, "Analysis of thermal and electrical properties of ZnO arrester block," *Current Applied Physics*, vol. 10, pp. 176-180, 2010.

[17] C. A. L. Almeida, *et al.*, "Intelligent detection and diagnosis of lightning arrester faults using digital thermovision image processing techniques," Orlando, FL, USA, 2005, pp. 109-120.

[18] C. Ying-Chieh and L. Yao, "Automatic Diagnostic System of Electrical Equipment Using Infrared Thermography," in *Soft Computing and Pattern Recognition, 2009. SOCPAR '09. International Conference of*, 2009, pp. 155-160. R. Nicole, "Title of paper with only first letter of the first word capitalized", J. Name Stand. Abbrev., submitted for publication.

A010

STREAK OBSERVATION OF DC PRE-BREAKDOWN PHENOMENON IN SILICONE OIL/LOW DENSITY POLYETHYLENE (LDPE) BY USING A 20M LONG IMAGE GUIDE SCOPE

Amir I. Mohamed*, Y. Miyamoto, K. Kadowaki
Ehime University
*University Malaysia Pahang
amirizzani@ump.edu.my

Keywords : dc breakdown, streak observation, insulation composite

Abstract: We observe streak images of dc pre-breakdown light images in silicone-oil (10cSt and 10000cSt) / low density polyethylene (30μm in thickness) insulation composite under needle/sphere electrode by using a 20 meter long image guide scope and a streak camera. In the case of insulation composite with 10cSt of silicone-oil, breakdown light propagates from the needle side under the both voltage polarity. However, in the 10000cSt case, breakdown light propagates from the film side under the negative voltage polarity.

I. INTRODUCTION

Insulators exist as gas, liquid or solid form. Every type has their own special characteristic. The combination of those insulators i.e. liquid and solid can be regarded as a good move as the liquid has the ability to recover while solid has high-voltage withstand. However, this was proved to be wrong. Narasaki and Kudo previously reported that the breakdown voltage of liquid / solid(thin film) composite insulation under dc stress was reduced as compared to that in neat oil case(1). In order to understand this phenomenon physically, we develop a photographic observation system by using a light delay path (a 20m long image guide scope, note as IGS) and image intensifier with high speed gate. The intensified breakdown light image was captured by a video camera with frame rate of 60fps. By using this system, photograhic observation on liquid/solid composite insulation system was carried out.

In this paper, another improvement of the observation system was carried out. Image intensifier with high speed gate and video camera was replaced by a streak camera. In the previous system, we were only able to capture either a pre-breakdown light image (at film or at either one of the electrodes) or a complete breakdown light image (light bridges between the gaps). However, by using a streak camera, transition process from pre-breakdown to complete breakdown can be observed.

II. MATERIALS AND METHODS

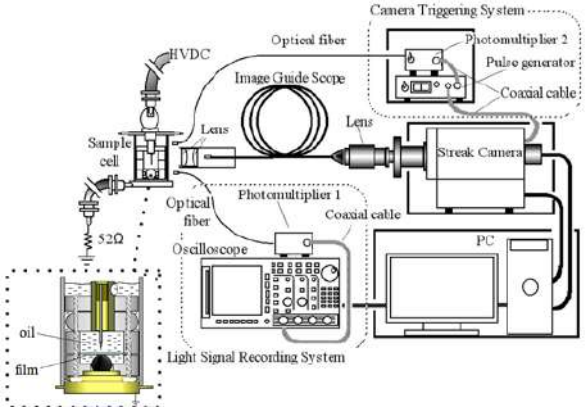

Figure 1. Observation system

Low-density polyethyelene with thickness of 30μm (Japan Polychem LF440HB, is noted as LDPE) and Silicone Oil (MOMENTIVE Performance Material) with viscosity of 10cSt (TSF451-10) and 10000cSt (TSF451-1M) are used as samples. A needle (with 10μm tip of radius) and a stainless steel sphere (10mm of diameter) is used as high voltage and ground electrode respectively. The LDPE film is placed on sphere electrode and the surrounding space is filled with silicone oil.

Experiment is explained as follows. After the sample cell is placed on experiment stage, voltage is applied by ramp speed of 0.1, 0.5 and 1.0kV/s until breakdown occurs. High voltage with negative and positive polarities are used. Once breakdown occurs, breakdown light will pass through 2 route ; 1) IGS and 2) to camera trigger. The breakdown light image is delayed for 100ns (travelling speed inside IGS 2.0×108 m/s). During this time, camera should be triggered. The arrival time of breakdown light image to the camera and the time of camera triggering signal should be syncronized in order to capture a streak image. The streak camera (Optronis GmBH SC-10, time resolution 2ps) sweep speed is set to 500ps/mm so that a streak image of 10ns can be obtained (phosphor screen size is 20mm). The observation system is shown in fig. 1. The observation system is explained in detail elsewhere(2). Sample number in each conditions is limitied to 5.

III. RESULTS AND DISCUSSION

Figure 2 shows the obtained streak images under all conditions with streamer propagation velocity and silicone oil

*Amir Izzani Mohamed (on study leave), Ehime University Japan, amirizzani@ump.edu.my, +81 89 9279786

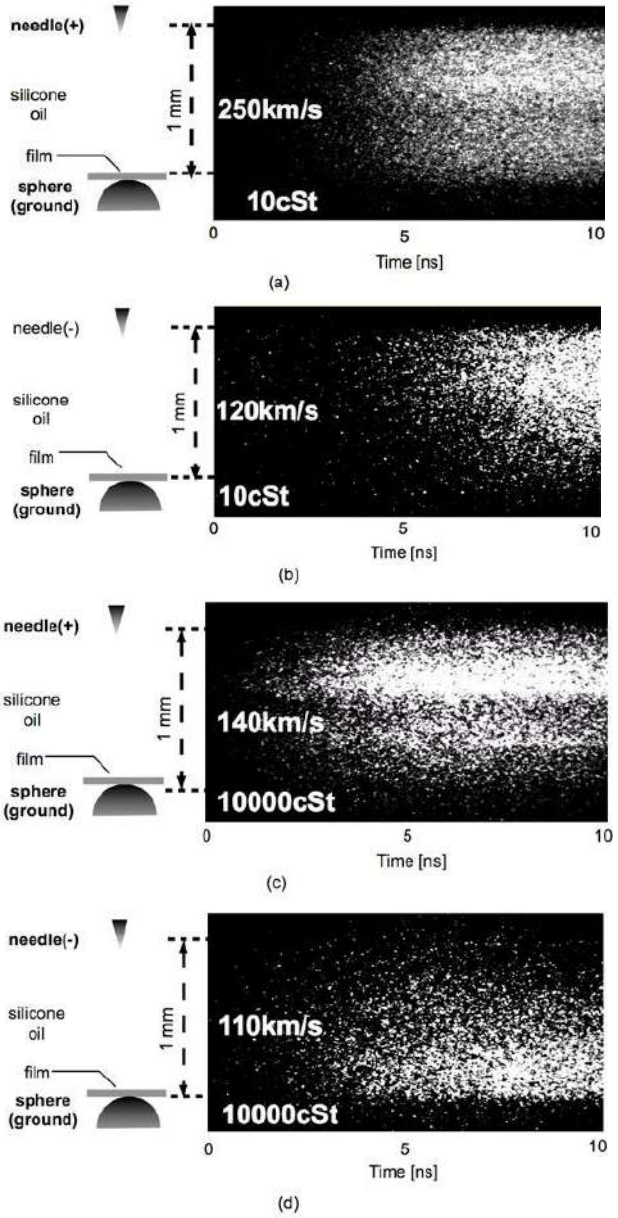

Figure 2. Obtained streak images, (a) positive polarity voltage with 10cSt oil, (b) negative polarity voltage with 10cSt oil, (c) positive polarity voltage with 10000cSt oil, (d) negative polarity voltage with 10000cSt oil.

viscosity is also noted in the image. Different in voltage ramp speed did not give a significant change in the initiation place of breakdown in all the samples. Streamer propagation velocity is higher under positive voltage application in both viscosity of the silicone oil. From figs. 2(a), 2(b) and 2(c) it was understood that breakdown initiated from needle electrode. Combination of positive polarity voltage and low viscosity factors yielded a fast streamer as shown in fig. 2(a).

However in fig. 2(d) breakdown was initiated at film. This phenomenon can be explained as follows. Application of negative polarity voltage release negative charges (assumably electron) from needle electrode. The charges travel across the oil bulk and accumulate in the film surface. The acumulated charges increase by time and upon reaching critical point, film breakdown occurs. On the other hand, this phenomenon was not observed in silicon oil (10000cSt) / LDPE under positive polarity voltage.

We assumed that the different in ramp voltage speed could show a significant change in breakdown initiation position. Slow ramp speed should initiate breakdown at film (as the charges have longer travelling time to counter electrode and accumulate at film) while fast ramp speed will show more breakdown initiation at needle electrode. However this assumption was ignored by the fact that breakdown initiates at needle electrode regardless the ramp speed in most cases. The existence of space charge under dc voltage application in an undeniable fact. However there is still no sufficient explanation on their role in dc breakdown phenomenon either in solid or liquid insulation. Therefore, study on this matter is still of important as it applies in many composite insulation system and useful for high voltage system designer in order to produce a better system.

IV. CONCLUSION

This study which use silicone oil / LDPE composite insulation is concluded as follows :

1. Breakdown initiates from needle electrode in most cases except in sample with 10000cSt viscosity of silicone oil under dc negative polarity voltgae application.
2. Streamer with speed of 250 km/s is recorded in sample with 10cSt viscosity of silicone oil under positive polarity voltage application. Streamer with speed of 110 km/s is recorded in sample with 10000cSt viscosity of silicone oil under negative polarity voltage application.

REFERENCES

[1] N. Narasaki and K. Kudo, "Direct Voltage Breakdown of Silicone Oil / Polymer Film Composite with Needle / Plane Electrode System", IEEE Trans. Electr. Insul, Vol.EI- 19, No.4, pp. 354-358, 1984.

[2] A. I. Mohamed and K. Kadowaki, "Streak Observation System for DC Pre-breakdown Using an Image Guide Scope", Jpn. J. Appl. Phys. Vol.51, 2012 (028003)

A011

CONSIDERING ON THE CURRENT TIME FRONT EFFECT ON THE VERTICAL ELECTRIC FIELDS DUE TO LIGHTNING CHANNEL AT NON-PERFECT GROUND CONDUCTIVITY CONDITION

Mahdi Izadi*, Mohd Zainal Abidin Ab Kadir, Chandima Gomes
Centre of Excellence on Lightning Protection (CELP), Faculty of Engineering, Universiti Putra Malaysia, 43400 UPM Serdang, Selangor, Malaysia.

Keywords : Electric field, Lightning, Ground conductivity

Abstract: In this study, the effect of time front of lightning channel base current on the vertical electric field due to lightning channel are considered while the ground conductivity conditions are set for both perfect ant non-perfect cases. Therefore, the behavior of field peaks versus time front changes under different values of ground conductivity are considered and the results are discussed.

I. INTRODUCTION

Several studied have been done to evauate electromagnetic fields assosiated with lightning channel at perfect and non-perfect ground counductivity cases while the ground counductivity can be effective on the peak and the rise time of electromagnetic fields[1-3].On the other hand,the rise time of return stroke current is more effective on the first peaks of electromagnetic fields while it has direcctly relationshipe with radiation component of electromagnetic fields[4].Therefore,In this study,the effect of current rise time on the vertical electric field at different conditions of ground counductivity will be considered and the resualts will be discussed accordingly. The basic assumptions in this study are as follow;

1. The lightning channel is as a vertical channel without any branches.
2. The ground surface is assumed to be flat.

II. RERURN STROKE CURRENT

In this study,the DU current function (improvement of Dieonorfer and Uman on the Heidler current function) is used for simulation of channel base current while the current function is expressed by equation (1) and the typical current parameters are listed at Table.1 as follow[5];

$$i(0,t)=\left[\frac{i_{01}}{\eta_1}\frac{\left(\frac{t}{\Gamma_{11}}\right)^{n_1}}{1+\left(\frac{t}{\Gamma_{11}}\right)^{n_1}}\exp\left(\frac{-t}{\Gamma_{12}}\right)+\frac{i_{02}}{\eta_2}\frac{\left(\frac{t}{\Gamma_{21}}\right)^{n_2}}{1+\left(\frac{t}{\Gamma_{21}}\right)^{n_2}}\exp\left(\frac{-t}{\Gamma_{22}}\right)\right] \quad (1)$$

Where
i01,i02 are the amplitudes of the channel base current,
Γ11,Γ12 are the front time constants,
Γ21,Γ22 are the decay- time constants,
n1,n2 are the exponents (2~10),

$$\eta_1=\exp\left[-\left(\Gamma_{11}/\Gamma_{12}\right)\left(n_1\times\frac{\Gamma_{12}}{\Gamma_{11}}\right)^{\frac{1}{n_1}}\right],$$

$$\eta_2=\exp\left[-\left(\Gamma_{21}/\Gamma_{22}\right)\left(n_2\times\frac{\Gamma_{22}}{\Gamma_{21}}\right)^{\frac{1}{n_2}}\right].$$

Table.1. The typical current parameters for the DU current function[6]

1_{01} (kA)	1_{02} (kA)	Γ_{11} (μs)	Γ_{11} (μs)	Γ_{11} (μs)	Γ_{11} (μs)	n_1	n_2
19.5	12	1	2	8	30	2	2

Furthermore,the MTLE (Modified Transmission line with Exponential Decay model) current model is applied for simulation of currents behaviour at different heights along lightning channel whereas it is expressed by equation (2) as follow[1];

$$i(z',t)=\begin{cases} i(0,t-z'/v)\exp(-z'/\lambda), & z'\le vt \\ 0, & z'>vt \end{cases} \quad (2)$$

where
z' is the instantaneous height along lightning channel ,
λ is the decay constant which allows the current to reduce its amplitude with height.
v is the return stroke current velocity along lightning channel
In this study the typical velues of v and λ are set at 1×108 m/s and 1500m, respectivelly.

III. THE ELECTROMAGNETIC FIELDS

The vertical electric field assosiated with lightning channel will be considered by using 2nd FDTD method[6]. Also,the ground counductivity effect on the vertical electric field will be considered by using Cooray expressions directly in the time domain[4].

REFERENCES

[1] Nucci.C.A, "Lightning-induced voltages on overhead power lines. Part I: return stroke current models with specified channel-base current for the evaluation of the return stroke electromagnetic fields," Electra, vol. 161, pp. 75–102, 1995.
[2] R. Thottappillil and V. Rakov, "Review of three equivalent approaches for computing electromagnetic fields from an extending lightning discharge," Journal of Lightning Research, vol. 1, pp. 90-110, 2007.
[3] R. Thottappillil, V. A. Rakov, and N. Theethayi, "Expressions for far electric fields produced at an arbitrary altitude by lightning return strokes," J. Geophys. Res, vol. 112, 2007.
[4] Cooray.V, The lightning flash: IET Press, 2003.
[5] Diendorfer.G and Uman.M, "An Improved Return Stroke Model with Specified Channel-Base Current " Journal of Geophysical Research-Atmospheres, vol. 95, pp. 13,621–13,644, 1990.
[6] M. Izadi, M. Kadir, C. Gomes, and W. Wan Ahmad, "An Analytical Second-FDTD Method For Evaluation of Electric and Magnetic Fields at Intermediate Distances From Lightning Channel," Progress In Electromagnetic Research (PIER), vol. 110, pp. 329-352, 2010.

*Mahdi Izadi,Email:aryaphase@yahoo.com

A012

CONDITION ASSESSMENT OF HIGH VOLTAGE INSTRUMENT TRANSFORMER USING PARTIAL DISCHARGE ANALYSIS

Mohd Aizam Talib*, A. Suffian. A. Bakar[1], S. Gobi Kannan[2]
TNB Research Sdn Bhd*[1]
No 1 Jalan Air Itam,
43000 Kajang, Selangor
Malaysia
Transmission Division, TNB[2]
Aras 4, Crystal Plaza
Jalan 223/51A, 46100 Petaling Jaya
Selangor, Malaysia

Keywords: Partial discharge, Instrument Transformer, On-site Diagnosis

Abstract: Determining the incipient faults in high voltage apparatus is important because failure without warning can result in damage to adjacent equipment, personnel injures, customer dissatisfaction and disruption to economic activity. The failure of several high voltage instrument transformers during in-service prompted Tenaga Nasional Berhad (TNB) to identify more effective diagnostic tool to predict insulation breakdowns. The viability of partial discharge (PD) measurements in the field on instrument transformers is investigated. This paper presents the results of partial discharge tests that have been carried out under laboratory experiments and field measurement on high voltage instrument transformers.

I. INTRODUCTION

During in-service high voltage instrument transformers are exposed to different kinds of stresses namely; electrical, thermal, mechanical and environmental stresses that can cause deterioration of insulation system (oil/paper) and associated with partial discharges (PD) activity. Catastrophic failures of instrument transformers may result in damages to adjacent equipment, personnel injures and represents highly replacement costs. TNB has over 20650 instrument transformers installed in 532 transmission substations operating at 132kV, 275kV and 500kV. The routine method used by TNB to verify the condition of in-service instrument transformers is off-line power factor (or dissipation factor) and capacitance measurement. However, the cost incurred to evaluate each instrument transformer off-line when considering the large amount of units installed on each substation. Dissolved gas analysis (DGA) is not recommended due to the limited amount of oil contained in the instrument transformer. From year 2001 to 2008, over 30 failures of in-service high voltage instrument transformers were recorded in TNB substation. On-line partial discharge detection technique was currently used by TNB to assess deterioration of insulation in instrument transformers.

In this paper, the partial discharge phenomena in instrument transformer is studied by analysis the PD data from small scale test objects, instrument transformer tested in the lab and instrument transformer installed at site. Preliminary results demonstrated that partial discharge analysis can provide useful information about the condition of instrument transformer thus allowing better management of installed instrument transformer in large transmission grid.

REFERENCES

[1] Christophe Moreau and Xavier Charpewtier, “On line Partial Discharge Detection System for Instrument Transformer”, IEEE International Symposium on Electrical Insulation, pp. 65-68, 1996.
[2] C. G. Azcarraga, V.R. Garcia-Colon, and A. Nava G, “On-site Testing of Instrument Transformers”, IEEE Conference on Electrical Insulation and Dielectric Phenomena, pp 39-42, 2006
[3] T.R. Blackburn, B.T. Phung, Z. Liu and R.E. James, “On-line Partial Discharge Measurement on Instrument Transformers”, IEEE International Symposium on Electrical Insulating Materials, pp 497-500, 1998
[4] A. Cavallini, and G. C. Montanari, “Condition assessment of Instrument Transformer by Partial Discharge Analysis: A Comprehensive Approach”, IEEE Transmission and Distribution Conference, pp 596-600, 2006
[5] V. R. Garcia-Colon, R. Lifih-Garcia and M.A. Jacob, “On-line Condition Assessment of High Voltage Current Transformers”, IEEE International Symposium on Electrical Insulation, pp 182-185, 2004.

*Mohd Aizam Talib is affiliated with TNB Research Sdn Bhd, Malaysia (e-mail: mohdaizam@tnbr.com.my)

A013

OZONE GENERATION PROPERTIES OF SCREW ELECTRODE OZONIZER BY ELECTRODES WITH DIFFERENT SCREW THREAD

Satoshi Myoyo*, Takuma Tanaka , Bunpei Ueda, Tomoyuki Fujishima, Takahiko Yamashita
Nagasaki University
1-14 Bunkyo-machi, Nagasaki, Japan

Keywords: Ozone, Dielectric Barrier Discharge, Screw Thread Intervals

Abstract: Methyl bromide has been used as agricultural chemicals. However, the use of the methyl bromide will be prohibited by 2015. Then ozone is expected as a substitute for methyl bromide. Therefore, we develop an ozone development system suitable for soil sterilization, and study the ozone generation characteristic. In our ozone generation system, ozone is generated by the dielectric barrier discharge. The inner electrode of the cylindrical ozone reactor is screw type electrode of stainless steel. The outer electrode is a copper plate which wrapped around the dielectric quartz glass tube. This time in order to change the electric field at the tip of a screw electrode, we changed screw thread intervals of the inner screw electrode on ozone generation properties. So, we report that investigations about influences of screw thread intervals of the inner screw electrode on ozone generation properties. As results, since the maximum electric field at the tip of the inner screw thread electrode is different, high ozone concentration is generated by using with larger interval of the inner screw thread electrode.

I. INTRODUCTION

Against the global environmental problem such as the global warming, we are regulated strictly in order to prevent it. Also in the agricultural sector, that is not an exception. Methyl bromide (CH3Br) is widely used as agricultural chemical to sterilize the soil. However, use of methyl bromide will be prohibited by 2015 because it brings on destruction of the ozone layer [1]. Then ozone is expected as a substitute for methyl bromide. Ozone has strong oxidation ability and no residual toxicity. And ozone can generate from oxygen in the air. High ozone concentration and high ozone generation efficiency are required for the ozone generation system which is suitable to the soil sterilization. Therefore, we have been developing an ozone generation system which is suitable to the soil sterilization, and studying ozone generation characteristics. From our previous research, we have found that ozone concentration depends on the width of the outer electrode, dividing of the outer electrode, the flow rate of the source gas and the applied voltage [2]-[4]. This time in order to change the electric field at the tip of a screw electrode, we changed screw thread intervals of the inner screw electrode on ozone generation properties. So, we report about the influence of the screw electrode interval and the electric field.

II. EXPERIMENTAL METHOD

In our ozone generation system, ozone is generated by the dielectric barrier discharge. Fig.1 shows detail of ozone reactor. The inner electrode of the cylindrical ozone reactor is the screw-type electrode of stainless steel. The diameter of the inner electrode of the cylindrical ozone reactor is 12mm. The outer electrode is a copper plate which wrapped around the dielectric quartz glass tube. The diameter of the outer electrode is 16mm. The discharge is generated easily because of high electric field at tips of the screw. Fig. 2 shows different screw electrodes of the screw thread interval (1.00mm or 1.75mm) used in this experiment. This time in order to change the electric field of the tip of a screw electrode, we used two screw electrode of different screw thread intervals. To prevent that ozone is broken down by heat, we make a hole in the inside of the inner screw electrode and let water flow inward. A diameter of the hole is 6mm. The dielectric barrier discharge is generated in the gap of 1mm between the inner electrode and the dielectric quartz glass tube. The diameter of inner side of the dielectric quartz glass tube is 14mm. A source gas (artificial air or air) flows between the inner electrode and the dielectric quartz glass tube. A flow rate of the source gas is adjusted by a flow meter in the range of 0.1 -1.0L/min.. An AC power source of low frequency (60Hz) is used. The applied voltage (0 – 15 kV) is supplied by using a neon transformer.

Ozone concentrations were measured by an ozone monitor. During the ozone generation, waveforms of the applied voltage and the discharge current were measured and recorded by a digitizing oscilloscope through a high voltage probe and a resistor (50Ω). The discharge power was calculated from the Q-V Lissajous figure obtained by using a capacitor of 0.47μF.

In this research, to investigate the influence of the interval of the inner screw electrode on ozone generation properties, we used experimental conditions as follows; screw thread intervals (1.00 mm or 1.75mm) of inner screw electrodes, source gases (artificial air or air), applied voltages (0-15 kV) and flow rates of source gases (0.1L/ min., 0.5L/min. or 1.0L/min.). In this paper, we will discuss ozone generation characteristics in the case of the flow rate of 0.1L/min. and outer electrode width of 11cm.

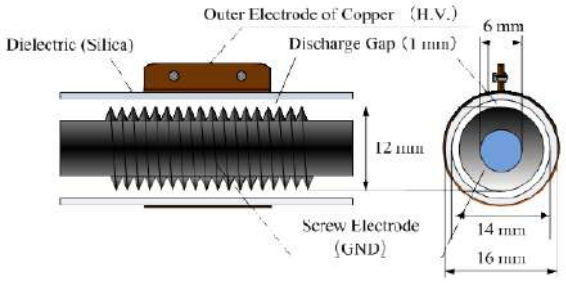

Figure 1. Detail of ozone reactor.

Figure 2. Different screw electrodes of the screw thread interval (1.00mm or 1.75mm).

*Tomoyuki Fujishima 1-14 Bunkyo-Machi, Nagasaki 852-8521, JAPAN t-fuji@nagasaki-u.ac.jp +81-95-819-2558 +81-95-819-2537

III. RESULTS AND DISCUSSION

Fig.3 shows relation of discharge power and ozone concentration in flow rate 0.1L/min. and the width of the outer electrode of 11cm. This Fig. 3 shows that ozone concentration increases for discharge power increase. But, it is able to ascertain that the rate of increase of ozone concentration is decreasing as electric discharge electric power becomes high. If electric discharge electric power becomes high, it will be thought that decomposition of the ozone by the electronic collision started.

Next, the intervals of a pitch compare 1.00 mm and 1.75 mm. The table 1 shows the ozone generation characteristic which changed with the difference in a screw thread interval of screw electrode by using the artificial air. In the case of using the artificial air, if the ozone concentration obtained by the difference in the interval of the screw thread electrode compare, that is ozone concentration of about 1.15 times in comparison with a screw electrode which is the interval of 1.75mm and 1.00mm. The table 2 shows the ozone generation characteristic which changed with the difference in a screw thread interval of screw electrode by using the air. In the case of using the air, if the ozone concentration obtained by the difference in the interval of the screw thread electrode compare, that is ozone concentration of about 1.28 times in comparison with a screw electrode which is the interval of 1.75mm and 1.00mm. If the screw thread interval becomes too narrow, it is thought that electric field at the screw thread tip is relaxed. Hence, it is thought that the ozone concentration became low

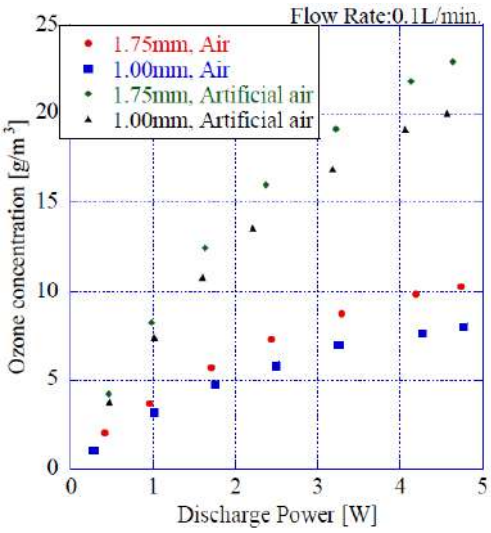

Figure 3. Relation of discharge power and ozone concentration in flow rate 0.1 L/min. and the width of the outer electrode 11cm.

Table 1. The ozone generation characteristic by artificial air

Screw Thread Interval Of Screw Electrode (mm)	Ozone concentration (g/m3)	Discharge electric power (W)
1.00	20.0	4.6
1.75	22.9	4.6

Table 2. The ozone generation characteristic by air

Screw Thread Interval Of Screw Electrode (mm)	Ozone concentration (g/m3)	Discharge electric power (W)
1.00	8.0	4.8
1.75	10.3	4.7

Fainally, we describe about comparing the artificial air and the air. The ozone concentration that was obtained by the interval of 1.75mm is about 2.22 times in comparison with the source gas of the artificial air and the air. Moreover, the ozone concentration that was obtained by the interval of 1.00mm is about 2.49 times in comparison with the source gas of the artificial air and the air. Since the rate of increase of ozone concentration is almost the same in about 2.22 times and 2.49 times even if source gas changes, screw thread interval of screw electrode is thought not dependent on source gas.

IV. CONCLUSION

We studied ozone generation characteristics of the ozone reactor with the screw-type electrode by changing screw thread intervals of the inner screw electrode (1.75mm or 1.00mm), using the width of the outer electrode (11cm) and changing source gases (artificial air or air). Results obtained in this work are summarized as follows.

(1) Ozone concentration generated by the screw thread interval of 1.75mm was higher than ozone concentration generated by the screw thread interval of 1.00mm.

(2) Maximum ozone concentration is 22.9 g/m3 with conditions of 0.1L/min., the width of outer electrodes of 11cm, the screw thread intervals of 1.75mm.

REFERENCES

[1] Ministry of Foreign Affairs notification, “Montreal Protocol on Substances that Deplete the Ozone Layer”, No.243, p.8, 2008. (in Japanese).

[2] T. Matsumoto, T. Fujishima and T. Yamashita: “Ozone Generation Characteristics of Compact Ozonizer Using Screw-Type Electrode with Oxygen or Artificial air”, Proc. 10th Korea-Japan Joint Symposium on Electrical Discharge and High Voltage Engineering, Paper No. 16P-41, pp. 395-398, 2007.

[3] Y. Iwase, T. Matsumoto, T. Fujishima and T. Yamashita: “Ozone Generation Characteristics of Compact Ozonizer Using Screw-type Electrode with Actual Air”, Proceedings of 14th Asian Conference on Electrical Discharge, Paper No. P-13, 2007, pp. 262-265, 2007.

[4] B. Ueda, T. Fujishima and T. Yamashita: “Effect of Divided Electrode of Screw-type Ozonizer for Ozone Generation and Basic Study of Ozone Sterilization Effect against Bacteria in Soil”, TENCON2010, Paper ID A77, pp.2119-2121, 2010.

A014

INFLUENCE OF DIVIDED ELECTRODES ON OZONE GENERATION PROPERTIES AND EFFECT OF OZONE CONCENTRATIONS ON SOIL STERILIZATION

Takuma Tanaka*, Satoshi Myoyo, Bunpei Ueda, Tomoyuki Fujishima*, Takahiko Yamashita
Nagasaki University
1-14 Bunkyo-machi, Nagasaki, Japan

Keywords: Ozone, Screw-type Electrode, Pure Oxygen, Soil, Sterilization

Abstract: The methyl bromide of a soil disinfectant will be prohibited from using except for an indispensable use by 2015. Then, we pay attention to ozone as a means of the soil sterilization replaced with a methyl bromide. Our ozone reactor has cylindrical shape, the screw electrode is used for the inner side electrode, and ozone was generated by dielectric barrier discharge. We investigated the influence of ozone generation characteristic of the screw electrode ozonizer by changing of outer electrodes, applied voltages, and flow rates of source gas (oxygen). In the soil sterilization experiment, the existence or non-existence of the bactericidal effect by ozone of ozone concentration 30, 20 and 10g/m^3 was examined.

I. INTRODUCTION

The regulation is performed on a worldwide scale to global environment problems such as ozone layer destruction. The methyl bromide of the soil disinfectant will be prohibited from using except for an indispensable use by 2015[1]. Then, we pay attention to ozone as a means of the soil sterilization replaced with a methyl bromide. Ozone has a bactericidal action by the strong oxidization power, and there are no worries about residual toxicity since it is decomposed with progress of time to oxygen. Moreover, by using an ozonizer, since there is an advantage of being able to supply from the air and the electricity, the use to soil sterilization is beginning to be expected [2]. We have been developing an ozone generation system which is suitable to the soil sterilization and studying soil sterilization with the ozone [3]. Moreover, it turns out that it is important to sterilize filamentous bacteria in the soil sterilization by the ozone.

This time, we investigated the influence on the ozone development characteristic when we used the outer electrode of 3cm or divided outer electrode of 1cm×3. And we also investigated the influence of the space of divided electrodes.
Moreover, when actually using ozone, it is necessary to consider that ozone has influence on an organic matter, an inorganic substance, a microbe, agricultural products, etc. in soil. But, it is difficult to solve these influences immediately at present. In this research, we investigated ozone concentration required for soil sterilization.

II. EXPERIMENTALMETHODS

Our ozone generator has cylindrical shape, the screw electrode (JIS screw, M12) of stainless steel is used for the inside electrode and copper plates wound around the outside of the dielectric (silica glass tube) is used for the outside electrode. Source gas (Oxygen) flows in the gap (1mm) between the screw electrode and the dielectric, ozone is generated by the dielectric barrier discharges (DBD). The electric discharge is made easily because electric fields of near the tip of the screw become strong by using a screw electrode. The applied voltage is supplied by using the neon transformer (Daihen, NA-1015P-H) which can be handled easily in the actual field. The oxygen of flow rate is adjusted by using the gas flowmeter (Koflok, RK-1200). The ozone concentration is measured by an ozone monitor (Ebara, EG-2001A). We made experiments under different conditions of applied voltages (5.3 – 15kV) and flow rates (0.1, 0.5, 1.0L/min.) of the oxygen. At the time of ozone generation, the waveform of applied voltage and the discharge current waveform were observed by the digital oscilloscope (Iwatsu, HV-P60). Discharge power is calculated from the Q – V Lissajous figure obtained by using the capacitor (0.47μF). Also, the ozone generation efficiency was calculated. Fig. 1 shows divided outer electrodes. In the ozone generation experiment, in order to investigate the influence of the space of divided electrodes, the outer electrode of 3cm, the outer electrodes of 1cm×3 (electrode spaces of 1cm) and outer electrodes of 1cm×3 (electrode spaces of 4cm) were used.

Next, soil sterilization experiment is explained. The ozone gas generated by the ozone reactor is poured from the underside of ozone injector to the upside. Ozone which didn't react with the soil is decomposed by using the activated carbon and excreted to the air. Also, the bottom of ozone injector is covered with the mesh of stainless (thickness 0.2mm, 70mesh) as a partition. By covering with the soil so that the whole of mesh will hide and let the thickness of the soil be 1mm, the deviation of the soil reacted with ozone is decreased. Applying ozone to soil is continued for 8 hours. Also, we shake the ozone injector every 30 min. so that

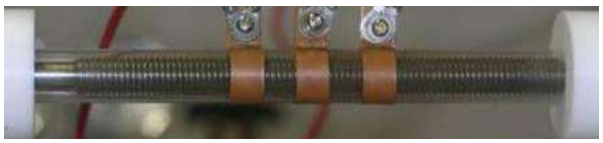

(a) Electrode spaces of 1cm

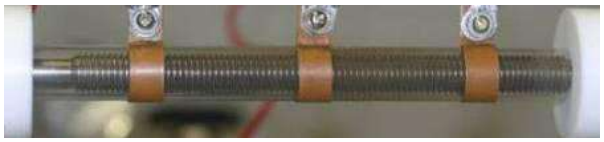

(b) Electrode spaces of 4cm

Figure 1. Divided outer electrodes

ozone can react with the soil evenly. The stump culture medium (atect, PT1025) and the incubator (Isuzu, SSR-115) were used for culture of the bacillus contained in the soil. The sterilized soil and unsterilized soil are attached respectively to stump culture medium. These are put into the incubator which preset temperature is 36 degrees, and are cultured for 24 hours. To make comparison of the culture results of the both soils, we

*Tomoyuki Fujishima; 1-14 Bunkyou-Machi, Nagasaki 852-8521, Japan E-mail: t-fuji@nagasaki-u.ac.jp, phone: +81-95-8192537 facsimile: +81-95-8192558

observe the occurrence time and place of colonies and the kind (circle shape or filament shape) of colonies.

Then we examined for the existence or nonexistence of bactericidal effects against the bacillus in the soil by generated ozone. In this research, in order to ascertain the lowest limit of the ozone concentration, which can sterilize the soil by the generated ozone, soil sterilizations were tried with the ozone concentration of 30g/m^3, 20g/m^3 and 10g/m^3.

III. RESULTS OF EXPERIMENTS

Fig. 2 shows relations between the applied voltage and the ozone concentration. Maximum values of the ozone concentration were 34.6g/m^3 in case of the outer elect rode of 3cm, 45.8g/m^3 in case of the outer electrode of 1cm×3 (electrode spaces of 1cm), and 55.4g/m^3 in case of the outer electrode of 1cm×3 (electrode spaces of 4cm). The ozone concentration was about 1.3 times in comparison with the outer electrode of 3cm and 1cm×3 (electrode spaces of 1cm), and was about 1.6 times in comparison with the outer electrode of 3cm and 1cm×3 (electrode spaces of 4cm). In our screw electrode ozonizer, surface corona discharge occurred from the both ends of outer electrodes, and there were functioning as effective outer electrodes. From these phenomena, we could increase the volume of the discharge space by dividing the electrode. Because O_2 were more exposed to DBD. In this way, we guess that high concentration ozone was generated.

Next, soil sterilization experiment is explained. Fig. 3 shows colonies generating situation (At 24 hours after the culture started). In case of non-sterilization, at 24 hours culture (Fig. 3 (a)), circular colonies and filamentous colonies generated from all soils. In cases of sterilization by the ozone concentration of 30g/m^3 (Fig. 3 (b)), circular colonies and filamentous colonies were not generated. It turned out that bacteria in the soil were completely sterilized by the ozone concentration of 30g/m^3. In cases of sterilization by the ozone concentration of 20g/m^3, circular colonies had generated from part of soils, but filamentous colonies were not generated from all soils. It turned out that bacteria which form filamentous colonies were completely sterilized by the ozone concentration of 20g/m^3.

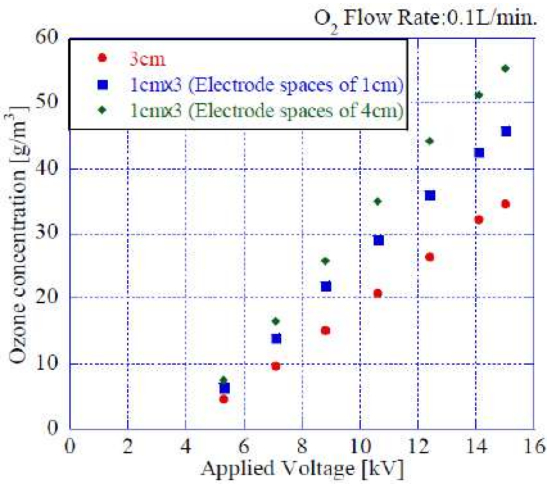

Figure 2. Relations between the applied voltage and the ozone concentration with different outer electrodes.

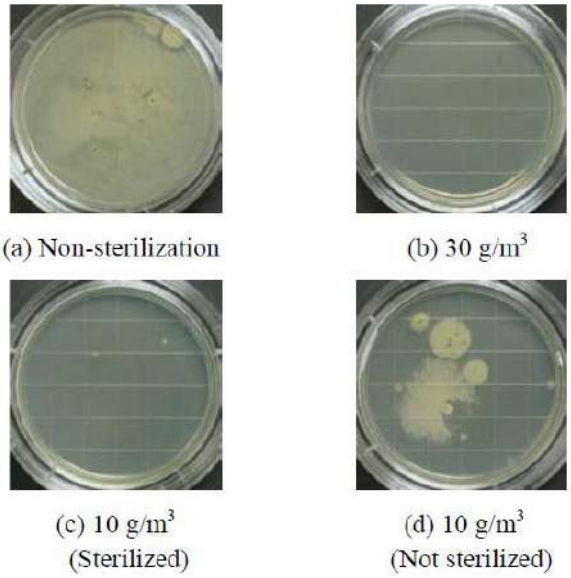

Figure 3. Colonies generating situation (At 24 hours after the culture started)

In cases of sterilization by the ozone concentration of 10g/m^3, there were both cases; soils were sterilized and soils were not sterilized. When sterilized (Fig. 3 (c)), the same result with the ozone concentration of 20g/m$_3$ was obtained. And when it was not sterilized (Fig. 3 (d)), circular colonies and filamentous colonies were generated from all soils. But it found that colonies were relatively small as compared with non-sterilization. These results indicate that there was the variance of bactericidal effects to bacteria during the sterilization by the ozone concentration of 10g/m^3, the probability of the sterilization was about 50%. In the soil, bacteria may form spores. Spores are difficult to sterilize. From this reason, we guess that there are bacteria which are not sterilized by the ozone concentration of 10 g/m^3.

IV. CONCLUSION

Results obtained by this research are summarized as follows.

(1) By dividing outer electrodes and extending electrode spaces, high concentration ozone has been generated relatively efficiently.

(2) Bacteria in the soil were completely sterilized by the ozone concentration of 30g/m^3.

(3) Ozone concentrations of at least 10~20g/m^3 are required in the soil sterilization by the ozone.

REFERENCES

[1] Ministry of Foreign Affairs notification, “Montreal Protocol on Substances that Deplete the Ozone Layer”, No.243, p.8 (2008). (in Japanese)

[2] K. Ebihara, H. Stryczewska, T. Ikegami, F. Mitsugi, J. Pawlat, ”On-site ozone treatment for agricultural soil and related applications”, Prizeglad Elektrotechniczny (Electrical Review), ISSN 0033-2097, R. 87 NR, pp. 148-152 (2011).

[3] B. Ueda, T. Fujishima and T. Yamashita, “Generation of High Concentration Ozone Using Dielectric Barrier Discharge with Divided Outer Electrode”, Proceedings of the 15th Asian Conference on Electrical Discharge, Paper ID A77, pp.243-246 (2010).

A015

COMPARATIVE STUDY ON SPACE CHARGE DISTRIBUTION MEASUREMENTS USING PEA AND PWP METHODS ON HIGH VOLTAGE INSULATION.

N. A. Othman , M. A. M. Piah, Z. Adzis,
Faculty of Electrical Engineering, University Teknologi Malaysia (UTM), Malaysia
nazlin7@live.utm.my, fendi@fke.utm.my, zuraimy@fke.utm.my

Keywords: ageing, space charge, PWP, PEA

Abstract: Space charge measurement has been extensively researched in recent years and has become a common method of investigating solid insulator properties. Comprehension of space charge build-up in solid insulator is crucial to determine how aging occurs, thus enabling the prediction of insulator lifetime. Pressure Wave Propagation (PWP) and Pulsed Electro-Acoustic (PEA) are non-destructive dielectric testing methods to determine the space charge distribution within the insulation. This paper presents the review and comparison of results from several published papers on application of PWP and PEA methods to investigate space charge accumulation.

I.INTRODUCTION

Space charge measurement has become a major concern of the electrical industry to investigate solid insulating material under high electric field. The presence of space charge greatly influences the electric field distribution within the material. The formation of space charge results in enhancement of local electric fields which may lead to breakdown of insulation under nominal voltage.

Many methods have been developed for probing space charge distribution in solid dielectrics. The most common method is by detecting the acoustic waves, as applied in PWP and PEA methods [1], developed in Europe in late 70's and in Japan during the 80's [2].

In PWP [3, 4], an acoustic wave is usually generated externally either by a laser or piezoelectric transducer. This can be done by impinging the laser pulse on an absorbing target adjacent to the sample, where the piezoelectric transducer was acoustically coupled. Hence, methods such as Laser Induced Pressure Pulse (LIPP) and Piezoelectric Induced Pressure Pulse (PIPP) are developed. Both methods have the same principle of space charge measurement but different principles in the generation of acoustic waves.

As opposed to PWP, an acoustic wave is internally generated in the PEA method [3, 4]. The generation of acoustic wave in PEA is usually done by applying a voltage pulse to the sample which exerts a force on the existing charges.

II. MATERIALS AND METHODS

A schematic diagram explaining the principles of PWP method is shown in Figure 1. An acoustic wave is generated when a pulsed electric field, $e_p(t)$ is applied to a piezoelectric transducer. The charges in the sample are moved (perturbed) in turn as the generated acoustic waves propagate through the sample at the velocity of sound. This movement slightly modifies the internal electric field and causes a change of surface charge on the electrodes. The time (domain) signal of displacement current indicates the charge distribution within the sample. The charge distribution is obtained by measuring the displacement current between the electrodes [1, 4, 5, 7, 9].

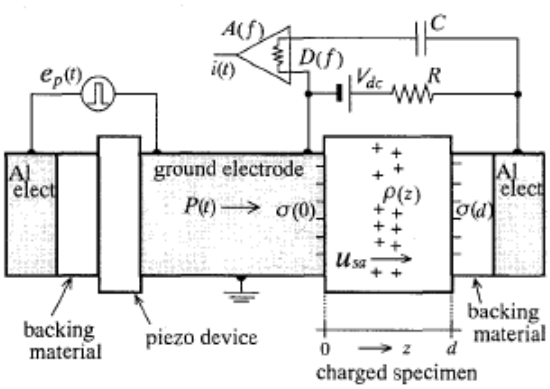

Figure 1. PWP space charge measurement [9]

The principles of PEA may be considered as the inversion of the PWP method since the relationship between the two methods resembles a mirror image. A schematic diagram of the theory of PEA method is explained using Figure 2. A perturbation force on each charge will be induced when a pulsed electric field, $e_p(t)$ is applied to a sample containing space charge. This force causes the charge to move slightly. The sudden movement of the charges launches an acoustic wave that is proportional to the charge distribution in the sample. These waves are detected by a piezoelectric transducer attached to the electrode, which converts the acoustic signal to an electric signal. The amplitude of the signal is related to charge density, and the delay indicates distance from the electrodes [1, 2, 4, 5, 7-9]. A piezoelectric sensor is usually made with polyvinylidene fluoride (PVDF) or lithium niobate ($LiNbO_3$).

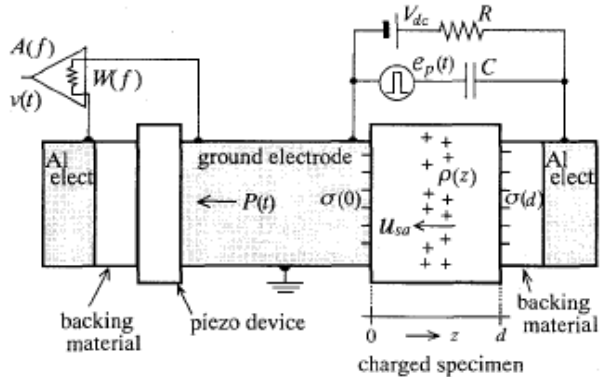

Figure 2. Principle of the PEA method [9]

*N.A. Othman, Faculty of Electrical Engineering, Universiti Teknologi Malaysia, 81310 Skudai, Johor, fendi@fke.utm.my, 07-5535697

III. RESULTS AND DISCUSSION

Figure 3 shows an example of charge, electric field and potential distribution waveform represented by red line (q), blue line (E) and green line (P) respectively. These three profiles are obtained when a DC bias voltage is applied to a polystyrene sheet [5] which does not contain internal charge. Since the sample contains no space charge, only the induced charges on the electrode were observed. The electric field distribution E(z) is obtained by integrating the charge profile, while the integration of E(z) provides the distribution of electric potential.

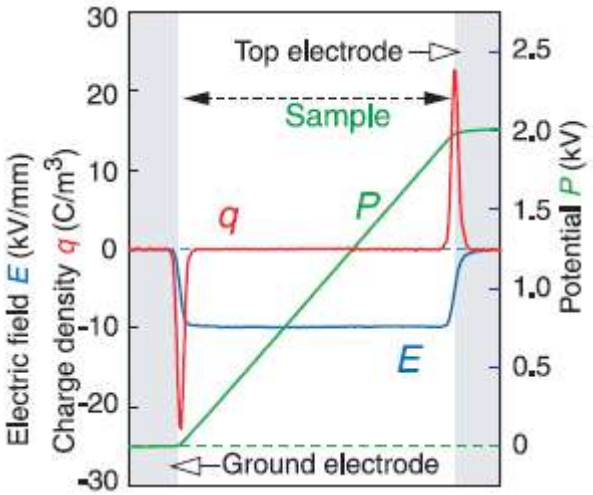

Figure 3. Example of profile obtained by PEA [5]

The resolution of the measurement system can be obtained from the widths of the peak and valley of the space charge density waveform. The peak and valley is actually representing the induced surface charges on the electrode. The system is said to have a high resolution when the widths between the peak and valley is narrower. It can be seen from the charge distribution profile in Figure 3 that there is no other peak or valley appearing in between them since the sample does not include any space charge.

The occurrence of space charge within an insulation material would introduce an early ageing effect which will lead to eventual failure. The presence of space charge can be investigated by PWP or PEA method. Researchers in [4] have designed a system based on the PWP method, allowing measurements at up to 3.2 kHz without signal averaging. A special piezoelectric transducer for pressure pulses generation and a storage unit have been developed for that purpose. A portable space charge measurement system using PEA method had been developed in [10] employs a new voltage waveform generator. The output signal shows the space charge distribution directly, without the need for deconvolution. Since the space charge profiles change with time, researchers in [11] have developed space charge measurement system using PEA method that can measure the space charge profiles for every 10μs in order to observe the transient behaviour of the system. This system utilizes the latest digitising oscilloscope model and a semiconductor switch to achieve high repetition rate PEA system.

Between these two methods, PEA has received much interest by researchers throughout the world as can be seen by many papers published recently. Hence, many research are conducted in the development of PEA including portable and mountable PEA, three-H PEA (high voltage, high repetition rate and high spatial resolution) and 3D space charge profile mapping [2, 3].

REFERENCES

[1] N. H.Ahmed and N.N.Srivinas. "Review of Space Charge Measurements in Dielectrics", IEEE Transactions on Dielectrics and Electrical Insulation, Vol. 4, pp. 644-656, October 1997.

[2] J. Li, Y.Zhang, X. Qin, Z. Xia, and T. Takada. "A Combined System of Piezo-PWP/PEA Methods for Measuring Space Charge Distribution in Solid Dielectrics", 10th IEEE International Symposium on Electrets, pp. 281-284, September 2004.

[3] R. J. Fleming. "Space Charge Profile Measurement Techniques: recent Advances and Future Directions", IEEE Transaction on Dielectrics and Electrical Insulation, Vol. 12, pp. 967-978, October 2005.

[4] S. Bamji, M. AbouDakka, and A. Bulinski. "Phase- Resolved Pulsed Electro-Acoustic Technique to Detect Space Charge in Solid Dielectrics Subjected to AC Voltage", IEEE Transaction on Dielectrics and Electrical Insulation, Vol. 14, pp. 77-82, February 2007.

[5] Kaori Fukunaga. "Innovative PEA Space Charge Measurement Systems for Industrial Applications", IEEE Electr. Insul. Mag., Vol. 20, No.2, pp. 18-26, 2004.

[6] N. Adachi, X. Qin, Y. Tanaka, and T. Takada. "Comparison between The PEA Method and The PWP Method for Measuring Space Charge Distributions", International Conference on Electrical Insulation and Dielectric Phenomena, 1998.

[7] S. Hole, C. Alquie, and J. Lewiner. "Measurement of Space Charge Distributions in Insulators under Very Rapidly Varying Voltage", IEEE Transaction on Dielectrics and Electrical Insulation, Vol. 4, pp. 719-724, 1997.

[8] S. Hole, T. Ditchi, and J. Lewiner. "Non-destructive Methods for Space Charge Distribution Measurements: What are the Differences?", IEEE Transaction on Dielectrics and Electrical Insulation, Vol. 10, pp. 670-677, August 2003.

[9] T. Takada, Y. Tanaka, N. Adachi and X. Qin. "Comparison between the PEA Method and the PWP Method for Space Charge Measurement in Solid Dielectrics", IEEE Transaction on Dielectrics and Electrical Insulation, Vol. 5, pp. 944-951, 1998.

[10] Takashi Maeno. "Portable Space Charge Measurement System Using the Pulsed Electroacoustic Method", IEEE Transaction on Dielectrics and Electrical Insulations, Vol. 10, pp. 331-335, April2003.

[11] M. Fukuma, T. Maeno, K. Fukunaga, and M. Nagao. "High Repetition Rate PEA System For In-Situ Space Charge Measurement During Breakdown Tests", IEEE Transaction on Dielectrics and Electrical Insulations, Vol. 11, pp. 155-159, February 2004.

A017

IMPEDANCE PROPERTY OF LIGHTNING IMPULSE DISCHARGE INWATER GAP

Daisuke Okano*
Liberal Arts Education Center, Tokai University
9-1-1 Toroku, Kumamoto, 862-8652 Japan

Keywords: lightning, impulse discharge, impedance, water

Abstract: The intrusion routes of lightning flashes and their surges into green power generation systems are divided as follows: The first is the route from air to ground, the second is the route from air to river or sea, and the third is the route from ground or water to building walls made of mortar or reinforced concrete. For all the routes, it is important to investigate the discharge impedance from the view point of the lightning power distribution. We demonstrate a simple method for determining discharge impedance in the liquid region by analyzing periodic, attenuated discharge waveforms with high-frequency components. We report the experimental results related to discharge impedance to lightning impulse discharges in the tap-water gap; (1) the discharge waveforms indicate the periodic attenuated ones for one period and the voltage waveforms indicate amplitude distortions; (2) the analyzed discharge resistance ranges from 0.05 to 10 Ω for positive and negative discharges; (3) the regressions of discharge inductance ranges from 4.0 to 100 μH and 2.0 to 100 μH for positive and negative discharges, respectively.

I. INTRODUCTION

It is important to protect green energy facilities such as photovoltaic or wind power generation systems that are near river basins, on the coast, or offshore against lightning flashes and their surges [1, 2]. Partial discharges due to coronas or surges can damage the power conditioner of the power generation systems including the electrical and electronic devices by the intrusion of lightning surges via space, ground, and river or sea. From the view point of controlling electrical damage to electric facilities due to lightning-power concentration, it is important to investigate the impedance in the corona or streamer discharge regions.

Existing methods such as the triple probe (TP) method [3, 4] and laser Thomson scattering (LTS) [5, 6] are unsuitable for the impulse discharges because the TP and LTS methods need the conditions of non-electric field and a fixed discharge path, respectively.

Our proposed method [7] has the following advantages: First, it does not require knowledge of both the electron temperature and plasma density so that Spitzer's expression can be used for the resistivity [8]. Second, it can provide a unique solution for dc, ac, or impulse discharge attenuated waveforms. Finally, it determines simultaneously all elements assumed in the series circuit, and can give the time dependence of the impedance.

In this paper, we present the dependence of the impedance on time after the occurrence of the lightning impulse discharge with the standard lightning impulse generator in the water gap.

II. EXPERIMENTS

Our standard lightning impulse generator (SLIG, 1.2/50 μs waveforms) is classified as a Marx circuit type with triple capacitor stage. The SLIG has a series circuit [7] consisting of passive circuit elements: a capacitor, inductor, and output resistor. It usually outputs a lightning voltage waveform with either positive or negative polarity. However, the SLIG also outputs a bipolar voltage waveform by satisfying the oscillation condition in a transient circuit when its output resistance is connected in parallel to a small resistance. Therefore, the oscillating waveforms of the voltage and current during the discharge may contain useful information for determining the discharge impedance. To determine the discharge impedance in the water gap, the impulse discharges were performed under oscillating conditions.

The liquid gap between the rod (φ 3.0 mm x 50 mm) and plate (φ 200 mm x 200 mm) electrodes made of SUS304 is consisted of the tap-water as shown in Fig. 1. The liquid gap (d_w) filling in the tap-water with the conductivity of 198 mS/m is d_w = 100 mm. A set of voltage and current values was measured by a digital storage oscilloscope (DSO). The discharge voltage was measured by a high-voltage probe (HVP) using a resistor-divider with an ratio of 1/5000 and a response time of less than 1 ns. The discharge current was measured by a high response current probe (HRCP) including the Rogowski coil with an attenuation ratio of 1/100 and a response time of 3.3 ns.

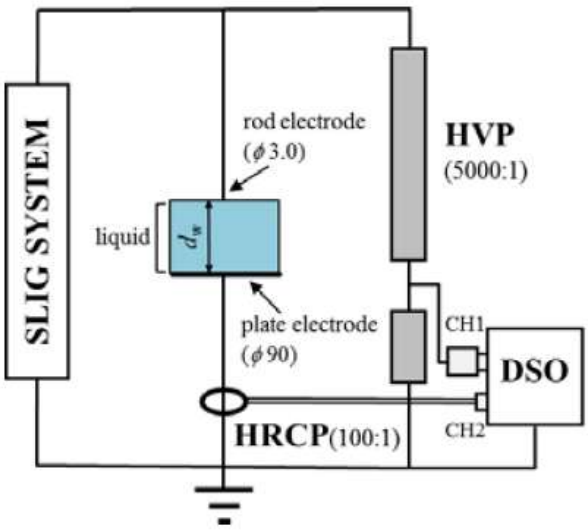

Figure 1. Schematic diagram of impulse discharge system.

III. EXPERIMENTAL RESULTS AND DISCUSSION

The conditioned discharge waveforms of the voltage (V_d) and current (I_d) are shown in Figs. 2 (a) and (b) for positive and negative discharges, respectively. These waveforms were determined with the synchronous averaging method using six raw voltage and current waveforms. As a result, smoothed discharge waveforms appeared, and the voltage waveforms indicated different amplitude distortions in both the positive and negative discharges compared to those of the current waveforms.

*Daisuke Okano, same address as mentioned above, okano@ktmail.tokai-u.jp, tel/fax:+81-96-386-2646

We confirmed that the period (T) of the voltage and current waveforms was approximately equal to 40 μs (corresponding frequency of f = 25 kHz). We also concluded that the discharge voltage period in the composite gap is 3 μs shorter than the case of the air gap reported in [7] and the duration of the discharge waveforms is 57 % of that in the case of the air gap.

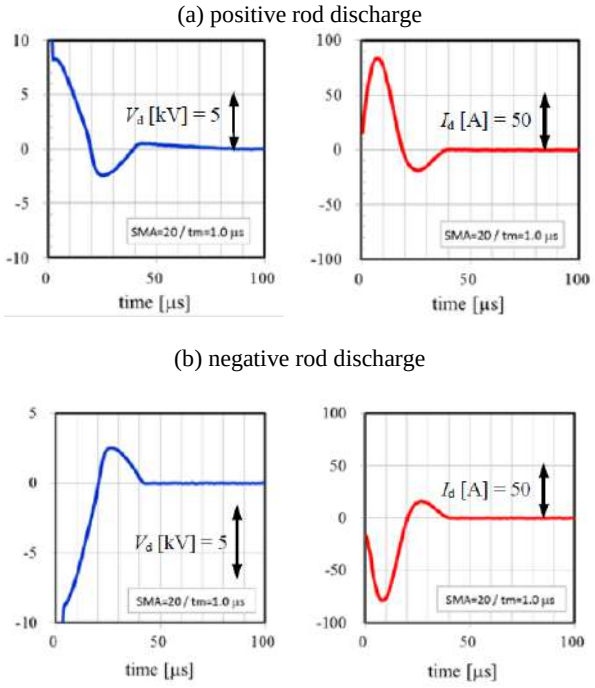

Figure 2. Conditioned waveforms of (a) positive and (b) negative discharges.

Our circuit model for the discharge impedance can be treated as a serial-connected circuit between a resistor and inductor during the discharges. The existence of the resistance was detected from the oscillating and attenuating waveforms, as shown in Figs. 2 (a) and (b). When the time lag between the voltage and current waveforms was carefully examined, we found that the current waveforms in the positive and negative discharges commonly had a delay time of around 3 μs against the voltage waveform. Thus, the discharge currents also may include an inductive component.

In general, the discharge impedance can be obtained by successively solving the simultaneous voltage equations [7] in the equivalent circuit. When the discharge period is approximately given by the average one between V_d and I_d in our case, the calculation was performed for 60 μs, which covered more than one cycle of the voltage and current value set.

The results and smoothing solid lines of inductance are shown in Figs. 3 (a) and (b) as a function of time for the positive and negative discharges, respectively. The resistance and inductance are represented by R and L, respectively, and the solid line is a regression of the inductance. From these results, R gradually increased over time but displayed curved regions, and as the R value at the bottom of the curved region is slightly lower than the other points, this suggests the existence of electron acceleration (EA). The EA was maintained for a duration that is 6 times greater than the 2 μs of the air gap reported in [7]. The L value, however, largely oscillated before synchronizing with the current period different from the constant values in the air gap. The values for each circuit element and the series impedance with respect to time can be summarized as R = 0.05–10 Ω, L = 4.0–100 μH for the smoothing curve, and Z = 0.63–19 Ω for the positive discharge; and R = 0.05–10 Ω, L = 2.0–100 μH for the smoothing curve, and Z = 0.32–19 Ω for the negative discharge.

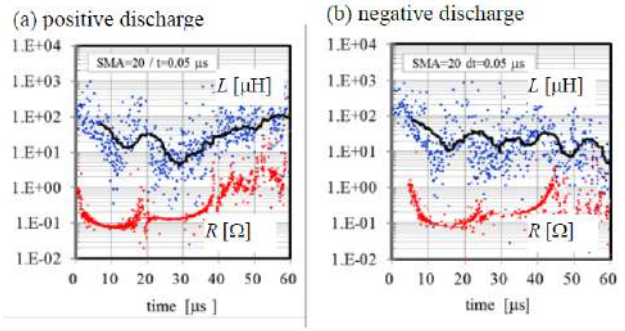

IV. CONCLUSIONS

We investigated experimentally the impedance to lightning impulse discharge in the liquid gap with the tap-water. The impedance depending on time after the discharges ranges are Z = 0.63–19 Ω for positive discharge and Z = 0.32–19 Ω for negative discharge. The electron acceleration in the short composite gap was maintained for ~12 μs longer than that for the air gap.

ACKNOWLEDGEMENT

This work was supported in part by KAKENHI (no. 23560339) from the Japan Society for the Promotion of Science (JSPS) in the Ministry of Education, Culture, Sports, Science and Technology (MEXT).

REFERENCES

[1] V. A. Rakov and M. A. Uman, "Review and Evaluation of Lightning Return Stroke Models Including Some Aspects of Their Application", IEEE Transactions on Electromagnetic Compatibility, Vol. 40, pp. 403-426, 1998.

[2] V. A. Rakov, "Some inferences on the propagation mechanisms of dart leaders and return strokes" J. Geophys. Res., Vol. 103, pp. 1879-1887, 1998.

[3] S. L. Chen and T. Sekiguchi, "Instantaneous Direct-Display System of Plasma Parameters by Means of Triple Probe", Journal of Applied Physics, Vol. 36, pp. 2363-2375, 1965.

[4] K. Urushihara, S. Ono, and S. Teii, IEEJ (in Japanese), Vol. A119, pp. 37-43, 1999.

[5] K. Muraoka, K. Uchino, Y. Yamagata, Y. Noguchi, M. Mansour, P. Suanpoot, S. Narishige, and M. Noguchi, Plasma Sources Science and Technology, Vol. 11, pp. A143-A149, 2002.

[6] T. Tsuji, C. Honda, M. Uchiumi, T. Tanaka, K. Muraoka, T. Takuma, M. Akazaki, F. Kinoshita, and O. Katahira, IEEJ (in Japanese), Vol. A115, pp. 583-588, 1995.

[7] D. Okano, "Simple method of determining plasma impedance of streamer discharge in atmospheric air", Review of Scientific Instruments, Vol. 82, pp. 123502-1~123502-5, 2011.

[8] L. Spitzer, *Physics of Fully Ionized Gases*, 2nd ed., John Wiley & Sons, Inc.: New York, pp. 136-143, 1962.

A019

INFLUENCE OF GAS PRESSURE ON SF_6 DISSOCIATION AND SIMULATION IN INITIAL DECOMPOSITION PRODUCTS UNDER AC CORONA DISCHARGE

Yan-Bo Yang*, Ming Dong [1], Jin Miao [1], Zhong Ren [1], Xue-Zhou Wu [1]
High Voltage Division, School of Electrical Engineering, Xi'an Jiaotong University
28 West Road of Xianning, Xi'an, Shaanxi Province, P. R. China, 710049

Keywords: SF_6, decomposition products, AC corona discharge, FTIR, Simulation

Abstract: To detect all the SF_6 decomposition products and investigate their concomitance laws, FTIR is used in on-line monitoring the whole gas formation process in SF_6 tank under AC corona discharge. The transported charge in experimental is controled from 0 to 10 C (mean discharge current intensity: 20μA and 40μA), and gas pressure that range from 0.1MPa to 0.4MPa. The main gas by-products detected are SO_2, H_2S, HF, SO_2F_2, SOF_2 and SOF_4. The results indicate that gas pressure have complicated effect on the gas decomposition products for current of 20μA. The yields of SO_2F_2, SOF_4 are independent of gas pressure while SOF_2 is affected by gas pressure signally. The levels of SO_2F_2 and SOF_4 are proportional to the charge transported, but SOF_2 grows linearly with charge transported initially and then reach equilibrium concentration. To explain the study result, we established a plasma model and mainly use cross section data to simulate the electron density and electron energy under different gas pressure in order to get the yields of initial products, such as SF_5, SF_4 and SF_2. The diversity of main gas by-products can be explained by different yields of initial products with chemical reaction followed, and gas pressure's role played in the process of SF_6 decomposition under AC corona discharge is discussed.

I. INTRODUCTION

Gas insulated substations (GIS) which are insulated by sulfur hexafluoride (SF_6) as arc extinguishing dielectric are widely applied today due to its excellent performances, i.e., small floor area, reliable operation. Currently monitoring the activities of partial discharge in SF_6 is treated as an effective method to evaluate the insulation condition of GIS, but how to distinguish real discharge with on-site noise is main dilemma of PD detection. So some kinds of incipient faults could not be found by PD measurement, which may lead to early low-energy discharges such as corona or partial discharge due to the conductor surface burrs left in GIS during transportation and installation.

Pure SF_6 gas is a colorless, odorless, nontoxic and noncombustible inert gas. Some former research results indicate that the stable gaseous by-products formed under corona or partial discharge are SF_4, SO_2F_2, SOF_2, SOF_4, SO_2, HF, etc. Considerable investigation of the types and contents of SF_6 gas decomposition products under corona discharge in different energy, voltage type, current intensity, gas pressure was carried out by Van Brunt, Chu F Y and other researchers[1-3]. In particular, A zonal plasma chemical model was proposed to account for the observed decomposition of SF_6 subjected to a negative, point-to-plane corona discharge by Van Brunt[3], which can provide a reference and guidance to explore SF_6 gas decomposition mechanism under AC corona discharge. From their work, SOF_2 was the dominant species formed in the decomposition products under corona discharge; and if pure SF_6 was contaminated by oxygen and moisture, the main stable gas by-products were SOF_2, SO_2F_2 and SOF_4; a modification of the surface state of the electrodes had a significant influence on value of corona current intensity and reactions of SF_6 decomposition products. In recent years, some researchers began to establish different SF_6 plasma model or change the condition of the model in order to get more ingormation about initial products and surface reactions[4]. Their works helped us understand the SF_6 decomposition mechanism in first part and they explained the phenomenon in electro-discharge of SF_6, however, their work had little connection with final products like SOF_2, SO_2F_2 and SOF_4 so it was hard to get the relationship between decomposition products and plasma model. The research on SF_6 decomposition characteristics under AC corona discharge is not deep enough to gain a clear understanding of the decomposition mechanism.

The emphasis in this paper was on the gas pressure's effect on the contents of SF_6 gas decomposition products under 50Hz AC corona discharge. We made a combination analyze of both initial products and final decomposition products so we make a more clear explaination of the role gas pressure played during the different process in SF_6 decomposition. Influence of gas pressure on decomposition products under different condition(electrode material, charge transported, mean current) had also been tested to further prove our results. According to phenomenon and conclusions of tests, the general decomposition mechanism of SF_6 gas under AC corona discharge is discussed.

II. MATERIALS AND METHODS

A. Gas reaction cell

To investigate gas by-products under corona discharge, a stainless steel discharge cell of which the diameter was 20cm and the height was 30cm was constructed, as shown in Figure 1. In order to replace electrodes, clean the gas chamber and observe discharge phenomenon conveniently, a hinge door sealed by seal ring is designed in which a pane of quartz glass with thickness of 13mm was embedded. The 50Hz ac corona discharge was generated between point-to-plane electrodes with a gap spacing of 5mm at room temperature. The needle point (radius of curvature 0.5mm) was made of stainless steel or copper and was replaced for each test. The plane electrode was made of stainless steel or brass. The holder of the electrodes was made of copper.

*Yan-bo Yang, 28 West Road of Xianning, Xi'an, Shaanxi Province, P. R. China, 710049. E-mail: yangyanbo@stu.xjtu.edu.cn. Tel: 13772005596, (+86-29)82668169

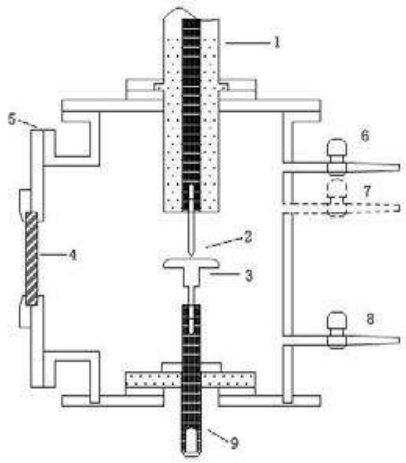

Figure 1. Schematic of discharge cell.

1: High voltage bushing; 2: point electrode; 3: Plane electrode. 4: quartz glass; 5: hinge door; 6: intake valve; 7: exhaust valve; 8: sample valve; 9: copper holder.

B. Decomposition products measurement

The detection equipment of SF_6 gas decomposition products was an FTIR spectrometer from Shimadzu (Japan) equipped with a KBr-5 interferometer shutters and a DLATGS detector.

III. RESULTS AND DISCUSSION

(a)The yields of SO_2F_2, SOF_4 seemed independent of gas pressure while SOF_2 was affected by gas pressure signally. The levels of SO_2F_2 and SOF_4 were proportional to the charge transported, but SOF_2 grew linearly with charge transported initially and then reached equilibrium concentration

(b) With the gas pressure rise, the development and amplitude of external current would be restricted and electron energy was lower, so among the initial dissociation products, the yield of SF_4 was higher than small fragments like SF_2 in high pressure for its higher cross section data.

(c) The yields of final dissociation products SOF_4, SOF_2 and SO_2F_2 in different gas pressure mainly relied on chemical reaction after ion-surface reaction which produced raw materials like SF_4 and SF_2 happened close to electrode.

(d) The reason that gas pressure mainly effects the level of SOF_2 may be that the equilibrium between moisture absorbed by metal electrodes and surface inside the chamber was changed for different level of gas pressure, while impurity oxygen spread in the chamber which was not related to gas pressure and the formation of SO_2F_2 and SOF_4 mainly depends on oxygen. Thus, the levels of SO_2F_2 and SOF_4 are independent of gas pressure.

REFERENCES

[1] Chu F Y. SF_6 decomposition in gas-insulated equipment [J]. IEEE Trans. Electr. Insul.., 1986, EI-21(5): 693-725.

[2] Van Brunt R J, Herron J T. Fundamental processes of SF_6 decomposition and oxidation in glow and corona discharges [J], IEEE Trans. Electr. Insul., 1990, 25(1): 75-94.

[3] R. J. Van Brunt and J. T. Herron. Plasma chemical model for decomposition of SF_6 in a negative glow corona discharge [J].Physica Scripta.,1994,T53:9-29.

[4] George Kokkoris, Apostolos Panagiotopoulos, Andy Goodyear et al. A global model for SF_6 plasmas coupling reaction kinetics in the gas phase and on the surface of the reactor walls[J]. Journal of Applied Physics, 2009,42:055209.

ACKNOWLEDGEMENTS

This work is supported by National Natural Science Foundation of China (50907051).

A020

BREAKDOWN CHARACTERISTICS OF TRANSFORMER OIL-BASED NANOFLUIDS

Jin Miao*, Ming Dong[1], Liang-Ping Shen[2], Yan-Bo Yang[1]
High Voltage Division, School of Electrical Engineering, Xi'an Jiaotong University
Faculty of Physics and Electronic Technology, Hubei University
28 West Road of Xianning, Xi'an, Shaanxi Province, P. R. China, 710049

Keywords: Nanofluids, Transformer oil, Breakdown strength, Electrical characteristic

Abstract: Oil-paper insulation is widely used in main power equipment, and its condition determines the usage lifetime, especially for power transformers. It is already known that the heat transfer efficiency of transformer oil could be effectively improved by adding suitable nanoparticles, which also would affect the oil's electrical properties and breakdown strength. In this paper, different kinds of nanoparticles were dispersed steady in transformer oil through ultrasonic treatment. In order to identify the influence of nanopaticles on electric characteristics, dissipation factor (tanδ), electrical conductivity and relative dielectric constant were measured. Further more, the AC and impulse breakdown strength of transformer oil-based nanofluids and mineral oil were measured, respectively. The results show that the AC breakdown voltage of transformer oil with suitable nanoparticles is close to ordinary oil, while the impulse breakdown vlotage has a great improvement under extremly non-homogeneous electric field, and the PD inception voltage increases at the same time. It is also founded that nanoparticles may induce the increasment of dissipation factor and electrical conductivity.

I. INTRODUCTION

The insulation system of power equipment is required to have better performance with growing energy needs and extreme reliability demands. Oil-paper insulation is widely used in main power equipment, i.e., power transformer, electrical cable, and its condition largely determines usage lifetime. In oil-paper insulation system, oil plays a dual role of cooling and insulation, and its heat dissipation and dielectric properties have great influence on the reliability of transformer in the long-term operation. In 1990s nanoparticles were added into transformer oil to enhance the heat transfer within itself. Segal et al. found that nanofluids can increase the withstand voltage under positive lightning impulse. The PD inception voltage increase up to 130% as compared to transformer oil [1]. J. George Hwang et al. thought that electron charging of nanoparticles can convert fast electrons from field ionization to slow negatively charged particles and decrease the positive streamer velocity[2].

In principle, nanofluids is a colloidal suspension of particles (average size is in the range of a few nanometers, two to three orders of magnitude smaller than micrometer) in transformer oil. From a conventional point of view, additional particles in transformer oil is detrimental to dielectric strength. It is a traditional way to purify the oil to a maximum degree as high as possible. It must be noted, however, that except for enhancement of heat transfor, nanofluids at its optimum composition has some special electric characters and improvement in dielectric strength.

This paper mainly concerns the breakdown characteristics of transformer oil-based nanofluids and mineral oil in different kinds of eletric field. In addition, the basic electrical characters of nanofluids: dielectric dissipation factor, electrical conductivity and relative dielectric constant were also measured.

II. MATERIALS AND METHODS

A. Nanofluids preparation

All the experiments presented in this paper were performed using 25# transformer oil as carrier oil, and ZnO, TiO_2, SiO_2 were chosen as nanoparticles (average size is 50 nm) without surface modification. Four kinds of nanofluids were contained in this paper whose volumn fractions are 0.025%, 0.05%, 0.1% and 0.2%, respectively.

B. Breakdown strength measurements

The AC breakdown voltage at power frequency was tested according to IEC 60156 standard using Mingsheng MS2673-IIB insulating liquids breakdown voltage tester. The impulse withstand voltage was measured as the illustration below, in accordance with IEC 60897 standard. Except for the needle to sphere electrode, this experiment also introduced needle to needle electrode to simulate extremly non-homogeneous electric field.

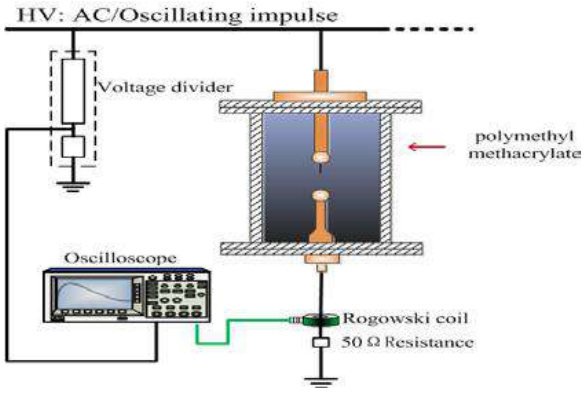

Figure 1. Illustration of impulse voltage measurement

III. RESULTS AND DISCUSSION

(a) At the optimium composition, transformer oil-based 2 nanofluids has the AC(50Hz) breakdown voltage close to that of the carrier oil, however the impulse breakdown strength is much higher, especially for the positive impulse.
(b) The PD inception voltage of nanofluids increased more than 20% compared with that of the ordinary oil.
(c) The streamer acrossing electrode gap under positive impulse was faster than the negative impulse.
(d) The transformer oil-based nanofluids had better properties than ordinary oil including impulse withstand voltage, PD inception voltage and suppressing streamer development.

*Jin Miao, 28 West Road of Xianning, Xi'an, Shaanxi Province, P. R. China, 710049. E-mail: miaojin@stu.xjtu.edu.cn. Tel: 15929985022, (86-029)82668169

(e) Nanoparticles added into transformer oil may cause the increase of dissipation factor and electrical conductivity to varying degrees, which was not expected by researchers.

REFERENCES

[1] Vladimir Segal, Arne Hjortsberg, Arnold Rabinovich, et al. AC(60 Hz) and Impulse Breakdown Strength of a Colloidal Fluid Based on Transformer Oil and Magnetite Nanoparticles[C]. IEEE Symposium on Electrical Insulation, Arlington, Virginia, USA, June 7-10, 1998.

[2] J. George Hwang, Markus Zahn, Francis M. O'Sullivan, et al. Effects of nanoparticle charging on streamer development in transformer oil-based nanofluids[J]. Journal of Applied Physics, 2010,107,014310.

A023

EXPERIMENTAL STUDY OF HOMOGENOUS DIELECTRIC BARRIER DISCHARGE IN ATMOSPHERIC-PRESSURE AIR

Junxia Ran, Haiyun Luo*, Seongling Yap, Xinxin Wang
State Key Laboratory of Power System, Department of Electrical Engineering,
Tsinghua University, Beijing 100084, China

Keywords: Dielectric barrier discharge, Homogeneous discharge, Gas discharge, Townsend discharge

Abstract: Homogenous dielectric barrier discharge (DBD) in atmospheric-pressure air was first generated in as larger as 3 mm air gap between two plane-parallel electrodes of 50 mm in diameter each covered by a specific ceramic plate with a thickness of 1.5~3.25 mm, which was not reported in previous literatures. The discharge free of filaments was confirmed to be a homogenous Townsend discharge by electrical measurement and fast photograph. By subtracting the displacement current from the total current, there was one current peak per half cycle of the applied sinusoidal voltage, as was typical for homogeneous DBD. The current peak was 1 mA in amplitude and about 85 μs in FWHM (full width at half magnitude). Side-view photographs with 10 ns exposure time taken at the peak of the current pulse showed that there were no filaments in the discharge gap. A luminous layer close to the instantaneous anode was observed, indicating the homogeneous DBD was a Townsend discharge. When choosing a ceramic thinner than 1.5 mm, some filaments randomly appeared in the gap, as was called a mixed mode of homogenous and filamentary DBD. This was because in DBD the dielectric capacitance played an important role in the limitation of the discharge current. A smaller capacitance would help to avoid an electron avalanche overdeveloping to a streamer. When a stable Townsend discharge was maintained, the breakdown voltage was determined to be only 8.3 kV, much lower than the static breakdown voltage of 11.2 kV for the same air gap of 3 mm in length. The formation of Townsend discharge was attributed to the uniqueness of the shallow traps on the surface of the specific ceramic plate and the common effect of the current limitation by dielectric.

I. INTRODUCTION

Dielectric barrier discharge (DBD) in air at atmospheric pressure normally occurs in a large number of short-lived and narrow current filaments that are randomly distributed in time and space over the dielectric surface [1]. Non-thermal plasma produced by homogeneous DBD in air is most attractve for the industrial applications. However, the realization of homogeneous DBD is usually much more difficult in air than in noble gases and other gases. Air is an electronegative gas consisting of oxygen, nitrogen and water vapour. The oxygen molecules in air efficiently quench nitrogen metastable species and tend to induce electron attachments in air discharges, so the DBD atmospheric-pressure air usually exhibits a filamentary mode. In recent years, the generation of homogeneous DBD in atmospheric air is one of the most remarkable research works in the plasma field. For obtaining a homogeneous DBD in atmospheric air, many methods and special barrier materials have been explored. [2–13]. Ráheĭ J found within the frequency range 1~15 kHz, discharge gaps smaller than 1.5mm a diffuse discharge could be obtained in air at at atmospheric pressure[2-3]. Garamoon A A and El-zeer D M found a uniform discharge can be obtained with a frequency 50 Hz and a gap distance 1.1mm[4]. Up to now, there was no report of a homogeneous DBD in atmospheric-pressure air with a gap distance larger than 2mm in high frequency.

In this paper we firstly report a homogenous DBD in as larger as 3 mm air gap at atmosphric pressure. Experimental setup, the generation and diagnostics of the discharge were introduced, and the discussion focus on the effect of the ceramic.

II. MATERIALS AND METHODS

The arrangement of the experimental was similar to our previous works[6]. Ceramic plates with various thicknesses between 0.5~3.25mm were chosen as the dielectric barriers. The air gap *d* is fixed at 3mm. A sinusoidal high voltage with a frequency that could be continuously changed from 1k~10 kHz was applied to the electrodes. An intensified-CCD- camera was used to take the discharge photographs with an exposure time down to 10 ns.

III. RESULTS AND DISCUSSION

3.1 Generation of the homogeneous DBD in air

It showed that when the barrier thickness was smaller than 1.5mm, a mixed mode of diffuse and filamentary discharge was found and the current shown many short-pulse per half cycle of the applied voltage. For example, when the barrier thickness was 0.5mm , the filamentary discharge is very intensity and its current pulse is unorderly. With the barrier thickness increasing, the filaments began to decreasing. When the barrier thickness was greater than 1.5mm, the filaments disappeared and a stable homogeneous discharge was produced. It was characterized by one current pulse per half cycle of the applied voltage.

3.2 The characteristic of the homogeneous DBD

In order to investigating the discharge characteristic of the homogeneous discharge, the time resolution photograph was measured by ICCD with a gap distance 3mm and ceramic plate thickness 2.285mm, In order to obtain bigger current the applied frequency f is 1.32kHz. the typtical waveform was shown in Figure 1. Side-view photographs with 10 ns exposure time taken at the time about the peak of the current pulse showed that there were no filaments in the discharge gap. A luminous layer

E-mail:Lhy@tsinghua.edu.cn

close to the instantaneous anode was observed, indicating the homogeneous DBD was a Townsend discharge, as shown in Figure 2.

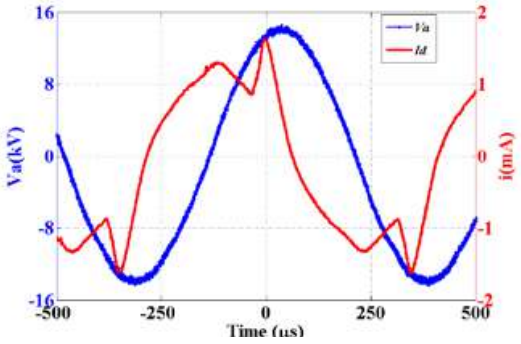

Figure 1. Applied voltage(*Va*) and total current(*I*)

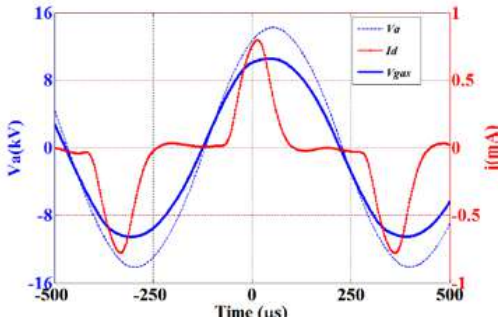

Figure 3. Calculated discharge current *Id* and gap votlage *Vgas*

By subtracting the displacement current from the total current, the discharge current and gap voltage was calculted. It was shown in Figure 3. It appears one current peak per half cycle of the applied sinusoidal voltage, which was typical for homogeneous DBD. The current peak was 1 mA in amplitude and about 85 μs in FWHM (full width at half magnitude). The breakdown voltage was determined to be only 8.3 kV, much lower than the static breakdown voltage of 11.2 kV for the same air gap of 3 mm in length.

The results prove a stable homogeneous discharge in air at atmospheric pressure was a Townsend discharge. It was suggested that the unique feature of the shallow traps on the surface of the specific ceramic plate and the common effect of the current limitation by dielectric barrier play important roles in the formation of theTownsend discharge. The details of the mechanism for the Townsend discharge were still under investigation.

3.3 The influence of ceramic plate

The Townsend discharge can only be produced under the condition that both electrodes were covered by a specific ceramic plate with a thickness of about 2 mm. If the ceramic plate was too thin, the discharge would transit to filamentary discharge. If the ceramic plate was too thick, the Townsend discharge would be too weak to observe. The formation of Townsend discharge in air was attributed to that the release of the shallowly trapped electrons on the surface of the dielectric covering the cathode provide the discharge with a limited amount of the seed electrons, which leaded to an extraordinary extinction of the Townsend discharge and made the glow discharge not to be reached. Next work was to do some diagnostic of the ceramic.

IV CONCLUSIONS

Homogenous Townsend dielectric barrier discharge (DBD) in atmospheric-pressure air was generated in 3 mm air gap. Ceramic plates as the barrier material had great impact on generating homogenous Townsend DBD. Next work was to do on the ceramic and the mechanism for the Townsend discharge .

ACKNOWLEDGMENTS

The research was supported by the National Natural Science foundation of China under contracts 51107067, 51077082 and by research fund from the State Key Laboratory of Power System for under contracts SKLD09M22 and SKLD11M05.

REFERENCES

[1] Kogelschatz U, “Dielectric-barrier Discharges: Their History, Discharge Physics, and Industrial Applications”, Plasma Chemistry and Plasma Processing Vol. 23, No. 1, pp.1-46, 2003.

[2] Ráheľ J, Sherman D M, “The transition from a filamentary dielectric barrier discharge to a diffuse barrier discharge in air at atmospheric pressure” J. Phys. D: Appl. Phys., Vol.38, No.4, pp. 547-554, 2005.

[3] Rahel J, Sira M, Stahel P, Trunec D., “The Transition Between Different Discharge Regimes in Atmospheric Pressure Air Barrier Discharge”, Contrib. Plasma Phys. vol.47,No.1-2, pp. 34-39,2007.

[4] Garamoon A A, El-zeer D M, “Atmospheric pressure glow discharge plasma in air at frequency 50 Hz”, Plasma Sources Sci. Technol. Vol.18, pp.0450064 , 2009.

[5] Fang Z, Qiu Y, Zhang C and Kuffel E “Factors influencing the existence of the homogeneous dielectric barrier discharge in air at atmospheric pressure”, J. Phys. D: Appl. Phys. Vol.40,No.140,pp.1–7 , 2007.

[6] Wang X, Luo H, Liang Z, Mao T and Ma R, “Influence of wire mesh electrodes on dielectric barrier discharge” , Plasma Sources Sci. Technol. Vol.15 No.4, pp.845–8, 2006.

[7] Okazaki S, Kogoma M, Uehara M and Kimura Y, “Appearance of stable glow discharge in air, argon, oxygen and nitrogen at atmospheric pressure using a 50 Hz source”, J. Phys.D: Appl. Phys.Vol. 26,No.5, pp. 889–892,1993

[8] Tepper J and Lindmayer M Proc., “Investigations on two Different Kinds of Homogeneous Barrier Discharges at Atmospheric Pressure”, HAKONE 7th Int.Symp. High Pressure Low Temperature Plasma Chemistry (Greifswald, 10–13 September 2000) vol.1 pp. 38, 2000

[9] Liu S and Neiger M, “Excitation of dielectric barrier discharges by unipolar submicrosecond square pulses” J. Phys. D: Appl. Phys. Vol.34 ,No.11,pp.1632–8, 2001

[10] Kruger C H, Laux C O, Yu L, Packan D M and Pierrot L , “Nonequilibrium discharges in air and nitrogen plasmas at atmospheric pressure”, Pure Appl. Chem. Vol. 74, No. 3, pp. 337–347, 2002.

[11] Choi J H, Lee T, Han I, Oh B Y, Jeong M C, Myoung J M and Baika H K, “Improvement of plasma uniformity using ZnO-coated dielectric barrier discharge in open air”, Appl. Phys. Lett., Vol.89, pp.081501,2006

[12] Walsh J L and Kong M G, “10 ns pulsed atmospheric air plasma for uniform treatment of polymeric surfaces”, Appl. Phys. Lett. Vol.91 pp.251504, 2007

[13] Takaki K, Kirihara H and Noda C, “Production of an Atmospheric- Pressure Glow Discharge Using an Inductive Energy Storage Pulsed Power Generator”, Plasma Process. Polym. Vol.3, pp.734–42, 2006.

A024

CURRENTS AND ELECTRIC FIELDS INDUCED IN ANATOMICALLY-REALISTIC HUMAN MODELS BY ELF ELECTRIC FIELDS

Hiroo Tarao[1]*, Noriyuki Hayashi[2], Takashi Matsumoto[3], and Katsuo Isaka[4]
[1]Kagawa National College of Technology, Japan,
[2]University of Miyazaki, Japan,
[3]Anan National College of Technology, Japan,
[4]The University of Tokushima, Japan

Keywords: Power transmission lines, Substations, External E-fields, Induced body currents, SPFD method

Abstract: There has been increasing public concern about biological interactions and the potentisl health effects of low frequency electric and magnetic fields. Recently, the ICNIRP has published new guidlines. The aim in this paper is to demonstrate induced currents and electric fields in human body by ELF external electric fields, using numerical human models of anatomically-realistic human body, and to compare those results with the basic restrictions of the new gauidlines.

I. INTRODUCTION

There has been increasing public concern about biological interactions and the potential health effects of low-frequency electric and magnetic fields (LF-EMFs). Human exposure to the LFEMFs results in induction of the electric fields and the resultant current densities in a body. The International Commission on Non-Ionizing Radiation Protection (ICNIRP) has published new guidelines for LF-EMFs [1], in which the physical quantity of the basic restrictions has been changed into internal electric fields from current densities. The aim in this paper is to demonstrate induced currents and electric fields in human body by ELF external electric fields, using numerical human models of anatomically-realistic human body, and to compare those results with the basic restrictions of the new ICNIRP guidelines.

II. MATERIALS AND METHODS

The induced electric fields in the voxelized human model, exposed to ELF external electric fields, are calculated using a two-stage approach, based on the scalar potential finite difference (SPFD) method. This method is originally for the low-frequency induction by magnetic fields but has been improved for electric field exposures. First, an electric field calculation solution for the whole computational domain including both a coarse voxel model and the air region is performed. Then, the resulting scalar potential is extracted from the results and interpolated onto a surface of the bounding box of a finer voxel model. The interpolated potential on the surface of the coarse voxel model serves as the electrode potentials for post-processing calculation in the bounding box of the finer voxel model [2].

Two realistic human models of an adult male (Duke) and a young male (Luis), comprised of 77 tissues or organs are used for the numerical calculation[3]. There are some sets of the models consisting of an array of cubic voxels in the same size bounding box. Of the set, voxel size of 5 mm and 2 mm are used in this study; the former and the latter models are for preliminary and post-processing, respectively.

III. RESULTS AND DISCUSSION

Two typical exposure scenarios are considered with the human model in external electric fields: one is a human body standing barefoot on the ground and the other is a human body standing in a free space. For the two scwnarios, an ambient electric field of 1 kV/m at 60 Hz is vertically aplied.

From the distribution of the induced electric fields on the coronal plane inside the adult male model, the induced fields can be found to be wholly higher for the grounded than for the isolated, as expected. Especially, at the feet for the grounded, the induced fields are very high as the induced currents converge on the feet. Table 1 indicates the current passing through each part of the body for the different scenarios of the two human models. For both models, the currents through the arm, where is most likely to perceive to electricity,for the grounded are five to six times higher than those for the isolated, as well as for the ankles. Electric fields induced in the human models are compared with the basic restrictions published in the new ICNIRP guidelines. The induced fields for the central nervous system tissues in the head of the body do not exceed the basic restrictions.

Table 1. Currents in μA through each part of the human body exposed to E-field of 1 kV/m at 60 Hz.

	Luis		Duke	
	Grounded	**Isolated**	**Grounded**	**Isolated**
neck	4.69	2.66	4.86	2.77
left upper arm	1.35	0.29	1.59	0.26
right upper arm	1.28	0.22	1.68	0.27
abdomen	12.77	5.54	14.56	6.09
left ankle	16.08	1.61	6.50	1.62
right ankle	0.07	1.54	11.73	1.64

REFERENCES

[1] ICNIRP, “Guidelines for limiting exposure to time-varying electric and magnetic fields (1 Hz to 100 kHz), Health Physics, Vol.99 , pp. 818-836, 2010.
[2] H. Tarao, N. Hayashi, L. Korpinen, T. Matsumoto, and K. Isaka: “Calculation of induced electric fields in human models exposed to ELF magnetic and electric fields”, Proceedings of ISH 2011.
[3] A. Christ et al.: “The virtual family- development of surface-based anatomical models of two adults and two children for dosimetric simulations”, Phys. Med. Biol. Vol.55, pp.N23-N38, 2010.

*Hiroo Tarao, Dept. of Electrical & Computer Eng., Kagawa National College of Tech., Takamatsu-shi, Kagawa 761-8058, Japan tarao@t.kagawa-nct.ac.jp

A026

RVM VERSUS PDC METHODS FOR INSULATIONS CONDUCTIVITY AND MOISTURE CONTENT MONITORING

R. A. Zainir[1], N. A. Muhamad[1], Z. Adzis[1], N. A. M. Jamail[1, 2], M. A. M. Piah[1], N. F. Kasri[1]
[1]Faculty of Electrical Engineering, Universiti Teknologi Malaysia (UTM), Skudai, Johor, Malaysia
[1]Faculty of Electrical and Electronic, University of Tun Hussein Onn Malaysia (UTHM), Batu Pahat, Johor, Malaysia
rabiadza@gmail.com, norasiah@fke.utm.my, zuraimy@fke.utm.my, norakmal@uthm.edu.my, fendi@fke.utm.my, akta1988@live.com

Keywords: ageing, degradation, conductivity, moisture content, PDC, RVM

Abstract: Degradation due to ageing is a major concern for the life span of high voltage insulators. In maintaining the insulation system's performance, it is crucial to monitor the insulator condition as it contributes to the whole system's efficiency and safety. Many diagnostic methods have been introduced, and in use for condition monitoring the insulation. They analyze measurements in either frequency or time domain. Condition-based monitoring (CBM) is in growing interest lately, compared to time-based monitoring due to the increasing population of aged insulators being utilized in existing power systems. Time-based monitoring has then been integrated with CBM. CBM's ability to enhance reliability, improve safety and reduce hazard of a system has been recognized by many researchers and utilities. This paper presents the study and comparison of two time domain CBM techniques namely the polarization and depolarization current (PDC) measurement and return voltage measurement (RVM). The findings of previous researches on determining the insulator's moisture content and conductivity by both methods will be reviewed in detail. The study concludes which method is better suitable for applications on "solid and liquid" type insulators.

I. INTRODUCTION

Condition-based monitoring also known as condition based maintenance (CBM) differs from the time-based monitoring (TBM), whereby CBM enables prediction of required maintenance. It is conducted due to the degrading insulation condition of high voltage equipments under continuous high voltage stress. The predictive maintenance is performed after one or more indicators show degraded condition of the equipment's insulation. Popular methods in assessing the condition of the insulation include polarization and depolarization current (PDC) measurement as well as return voltage measurement (RVM). Time domain measurements based on polarization/depolarization current (PDC) measurement and return voltage measurement (RVM). The time domain measurements based on PDC and RVM has gained significant importance over the last ten years. Coupled with computer-aided technique, which is capable to record and process large amounts of data has improved the possibilities of analyzing the insulation's condition in both methods.

The ageing status and moisture content of the insulation can be determined from measurements of PDC and RVM [1]. Findings from the previous research around the world will be discussed in this paper. The focus is on PDC method as an alternative to the conventional RVM method.

II. METHODOLOGY

This paper reviewed two condition-based monitoring methods: PDC and RVM. PDC is measured in the current while voltage been measured in RVM. Both methods have specific parameters to be identified such as charging/discharging time and test voltage. The paper is focusing on application of both methods in diagnosing solid and liquid type of insulator. These parameters then been investigated on the effects of moisture content and the conductivity level.

III. MATERIALS AND METHODS

The principle of measurement in PDC is based on the application of a DC voltage across a test object for a period of time, in which current will flow from the polarization process in the test object with different time constants. This current depends on the insulation material and its conductivity. This current is called as polarization current. Next, the voltage is removed and the test object is short-circuited. The activation from the previous polarization process now gives rise to the discharging current in the opposite direction. This process in which the current flows in the relaxing state is called depolarization current [2-5, 9].

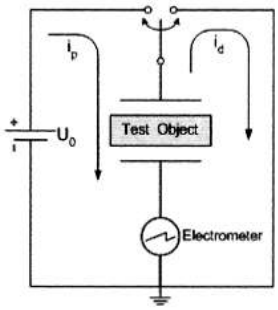

Figure1: Basic PDC measuring Circuit

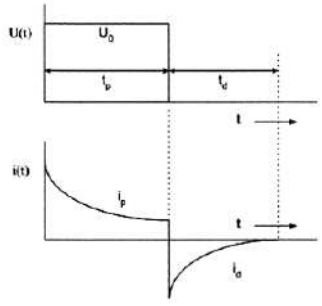

Figure 2. Waveform of polarization and depolarization currents

The basic principle RVM is charging the sample for a long period of time, t_c. Then, the sample is isolated from the HV source and short-circuited for a shorter period of time, t_d. Then

*R. A. Zainir, Faculty of Electrical Engineering, Universiti Teknologi Malaysia, 81310 Skudai, Johor, norasiah@fke.utm.my, 07-5535263

the short circuit is disconnected, and the charge bounded by the polarization process will turn into free charges. This return voltage appearing between the electrodes is then measured to assess the insulation's condition via the maximum spectra of recovery voltage and the recorded charging time [1, 6- 8].

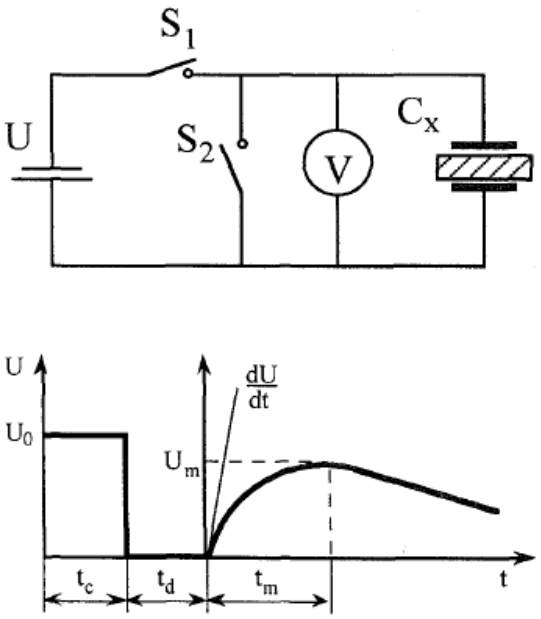

Figure 3. Principle of return voltage measurement

Moisture content for paper can be obtained independently using RVM and PDC measurement while for oil based insulator, the results can only be obtained from PDC tests [1]. The researchers in [1] thus introduced an expert system (ES) for the system operations and insulation diagnosis. ES which is a ruled based artificial intelligence technique has been applied by the several researchers. ES aims at assisting the user to make unambiguous, reliable and quick decision in insulation condition assessment of the transformers using PDC and RVM techniques [1].

IV. RESULTS AND DISCUSSION

Ageing and degradation of high voltage equipment can be determined by the conductivity and moisture content of the insulation. These two parameters can be identified using PDC and RVM. The polarization conductivity is proportional to the initial slope of the return voltage for the transformer's insulation. Conductivity is a good indicator for determining the moisture content in the insulator. The same goes to the PDC method where the higher current at the initial part of the measurement make the insulator is not in the good condition. Further, among the RV parameters, central time constant was found to be most sensitive to ageing and moisture, but the oil and paper insulation cannot be evaluated separately. However PDC analysis is able to analyze the oil and paper insulation, separately. The simple and reliable method of analysis in assessing the insulation system makes PDC measurement more advantageous than RVM.

REFERENCES

[1] Tapan K. Saha and Prithwiraj Purkait, "Investigation of An Expert System for the Condition Assessment of Transformer Insulation Based on Dielectric Response Measurements", IEEE Transactions on Power Delivery, Vol. 19, pp. 1127-1134, July 2004.

[2] T.K.Saha and P.Purkait, "Investigation of Polarization and Depolarization Current Measurements for the Assessment of Oil-Paper Insulation of Aged Transformers", IEEE Transactions on Dielectrics and Electrical Insulation, Vol.11, pp. 144-154, February 2004.

[3] N.A.M.Jamail, M.A.M.Piah and N.A.Muhamad, "Comparative Study on Conductivity using Polarization and Depolarization Current (PDC) Test for HV Insulation", International Conference on Electrical Engineering and Informatics, July 2011.

[4] T.K.Saha and P.Purkait, "Investigating Some Important Parameters of the PDC Measurement Technique for the Insulation Condition of Power Transformer", Sixth International Power Engineering Conference (IPEC2003), November 2003.

[5] Walter S.Zaengl, "Dielectric Spectroscopy in Time and Frequency Domain for High Voltage Power Equipment, Part I: Theoretical Considerations", Feature Article, Vol.19, pp.5-19, September/October 2003.

[6] A.Krivda, R.Neimanis and S.M.Gubanski, "Assessment of Insulation Condition of 130kV Oil-Paper Current Transformers using Return Voltage Measurements and an Expert System", IEEE Annual Report-Conference on Electrical Insulation and Dielectric Phenomena, pp. 210-213, October 1997.

[7] Omar Hassan, et al., "Diagnostic of Insulation Condition of Oil Impregnated Paper Insulation System with Return Voltage Measurements", Annual Report Conference on Electrical Insulation and Dielectric Phenomena, pp. 153-156, 2003.

[8] T.K.Saha and T.Y.Zheng, "Experience with Return Voltage Measurements for Assessing Insulation Conditions in Service Aged Transformers", IEEE Transactions on Power Delivery, Vol.18, pp. 128-135, January 2003.

[9] T.K.Saha and P.Purkait, "Impact of the Condition of Oil on the Polarisation based Diagnostics for Assessing the Condition of Transformers Insulation", IEEE Power Engineering Society General Meeting, pp.1881-1886, June 2005.

A027

EFFECT OF SWITCHING METHOD IN POLARIZATION AND DEPOLARIZATION CURRENT (PDC) MEASUREMENT TECHNIQUE

N. F. Kasri[1], M. A. M. Piah[1], N. A. Muhamad[1], N. A. M. Jamail[1, 2], R. A. Zainir[1]
[1]Faculty of Electrical Engineering, Universiti Teknologi Malaysia, Johor Bahru, Johor, Malaysia
[2]Faculty of Electrical and Electronic, University of Tun Hussein Onn Malaysia, Batu Pahat, Johor, Malaysia
akta1988@live.com, fendi@fke.utm.my, norasiah@fke.utm.my, norakmal@uthm.edu.my, rabiadza@gmail.com

Keywords: high voltage switch, series connection, voltage unbalance, HV relay, IGBT, PDC

Abstract: Switching method in Polarization and Depolarization (PDC) measurement technique is an interesting area to look at, especially in terms of its behavior over the time based monitoring. Pervious researches on PDC measurement technique did not take into account the effect of switching method in process of PDC measurement technique. Most of the researcher used conventional HV relays that act as a switching component. This paper studies the behavior of PDC measurement results and its relationship with the types of switching methods used. It is due to the research's hypothesis which is different switching method may produce slightly difference of PDC measurement results. Determination of which is the best switching method that suit with this technique can be made when comparing the PDC measurement results and through this path, which result is more similar with the reference is consider as the best switching method. Two different switching methods will be considered in this research, which is HV relays and series-connected of 600V, 30A, Insulated Gate Bipolar Transistor (IGBT).

I. INTRODUCTION

Polarization and depolarization current (PDC) measurement is the time domain measurement in assessing the condition of the high voltage equipment likewise the return voltage measurement (RVM) methods. Time domain measurements based on polarization/depolarization current (PDC) measurement and return voltage measurement (RVM) has gained significant importance over the last ten years [1]. Amongst these two dielectric diagnosis techniques, the resemblances can be perceived in terms of its circuit in which switching circuit is involved. Figure 1 shows the similarities of these two different circuits.

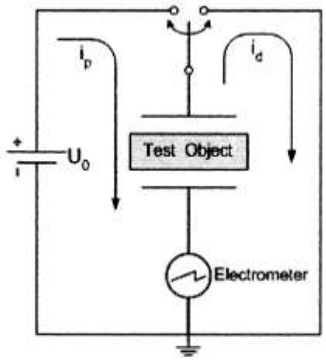

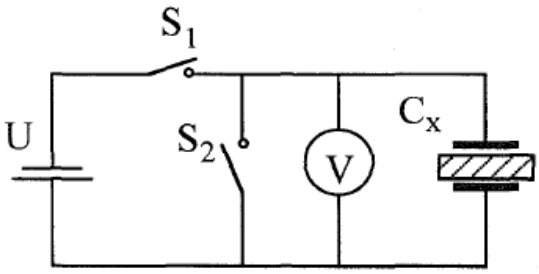

Figure 1. The resemblances between (a) PDC circuit and (b) RVM circuit (shows in dash circle)

II. METHODOLOGY

Switching Method: High Voltage (HV) Relay

This switching method is commonly used by the previous researchers and also in industrial application. The advancement in relay technology makes a very drastic implication in switching world and simultaneously, the monopoly legacy in high voltage switching field has been made by relays. There are many types of relays that can be found in the market and different types of relay are made with specific application. For example, if the rating operation voltage of relays is 5kVdc, means it cannot be used for higher voltage than that and if the relays are for 'make and brake' load or SPDT (Single Pole Double Throw) means it suitable to be used as a switch between two terminals. Figure 2 shows basic principle of electromagnetic relay.

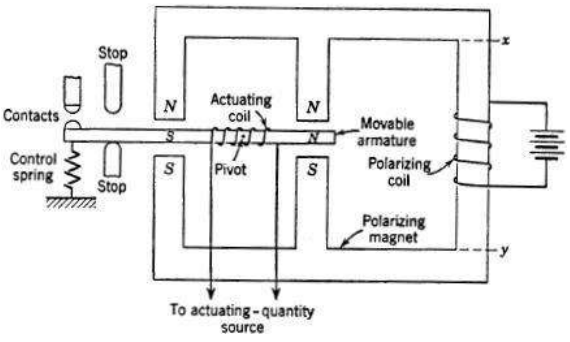

Figure 2. Directional relay of the electromagnetic-

*N.F.Kasri, akta1988@live.com, +60137019145

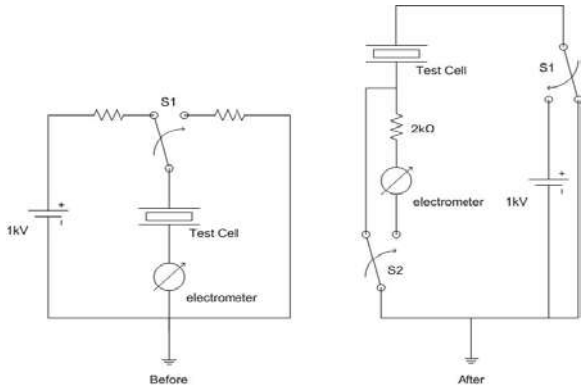

Figure 3. The test setup for PDC measurement before and after improvisation

Figure 3 above shows the test setup for PDC measurement and the circuit has been develop to suit with the purpose of PDC measurement technique. Some improvisation has been done to it specifically in protection system even though the numbers of HV relay increase from 1 unit to 2 units. S1 and S2 are the switching component and it represents the SPDT type of HV relay. S2 which act as a protection circuit is arranged and controlled in such a way that all transient currents bypass the electrometer. A 2 kΩ resistor is used to avoid instantaneous high current through the electrometer during a possible low impedance faulty connection [3]. As a result, the polarization current can be measured with no introduced of harm to the electrometer.

Switching Method: Series-connected IGBTs

In this method, the difference that can be perceived from previous method is only on its switching component and others are the same. Today, there are various power semiconductor devices in the market since power semiconductor device technology has been continually developed far to get higher voltage/current ratings, lower conduction/switching losses, and easier drive. Among various power devices, the Insulated Gate Bipolar Transistor (IGBT) is becoming the best selection from low-to high-power applications because it has advantages which include high voltage/current rating, fast switching, and easy drive capabilities [4]. In this research, the IGBT used has 600V/30A rating. Figure 4 shows the exact circuit of the series-connected IGBTs that replace HV relay.

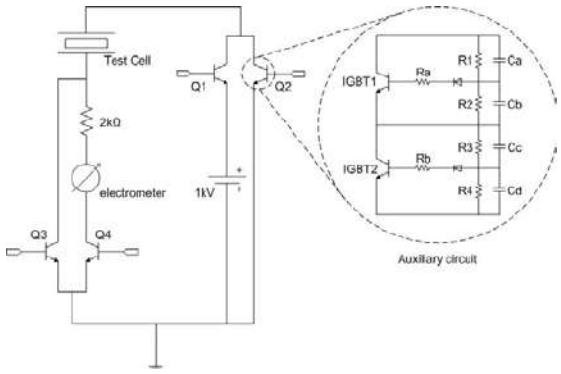

Figure 4. Series-connected IGBT with auxiliary circuit

The main problem that will be confronted is voltage unbalance for each device. Because of differences in IGBT-parameters and gate-drive-circuits, a method for voltage-balancing is needed to ensure, that each element overtakes the correct amount of collector-emitter voltage in the dynamic and static phases. Only with balanced voltages is an economical realization of applications with series connected IGBTs possible [5].

To overcome the unbalance voltage problem on each device, an auxiliary circuit technique has been introduced. This circuit, which consists of two small capacitors, three small resistors, and one small diode, is attached to each device and provides an active gate control effect [4]. If without any presence of voltage balancing techniques, the risk that needs to be taken is destruction of the elements due to voltage and power dissipation stress [5].

III. RESULT AND DISCUSSION

From both switching method that has been explained above, the expected result for HV relay is it will act perfectly like a switch as the existence of relay is for switching purpose only and automatically controlled by the LabVIEW software via NI USB-6211 (multifunction DAQ). For series-connected IGBTs, unbalance voltage problem on each device will be solved with a presence of auxiliary circuit and it can perform perfectly as a switch which can handle a voltage up to 1kV. Determination of the best switching method is depending on the PDC measurement result. By comparing the acquired result with the reference result, it may lead this research to achieve its objective.

REFERENCES

[1] T.K.Saha, *Review of Modern Diagnostic Techniques for Assessing Insulation Condition in Aged Transformer*, IEEE Transactions on Dielectrics and Electrical Insulation, Vol.10, pp. 903-917, October 2003.

[2] Mason, C. R, *Art & Science of Protective Relaying, Chapter 2, GE Consumer & Electrical*, Retrieved October 09, 2011.

[3] Ekanayake, C., Saha, T.K., Ma, H., Allan, D., "*Application of Polarization Based Measurement Techniques for Diagnosis of Field Transformers*", *Power and Energy Society General Meeting, 2010 IEEE*, on page(s): 1 - 8, Volume: Issue: 25-29 July 2010.

[4] J. W. Baek, D. W. Yoo, H. G. Kim: "*High Voltage Switch Using Series-Connected IGBTs with Simple Auxiliary Circuit*", Industry Applications Conference, 2000. Vol.4, 8-12 Oct. 2000 pp.: 2237-2242.

[5] C. Gerster, "*Fast High Power/High Voltage Switch Using Series Connected IGBT's With Active Gate-Controlled Voltage Balancing*", *Proc. IEEE APEC'94*, pp.469 - 472, 1994.

A028

PARTIAL DISCHARGE DETECTION IN GIS UNDER IMPULSE VOLTAGE BY USING PHOTOELECTRIC SENSORS

Zhong Ren*, Ming Dong, Ming Ren, Haibin Zhou, Lei Zheng
State Key Laboratory of Electrical Insulation for Power Equipment, Xi'an Jiao Tong University
28 West Road of Xianning, Xi'an, Shaanxi Province, P. R. China, 710049

Keywords: Gas insulated substation, Partial discharge, Photomultiplier tube, Impulse voltage, Spectrum

Abstract: In the past few years some facilities of gas insulated substation(GIS) still occurs failures even after passing partial discharge test under power frequency voltage according to the actual operational cases in China, more effective method is in urgent needs. For this reason, whether the PD takes place or not under more kinds of strict conditions has been treated as a new possible proposal, i.e., amplitude, waveform, frequency, etc. In this paper, the measurement and analysis of PD under impulse voltage in GIS is investigated, and some PD characteristic is also presented. Different artificial defect models are placed into a sealed tank filled with SF6, and a MARX generator is used to produce high-voltage impulse waveform. Since PD measurement based on pulse current method is incapable of receiving high frequency signal and preventing interference, a high sensitivity and good shielding performance of photomultiplier tubes is used to recognize the PD spectrum and optical pulses. Studies have shown that spectrums of partial discharge in GIS under oscillating impulse voltage distribute mainly from 350nm to 850nm, and are often influenced by the electrode spacing and voltage levels. Additionally, waves in time domain of the light pulse and electric pulse have a good synchronization; the time-frequency spectrum obtained by signal transformation could describe the frequency characteristics of optical pulse in detail.

I. INTRODUCTION

Due to the reliability and compactness of GIS, it has been widely used in power system. For various reasons in China, i.e., design, manufacture, transportation and installation, the failure rate of GIS is highest. Because the partial discharge is an important method for GIS, PD measurement has applicability as a diagnostic tool. But some facilities still occur failures even after passing PD test under power frequency voltage according to the actual operational cases in the past few years.

So far some studies in the world have showed that the streamer and leader discharges are more likely to appear in the needle-plate type defects in GIS when the defects are under the impulse voltage with short-wave head and the rapid oscillating voltage, [1,2,3]. The CIGRE organizations proved by experiments that it's more helpful for diagnosing some faults and defects i.e., surface defects, conducting particle defects, in GIS to conduct PD tests under impulse voltage than under power frequency voltage. However, the partial discharge pulse in GIS under impulse voltage of short wave head is extremely weak and influenced by electromagnetic interference, and the pulse current method is difficult to meet the measurement needs. As a non-electrical measuring method, the optical method can effectively suppress electromagnetic interference, provide strong evidences of the presence of partial discharge signal, and create a new thought to study partial discharge mechanism in depth. Recently, some scholars have been using high-sensitivity photomultiplier tube to analyse the partial discharge signals in GIS under impulse voltage and have got some conclusions [4,5,6].

This paper researches and analyses spectrums of partial discharge, time-frequency spectrums of optical pulses in GIS under impulse voltage by using a high sensitive and low noise photomultiplier tube. The waves in time domain of the light pulse and electric pulse are also compared.

II. MATERIALS AND METHODS

Figure 1 shows a comprehensive partial discharge measurement system based on optical and electrical sensors. In order to accurately observe the waveform of a single pulse of partial discharge signal, a Lecory64Mx-B oscilloscope, whose sampling rate is 10GS/s and bandwidth is 600MHz, was used. The PMT(photomultiplier tube) has a wavelength range from 185nm to 900nm, and its pulse response time is 2.2ns. The lower cut-off frequency and upper cut-off frequency of the Rogowski coil is respectively 60kHz and 140MHz. The Rogowski coil and PMT are placed in two metal shielding boxes to shield the interference of external electromagnetic signals.

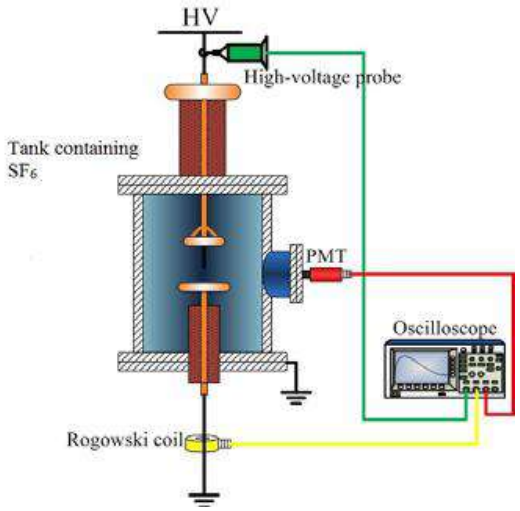

Figure 1. Partial discharge detection system of GIS defect model under impulse voltage

III. RESULTS AND DISCUSSION

(a) Spectrums of partial discharge in GIS under oscillating impulse voltage distribute mainly from 350nm to 850nm, but are influenced by many factors i.e., electrode spacing, voltage levels, defect type, etc.

(b) Results of experiments in this research show that waves in time domain of the light pulse and electric pulse have a good synchronization. However, characteristics of the light pulse and that of the electric pulse are different, which may be caused by differences between circuit structure of PMT and that of Rogowski coil.

*Zhong Ren, 28 West Road of Xianning, Xi'an, Shaanxi Province, P. R. China, 710049. E-mail: renzhong1989@yahoo.cn. Tel: 15829394990, (86-029)82668169

(c) The time-frequency spectrums of optical pulses obtained by signal transformation in this research accurately describe the frequency characteristics of optical signal of PD, reflect the signal changes in time-frequency plane, which provides references for pattern recognition of partial discharge in GIS.

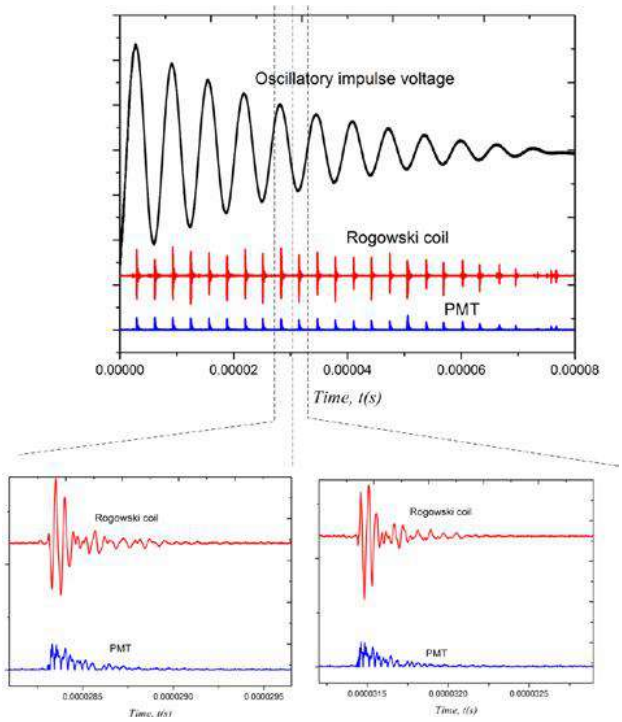

Figure 2. Partial discharge pulse waveform of rod-plane defect under oscillatory impulse voltage (Oscillatory frequency *f*=159 kHz, Applied voltage Um=48.59kV)

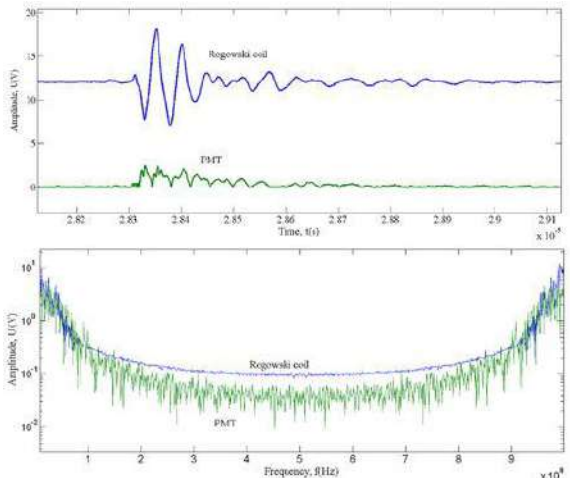

Figure 3. Frequency spectrum of partial discharge pulse of rod-plane defect under oscillatory impulse voltage

REFERENCES

[1] CIGRE Joint Working Group 33/23.12, Insulation coordination of GIS: Return of experience, on site tests and diagnostic techniques, ELECTRA, 176, pp. 67-97(1998)

[2] Silvio Stangherlin, Gerhard Salge and Friedrich Koenig. On the Discharge Phenomena in the Gas Mixture under Fast Oscillating impulse Conditions[C]. Conference Record of the 2002 IEEE International Symposium on Electrical Insulation, Boston, MA USA, 2002:417-420.

[3] S. Tenbohlen, D. Denissov and S. M. Hoek. Partial Discharge Measurement in the Ultra High[J]. IEEE Transactions on Dielectrics and Electrical Insulation. 2008, 15(6):1544-1552.

[4] N. Hayakawa and H. Okubo. Impulse Partial Discharge and Breakdown Characteristics of Rod-Plane Gaps in Gas Mixtures[J]. IEEE Transactions on Dielectrics and Electrical Insulation. 2005, 9(4):544-550.

[5] Toshiaki Ueda And Hitoshi Okubo. Impulse Partial Discharge Characteristics and Their Mechanisms under Non-uniform Electric Field in Gas Mixtures[J]. IEEE Transactions on Dielectrics and Electrical Insulation. 2005, 12(5):1035-1042.

[6] Xuefeng Zhao, Xiu Yao, Zhifeng Guo and Junhao Li. Characteristics and Development Mechanisms of Partial Discharge in SF6 Gas Under Impulse Voltages[J]. IEEE Transactions on Plasma Science. 2011, 39(2):668-674.

A030

MEASUREMENT OF 2-DIMENSIONAL ELECTRON DENSITY DISTRIBUTION IN EXTINGUISHING ATMOSPHERIC ARC USING SENSITIVE SHACK-HARTMANN TYPE LASER WAVEFRONT SENSOR

Yuki Inada*, Shigeyasu Matsuoka, Akiko Kumada, Hisatoshi Ikeda, Kunihiko Hidaka
Department of Electrical Engineering and Information Systems, The University of Tokyo, Japan
Mailing Adress: 3-1, Hongo, 7-chome Bunkyo-ku, Tokyo, Japan
E-mail: inada@hvg.t.u-tokyo.ac.jp
Phone: +81-3-5841-6725
Fax: +81-3-5841-8577

Keywords : Shack-Hartmann, laser wavefront sensor, electron density, arc discharge

Abstract: The measurement sensitivity of Shack-Hartmann type laser wavefront senor was improved by the implementation of microlens arrays with a long focal length of 238mm in order to measure 2-dimentional electron density distributions in an arc channel in an extinguishing phase. The sensitive sensor was applied to pulsed arcs in 3-mm air gap between rod-to-rod tungsten electrodes with a diameter of 1mm. Electron densities in the arc discharges with currents of several amperes were lower around the gap centre than near the anode and cathode.

I. INTRODUCTION

Optical measurement of 2-dimmentional electron density distributions in extinguishing arc channels is a promising method for developing highly reliable gas circuit breakers. However, arc discharges in an extinguishing phase do not always take the same discharge path. Moreover, the measurement sensitivity of standard optical system with potential of acquiring 2-dimmentional electron density distributions by only a single measurement is limited to relatively high electron densities above 10^{23}m^{-3}. Here, microlens arrays with a long focal length of 238mm were investigated and implemented to Shack-Hartmann type laser wavefront sensor to improve the measurement sensitivity by one order of magnitude. This paper describes electron density distributions over atmospheric arc channels in an extinguishing phase with low currents of several amperes. The experimental results obtained by a single measurement using a sensitive Shack-Hartmann sensor demonstrate the feasibility of fully understanding the unstable extinguishing process of atmospheric arcs.

II. RESULTS AND DISCUSSION

Figure 1. shows voltage and current waveforms of atmospheric arc discharges. The peak value and damping time constant of arc currents were 0.8kA and 25μs, respectively. The time when breakdowns occurred was defined as t=0s. Measuremnets of electron density distributionws were carried out at t=130μs. The arc current at t=130μs was below 10A.

Figure. 2 shows the overall electron density distributions at t=130μs. The order of electron densities over the arc channels ranged 10^{22} to 10^{23}m^{-3}. The minimum detectable electron density and measurement error of the sensor were 3×10^{23}m^{-3}and 2×10^{23}m^{-3}, respectively.

The electron densities in an extinguishing phase shown in Figure. 2 were lower around the gap centre than near the anode and cathode. The higher electron densities around the anode are thought to be due to contamination of metallic vapour from an anode. On the other hand, one of the most reasonable supports for higher electron densities around the cathode is the electron emission from the cathode due to the collision of positively charged ions.

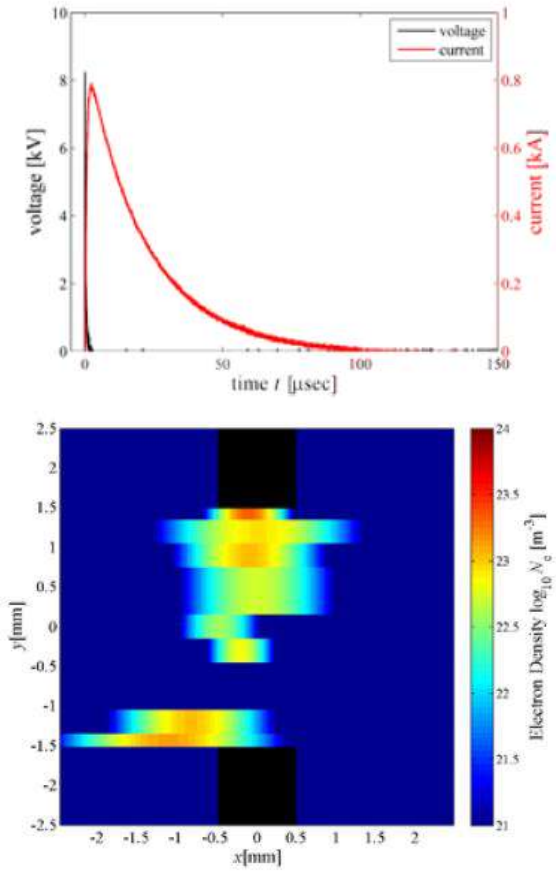

Figure 2. Overall electron density distribution at t=130μs

A031

OPTICAL MEASUREMENTS OF HIGH ELECTRIC FIELD STRENGTH IN A DIELECTRIC LIQUID WITH LARGE KERR CONSTANT

Hayato Nakao*, Masaharu Fujii, Haruo Ihori
Faculty of Engineering, Ehime University
3, Bunkyo-cho, Matsuyama, Ehime, 790-8577, Japan
Phone : +81-89-927-9893 , FAX : +81-89-927-9893
otayah501@gmail.com

Keywords: Kerr effect, Electric field distribution, Dielectric liquid

In order to measure electric field strength, Kerr electrooptical method is very usful. The phase retardation due to Kerr effect is generally measured as the chage of a light intensity by an optical system with optical wedges. Therefore, since the change of the light intensity changes priodically to a given field strength, there are some cases that the field strength can not decieded in a relatively large kerr constant.

We have investigated the measurement of electric field vector distributions in liquids by Kerr optical method. Recently, time series analysis of the electric field distribution was carried out. Then, in some cases, the strength was larger or smaller than a static value caluclated from an electrode system and an applied volatage. therefore, in orde to carried out experiments under various experimental conditions, it is neccesary to develop a system for measurement of more larger strength. So, we studied about the measurement of the high electric field strength.

A-system shown in Fig. 1 was our ordinary measurement system for the measuremenr of the electric field strength. Figure 2 shows theoretically the change of the light intensity corresponding to the field strength for A-system. As a sample liquid, Propylene carbonate (C4H6O3, Kerr constant was about 1*10-12 m/V2) was used. If, for example, the ratio was -0.4, the electric field strength is either 15 kV/cm or 22 kV/cm but it cannot be decided. The optical system called B-system, which consisted of only a polarizer and an analyzer, was added to A-system, as shown in fig.1. The ratio of light intensity obtained by B-system was shown in Fig.3. The ratio obtained by B-system changes very little when the electric field strength was less than 10kV/cm. For more than 10kV/cm, the ratio increased linearly with the field strength.

Consequently, from the ratio measured by A-system and B-system, the electric field strength was decided by the following procedure.

If the ratio obtained by A-system was negative value, the electric field strength was less than about 27kV/cm. And if the electric field strength calculated from the ratio by B-system was more than 15kv/cm, it was the measurement value. If the electric field strength by B-system was less than 15kv/cm, the field strength measured by A-system was the measurement value. If the ratio obtained by A-system was positive, the decision of the electric field strength would require to carrying out further case analysis.

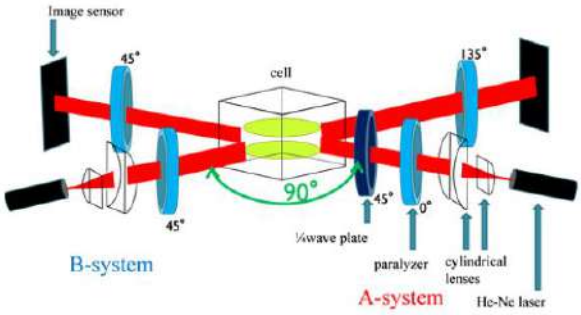

Figure 1. Optical system for measurement of high electric field strength

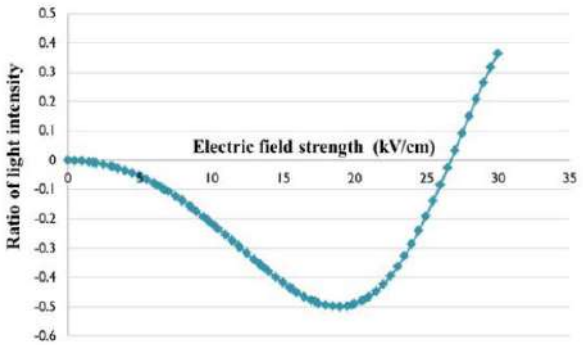

Figure 2. Ratio of light intensity obtained by A-system

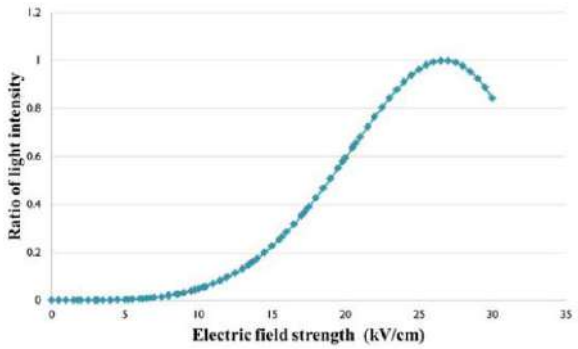

Figure 3. Ratio of light intensity obtained by B-system

A032

THE PROPAGATION SPEED OF LOW PRESSURE DISCHARGE WITH SPECIAL ATTENTION TO BLUE JETS AND SPRITES

Mahbubur Rahman and Vernon Cooray
The Ångström Laboratory, Division for Electricity, Department of Engineering Sciences, Uppsala University, Box 534, SE-752 21 Uppsala, Sweden
E-mail: Mahbubur.Rahman@angstrom.uu.se

Abstract: After the first recording of luminous phenomena above cloud tops, obtained in 1989 by Franz et al. [1], the low-luminosity transient optical phenomena is classified into three general types and they are: red sprites, blue starters and blue jets, elves. They all take place in the region between the cloud tops and the lower ionosphere. To understand these phenomena it is important to find out their speed of propagation. In 1995 Wescott et al. [2] reported a newly documented type of optical emission, so called "Blue jets", that appear to propagate upwards from the tops of thunderstorms at speeds of about 100 km/s. Later in 1996 Wescott et al. [3] reported a new stratospheric phenomenon associated with thunderstorms, which they have called "blue starters" and they found that the velocity of blue starters varies from 27 km/s up to 218 km/s. Stanley et al. [4] found that the initial development of sprites appears to be dominated by corona streamers with velocities in excess of 107 m/s.

In this paper the propagation speed of a laboratory discharge at low pressure is reported. The experiment was conducted at pressures ranging from 120 torr down to 10 torr, which correspond to an altitude from about 18 km up to 33 km above earth surface. This region is where blue jets and the lower part of the red sprites have been observed. The discharge was produced by applying a pulse voltage to a small electrode at one end of a long tube that contained unionized air at low pressures. The discharge tube consists of two metal electrodes placed 365 mm apart in a glass tube of 40 mm diameter. Total length of the tube is 650 mm. The glass tube is capable of sustaining a pressure of at least 3·10-2 mbar. The electrodes were 16 mm thick, and of 40 mm diameter with 6 mm diameter holes in the center. By recording the optical emission generated by the discharge the propagation speed was calculated.

A cable generator is used to produce an impulse voltage that is applied to the electrodes in the discharge tube, by means of a mechanical switchbox. The switchbox is made of copper with a large copper plane attached to it. The copper plane is attached to the grounded table at which the experiment is performed. The cable generator consists of a Hipotronics high voltage DC power supply (max 50 kV), connected through a 500 MΩ resistance to a 60 m long RG-8 coaxial cable with 50 Ω characteristic impedance. The coaxial cable is charged to the desired voltage in a certain time determined by the time constant of the circuit, with C=100 pF/m for the RG-8 cable and R=500 MΩ for the charging resistor. By manually triggering the mechanical switch in an isolated switchbox, the cable is discharged. The output from the cable is an impulse,mwhich looks different depending on the load to which it is discharged. In the case of a matched load, the output will be a square impulse. In the case of a mismatched load, multiple reflections will take place, slowly decreasing the output to zero [5]. A typical output with rise time 170 μs and 1300 μs duration is shown in Figure 1. The cable was terminated with 500 MΩ resistances at the end. A vacuum pump is used to create low pressure in the tube, monitored by a Balzers manometer. Two optical fibers connected to photomultipliers are placed near the anode and cathode, detecting light from the discharge. At the cathode, a Pearson current probe model 2878 with 5 ns rise time, max 400 A, measures the cathode current. The applied voltage pulse is measured using a Tektronix P6015A high voltage probe with 75 MHz bandwidth, 100MΩ impedance, 1000x attenuation and 40 Kv impulse maximum, at the anode. A four-channel LeCroy LC574AL oscilloscope (max 1GS/s) powered by a UPS, placed in a grounded metal cabinet, records current, voltage and light signals simultaneously. The signal cables from voltage and current probes have been covered with an extra grounded shield to minimize noise. Voltage, current and optical signal cables are connected to the cabinet via contacts.

In experiments at higher pressure range the cable generator and the switch box were replaced by Marx generator and a standard lightning impulse voltage with 1.2 μs rise time and a 50 μs decay time was applied. Once the experimental set-up is assembled, the operation is fairly straightforward. The vacuum-pump is used to create a stable desired pressure. The oscilloscope is set to simultaneously record current and light signals. The channel recording light from the fiber at the anode is set as trigger. Appropriate trigger level was chosen to -60 mV or -100 mV (Marx generator case). Time window was set to 100 μs or 500 μs (Marx generator case), at a sampling rate of 1 GS/s. Immediately after discharging the generators visible optical emission appears in the tube. At very low voltages in some experiments there were no visual light for human eyes but the optical fiber could detect signal. During the experiments, the room temperature varied between 17 to 22^{0}C and the relative humidity varied between 17 to 44%.

Figure 2 shows the optical signals measured at anode (blue signal) and at cathode (red signal). The result show that the propagation speed depends on applied voltage and pressure. Table 1 shows result from the experiments conducted with lightning impulse voltage. The speed gets faster for higher applied voltage. It also increases almost linearly with decreasing pressure. The preliminary results also show that discharges with low-luminosity have an average speed of about 3·106 m/s. This speed for prebreakdown optical phenomena exceeds more than 1·107 m/s for faster applied impulses with higher applied voltage. The result found here agrees with a similar study by Winn [6].

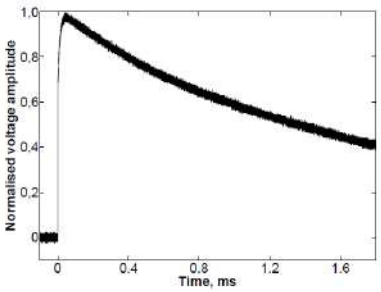

Figure 1. The applied impulse voltage.

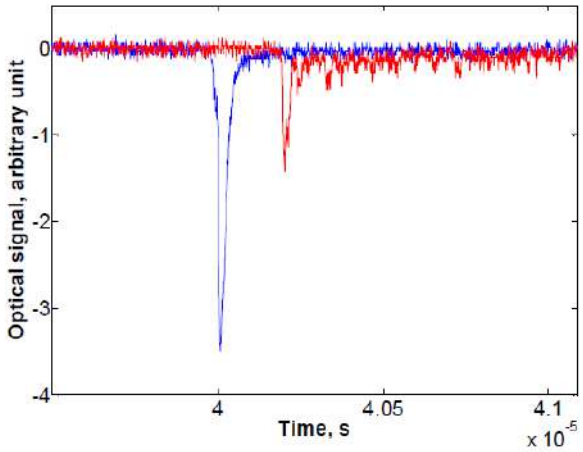

Figure 2. The measured optical signals, blue at anode and red at cathode.

Table 1. Estimated propagation speed under different pressures. Standard lightning impulse was applied with amplitudes 180 kV and 300 kV

Nr.	Pressure, torr	Estimated speed, m/s for 180 kV	Estimated speed, m/s for 300 kV
1	120	$12 \cdot 10^6$	$17 \cdot 10^6$
2	100	$17 \cdot 10^6$	$19 \cdot 10^6$
3	80	$18 \cdot 10^6$	$22 \cdot 10^6$
4	60	$20 \cdot 10^6$	$25 \cdot 10^6$
5	40	$30 \cdot 10^6$	$33 \cdot 10^6$

REFERENCES

[1] R. C. Franz, R. J. Nemzek, J. R. Winckler, “Television image of a large upward electrical discharge above a thunderstorm system”, Science, Vol. 249, pp. 48-51, July 1990.

[2] E. M. Wescott, D. D. Sentman, D. L. Osborne, D. L. Hampton, M. J. Heavner, “Preliminary results from the Sprites94 aircraft campaign 2, Blue jets”, Geophysical Research Letter, Vol. 22, No. 10, pp. 1209-1212, May 1995.

[3] E. M. Wescott, D. D. Sentman, M. J. Heavner, D. L. Hampton, D. L. Osborne, and O. H. Vaughan, “Blue starters: brief upward discharges from an intense Arkansas thunderstorm”, Geophysical Research Letter, Vol. 23, No. 16, pp. 2153-2156, August 1996.

[4] M. Stanley, P. Krehbiel, M. Brook, C. Moore, W. Rison, and B. Abrahams, “High speed video of initial sprite development”, Geophysical Research Letter, Vol. 26, No. 20, pp. 3201-3204, October 1999.

[5] L. Liljestrand, V. Scuka, “A 200 kV cable generator with nanoseconds rise time”, UURIE 191:86, Uppsala university, Sweden.

[6] W. P. Winn, “A laboratory analog to the dart leader and return stroke of lightning”, Journal of Geophysical Research, Vol. 70, No. 14, pp. 3265-3270, July 1965.

A033

STREAMER-TO-LEADER TRANSITION ACROSS SURFACE/GASEOUS GAP IN SF_6/N_2 GAS MIXTURE

Hiroshi Moriyama*, Shigeyasu Matsuoka, Akiko Kumada, Kunihiko Hidaka
Department of Electrical Engineering and Information Systems, The University of Tokyo, Japan
Mailing Adress: 3-1, Hongo, 7-chome Bunkyo-ku, Tokyo, Japan
moriyama@hvg.t.u-tokyo.ac.jp

Keywords: surface discharge, streamer-to-leader transition, SF6/N2 gas mixture, precursor model, high time-resolved measurement, pockels effect

Abstract: This study shows the experimental analysis of streamer-to-leader transition in SF6/N2 gas mixture. The streamer to leader transition process were observed with a streak camera and a framing camera. In the gas mixture, a 'leader precursor' was clearly observed in the transition from a streamer to leader. The transient change in the potential distribution along a surface leader propagating in the gas mixture was also measured with a pockels measuring system. The electric field and charge distributions were calculated from the measured potential profile. The electric field and charge distributions were compared with ICCD images. These results indicate that streamer-to-leader transition can be explained by the precursor model.

I. INTRODUCTION

Surface discharge on a dielectric material has a great influence on the insulating performance of electrical apparatuses and electronic devices. The phenomena of leader inception and propagation have been studied extensively. Precursor and stem models have been proposed to explain the leader transition process in gaseous gaps, but there still remains many things to be clarified for quantitative discussion.

This paper describes the experimental analysis of streamer-to-leader transition of positive discharge in SF6/N2 gas mixture with high time resolution. The streamer to leader transition process were observed with a streak camera and a framing camera (Specialized Imaging : SIM) .

II. RESULTS AND DISCUSSION

Figure 1 shows streamer-to-leader transition in SF6/N2 gas mixture taken with a streak camera and a digital camera. A pin-to-plate electrode was installed in a chamber filled with SF6/N2 gas mixture, whose mixture ratio was 1 to 4. The impulse voltage of 94 kV was applied. Figure 1(a) is a picture of overview image by a dijital camera. Figure 1(b) is its streak images (sweep speed is 1.46μs/9.2mm). In Figure 1 (b), streamer occured around at t = 150 ns, and light-emitting chanel corresponding "precursor" occurred at t = 600 ns, and then leader occurred at t = 1.2 μs.

A surface discharge in SF6/N2 gas mixture was also observed. A chamber was filled with SF6/N2 gas mixture, whose mixture ratio was 1 to 4. The impulse voltage of 15 kV was applied. Figure 2(a) shows a voltage waveform, current waveform and capturing timing of a framing camera. Figure 2(b) shows framing images of streamer to leader transition taken by a ultra-high-speed camera (Specialized Imaging : SIM). A streamer propagated radially from the electrode (Frame 1), and two weak light-emitting channels corresponding precursors appeared in the streamer (Frame 2 and 3), and then subsequent streamers were formed at the tips of right emitting chanel (Frame 4), respectively. These results indicate that streamer-to-leader transition can be explained by precursor model.

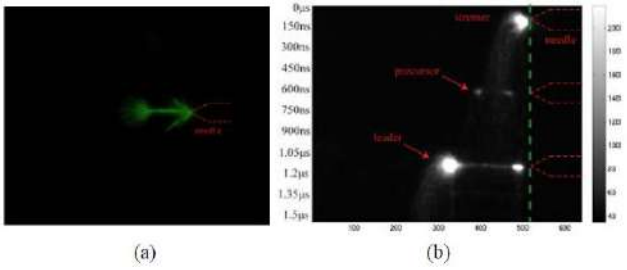

Figure 1. Gas discharge in SF6/N2 gas mixture
(a) Digital camera image (b) Streak camera image

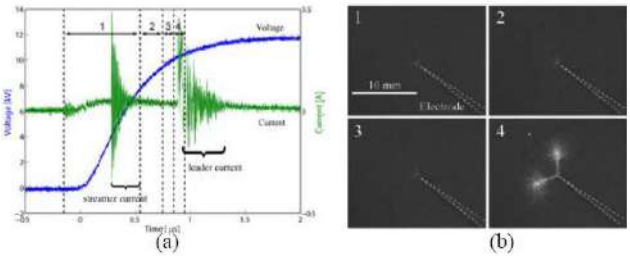

Figure 2. Surface discharge in SF6/N2 gas mixture
(a) Voltage waveform, current waveform and capturing timing (1: 700 ns, 2: 200 ns, 3: 100 ns, 4:100 ns) (b) SIM pictures

REFERENCES

[1] Gallimberti and N. Wiegart, "Streamer and leader formation in SF6 and SF6 mixtures under positive impulse conditions : II. Streamer to leader transition ", J. Phys. D: Appl. Phys.19,pp.2363-2379, 1986.

*Hiroshi Moriyama Department of Electrical Engineering, The University of Tokyo 7-3-1 Hongo, Bunkyo-ku, Tokyo, 113-8656 JAPAN TEL: 81-3-5841-6759; FAX: 81-3-5841-6725 Email: moriyama@hvg.t.u-tokyo.ac.jp

A034

PROPAGATION CHARACTERISTICS OF SURFACE DISCHARGE UNDER POSITIVE IMPULSE APPLICATION VOLTAGE

Junbo Deng[1], Shigeyasu Matsuoka[2] , Akiko Kumada [2] , Kunihiko Hidaka[2] , Haibao Mu[1], Guanjun Zhang[1]
([1]. State Key Laboratory of Electrical Insulation and Power Equipment, Xi'an Jiaotong University, Xi'an, 710049; [2]. The University of Tokyo, Tokyo, Japan, 113-8586)

I. INTRODUCTION

Flashover on insulator surface in the air at atmospheric pressure occurs as a sequence of several processes that leads to the formation of a plasma channel which bridges the electrode gap. The main stages of the flashover are the occurrence of initial seeding electrons, the development of electron avalanches, the inception and the propagation of streamers, the streamer-to-leader transition, the propagation of leader, and the formation of a breakdown[1, 2]. The streamer-to-leader transition is a very critical stage of such a breakdown since the leader can propagate a long distance with a low increment of application voltage. The streamer-to-leader transition and the propagation process of a leader are still the object of intensive experimental and theoretical studies[3-6].

In this paper, Potential distribution of residual charge under different positive impulse application voltage are investigated.

II. EXPERIMENTAL SETUP

The investigations are performed in a cylindrical insulator configuration in atmospheric air. The Schematic of experimental setups are shown in Figs. 1. One of the pair of ring electrodes is grounded and a positive 1.2/50μs standard lightning impulse voltage is applied to the other ring electrode so that a surface discharge occurs and propagates on the insulator surface.

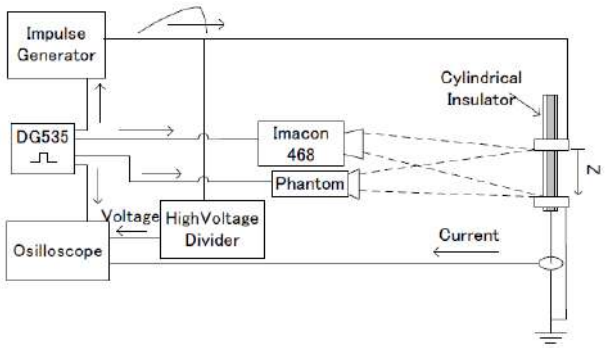

Figure 1. Experimental setup.

III. RESULTS AND DISCUSSION

Residual charge distributions of surface discharge under the application of positive impulse voltages are measured by the measuring system developed by the authors, and the potential distribution are calculated. The potential distributions of surface discharges under 12.5 kV, 13.5 kV, 14.5 kV, and 16 kV positive impulse application voltage are respectively measured.

Under the application of 12.5 kV impulse voltage, a lot of blush-like streamer discharges propagate in parallel from the high voltage electrode. When 13.5kV is applied, an arborescent discharge, which corresponds to a leader discharge, propagates towards the grounded electrode through the streamer region. The stem of such discharge is regarded as the leader part and the filamentary discharge ahead of the leader is regarded as the streamer part.

With the increase of the application voltage, more leader discharge occurs and develops for a longer distance. In the suburb of the high voltage electrode, some residual charge has disappeared due to the back discharge which occurred at the tail part of the impulse voltage.

Potential profiles along surface discharges are extracted from the measured potential distribution. The potential in the brush-like streamer decreases almost linearly with the distance from the electrode and its gradient is 0.6 kV/mm. It is found that the potential and charge density profiles along a leader discharge can be divided into two parts: leader parts and streamer parts. The potential gradient in the streamer part increases with the application voltage and its value is from 1.0 to 1.2 kV/mm. In the leader part, it is from 0.15 kV/mm to 0.20 kV/mm and decrease with the application voltage. The dividing point of the leader and streamer is about 6 - 8 kV, which corresponds to 400 - 600 pC/mm^2. The dividing point increases with the application voltage.

IV. CONSLUSION

In this paper, the propagation characteristics of surface discharge under impulse application voltage are studied.
Potential distributions under different application voltage are measured. With the increase of application voltage, the discharge changed from streamer discharge into leader discharge It is found that in the channel of the leader, the electrical field is very low and the conductivity is very high. At the periphery of the streamer zone, the electrical field is very high.

REFERENCE

[1] L. Niemeyer and F. Pinnekamp. *J.Phys. D: Appl. Phys.*, Vol. 16, pp. 1031-1045, 1983.
[2] L. Niemeyer, L. Ullrich and N. Wiegart. IEEE Trans. On Electrical Insulation, Vol. 24, pp. 309-324, 1989.
[3] Q. Zhang, L. Yang, Q. Chen, M Hara and Y. Qiu. *J.Phys. D: Appl. Phys.*, Vol. 36, pp. 1212-1216, 2003.
[4] O. Yamamoto, T. Hara and T. Takuma. *J.Phys. D: Appl. Phys.*, Vol. 31, pp. 2997-3003, 1998.
[5] Y. Qiu, W. Gu, Q. Zhang and E. Kuffel. *J.Phys. D: Appl. Phys.*, Vol. 31, pp. 3252-3254,1998.
[6] A. Kupershtokh, V. Charalambakos, D. Agoris and D. Karpov. *J.Phys. D: Appl. Phys.*, Vol. 34, pp. 936-946, 2001.

A035

PEARL-CHAIN-TYPE TREE IN SILICONE RUBBER GEL UNDER AC VOLTAGE

Masaharu Fujii*, Haruo Ihori, and Hyeon-Gu Jeon
Graduate School of Engineering, Ehime University
3 Bunkyo, Matsuyama, Ehime 790-8577, Japan

Keywords: tree, breakdown, silicone rubber, gel, pearl-chain-type tree

Abstract: Trees have been observed in two-dimensional specimen of silocone rubber/gel under AC voltage. Under certain conditions of gel, tree has been developing with bubble-like and string-like pattern alternatively. This tree is called pearl-chain-like tree. At first the tree developed like bubble and then a projection arosed like cone on the surface. After some growth, the tip of the cone expanded and formed bubble. This process was repeated and the branching started when the two cones formed on the surface on the bubble. The shape of three is like perl-chain.

I. INTRODUCTION

Development of electrical trees has been oberved to investgate the mechanism of the tree under various appledf voltages. When the silicone rubber gell was used as specimen, it is easy to observe the development of the tree because the growth speed is vely slow inder AC voltage. The stages of the development has been classifed into three ones:(1)Linear tree at 1st stage, (2) The branches ioslated at 2nd stage, and (3) the development of selected branches at 3rd stage. The various type of tree has been observed by changing the fabirication conditions of silicone rubber; tree with no branch, spherical and buble one.

In this paper, the tree developed through different type of silicone rubber/gel has been investigated. The perl-chain-like tree has been observed/ the tree consited of a series of two parts; bubble and string one.

II. MATERIALS

Sewing needles were used as electrode. One was a needle electrode for high field and another was counter electrode. The gap length between the electrodes was 1 or 2mm. Silicone rubber (Shin-Etsu Chemical Co., Ltd. KE-1935A(base body) and B(cross-linking agent).) was used as specimen. Degassed silicone rubber was poured into the space between two slide glasses, and was heated for 4 hours at 80 degrees C. Silicone rubber gel was fabricated by changing the ratio of KE-1935A and B. Figure 1 shows two-dimensional composite specimen of silicone rubber that consits of two layers.

III. RESULTS AND DISCUSSION

Figure 2 shows The tree through the twolayers of silocone rubber(5;1)/gel(6;1). The tree started as conventional tree from the tip of the needle electrode in the rubber(1;1). In the gel(6;1) tree developed with bubble-like and string-like pattern alternatively as perl-chain in gel(6;1). At first the string-like tree from the bubble devolped as Taylor cone in electrospinning system. After some growth, the tip of the cone expanded and formed bubble. The tree had the branches. The branching started from the surface of the bubble part. This phenomena is very important to consider the model of tree development.

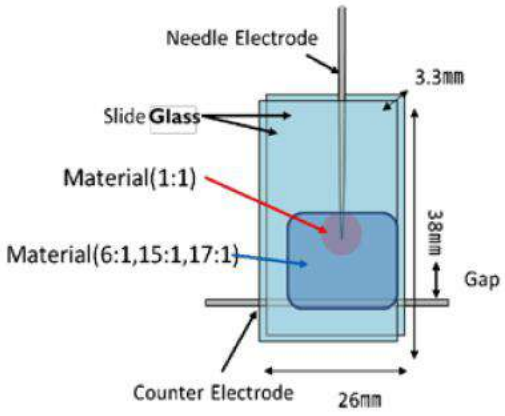

Figure 1. Composite specimen of silicone rubber/gel

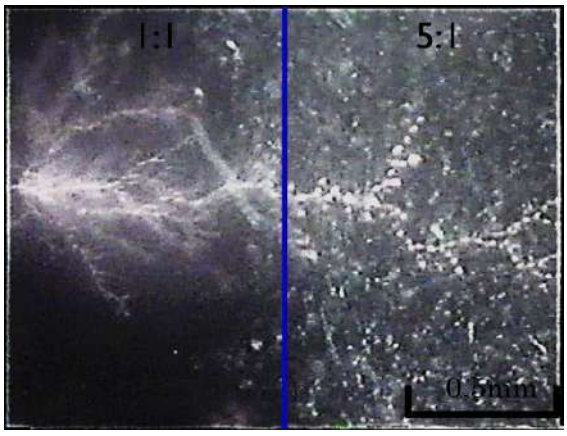

Figure 2. Tree through two layrs.
Conventional tree in left-side medium(1:1) and perk-chain-like one in (5:1)

M.Fujii, Graduate School of Engineering, Ehime University, 3 Bunkyo, Matsuyama, Ehime 790-8577, Japan, fujii.masaharu.my@ehime-u.ac.jp Tel : +81-89-927-9892 Fax: +81-89-927-9907

A037

STUDY OF POLLUTION PERFORMANCE ON A WIND TURBINE BLADE USING OES TECHNIQUE FOR LIGHTNING AND SWITCHING IMPULSE VOLTAGE PROFILES

V. Sathiesh Kumar*[1], Nilesh J. Vasa[1], R. Sarathi[2]
[1]Department of Engineering Design, Indian Institute of Technology Madras, Chennai 600036, India
[2]Department of Electrical Engineering, Indian Institute of Technology Madras, Chennai 600036, India

Keywords: wind turbine blade, lightning impulse, switching impulse, surface discharge, pollutant.

Abstract: Lightning damage to offshore wind turbine power plant requires an immediate action in order to avoid it from a stoppage for a long period. For blades placed in humid or polluted environment, the risk of lightning striking the blade is expected to be higher. The pollutant (Salt) which is transported through air gets deposited on the blade surface thereby reducing the dielectric breakdown strength of material. Wave profile and polarity also has an effect during discharge because of unique discharge formation process. In this paper, preliminary experiments at laboratory level were conducted to study the effect of pollutant deposited on a blade sample by adopting IEC 60507 standards. Experimental results clearly shows the increase in deterioration of sample surface with increase in salt concenteration.

I. INTRODUCTION

In recent years, there is an increasing use of wind turbines around the world, with an output power growth in rating from 30 kW up to 5 MW. Wind turbines are of large size, distinct shape, open air structures placed in often isolated, mountain regions or near coastal areas due to strong wind flow means that they are extremely vulnerable to lightning strikes [1]. Lightning can be classified into summer and winter lightning. These two forms can be further subdivided into positive and negative polarity respectively, the polarity being that of the charge transferred from the cloud to the ground. Winter lightning current has a much longer front time and tail time when compared to the summer lightning [2]. In off-shore wind power plants, most of the time the blades are subjected to moisture. Also soluble and non-soluble contaminations such as dust, sand and salt gets deposited on the blade surface. The deposited contaminants on the surface of blade form a conducting layer, thereby reducing the dielectric strength of the blade [3-5]. Lightning might break through the blade material. Hence it is necessary to study the effect of pollutant (NaCl) on a Glass fiber reinforced plastic (Basic material used in manufacturing of wind turbine blades) under the application of lightning impulse voltage (1.2 µs / 50 µs) and switching impulse voltage (250 µs / 2500 µs) of positive and negative polarity by adopting IEC 60507 standards.

II. EXPERIMENTAL SETUP

Generated impulse voltage (Lightning/Switching) was applied to two aluminium electrodes in which tip is cut for 45° (with edges smooth) placed on the sample as shown in Fig. 1. The distance between the two electrodes is fixed to 10 mm. The size of the Glass fiber reinforced plastic (GFRP) samples used in the experimental studies are of 6 cm x 6 cm. Mixture of kaolin clay and salt were deposited on the GFRP sample with its salt deposition density (SDD) ranging from 1 to 11 mg/cm2. For a particular applied voltage, surface discharge occurs on the sample and in addition to that optical emission can also be seen. The light which is emitted during surface discharge on sample is collected using a multi-mode fiber (low OH multimode fiber, 600 µm core diameter, 0.32 NA) and it is fed into a monochromator (190 mm,Carl Zeiss) with an NMOS linear image sensor (S3901 Hamamatsu). To perform neutral sodium atom (D-II line, 588.99 nm) emission life time studies, focused light during surface discharge is coupled using a multimode optical fiber to a sodium filter (≈ 589 nm) and photomultiplier tube (R562, Hamamatsu). Simultaneously flashover voltage and discharge current were measured using a voltage probe (Lecroy, EP-50k, 1000:1) and a current probe (ETS Lindgren: Model 94111-1).

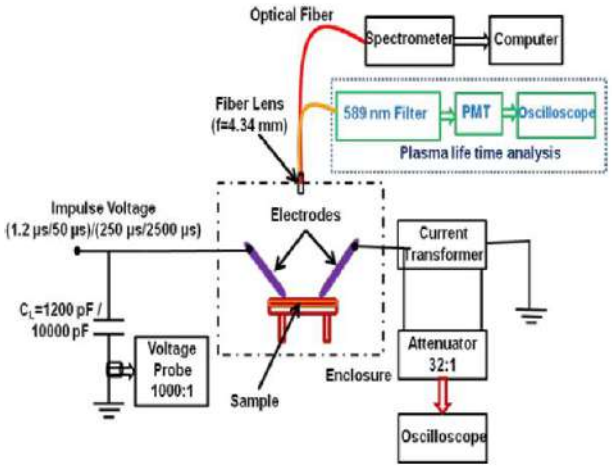

Figure 1. Optical Emission Spectroscopy Technique

III. RESULTS AND DISCUSSION

Flashover voltage reduces with increase in salt deposition densities irrespective of wave profile and polarity. Discharge current increases with increase in salt deposition densities since the electrical conductivity of layer increases with increase in salt concentration. During the initiation of the surface discharge process, the applied voltage collapses and forms a ringing pattern which leads to the ringing nature of the discharge current profile.

Figure. 2 shows the optical emission spectra of GFRP, Kaolin clay deposited on GFRP, Samples with SDD of 3 and 11 mg/cm2. The characteristic peak, obtained in spectra of samples is in agreement with the NIST database [6]. Samples with different salt deposition densities show a significant peak at 588.99 nm which relate to a neutral sodium atom (Na I) but chlorine peaks were not observed. With increase in SDD, the optical emission spectra of GFRP (underneath substrate) itself is observed representing surface damage leading to carbonization.

*V. Sathiesh Kumar, Department of Engineering Design, IIT Madras, Chennai 600036, India. E-mail: sathiieesh@gmail.com Contact No: +91 9444721638, +91-44-22574730

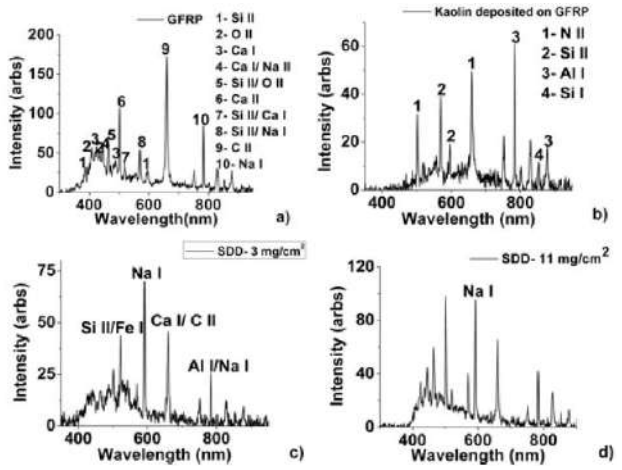

Figure 2. Optical Emission Spectra on different samples during positive lightning impulse surface discharge: a) GFRP. b) Kaolin clay deposited on GFRP. c) SDD= 3 mg/cm2. d) SDD= 11 mg/cm2.

The life time of neutral sodium (Na I) at 588.99 nm was estimated at 20% of the maximum emission intensity for lightning and switching impulse voltage profile and are listed in Table 1. Lifetime profile of Na I is similar to that of discharge current profile as shown in Fig. 3. Experimental results based on optical emission spectroscopy studies qualitatively is in agreement with the electrical discharge measurements.

TABLE 1. Lifetime of Na I emission line at 589 nm

WAVE PROFILE	LIFETIME (μS)
Lightning Impulse Voltage (1.2 μs/50 μs)	0.8-5.8
Switching Impulse Voltage (250 μs/2500 μs)	4-18

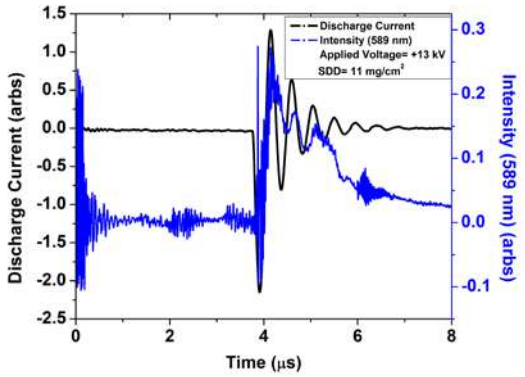

Figure 3. Lifetime profile of Na I (589 nm) for positive lightning impulse voltage.

IV. SUMMARY

An influence of pollutant (NaCl) on a glass fiber reinforced plastic, which is used in in manufacturing of wind turbine blades, under the application of lightning impulse voltage (1.2 μs / 50 μs) and switching impulse voltage (250 μs / 2500 μs) of positive and negative polarity is investigated using the optical emission spectroscopy technique. Samples with different salt deposition densities (SDD) show a significant peak at 588.99 nm corresponding to Na I. With increase in the SDD, the optical emission spectra of GFRP (underneath substrate) itself is observed representing surface damage leading to carbonization. This study also indicates it is essential to develop a technique, such as laser assisted remote sensing technique to measure the salt deposition density on wind turbine blades.

REFERENCES

[1] IEC TR 61400-24, “Wind turbine generator systems- Part 24: Lightning protection”, 2002.

[2] S. Sekioka, K. Yamamoto, M. Minowa and S. Yokoyama, ``Damages in Japanese Wind Turbine Generator Systems due to Winter Lightning", IX International Symposium on Lightning Protection, 2007.

[3] M. A. Douar, A. Mekhaldi and M. C. Bouzidi, ``Flashover Process and Frequency Analysis of the Leakage Current on Insulator Model under Non-Uniform Pollution Conditions", IEEE Transactions on Dielectrics and Electrical Insulation, Vol. 17, pp. 1284-1297, 2010.

[4] N. J. Vasa, T. Naka, S. Yokoyama, A. Wada and A. Asakawa, ``Experimental Study on Lightning Attachment Manner Considering Various Types of Lightning Protection Measures on Wind Turbine Blades", Proceedings on International Conference on Lightning Protection, 2006.

[5] T. Naka, N. J. Vasa, S. Yokoyama, A. Wada, A. Asakawa, H. Honda, K. Tsutsumi, S. Arinaga, "Study on Lightning Protection Methods for Wind Turbine Blades", IEEJ Transactions of Power Engineering, Vol. 125, pp. 993 -998, 2005.

[6] NIST Handbook of Basic Atomic Spectroscopic Data (http://physics.nist.gov/PhysRefData/Handbook/index.html).

A038

BREAKDOWN STRENGTH CHARACTERISTIC OF RBDPO AND MINERAL OIL MIXTURE AS AN ALTERNATIVE INSULATING LIQUID FOR TRANSFORMER

Yusnida M. Y, M Kamarol*, Shahid Iqbal
Universiti Sains Malaysia**,** 14300
Nibong Tebal, Pulau Pinang, Malaysia
yusnida_tiq@yahoo.com
eekamarol@eng.usm.my

Keywords: Refined Bleached Deodorized Palm Oil, Mineral Oil, Breakdown Strength

Abstract: Mineral oil (MO) works as an important electrical insulation and coolant in transformer which is non-biodegradable and nearly running out. Therefore, for sustainable and environmental concern, an alternative biodegradable insulating oil that potential to replace the mineral oil is introduced. In view of that, the breakdown strength properties of Refined Bleached Deodorized Palm Oil (RBDPO) and MO mixtures were investigated by varying the mixing percentage of RBDPO from 0% to100% at 40oC. The result shows that the breakdown strength of the oil mixture abruptly decline at 10% of RBDPO mixture and slightly increased when the ratio of the RBDPO is added. The highest breakdown strength achieve at 80% of RBDPO content.

I. INTRODUCTION

Petroleum based mineral oil (MO) is widely used in electrical power transformers for electrical insulation and cooling purposes. However, the MO is a poorly biodegradable oil. If leak occurs, the petroleum based MO can spill out of the transformer tank and contaminate soil andwaterways Furthermore, petroleum based MO are eventually going to run out in the feature. Thus the replacement of the MO should be considered [1].

One of the potential oil is vegatable oil. Tha vegetable oil is recognized readily biodegradable oil and environmentally friendly. Researchers are trying to replace the vegetable oil as insulating and cooling liquid in the transformer.

The extensive research into the use of vegetable oil as an alternative transformer oil has been carried out by many researchers [1,2,3]. Refined, Bleached and Deodorized Palm Oil (RBDPO) is one of the vegetable oil that has good potential to be used in electric power transformer as insulating oil. Although the dielectric properties of the RBDPO has been carried out, there is also important and meaningful to know the electrical characteristic of the mixture of this oil with MO. Thus, this paper presented the investigation of breakdown characterictic of RBDPO and MO mixture at 40˚C.

II. EXPERIMENTAL SETUP

RBDPO were mixed into MO with the ratio 0% to 100%. The breakdown voltage test was conducted by BA100 Breakdown Analyzer. The test was performed according to IEC 60156 standards. The test cell has a volume capacity of 400 ml consists of mushroom electrodes with the gap of 2.5 mm. The specimens were heated on a hot plate and stirred at 250-300rpm until the temperature reach 40oC. The AC voltage with frequency of 50Hz was applied automatically with increasing rate of 2kVs-1 until breakdown occurs. The breakdown voltage is taken in average of six measurements with 2 minutes pause between consecutive breakdowns.

III. RESULTS AND DISCUSSION

Figure 1 shows the results of breakdown voltage as a function of the mixture percentage of RBDPO. The breakdown voltage abruptly decreases when the MO is mixed with 10% of RBDPO. It is slightly increased with the increasing percentage of the RBDPO mixture. The highest breakdown voltage achieve at 80% of RBDPO which is higher compared to 100% MO. The breakdown voltage of the oil mixture was above 30kV which fulfilled the IEC standard. and break the bond of oil into glycerol and free fatty acid [5, 6].

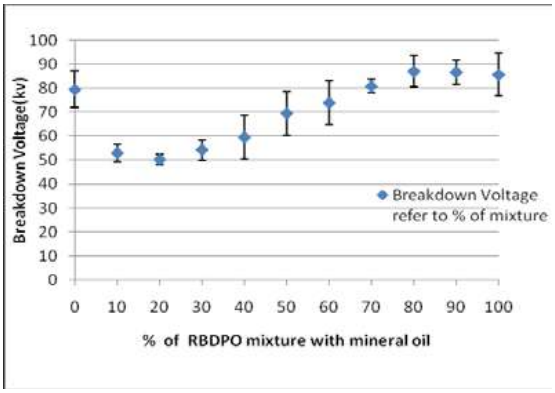

Figure 1. Dependence of breakdown voltage on RBDPO content

REFERENCES

[1] T. V. Oommen, "Vegetable oils for liquid-filled transformers," *Electrical Insulation Magazine, IEEE*, vol. 18, pp. 6-11, 2002.
[2] B. Sm, Y. Robia, and N. Amir, "Use of natural vegetable oils as alternative dielectric transformer coolants," *The Journal*, 2006.
[3] S. Aditama, "Dielectric properties of palm oils as liquid insulating materials: effects of fat content," 2005, pp. 91-94 Vol. 1.
[4] A. Rajab and S. Aminuddin, "Properties of RBDPO Oleum as a candidate of palm based-transformer insulating liquid," 2009, pp. 548-552.
[5] M. Kamarol, M. Zulhilmey, and Y. A. Arief, "Breakdown characteristics of RBDPO and soybean oil mixture for transformer application," pp. 219-222.
[6] T. Kanoh, H. Iwabuchi, Y. Hoshida, J. Yamada, T. Hikosaka, A. Yamazaki, Y. Hatta, and H. Koide, "Analyses of electro-chemical characteristics of Palm Fatty Acid Esters as insulating oil," 2008, pp. 1-4.

*Mohamad Kamarol, School of Electrical and Electronic Engineering Universiti Sains Malaysia Nibong Tebal Pulau Pinang Malaysia, eekamarol@eng.usm.my, +06 019 4561946

A039

DEVELOPMENT OF SINGLE STATION EARLY WARNING LIGHTNING ALARM SYSTEM

M. K. Koyamani@Hassan*, W. I. Ibrahim
Sustainable Energy & Power Electronics Research (SuPER)
Faculty of Electrical & Electronics Engineering
Universiti Malaysia Pahang, 26600 Pekan, Pahang
khairul_hassan@yahoo.com*, wismail@ump.edu.my

Keywords: Single-station, Lightning, LabVIEW,

Abstract: Lightning is one of the spectacular natural phenomena which happen on the earth. More than 2000 people are killed worldwide by lightning each year. The lightning monitoring system is important in developing an early alarm system and also to study about the pattern of the lightning strike at the monitored area. The purpose of this project is to develop a lightning warning alarm system which can monitor and observe the lightning activity and will trigger the warning system whenever a lightning strikes at a particular area where the lightning detector device is installed. The lightning detection system will constantly sent data to PC about the lightning activity at that area. The monitoring system will be developed by using LabVIEW software. The system will give information about time, strength and distance of the detected lightning signal.

I. INTRODUCTION

Lightning happens when two massively charged cloud is colliding in mid air. The collision releases huge amounts of energy in form of light, high volt, sound, heat, and many other more. It also produces electromagnetic field (EMF) and electrostatic field (EF). Due to its very high volt, it is very dangerous to human's life. It also can cause losses to communication equipments, power transmission line, power distributions system and more other expensive equipments. Development of a lightning warning alarm system is very important to monitor local lightning activity so that early precautions can be taken before any unexpected tragedy happen

II. METHODOLOGY

The complete process flow of this system is as in the flowchart in the Figure 1. This system is should operate according to the flow so that it will run without false and smoothly. As a whole, this lightning monitoring system have 3 main parts. They are hardware part, interfacing part and the software part.

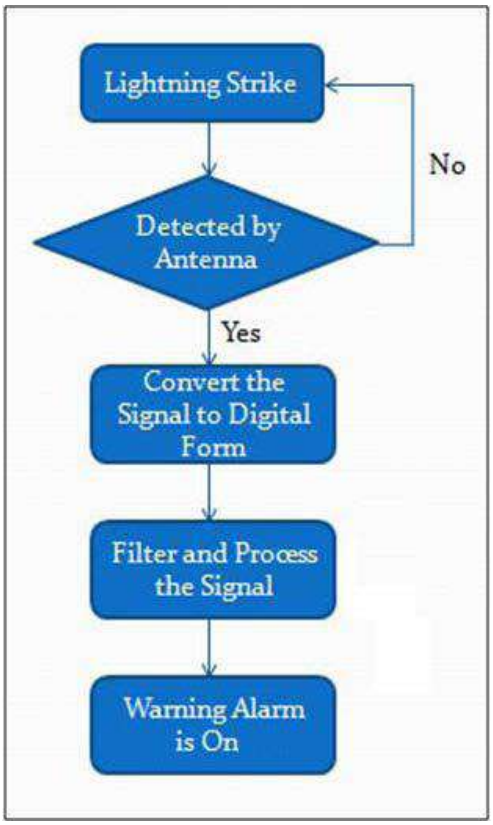

Figure 1. Process flow of the system

An amplifier circuit is used in this system to amplify the signal which is detected by the receiver as shown in Fig. 2. The signal is need to be amplified so that the weak signals will have high possibilities to be detected. This will make this detection and monitoring system is more efficient and reliable. This amplifier circuit is also consist element of protection which will protect the system in case of high voltage or current pass through the receiver system.

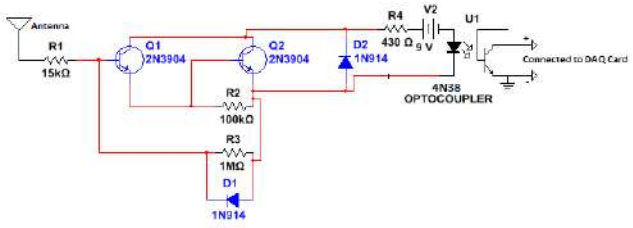

Figure 2. Amplifier circuit diagram

The PVC housing is designed in order to cover and protect the copper receiver and the amplify circuit from the heating sun and rain. The antenna system will be placed at a location where have no shade and have opened air for better chance for detecting the lightning's EMF signal. So a durable and water proof housing is a compulsory in order to make this system to successfully operate.

Interfacing

Type of interfacing device that used for this system is the National Instrument USB 6212 DAQ Card with sampling rate of 400kS/s.

Software

The development of lightning warning alarm system is not complete without the software part of this project, which is developing Graphical User Interface (GUI) by using National Instrument LabVIEW software. The purpose of this GUI is to monitor the lightning activity that happen at investigated area. The signal that detected by the detection system will be displayed at the GUI. The signal will be filtered so that only lightning ranged signal will be pass through the system. After the lightning signal is detected, the GUI will send signal so that the alarm is triggered.

III. RESULTS AND DISCUSSION

Electromagnetic field Detection

From the lightning activity for 1 hour period, they are several successful detection for the electromagnetic field radiation which is captured by copper wire antenna. The detection details are as in Table 1. Example of the lightning signal that detected is as in the Figure 3.

Table 1. Electromagnetic field detection, 8.30pm to 9.30pm on 4th May 2012

Time (PM)	Amplitude (v)	Type of Discharge
8.39	0.5	Positive
8.43	1	Positive
8.44	4.2	Positive
8.45	1.2	Positive
8.55	-2.6	Negative
8.56	0.5	Positive
9.02	0.55	Positive
9.02	-0.27	Negative
9.03	0.2	Positive
9.26	-0.4	Negative

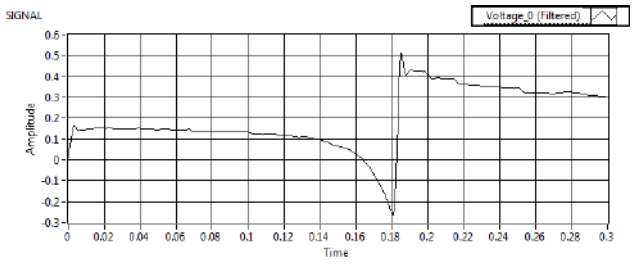

Figure 3. Lightning signal graph for 8.39pm, 4th May 2012

Distance

The formula that used for calculate the estimation value for the distance the lightning occurs is the electromagnetic field to electrostatic field ratio. The estimated distance of the lightning event that occurs on 4th May 2012, from 8.30pm to 9.30pm is as in the Table 2.

Table 2. Estimated distance, 8.30pm to 9.30pm on 4th May 2012

Time	EMF Amplitude (V)	EF Amplitude (V)	Estimated Distance (M)
8.39	0.5	0.0015	350
8.43	1	0.0025	400
8.44	4.2	0.0015	2800
8.45	1.2	0.00125	960
8.55	-2.6	0.002	1300
8.56	0.5	0.0022	300
9.02	0.55	0.005	110
9.02	-0.27	0.0006	450
9.03	0.2	0.0008	250
9.26	-0.4	0.00075	550

IV. CONCLUSION

A copper wire antenna, electromagnetic field detector was successfully developed and installed at the investigation area as planned. The detector was successfully detects signal during lightning days, interface with the software and display the relevant data that can be trusted on a GUI which is developed by using NI LabVIEW software. All the information that displayed in the GUI are important, such as date, time and distance of the lightning event. The alarm is also triggered as desired and suitable to be used as lightning warning alarm system.

REFERENCES

[1] Kenneth L. Cummins, Martin J. Murphy, Jeffrey V. Tuel "Lightning Detection Methods and Meteorological Application",Global Atmospherics, Inc. Tucson

[2] Noradlina Abdullah, Mohd Pauzi Yahya, Dr. Nadiah Salwi Hudi, "Implementation and Use of Lightning Detection Network in Malaysia", TNB Research Sdn. Bhd., PECon Dec 2008

[3] Mohd Pauzi Yahya, "Lightning Phenomenon in Malaysia", TNB Research Sdn. Bhd., ARSEPE Jan 2007

[4] Wu Yanjie, Fan Changyuan, Li Yiding, " Design of Lightning Location System Based on Photon and Infrasound Detection", Chengdu University of Information Technology, ICEMI' 2007

[5] Koay Kim Leong, "Lightning Strike Distance Detector", Universiti Teknology Malaysia, May 2009.

A040

MULTI-STATION SHORT BASELINE LIGHTNING MONITORING SYSTEM

A. S. M. Amir*, W. I. Ibrahim
Sustainable Energy & Power Electronics Research (SuPER)
Faculty of Elecrical & Electronics Engineering
Universiti Malaysia Pahang, Pekan 26600, Pahang.
adisyafiq89@gmail.com*,wismail@ump.edu.my

Keywords: Multi-station, Azimuth, Elevation, Time-of-Arrival.

Abstract: Lightning is a natural phenomenon where the charges generate due to cloud, air movement or other turbulence atmospheric condition. The lightning can occur between cloud to cloud, cloud to air and cloud to ground. The lightning strike gives a big impact in our daily life such as it will kill people and animal, interruption on transmission line; destroy the building and other electrical equipment. These problems can be managed by using Lightning Detection System and the location method to detect and locate the lightning strike. This paper introduced the multi-station short baseline of VHF using Time-of-Arrival (TOA) method. A NI-DAQ 6212 was used to connect the antennas to the personal computer for display and data storage by using LabVIEW. The azimuth and elevation angle was calculated to determine the location of lightning stroke.

I. INTRODUCTION

Lightning is a natural phenomenon that is of great concern to mankind and industry because of the detrimental impact on human safety, hazard and equipment failure due to AC main power conducting electrical transient. The lightning discharges produce energetic electromagnetic radiation. The quest of lightning distance can be solved by means of multi-station or single station techniques. Multi-station technique is the most accurate compare to the single station and several systems have been developed in the past decades [1].

Lightning VHF radiation source location system has been developed and applied widely. Many studies were done by several researchers that used Time-of-Arrival (TOA) method and this method was successful for lightning location studies. This method also can provide accurate locations at long ranges and if the antennas are properly sited, the systematic errors are minimal [2].

Multi-station has been setup for lightning detection system in short radius. The signals that come from the lightning strike will be capture by antennas and monitor from the personal computer. The signal then will filter, save and estimate the azimuth and elevation angles by using LabVIEW software.

II. METHODOLOGY

VHF short baseline broadband was used as a method to locate the position of the source of VHF impulse. Fig. 1 shows that the simplest short baseline consists of three separate antennas. The distance between each antenna is 10m. The system employed three broadband circulate flat antennas having diameter of 30cm each. The antennas were connected to a NI-DAQ 6212 through coaxial cable.

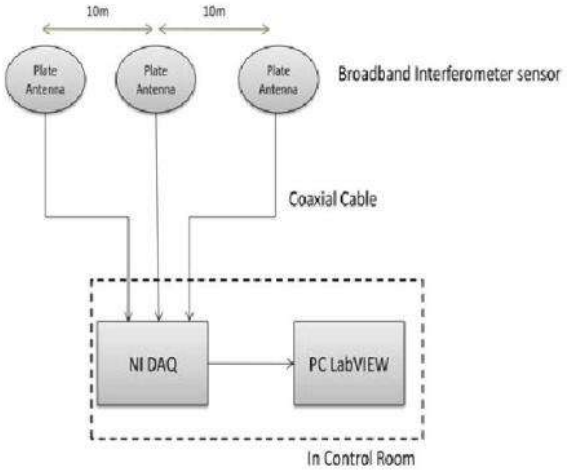

Figure 1. Multi-station short baseline

In order to determine the azimuth and elevation angle, the third antenna is added. The first and second antennas will be the first baseline while the second and third antennas will be the second baseline. These two baselines are perpendicular to each other. Figure 2 shows the geometry of the perpendicular baseline antennas.

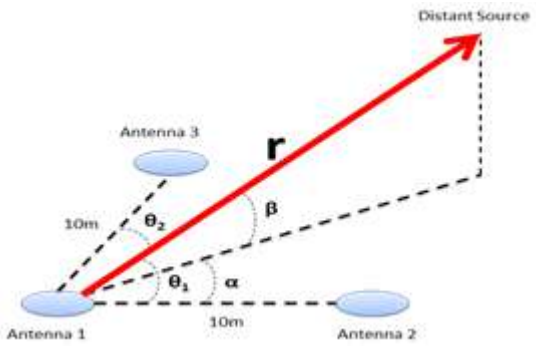

Figure 2. Baseline geometry of the short baseline broadband

III. RESULTS AND DISCUSSION

At this part, we will explain more about the data from a cloud to ground lightning strike which was detected by the plate antennas. Figure 3 shows a typical signal captured when lightning occur. From this figure, we can see that the difference of time delay for each signal.

*adisyafiq89@gmail.com, Fkee, Universiti Malaysia Pahang

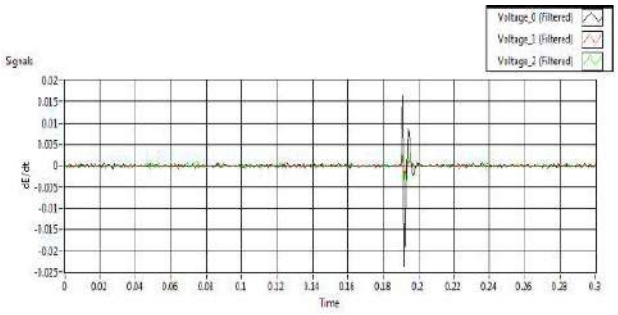

Figure 3. Lightning electromagnetic signal (dE/dt)

According to a simple geometry model that has been developed in Figure 2, three antennas are used to determine the angle of azimuth and elevation by the formulation as follows [3].

$$\alpha = \tan^{-1}\left(\frac{\Delta t_2}{\Delta t_1}\right) \quad (1)$$

$$\beta = \cos^{-1}\left(\frac{\Delta t_2}{dSin\alpha}\right).C \quad (2)$$

Where α is the azimuth angle of radiation source, β is the elevation angle and C is speed of light

Figure 4 shows time waveforms and radiation source location during the flash.

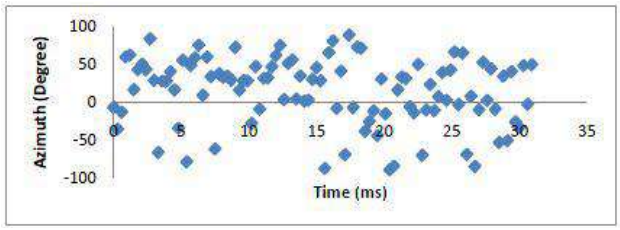

(a)

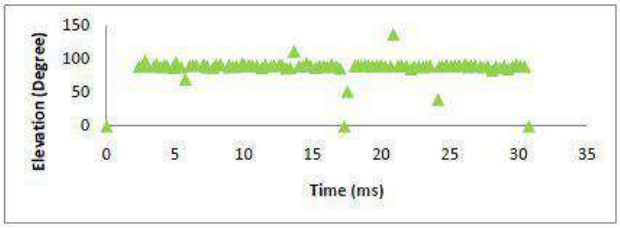

(b)

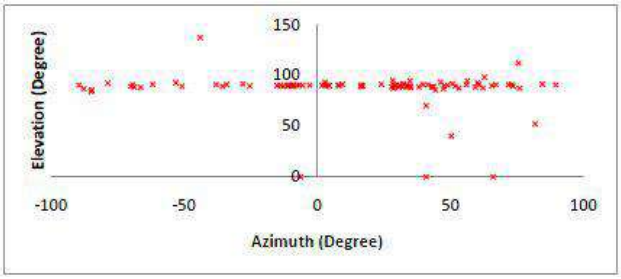

(c)

Figure 4. Radiation during a multi stroke CG flash at 14.15 pm on 2nd May 2012. (a) Azimuth angle versus time, (b) Elevation angle versus time, (c) Radiation source locations

It was obvious that the flash initiated in the cloud. The traditional atmospheric sign convection was adopted to present an electric field change. So, an abrupt negative change means that positive charges are lowered from the cloud to the ground. In this meaning, Figure 4 (a) and (b) is discriminated both negative and positive CG strokes. Both of figures show the activity during 30ms.

IV. CONCLUSION

This paper describes a short baseline lightning location system (LLS) using time-of-arrival (TOA) technique. This technique was performed into two dimensional.

From the analysis of CG multi stroke, we can conclude that the system works well. The system will be improved after this by increased the high speed of the DAQ so that it can be longer time to record

REFERENCES

[1] Ibrahim W. I., Malek Z. A., "Time-to-Thunder Method of Lightning Distance Determination", IEEE Int. Conf. on Power and Energy, pg 357-360, 2010.

[2] C. Dongjie, Q. Xiushu, D. Shu, Y. Jing, and X. Yuejion, "Observation of VHF Source Radiated by Lightning Using Short Baseline Technology", Sym. on Electromagnetic Compatibility (APEMC), Asia Pacific, 2010.

[3] R. Mardiana, and E. Mailadi, "A Technique for Lightning Reconstruction using Short-Baseline Broadband Time-of-Arrival", Proceed. 14th Asian Conf. on Electrical Discharge, 23-25 Nov, 2008.

A041

EFFECT OF PHASE ORDER ON MAGNETIC FIELD DISTRIBUTION UNDER EHV AND HV DOUBLE-CIRCUIT POWER LINES WHICH CHANGE THEIR DIRECTION

T. Matsumoto[1]*, H. Hirata[1], H. Tarao[2], N. Hayashi[3], and K. Isaka[4]
[1]Anan National College of Technology,
[2]Kagawa National College of Technology,
[3]University of Miyazaki,
[4]The University of Tokushima
Contact address: 265 Aoki, Minobayashi-cho, Anan-shi, Tokushima 774-0017, Japan

Keywords : Magnetic Field, EHV, HV, Power Line, Distribution

Abstract: Transmission power lines are a common source of ELF magnetic fields and are usually analyzed as serial lines in one direction. Overhead vertical-type EHV and HV double-circuit power lines, which are generally used in Japan. In this paper, a special emphasis is placed on the effect of EHV and HV double-circuit changing their direction on the total magnetic field distribution.

I. INTRODUCTION

With several epidemiological studies linking extremely low frequency (ELF) magnetic fields with higher rates of incidence of cancer, there is a persistent concern in the public mind regarding the potential health effects of these fields[1-4]. The transmission power lines are the typical facility which generates ELF magnetic fields. There are few analyses which considered the phase order configuration of EHV and HV double-circuit line conductors to decrease magnetic fields in the vicinity of the ground[5].

II. CALCULATION METHOD

The transmission line model is the overhead two vertical-type double-circuit power line, which is commonly used in Japan because of the limited space and reducing the construction cost. In this case, one double circuit is EHV and another double circuit is HV. Its line configuration is that a EHV vertical double-circuit line is placed above a HV vertical double-circuit line. Fig. 1 shows the power line configuration. The phase order of double-circuit of 154 kV is usually the same order. When we define it as (abc-abc), we describe the two vertical-type double-circuit power line as (abc-abc)(abc-abc). The minimum height of the power line is 25 m. It is assumed in the calculations of magnetic fields generated by transmission line that the line conductors are placed in parallel with flat ground, and that the line conductors carry a three-phase balanced current. The magnetic shielding effects of the steel tower and the ground wire are ignored. The magnetic fields are calculated at a height of 1 m above the ground and are the vector sum of 3-dimensional magnetic field components with the phase difference among the line currents. Total magnetic field at a point is the maximum value obtained by composing the magnetic field components.

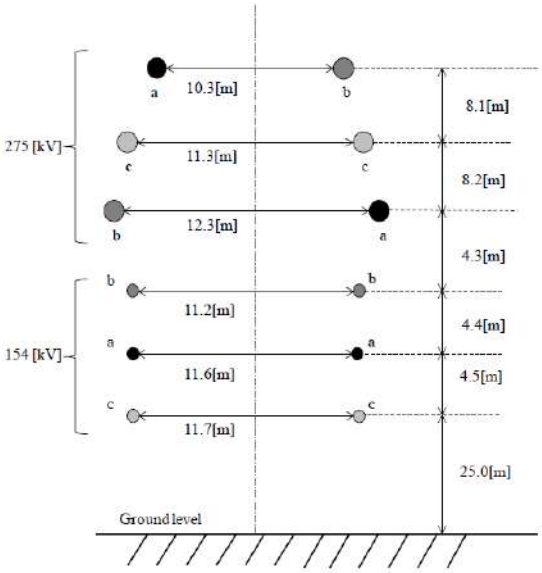

Figure 1. Power line configurations. I_{275kV}=224 A I_{154kV}=90 A

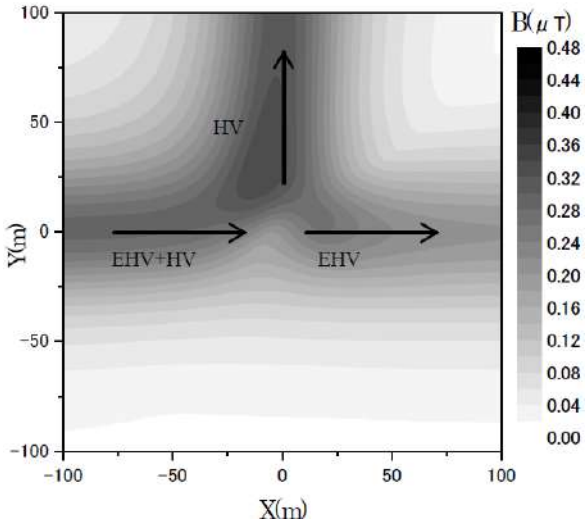

Figure 2. Distribution of total magnetic fields. (acb-bca)(bac-bac)

*T. Matsumoto, 265 Aoki, Minobayashi-cho, Anan-shi, Tokushima 774-0017, Japan, matumoto@anan-nct.ac.jp, +81-884-23-7171

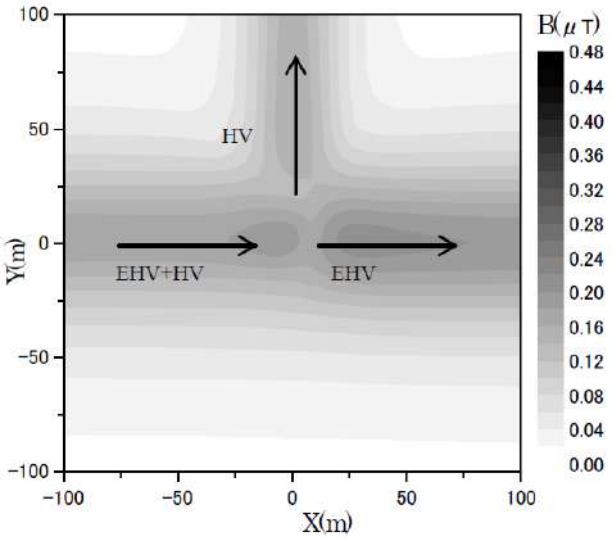

Figure 3. Distribution of total magnetic fields. (acb-bca)(bac-cab)

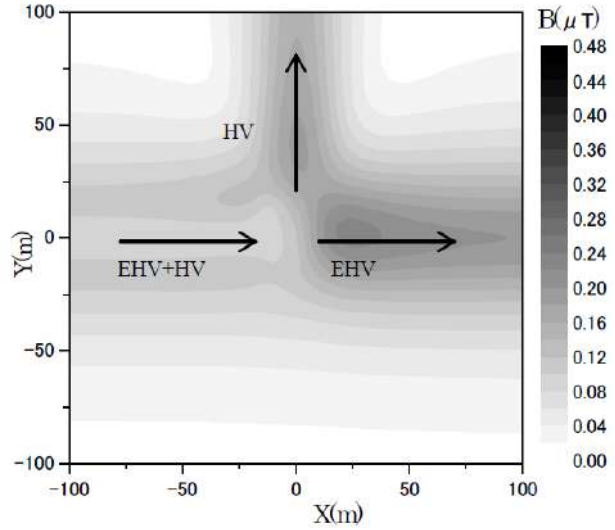

Figure 4. Distribution of total magnetic fields. (acb-bca) (bca-acb)

III. RESULTS AND DISCUSSION

We assume that only HV power lines change their direction in order to supply electric power to a load like a factory, and focus on the relationship between HV phase order and magnetic field distribution. We compare the three vertical-type HV double-circuit lines having different phase order. Fig. 2 shows the total magnetic field distributions at a 1 m above the ground under power lines in the case that the phase order is (acb-bca)(bac-bac). When HV power lines don't change their direction, the maximum of the total magnetic field is 0.28 μT. When HV power lines change their direction, the maximum of the total magnetic field is 0.34 μT in the case that the phase order is (*acb-bca*)(*bac-bac*). The magnetic field increase near the point where HV power lines change their direction showed in Fig. 2. In the case of the phase order (*acb-bca*)(*bac-cab*), the maximum of the total magnetic field is 0.21 μT showed in Fig. 3. It is decreased by 38 %. Furthermore, the maximum of the total magnetic field is 0.23 μT in the case of the phase order (*acb-bca*) (*bca-acb*) showed in Fig. 4. It is found that simple change of the phase order has an effect on the total magnetic field from EHV and HV double-circuit lines and can reduce the magnetic field.

REFERENCES

[1] N. Wertheimer and E. Leeper. Electrical wiring configurations and childhood cancer. Am J Epidemiology, 1979, 109(3): 273-284.

[2] D. Savitz, F. Barnes et al. Case-control study of childhood cancer and exposure to 60 Hz magnetic fields. American Journal of Epidemiology, 1988, 128(1): 21-38.

[3] M. Feychting and A. Ahlbom. Magnetic fields and cancer in children residing near Swedish high voltage power lines. American Journal of Epidemiology, 1993, 138(7): 467-481.

[4] M. Linet et al. Residential exposure to magnetic fields and acute lymhobrastic leukemia in children. New England Journal of Medicine, 1997, 337(1): 1-7.

[5] T. Matsumoto, H. Hirata, H. Tarao, N. Hayashi and K. Isaka, "Analysis of Magnetic Field Distribution Under Power Lines Which Carry Different Current and Change Direction", High Voltage Engineering, Vol. 37, No.11, pp. 2830-2835, 2011.

A042

INFLUENCE OF DISCHARGE MODE ON DECOMPOSITION OF TOLUENE GAS SUBJECTED TO VERY SHORT VOLTAGE PULSES WITH POLARITY REVERSAL

Atsushi Yoshida*, Kazunori Kadowaki
Ehime University
Graduate School of Science and Engineering, Bunkyo-cho 3, Matsuyama, Ehime, 790-8577, Japan

Keywords: VOC gas, decomposition, polarity reversed voltage pulse, surface discharge, DBD

Abstract: This paper presents an experimental study on mechanism and energy efficiency for toluene gas decomposition using repetitive discharges produced by polarity reversed voltage pulses. 300ppm of toluene with dry air is injected into a gap between coaxial double glass cylinders. Three kinds of discharge modes, surface discharge (SD) mode, dielectric barrier discharge (DBD) mode and hybrid (H) mode, are used for the decomposition test. Energy efficiency for toluene decomposition with 80 % removal ratio is over 10 g/kWh for SD-mode. We confirm that the energy efficiency can be further improved for DBD-mode and H mode. When a sinusoidal wave ac voltage is used as the voltage source, however, there is no remarkable difference on the energy efficiency between the three modes. Quantitative evaluation for by-products of toluene will be carried out with GC-MS analysis. Decomposition mechanism of toluene will be discussed on the basis of the results on the chemical analysis.

I. INTRODUCTION

There are many studies on application of dielectric barrier discharge (DBD) and surface discharge (SD) to decomposition of VOC (volatile organic compounds) gases. In general, a sinusoidal wave voltage is applied to a barrier-type plasma reactor because of easy control of input power into plasma. On the other hand, it is also known that intermittent application of rectangle high voltage pulse is effective way to obtain non-equilibrium plasma. An advantage of the voltage pulse with a very short rise time of the order of 10-8 s over sinusoidal wave voltage is that the very high dV/dt at the voltage front allows to make higher energy electrons because the external field strength in a gas gap subjected to the high voltage pulse can be higher than that subjected to the sinusoidal wave voltage. However, there are few reports on DBD and SD using the pulsed power technique. This is because residual charges produced by the application of a monopolar pulse are deposited on the barrier so that field strength in discharge gap is strongly reduced.

Recently, we reported an effect of polarity reversal of pulse voltages on NO oxidation in a barrier-type plasma reactor using a reciprocal traveling wave voltage pulse generator. In this study, we confirmed that the energy efficiency of the polarity reversed pulse discharge treatment was more than two times the energy efficiency of ac discharge treatment.

In the present study, influence of discharge mode on decomposition of toluene gas is discussed using a double cylindrial glass reactor. In order to understand the chemical reaction process of the decomposition, quantitative evaluation for by-products of toluene will be also carried out with GC-MS analysis.

II. EXPERIMENTAL PROCEDURE

Fig.1 shows a general view of a plasma reactor for toluene removal. The reactor consist of two cylindrical glass tubes and electrodes. A test tube (IWAKI Co., PYREX test tube, inner diam. 18.5 mm, outer diam. 21mm) with tungsten winding (wire diam. 0.10 mm) is adjusted coaxially with a qualtz cylinder (inner diam. 25 mm, outer diam. 28 mm). The plasma-chemical reaction of toluene is caused by the discharge from the wire electrode in the gap space between the two glass cylinder. For SD-mode, a high voltage is applied between the tungsten winding and a grounding aluminum rod (18 mm in diam.) inside the test tube, so that the discharge propagates along the inner glass surface. In order to suppress undesirable discharges at the inside of the test tube, the thin layer between the glass and Al rod is filled with NaCl solution

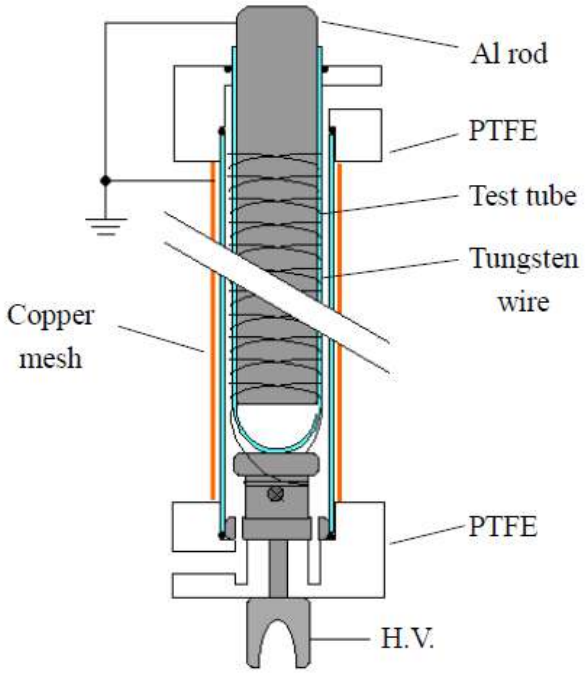

Figure 1. Sectional view of plasma reactor.

of 3 % in concentration. For DBD-mode, the grounding electrode is not set inside the test tube but set outside of the quartz tube. Since the quartz tube is covered by the grounding copper mesh in DBD-mode, streamer discharge from the wire electrode can propagate in the gap space along the radial direction. Both the inner aluminum rod and the outer copper mesh are used for H-mode, so that a hybrid pattern between SD and DBD must be observed.

The simulated VOC gas consisting of toluene (300 ppm), N2, (79 %) and O2 (21 %) is introduced into the reactor with a flowing speed of 0.4 L/min in all tests. Toluene concentration at the outlet of the reactor is measured by gas detecting tube

*E-mail: ryoumaden3@gmail.com, Tel : +81-89-927-9786, Fax : +81-89-927-9790

(Gastec Co., No.122). In addition, the exhausted gas is taken out by a sampling bag for GC-MS analyisis.

Energy efficiency for toluene decomposition [g/kWh] is calculated with the amount of removed toluene weight [g] and input energy [kWh] into the reactor. The input power into the reactor is calculated with the applied voltage and current waveforms measured by a voltage probe (Tektronix Co., P6015A) and a current monitor (Pearson Co. Model 2878) . The energy efficiency in each mode for the polarity reversed voltage pulse application is compared with that for a 60Hz ac voltage application.

III. RESULTS AND DISCUSSION

Typical waveforms of the polarity reversed voltage and discharge current are shown in Fig.2(a) for SD-mode, Fig.2(b) for DBD-mode and Fig.2(c) for H mode respectively. The discharge current in H-mode is highest in the three discharge patterns. This is because plasma volume in H-mode can expand due to the effect of the double grounding electrodes. The discharge energy calculated from the voltage and current waveforms is 24 mJ for Fig.2(a), 22 mJ for Fig.2(b) and 26 mJ for Fig.2(c). This fact suggests that the energy transform ratio from the stored energy in the pulse forming cable into the discharge energy is up to approximately 80 % for H-mode.

The relationships between the toluene removal ratio and the energy efficiency for H-mode are shown in Fig.3(a) for the polarity reversed pulse and in Fig. 3(b) for ac 60Hz. From Fig.3, it can be seen that the toluene removal ratio is 90% and energy efficiency is 18g/kWh for the polarity reversed pulse, while 57% toluene was oxidized to CO or CO2. And toluene of more than 30% is decomposed into different by-products in the dry air.

The quantitative evaluation of the by-product by GC-MS analysis is now in progress.

REFERENCES

[1] K. Kadowaki, and I. Kitani, “Physics and Application of Streamer Discharge Produced by Polarity-Reversed Voltage Pulse for Environmental Protection Technology”, IEEJ Trans. FM, Vol. 130, No. 10, pp.871-878, 2010

[2] K. Satoh, ”Decomposition of Volatile Organic Compounds and Environmental Hazardous Substances in Water using Discharge Plasma”, IEEJ Trans. FM, Vol. 130, No. 10, pp.941-948, 2010

[3] J. Van Durme, et al., “Abatement and degradation pathways of toluene in indoor air by positive corona discharge”, Chemosphere, Vol. 68, pp.1821-1829, 2007

[4] W. F. L. M. Hoeben, et al., “Oxidative degradation of toluene and limonene in air by pulsed corona technology”, J. Phys. D: Appl. Phys, Vol. 45, 2012

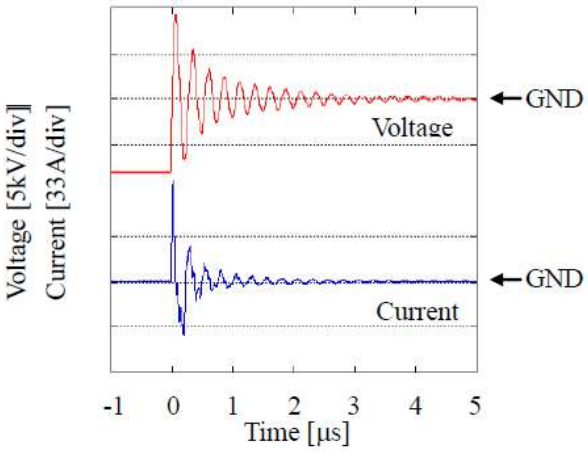

(a) SD-mode

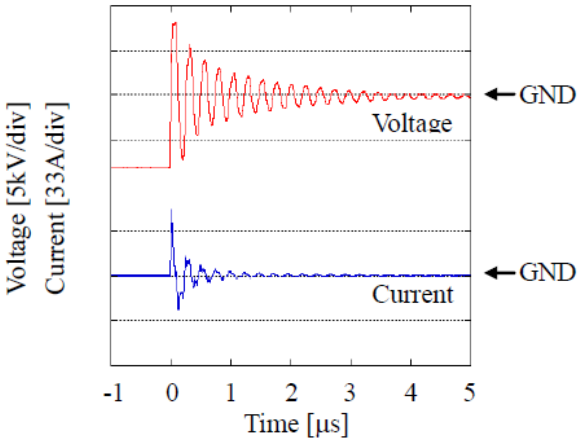

(b) DBD-mode

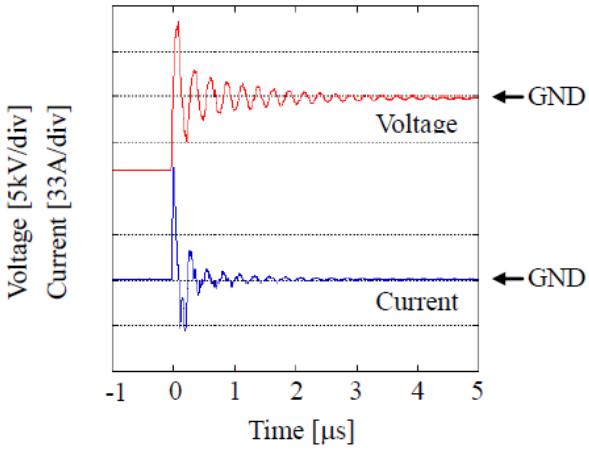

(c) H-mode

Figure 2. Typical waveforms of the polarity reversed voltage and discharge current for (a) SD-mode, for (b) DBD-mode and for (c) H-mode.

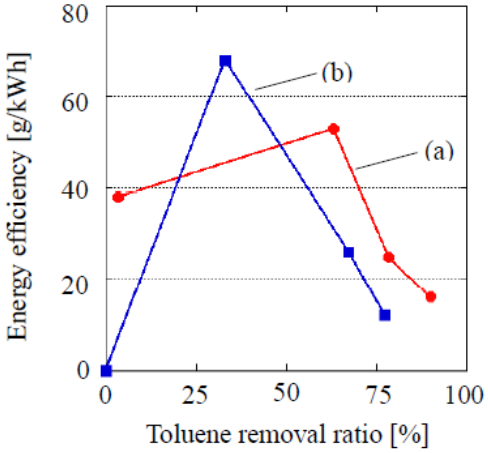

Figure 3. Relationships between the toluene removal ratio and the energy efficiency for (a) the polarity reversed pulse and for (b) ac 60Hz.

A043

DEPENDENCE OF BREAKDOWN TIME LAG OF LOW DENSITY POLYETHYLENE UNDER DC ELECTRIC FIELD

Takashi Akagi*, Amir Izzani Mohamed , Kazunori Kadowaki
Ehime University
Graduate School of Science and Engineering, Bunkyo-cho 3, Matsuyama, Ehime, 790-8577, Japan

Keywords : Space Charge, Pulsed Electro Acoustic Method, Low Density Polyethylene, Breakdown Time Lag

Abstract: This paper reports the results from a measurement of the breakdown time lag and space charge distribution when applying a high voltage DC to low-density polyethylene film. DC voltage is applied so that the applied field become +3.0MV/cm or +2.0MV/cm electric field. Space charge distribution is measured by a pulsed electro Acoustic (PEA) Method. If the sample does not breakdown in five hours, the measurement is terminated. The measurement is carried out for 20 samples for each applied electric field. It is interesting to notice that breakdown time lag is faster under 3.0MV/cm applied field than under 2.0MV/cm applied field. In space charge measurement, a packet-like positive charge penetrated deeper under 2.0MV/cm than under 3.0MV/cm applied field. In addition, positive packet-like charge in the sample freezes for a long time in the case of 3.0MV/cm than the case of 2.0MV/cm.

I. INTRODUCTION

Space charge penetration into bulk of polymer insulation material inducing distortion in local electric field and is considered as the reason of breakdown of the insulation material. Although a lot of studies have been made, the correlation between space charge and breakdown is still unclear. In this study, breakdown time lag of low-density polyethylene (LDPE) under dc high voltage application for 5 hours was carried out. As a result, breakdown time lag of samples under 2MV/cm applied field was found to be shorter than that under 3MV/cm applied field.

II. MATERIALS AND METHODS (when applicable)

LDPE pellet (Sumitomo Chem. Co. Ltd. : Sumikasen G201) was blended into a rough sheet. After that, it was hot-pressed so that the thickness of the centre area became (measurement area) approximately 200μm. In order to avoid breakdown at the electrode's edge, recess-type sample was prepared. Experiments were carried out under atmospheric pressure with temperature at electrode vicinity was controlled at 300C. Semicon rubber was used as upper electrode and evaporated-Aluminium was used as lower electrode. A total of 20 samples of each applied electric field (2.0MV/cm or 3.0MV/cm) were prepared. The experiment was stopped when breakdown occurs during 5 hours voltage application the time was recorded and plotted as Laue's plot.

III. RESULTS AND DISCUSSION

Fig. 1 shows an example of space charge profile under (a) 2.0MV/cm and (b) 3.0MV/cm electric field application in sample that did not breakdown for 5 hours. From both figures it is understood that packet-like positive charge penetrated into the bulk to vicinity of counter electrode with velocity that gradually decreasing. In the case of 2.0MV/cm applied field, after 80 minutes packet-like positive charge dissappeared. On the other hand, in the case of 3.0MV/cm applied field, after penetrating close to vicinity of counter electrode, the packet-like positive charge seem frozen. After 270 minutes, they dissappeared. The packet-like positive charge penetrated deeper (closer to counter electrode) under 2.0MV/cm than under 3.0MV/cm applied field. This result is in agreements with other report[1].

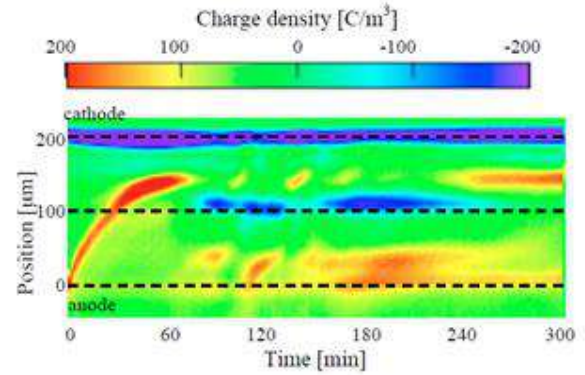

(a) 2.0MV/cm applied field

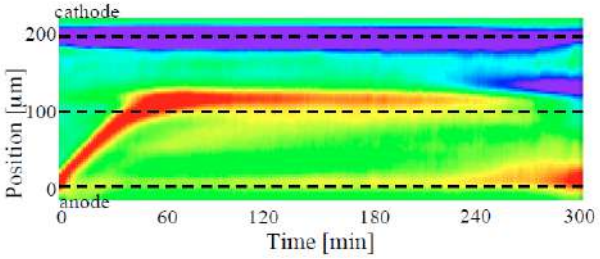

(b) 3.0MV/cm applied field

Figure 1. Temporal changes in space charge distribution in the no break down sample

Moreover, packet-like positive charge arrive at 100μm of penetration depth in 30 minutes under 2.0MV/cm and in 50 minutes under 3.0MV/cm. This shows that penetration velocity of packet-like space charge is faster under 2.0MV/cm applied field. In all samples, during voltage application until breakdown and space chargemeasurement, space charge profile and penetration velocity of the packet-like positive charge are almost similar to that in fig. 1. During voltage application for 5 hours, 5 out of 20 samples and 4 out of 20 minutes did not breakdown under 2.0MV/cm and 3.0MV/cm respectively.

Figure 2 shows temporal changes in maximum electric field from one the sample that did not breakdown under both applied field. From this fig., electric field reached maximum value shortly after voltage application. Under 2.0MV/cm applied field, electric field reached maximum value of 3.8MV/cm in 30 minutes. While under 3.0MV/cm applied field, electric field reached maximum value of 4.6MV/cm in 50 minutes. Ratio of applied field and maximum electric field is defined as electric field distortion rate. Electric field distortion rate is 1.9 under 2.0MV/cm and 1.5 under 3.0MV/cm showing that the rate is higher under a lower applied elctric field (2.0MV/cm). After

*Takashi Akagi, E-mail: t.akagi204@gmail.com , Tel :+81-89-927-9786,Fax: +81-89-927-9790

distortion rate reach maximum value, maximum electric field decreased slower in 2.0MV/cm applied field case than in 3.0MV/cm. This is corresponding to fig. 1 that shows the disappearence of packet-like positive charge at 80 minutes of voltage application under 2.0MV/cm and at 270 minutes of voltage application under 3.0MV/cm.

Figure 3 shows Laue plot of breakdown time lag under both applied field. Number of samples that did not breakdown under 3.0MV/cm in 5 hours is slightly higher than under 2.0MV/cm. However, it is interested to notice that samples under 3.0MV/cm tend to have a longer time lag to breakdown after 5 hours of voltage application. Under 2.0MV/cm, breakdown ocurred in 60 to 80 minutes range in most cases while under 3.0MV/cm breakdown ocurred in 80 to 110 minutes range in most cases. It is understood that breakdown ocurred during the decrease of electric field value after reaching maximum value under both applied field. In addition, breakdown ocurred only one case under 2.0MV/cm in longer time range while there are 4 cases as such under 3.0MV/cm. This is considered to be attributed by the slowly decrease of distortion rate under 3.0MV/cm case as compares to under 2.0MV/cm case.

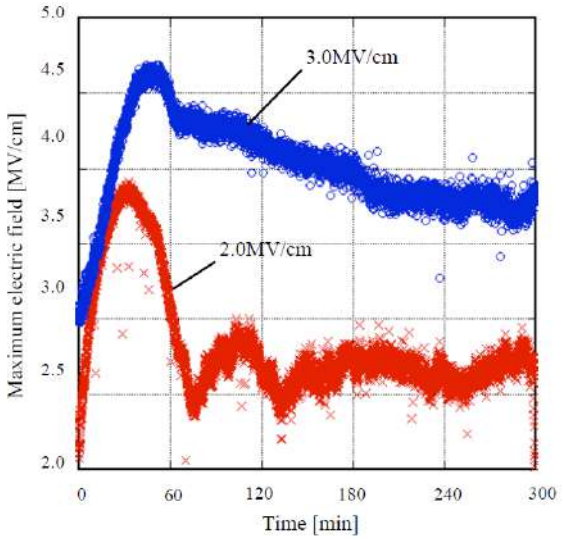

Figure 2. Temporal change of average of the maximum electric field in the no breakdown sample

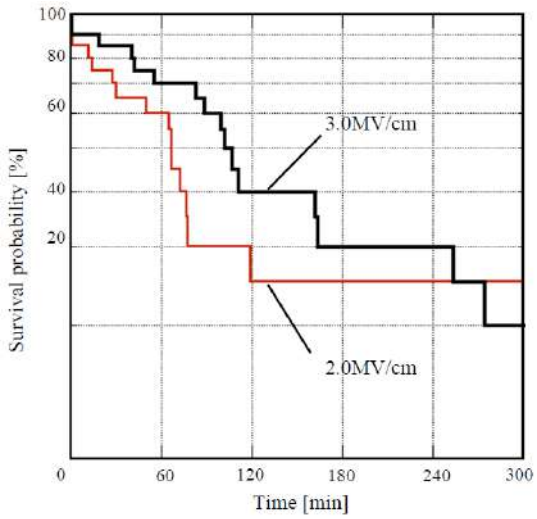

Figure 3. Laue plot of the breakdown time lag in each of the applied field

REFERENCES

[1] K. Matsui, Y. Tanaka, T. Takada, T. Fukao, T. Maeno and J.M. Alison, “Space Charge Behavior in Low-density Polyethylene at Pre-breakdown”, *IEEE Trans. DEI*, Vol. 12, No. 3, pp. 406-415, 2005

[2] T. Maeno, H. Kushibe, and T. Takada “Pulsed Electro-Acoustic Method for the Measurement of Volume Charges in E-Beam Irradiated PMMA”, CEIDP Ann. Rep., pp.389-397 (1985-10)

[3] K.Kadowaki, A. Mikano, S. Usuki, S. Nisimoto and I.Kitani : “Space Charge Dynamics in LDPE Film Subjected to Dc Step Voltage under High Pressure”, *Proceedings of the ICSD 2007*, pp.446-449, 2007

[4] Y. Tanaka, K. Matsui, T. Takada and T. Maeno : “Analysis of Packet-like Space Charge Behavior in Low -density Polyethylene”, *Proceedings of the ICSD 2007*, pp.482-485, 2007

A044

LIGHTNING FATALITIES IN MALAYSIA

Nur Najihah Abu Bakar, Noor Azlinda Ahmad*
Faculty of Electrical Engineering, Universiti Teknologi Malaysia, 81310 Johor Bahru, MALAYSIA
*Email: azlinda@fke.utm.my , gburn_nice@yahoo.com

Keywords: Lightning, lightning fatalities statistical data, Lightning injury mechanism, Human body modelling

Abstract: Lightning strike is the environmental phenomenon that dominates to the major factors of supplemental deaths as well as injury due to its extremely generous surge current and voltage. Many of fatalities caused by lightning have been reported where some of them were deaths and another some is able to survive by having injuries either in a short or long term effect; the worst is permanent injury. Since Malaysia is one of the countries in the world with highest lightning activities [24], a laudable statistics data about death and injuries is to increase public awareness on the danger of lightning. This thesis work manifests an overview, recent statistical data and analysis on lightning fatalities in Malaysia which includes the year, gender, age, status, month, state, activities and location of where the victim was hit by lightning. It bestows the favourable image to illustrate the jeopardy of lightning to the public by employing case study and statistical analysis based on medical report, blogger and newspaper. In addition, five main lightning injury mechanisms (direct strike, contact potential, side splash and ground current) were analysed using a human body electrical modelling. The results were presented in terms of current and voltage relationship across the significant part of the human body.

1. INTRODUCTION

Lightning usually being related with the electricity where the formation of lightning occur when there are discharge of the charged cloud to the ground. Lightning have the ability to cause severe electric injuries and may be seen as a result of an accident or in deliberate attempts at injury. This damage to the human body is caused by the sudden flow from the lightning strike of a large amount of electrical current in a range of several thousand amps to several hundred thousand amps.

There are an estimated 25 million lightning flashes in the United States each year. Documented lightning injuries in the United States shows the average of lightning fatalities is about 300 per year. For the undocumented injuries due to flaws in the reporting process of lightning-related occurrence, actual amount of lightning fatalities are likely much higher [5]. Malaysia likewise ranks as one of the highest countries with lightning injury in the world after Rwanda and Congo [24]. As comparison to United Stated that has the volume of 300 million people, the population in Malaysia is only 27 million. This means that, Malaysia lightning death and injuries rate is actually 10 times more than United Stated in the aspect of citizen capacity.

2. GENERAL OVERVIEW OF LIGHTNING ACTIVITIES IN MALAYSIA WITH METEOROGICAL INFO

Formation of lightning is influenced by environmental controls [1] for instance, geographical variations. Equator is one of the locations that tend to receive higher lightning flash [7]. Since Malaysia is located at the equator, lightning flash develops nearly every day due to the amount of sunshine received and consequently produces high vertical updrafts which generate cold fronts, and moist air [13].

The intensity of lightning is getting more critical due to the global warming and transforming in climate [4]. It drives more warm and moist air due to rise of the sea surface temperature which was the main provocation for thunderstorm. Growing the number of factories and releasing chemical to atmosphere in Malaysia favour to high frequency of thunderstorm. In addition, deforestation and land clearing for development will worsens the 'heat islands' effect especially in urban regions and probably contribute to storm cloud formation [16]. With this serious situation, more lightning injury and death cases can be expected to be occurred in Malaysia.

Figure 2 shows the density of lightning flash in peninsular Malaysia including Sabah and Sarawak. Based on the colour of the flash scale given, Malaysia was in the range of 25 up to 4000 thunderstorm activities.

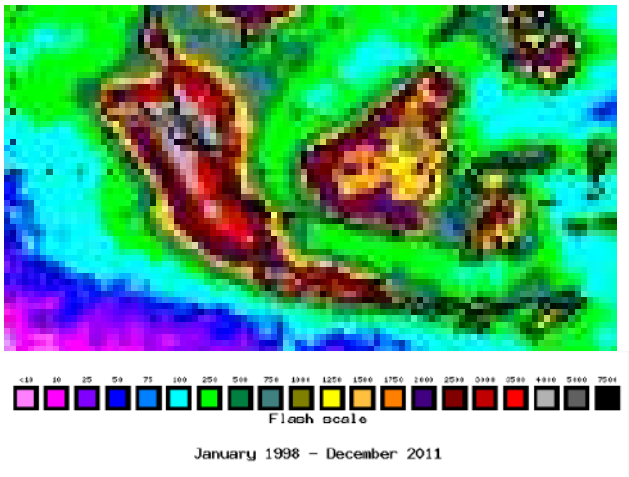

Figure 2. Malaysia isokeraunic map [4]

Based on Figure 3, the average number of thunderstorm (TD) days per year in peninsular Malaysia was in the range of 159 to 293. In contrast, TDs recorded by National Lightning Safety Institute (NLSI) of the US, Japan, Australia, Europe, and England show far fewer TD (below 70). Surprisingly, even lightning capital in USA, Florida has only 90-110 TDs[16].

*Noor Azlinda Ahmad, E-mail : azlinda@fke.utm.my, Tel: 07-5535432

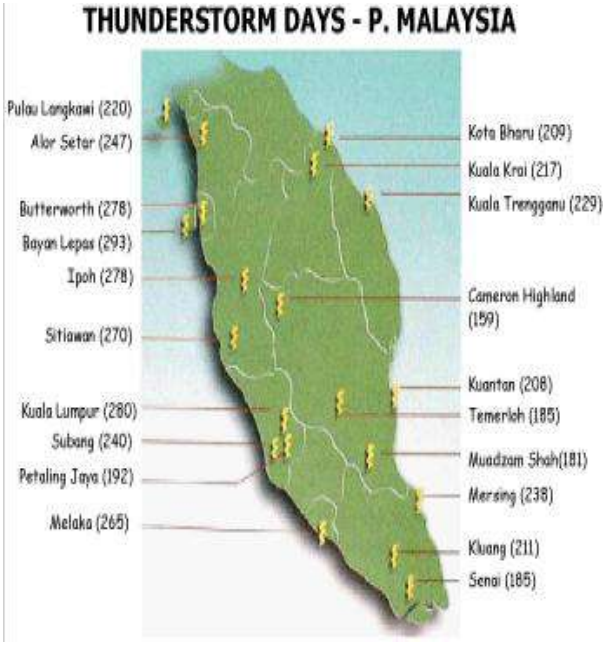

Figure 3. Thunderstorm distribution in peninsular Malaysia

3. STATISTICAL DATA OF LIGHTNING FATALITIES IN MALAYSIA

Governments are pressing the right to citizen for reporting lightning injuries as well as deaths case. However in Malaysia reliable statistics data on lightning fatalities is often difficult to accumulate. Apart from the completeness of medical facilities in each state of this country, some victim do not seek treatment at the time of the injury resulting medical data sources even more unreliable [16]. In fact, deaths are regularly better reported than injuries since it is mandatory [9]. Average of the lightning injuries was estimated about ten times the quantity of deaths [15].

Table 1 Lightning fatalities data in Malaysia (by month)

YEARS	BY MONTH												TOTAL
	JAN	FEB	MAR	APR	MAY	JUN	JUL	AUG	SEP	OCT	NOV	DEC	
2004					7								7
2006				6	2						3	1	12
2007	3										1		4
2008	1			2	1	1					2		7
2009					11					4		2	17
2010				4	2			2	1				9
2011	1	1	1			3	2	12	5	1	3	1	29
2012	6												6

In this study, a statistical data of lightning fatalities in Malaysia for the year 2004, 2006, 2007, 2008, 2009, 2010, 2011 and early 2012 is presented. Table 1 shows that the number of lightning fatalities in this country is increasing yearly. Although the number of cases is small in 2004, 2008 and 2010, the actual number may be considered larger because sometime, most survivors do not require a hospital admission and this may affect statistical database which relies on the report.

On the other hand, it appears that the number of male victim is higher than that of female. For 2006 and 2011, there are only two female victims have been recorded.

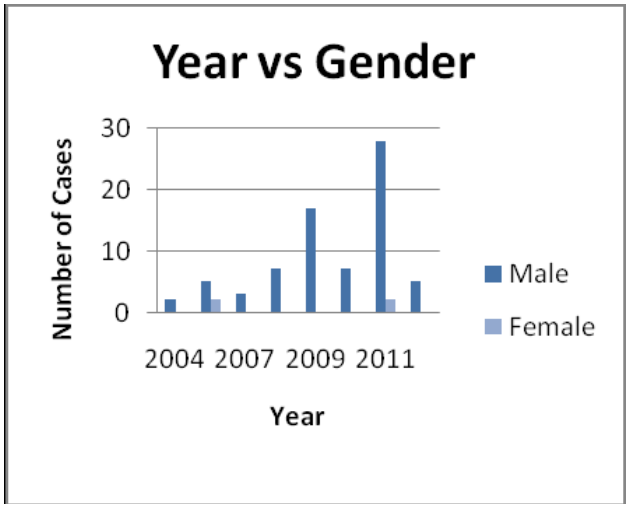

Figure 4 Bar chart year versus gender

Other than that, all the number cases were monopoly by male victims. The highest was in 2011 with 28 cases. Besides that, the primeval publications have proven the male ratio predominated over female's ratio [23]. This is due to a big number of groups per strike. It can be explained since males are more exposed to the outdoor activities than female. Furthermore, when lightning strike (either by direct strike or indirect strike), many victims will get involved due to multi-point grounds terminations [13].

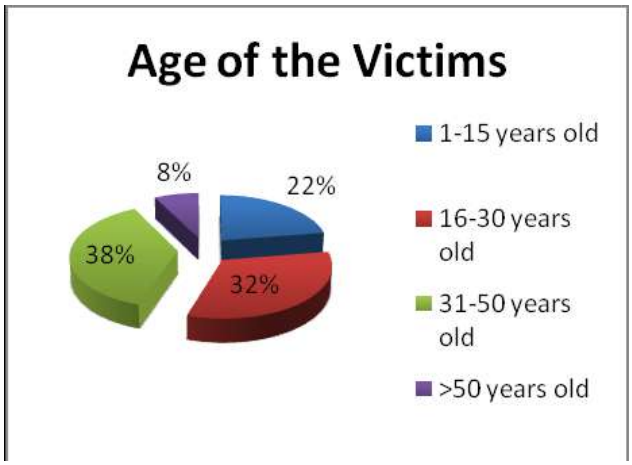

Figure 5 Pie chart ages of victims

Figure 5 graphically represent the age of victims. Majority of lightning victims aged between 31-50 years old (38%), followed by maturity age (16-30 years old) which contribute to approximately 32 %. Despite of their age both groups are dominating the number of lightning fatalities in Malaysia. This may be due to lack of awareness among citizen on the danger of lightning and the appropriate safety precaution.

This is clearly shown in Figure 6 where in most cases involve outdoor activities such as seeking shelter in unsafe places, fishing, using hand phone, planting, playing football, hockey game and playing golf.

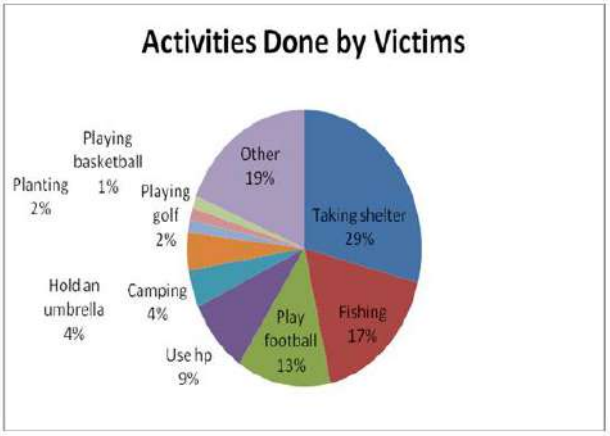

Figure 6 Percentage of activities done by the victim during the incident

Taking shelter outside contribute to the highest percentage with 29 %. Most of the victims were foreigner worker including Indonesian and Bangladesh where many of them work at the construction. Other (riding motorbike, chatting at the outside, selling, and archery training) dominates 19 % of the total cases. Fishing also has the large scale number of fatalities (17 %). This is probably due to the sea geographical condition which tends to generate higher density of moist air that will lead to the large lightning flash at the area.

One of the significant factors of lightning fatalities is the location of lightning strike. Obviously, lightning is prone to strike to an open place or field. Figure 7 shows that most of the fatalities occur at the field (53%) followed by sea which accounts for about 20 %. Direct strike often occurs to people who are standing in the open area because lightning tend to hit highest object at the area. If at the field, people is the tallest object then that people will have higher probability to get hit by the lightning. However, only 3 % of the cases happened when victims were standing under a tree.

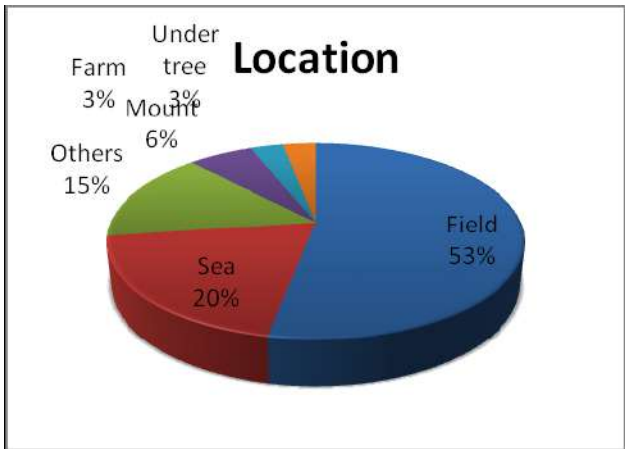

Figure 7 Location during the lightning incident

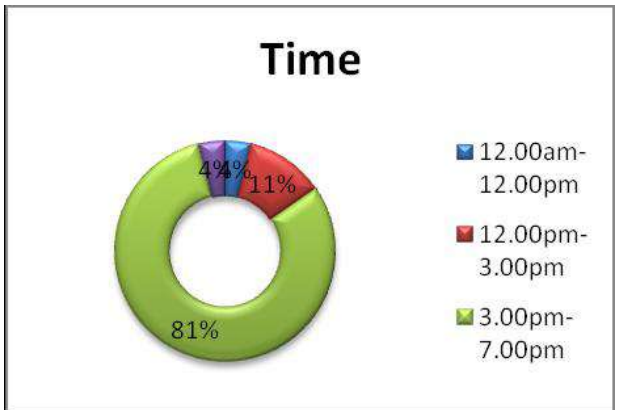

Figure 8 Time of the incident

Figure 8 indicates the time of victims was struck by lightning. Most cases happened in the evening between 3.00 pm to 7.00pm. During this time, Malaysia usually has heavy rain follow by the thunderstorm especially during the monsoon transition. However, slightly rain also may cause to lightning activities. Sometimes lightning can also strike from a perfectly blue sky [3]. Continual sense mistakes with lightning can be deadly. Waiting to see or hear the first stroke of lightning means that we have been at risk of a direct lightning strike for 30 minutes or more already [3]. Base on previous study, 60 % of injuries and fatalities occur after it seems a storm has passed.

4. LIGHTNING INJURY MECHANISM

Lightning injury may be accidental or non-accidental. Accidental lightning injury usually related to direct strike. However, non-accidental cases will occur when we do not realise it such as in EPR (Earth potential rise) case. When we was think of how lightning injuries, we always assume that it is due to the direct strike. However, it was shown in the previous research that a direct strike lightning was responsible for only a small percentage of lightning-related injuries with the estimated frequency in about 3% to 5 %, compared to other causes [7].

Types of lightning injuries and deaths depend on many factors, such as intensity of the lightning current, time the current takes to go through our body, pathway involved and type of strike [21]. Obviously there are four main mechanisms of lightning injuries (which may lead to deaths related cases) such as direct strike, EPR, side splash and contact voltage is very significant to ascertain [5].

4.1 Direct strike

Injury caused by direct strike happened when the victim was directly hit by lightning. Head entry is the most common site [5] and exit pathway is through the soles of the feet because in most cases, the victim was usually standing thus earthing him through the ground [21]. Figure 9 shows the clear image of exit pathway when someone gets injured by direct strike [21].

Figure 9 Exit pathway through feet when direct strike

For a given current path throughout human body, the danger depends mainly on the magnitude and duration of the current flow [23]. The rate of current directly enter the human body eagerly reach up to thousand amp and the standard rate of time is very short, that is 8/20u s [1]. According to Fish *et al* [8] a current of 20mA might bring human to fatal so human body could not support full strength of the current flow when was directly struck by lightning. Figure 10 illustrate the way of direct strike flash to human

Figure 10 Direct strike

4.2 Side splash

Side splash can be explain when flash of lightning hit an object such as tree and travels partly down through the object before jumping to a nearby victim. Side splash also be able to occur from one person to another [7]. This kind of lightning mechanism injury splash the lightning from tall object onto nearby object in order to reach the ground. Current divides itself between the two paths in inverse proportion to their resistances. Resistance of the jump path and additional path is separated from the path to earth from the stricken object [22]. This is the most common lightning injury phenomenon that occurs in real life. The lightning is deviated to the victim from another tall object. Figure 11 shows the portion of flash jumps to the victim after strike the tree.

Figure 11 Side splash mechanisms

4.3 Contact voltage

Beside direct strike and side splash another main cause of lightning injury is contact voltage. It occurs when a person is holding or touching something that can be categorize as metal such as weapon, umbrella and telephones poles. Lightning will strike this metal object, driving high current throughout the body of the victim due to the least resistance [21]. A voltage development is established on that object from the strike point to the ground, and the person in contact with the object is subject to the voltage between their contact point and the earth [22]. In the electrical field, electricity obligates a complete path (circuit) to flow and proceed. It can be observed either from theory or practical that there is no hazard shock without two contact points on the body for current to enter and exit. Figure 12 explain the circuit theory regarding to current flow that make human get shocked. Lightning current will flow from metal to the victim's body in order to find the shortest way to the ground. Figure 13 illustrate the situation of the contact voltage mechanism when the victim touching metal object before get shock.

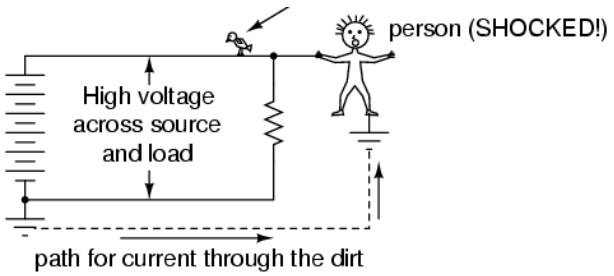

Figure 12. Shock current path through the circuit [25]

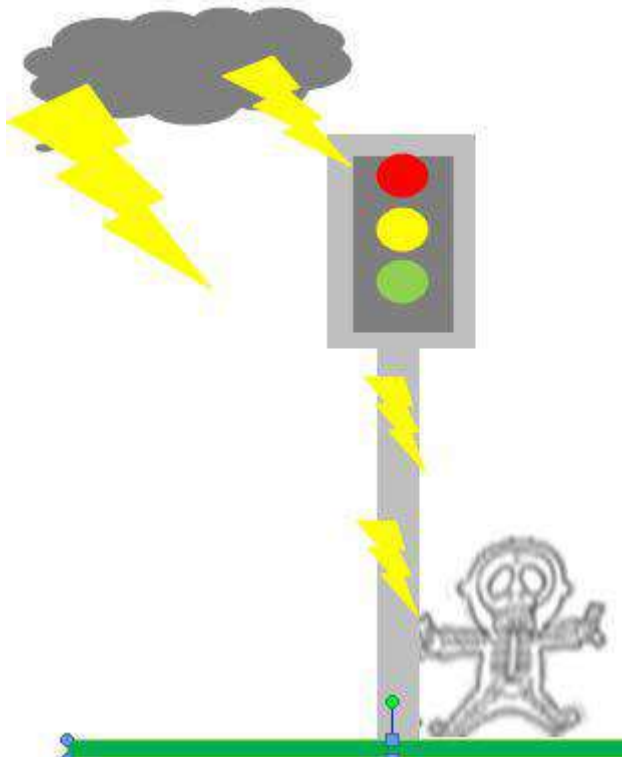

Figure 13 ` Contact voltage situation

4.4 Earth potential rise (EPR)

When lightning strike into the earth and travel through it, the voltage are set up in the ground before it jump to the people that walking or standing nearby the location where EPR is active [5]. One part of human leg contacts one voltage and another leg will contact a different voltage. The difference in voltage makes a circuit to drive current into the body. EPR strikes are less severe since the strength of the lightning current has been weakened by travelling through the ground [7]. However, for the both legs usually it will show severe burn as already shown in Figure 9 above.

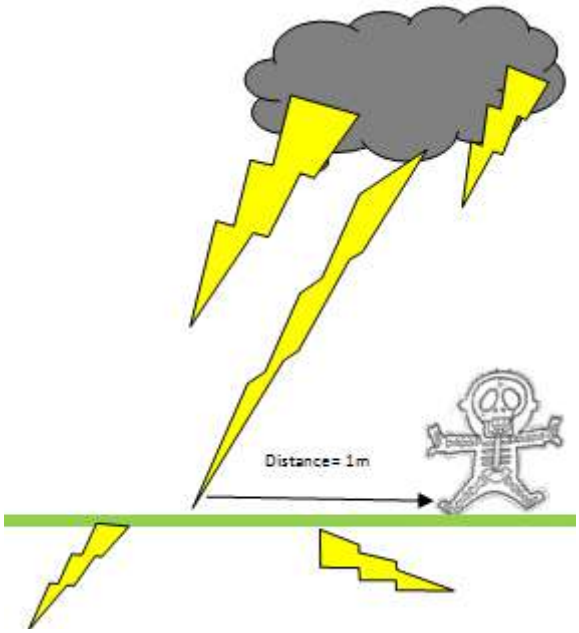

Figure 14. Earth Potential Rise

5. MODELLING HUMAN BODY AS AN ELECTRIC CIRCUIT

Injuries caused by electricity usually difficult to understand because it is invisible and cannot be seen through naked eyes. Because of the great improvement of the technology, it was recovered that human body can be represented as an electrical circuit to give clear explanation of the way current go through the human body and how this influences the nature of injuries in aspect of science and engineering. During normal activity, the characteristic of current flow in the body are carefully controlled by the body system to prevent injury. However, the body also subjected to uncontrolled electric current such as an accidental electric shock which may occur under varying circumstances [18] for instance lightning flash. This situation is occurring because lightning discharges are characterized by extremely high voltages and currents that bring millions value of voltages and thousands amperes per strike. In addition, the duration of current pulse is very short in about milliseconds [18]. Burn and branching zigzag red mark will appear after the victim was struck by lightning due to extravagated blood.

Human body has the resistance to allow current flow through its [17].The impedance in human body is the combination of two components consists of resistance and capacitance [1]. In general, skin is the main resistance for current to flow. Previous study state that 99% of the body's resistance to electric current flow is at the skin [17]. The components for skin resistivity are significantly larger than for the internal resistance consist of a parallel resistance and capacitance of 10kΩ and 0.25μΩ [1] as shown in Figure 16. Basically V=IR, meaning that current flow is increasing with decreasing value of impedance. However, current that move depends on several factor such as moisture content, wet or dry skin, temperature and physical properties. In the dry skin, the tendency for electrical current to travel is deeper into body meanwhile if the victim is wet there will be tendency for electrical to flow over the surface of the body, causing an effect known as "flashover" [3].

From the thermal effect aspect, when heat is produced in tissue as a result of shock electric, it will lead to severe burns through the body especially for direct current. The most familiar regarding to this is Ohmic heating [18]. It is more dangerous when current go through across the chest and may bring fatal to victim because it will affect the heart quickly.

The effective way to prevent from jeopardy of electric shock is to keep one's body from becoming a part of an electric circuit [19]. Unfortunately, lightning always find the easiest way to ground the flash. Usually the human body will be a part of the way.

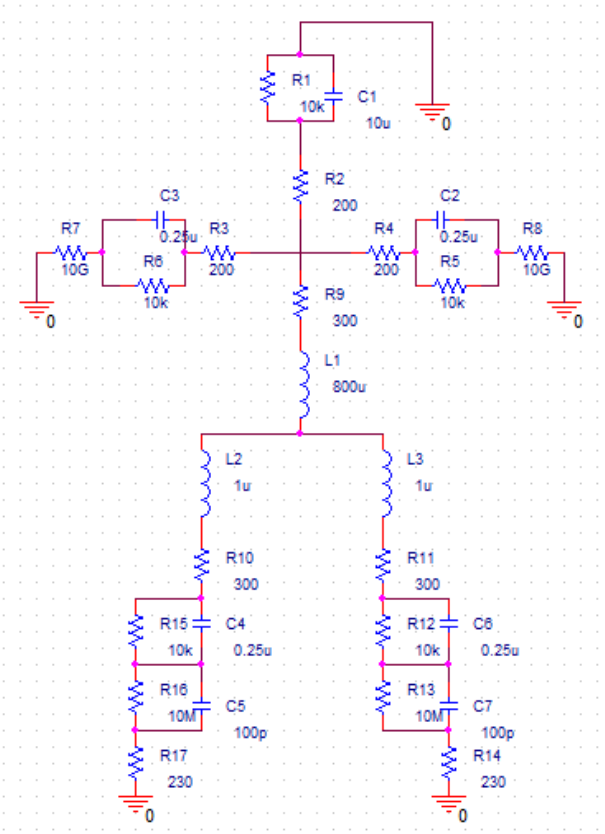

Figure 15. Human body modelling circuit

6. SIMULATION AND DISCUSION

Table 2 and 3 shows the simulation result of lightning strike to human body represented by an electrical circuit. The design and all element's value of equivalent circuit in Figure 16 was based on a model done by V Cooray and N.R.Misbah's[1] . In their work, the human body modelling was injected by standard lightning current impulse 5kA, 8/20µs waveshape [1]. It was shown that victim of lightning injuries will have severe injuries on his face, neck and trunk areas [12].

In our simulation, the measurement of current and voltage at six main point will be taken into account including head, chest, palm, arm, leg and foot for five lightning mechanism injury cases; direct strike, EPR, contact voltage and side splash. In order to illustrate this simulation several factors need to be considered during the modelling stage for all the cases. A structure equivalent circuit of an umbrella is designed for the contact voltage used as the metal object touch by the victim. In side splash cases, a distance between the victim and the object was assumed to be at 1m [7]. Meanwhile for the direct strike, the current was injected directly to the head. In contrast with the EPR, the current is injected at the foot.

Table 2: Measurement of current with respect to point of interest (POI) for four lightning injury mechanism (LIM)

LIM / POI	Direct Strike	EPR	Side Splash	Contact Voltage
Head	746.67A	5.45uA	1.16uA	0
Chest	746.67A	6.22nA	2.27mA	0
Palm	0	0	0	466.58mA
Arm	0	0	0	457.81mA
Leg	373.33A	26A	186.34A	0
Foot	29.87A	100.92uA	7.47mA	0

Table 3: Measurement of voltage with respect to point of interest (POI) for four lightning injury mechanism (LIM)

LIM / POI	Direct Strike	EPR	Side Splash	Contact Voltage
Head	2.07MV	0	1.78MV	0
Chest	1.92MV	9.44uV	1.71MV	0
Palm	0	0	0	4.70GV
Arm	0	0	0	9.28GV
Leg	199.10kV	36.48mV	99.94kV	0
Foot	86.17kV	9.66kV	43.01kV	0

The result shown in Table 2 and 3 tabulate the value of currents and voltages at the six point of interest brought by lightning to the human body through the simulation analysis. During direct strike, the highest current and voltage is at the head and chest with 746.67A and 2.07MV, respectively. This is due to the tendency of lightning to strike at the tallest object. So, the human head will be the main target. The current then will flow down to the leg and foot. However, value of current for palm and arm is zero because the part of arm is connected to the ground in the human body modelling for the simulation. If not, the current will be floating. Although this type of lightning injury mechanism is rare to happen, but the value of current that flow through the human body can bring fatal.

In the case of EPR, foot and leg are the targeted point hence receiving highest value of current and voltage. When lightning strikes the object such as trees, the energy travels along the ground surface known as ground current [21]. Anyone that stands near a lightning strike is highly potential to be the victim of ground current. Some more, the ground current has the ability to affect in a far distance and larger area. Typically, the current of lightning enter the body victim at the contact point closest such as foot, travels through the nervous systems and exits at the contact point farthest from the lightning [18]. This type of lightning injury mechanism might cause severe injury to the foot of the victim but often fatal to the livestock.

As for side splash, the highest current is at the chest with 373.33A. Main target to be struck by lightning in this case is at the chest and the current spread along the body. This occurs when the portion of the lightning that strikes a taller object jump to the near victim that have taken the shelter under a tree to avoid rain. In addition, the person acts as a 'short circuit' for some of energy in the lightning discharge [26]. Usually, a person which struck by side splash will have severe burn at the neck and the worst is fatal.

While in the case of contact voltage, there are no current flow through the head, leg and foot. As expected, current were highly developed at the arm and palm with 466.58mA and 457.81mA since the hand touches the object that was strike by lightning resulting current to flow through it. The potential of being fatal is very low because the muscular organ in the human body is not affected as well by the lightning current. So heart can be function as usual to keeps blood circulating by contacting rhythmically.

7. CONCLUSION

Nowadays, lightning fatalities has become major incident in Malaysia that cause to the injury and deaths as well. An update statistical data and meteorological info shows that lightning fatalities is increasing every year. Most lightning statistics in Malaysia are based on medical record and newspaper reports. However, a good statistical data is still not available because many cases that occur were left unreported especially for lightning injury since it is not compulsory.

Among four lightning mechanism injury (direct strike, side splash, contact voltage, EPR), EPR is the common cases that always happened due to high percentage of the incident around 40% to 50%. Although direct strike usually describe as the cause of injury and deaths, the previous study show that there are only small percentage of the cases up to 5%.

The human body that was stimulate by using P-Spice software with combination of resistor and storage element is to show the relationship of the lightning and injuries from the aspect of electrical field engineering. Results are found to be very useful in the numerical form for four main lightning injuries mechanism which it give easy understanding in order to illustrate the clear image of the risk point of interest when a person was strike by lightning.

8. REFERENCES

[1]Corray, V., The Lightning Flash, IET power and Energy Series 34,2003, Chap 1,pp 6-11, Chap 11, pp 549 – 56.

[2]Malaysia info website. [online] Available: http://kilatmalaysia.blogspot.com

[3] http://www.tbi.usa.com

[4] Lightning and Atmospheric electricity Research at the GHCC website. [online] Available: http://www.thunder.nsstc.nasa.gov

[5] Robert D, MD.B, Women's BC: Lightning Injury, Boston.

[6] Cooper MA, Ab Kadir MZA: Lightning Injury Continues to be a Public Health Treat Internationally. UPM, Selangor Malaysia, CELP, 2010.

[7] N.R. Misbah, Ab kadir MZA, C. Gomes: Modelling and Analysis of Different Aspect of Mechanisms in Lightning Injury. UPM, Selangor Malaysia, CELP.

[8] Fish, M. R., Geddes L. A., "Conduction of Electrical Current to and Through the Human Body: A Review",Journal of Plastic Surgery, (2009), Volume 9.

[9] Lopez RE, Holle RL, Heitkamp TA, Boyson M, Cherington M, Langford K:The Underreporting of Lightning Injuries and Deaths in Colorado. Bull. Amer,1993.

[10] Cherington M, walker J, Boyson M, Glancy R, Hedegaard Clark S: Closing the Gap on the Actual Numbers of Lightning Casualties and Deaths. Preprints, 11th Conference On Applied Climatology, Dallas, January 10-15, Boston, America Meteorological Society, 1999.

[11] http://www.alaboutcircuit.com

[12] Murty, O.P., "Dramatic Lightning Injury with Exit Wound," Journal of Forensic and Legal Medicine,14, Issue 4, (2007), 225-227.

[13] Ab Kadir MZA, Cooper MA, Chandima G: An Overview of the Global Statistics on Lightning Fatalities. Proceedings of the 30th International Conference on Lightning Protection-2010, (2010).

[14] http://www.nst.com.my

[15] Cooper MA, Holle RL: How to use Public Education to Change Lightning Safety Standards(And Save Lives and Injuries), Arizona, Chicago, U.S.

[16] Andrew S, Elizabeth T: Land of Lightning, Star Property, Malaysia, 2009.

[17] Raymond M.Fish, Leslie A.G: Conduction of Electrical Current to and Through the Human Body. Department Research lab.Vol.9.

[18] Odell, M., "The Human Body As An Electric Circuit," Journal Of Clinical Forensic Medicine, Vol. 4, Issue 1, (1997), pp. 1-6.

[19] Dalziel, Charles, F., "Electric Shock Hazard," Spectrum, IEEE, Vol. 9, Issue 2, (2009), pp. 41-50.

[20] IEC Standard 60479-1: 'Effects of Current on Human Beings and Livestock-Part 1'. IEC, 2005

[21] Seidl, S. "Pathological Features of Death from Lightning Strike," Forensic Pathology Reviews, Vol. 4, 1, (2006), pp. 3-23.

[22] Cooper, M. A., Holle, R. L., Andrews, A, "Distribution of Lightning Injury Mechanisms," 20th International Lightning Detection Conference, (2008), pp. 22-23.

[23] Ronald L, Holle: Lightning –Caused Deaths and Injuries in and Near Dwelling and Other Buildings. Holle Meteorology & Photography, Oro valley, Arizona.

[24] http://waghih.blogspot.com

[25] http://www.allaboutcircuits.com

[26] http://www.nws.noaa.gov

A046

MITIGATION OF FERRORESONANCE IN POWER TRANSMISSION SYSTEM USING SERIES COMPENSATOR

Amir Hasam Khavari*, Zulkurnain Abdul-Malek
Universiti Teknologi Malaysia (UTM)
hesamkhavari@fkegraduate.utm.my, zulk@fke.utm.my

Keywords: FACTS devise, Ferroresonance, Harmonic, Magnetic Flux Density.

Abstract: Nowadays power quality becomes critical issue in power electrical system. The connection of three-phase transformer through underground cables is growing fast in residential, commercial, industrial and rural applications. Due to this increasing situation, the possibilities of having a series connected capacitance and a non-linear inductance, prone to ferroresonance, become more probable. Because of that, it is necessary to have a general idea about what would be the best preventive decisions to take in order to avoid unexpected surprises. First of all it is necessary to have accurate model consist of ferroresonance then we should apply any device to smooth the sharp effect of it. In this paper serries compensator which is find into one of the FACTS devise has been applied, static synchronous series compensator (SSSC) to palliate ferroresonance.

I. INTRODUCTION

There is no doubt the enhancement of power quality and stability in power system is critical issues. Ferroresonance is a resonance situation with nonlinear inductance which is equal of capacitance in the network. The inductive reactance not only depends on frequency, but also on the magnetic flux density of an iron. Core coil (transformer iron- core).High overvoltage due to Ferroresonance can cause failures. Initially in 1920 a new definition of ferroresonance has been devised by Boucherot to illustrate the co-existing of two stable ultimate frequency operating points in a series resistors, capacitor circuit and nonlinear inductor. So we may like to control the power flow in a AC transmission line to (a) enhance power transfer capacity and or (b) to change power flow under dynamic conditions (for example disturbances such as sudden increase in load, line trip or generator outage) to ensure system stability and security. The stability can be affected by growing low frequency, power oscillations (due to generator rotor swings), loss of synchronism and voltage collapse caused by major disturbances such as ferroresonance. Power electronic based systems and other static equipment that provide controllability of power flow and voltage are termed as FACTS Controllers. It is to be noted that power electronic controllers were first introduced in HVDC transmission for not only regulation of power flow in HVDC links, but also for modulation to improve system stability (both angle and voltage). FACTS does not refer to any single device, but contains controllers such as SVC, Thyristor Controlled Series Capacitor (TCSC), Static Phase Shifting Transformer (SPST), and newer controllers based on Voltage Source Converters (VSC)-Static synchronous Compensator (STATCOM), Static Synchronous Series Compensator (SSSC), Unified Power Flow Controller (UPFC).

II. RESULTS AND DISCUSSION

Figure 1 shows the circuit and its detail such as R_1, R_2, X_1, X_2.

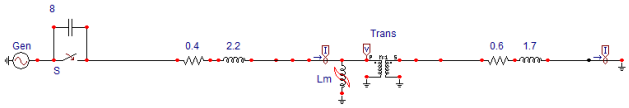

Figure 1. The ATP simulated structure of circuit to investigate ferroresonance

Table 1. Circuit Characteristic

Transformer	Ideal Transformer
Type	TYPE 18
R_1 (primary resistance)	0.4 Ohm
R_2 (secondary resistance)	0.6 Ohm
X_1 (primary inductance)	2.2 mH
X_2 (secondary inductance)	1.7 mH
Non-linear inductance	TYPE 96

Table 1 shows the primary and secondary of resistance and inductance of transformer.The purpose is to exhibit of ferroresonance occurring in the system.

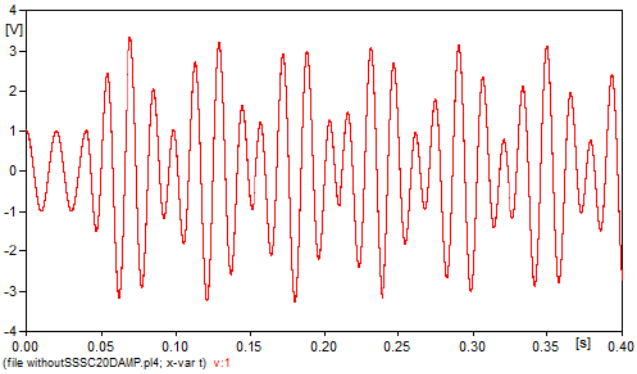

Figure 2. The transformer primary voltage waveform during ferroresonance at switching operation 0.04 s

In figure 2, the output voltage waveform during ferroresonance in the absence of compensator is illustrated. ferroresonance has a trend to produce.

Table 2. Fourier series analysis during ferroresonance after switching operation 0.04s (initial time 0.07-final time 0.09)

Harmonic	Amplitude	Phase	Harmonic	Amplitude	phase
1	2.1972	130.3	8	0.075197	-1.0574
2	0.50337	-6.3424	9	0.070713	-0.97776
3	0.3385	-4.7544	10	0.066737	-0.90596
4	0.25839	-3.7921	11	0.063187	-0.84077
5	0.21008	-3.7921	12	0.063187	-0.78119
6	0.17746	-2.6807	13	0.57114	-0.67583
7	0.13587	-2.0539	14	0.049925	-0.5438
THD=62.939%					

*3/5-1, Desa Skudai Apartment, Jalan Sejehtera15, skudai, johor, Malaysia, +60127556239

Table 2, shows Fourier series analysis during ferroresonance (initial time= 0.07, final time = 0.09). The fundamental harmonic amplitude is 2.1972 and all other harmonics have a value. The total THD reach to 62.939 % which shows that ferroresonance occurs and it can be predicted that this amount of harmonic change the topology of network.

The compensator model is shown in figure 3, Opening times of switch are 1 sec 0.12 sec 0.35 sec and Closing times of switch are 0.35 sec 0 and 0.12 are predominated respectively. Any variation in opening and closing time lead to lose mitigation method.

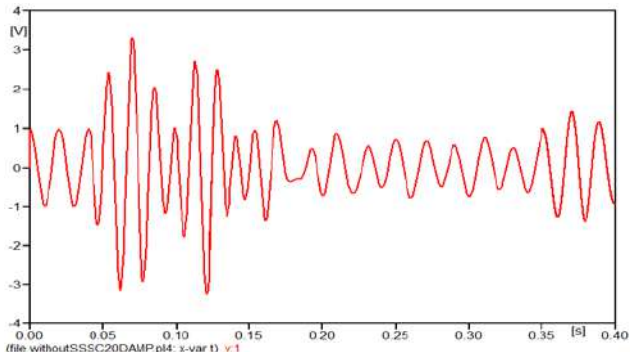

Figure 3. The transformer primary voltage waveform during ferroresonance and at last cycle by applying SSSC (initial time 0.38-final time 0.40)

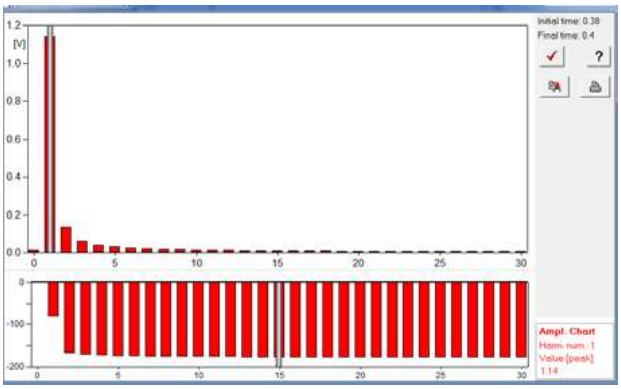

Figure 4. Fourier series analysis after compensation by serise compensator at last cycle (initial time 0.38-final time 0.40)

Figure 4, represents the harmonic analysis after ferroresonance in last cycle (initial time= 0.38, final time = 0.40).

REFERENCES

[1]K.R Padiyar, “FACTS devise controller in power transmission and distribution", new age international publisher, banglore, 2007.

[2]Rezaei-Zare, A.I., R.; Sanaye-Pasand, M.; Mohseni, H.; Farhangi, S., An Accurate Hysteresis Model for Ferroresonance Analysis of a Transformer. Power Delivery, IEEE Transactions, July 2008. 23(3): p. 1448 – 1456.

[3]Arab, H.F., F., Implementation of Preisach-type model for studying of B-H curve influence on the behavior of flux-coupling type SFCL. October. 2009 p. 1 – 6.

[4]Li, H.L.Q.L.X.-b.X.T.L.L., A Modified Method for Jiles-Atherton Hysteresis Model and Its Application in Numerical Simulation of Devices Involving Magnetic Materials. Electromagnetic Field Computation (CEFC), 2010 14th Biennial IEEE Conference, May 2010 p. 1 - 1

A047

LOCALISED SINGLE-STATION LIGHTNING DETECTION BY USING TOA METHOD

Behnam Salimi*, Saeed Vahabi Mashak, Kamyar Mehranzamir, Hadi Nabipour Afrouzi, Zulkurnain Abdul-Malek
Institute of High Voltage and High Current (IVAT), Universiti Teknologi Malaysia
81310 UTM Skudai, Johor, Malaysia
{ sbehnam3,vmsaeed3,Mkamyar3,Nahadi4}@live.utm.my, zulk@fke.utm.my

Keywords: Lightning Locating; Time of Arrival; Short Baseline;

Abstract: This project attempts to provide instantaneous detection of lightning strike lightning location using the Time of Arrival (TOA) method of a single detection station (comprises of four antennas). It also models the whole detection system using suitable mathematical equations so as to give some understanding on the differences between the measured and calculated (theoretical) results. The measurement system is based the application of mathematical and geometrical formulas. Several parameters such as the distance from the radiation source to the station and the lightning path are significant in influencing the accuracy of the results (elevation and azimuth angles). The role of each parameter is examined in detail using Matlab. This study solved the resultant non-linear equations by Newton-Raphson techniques. Methods to determine the radiation source which include the exact coordinate of a given radiation source in 3-dimensions were also developed. Further clarifications on the cause of errors in the single-station TOA method and techniques to reduce the errors and are given.

I. INTRODUCTION

Nowadays, the higher the rate of urbanism and building construction especially in tropical areas, the bigger concern on the safety of facility and human beings due to lightning strikes. Issues related to lightning locating systems are actively being researched. The research is very useful for the purpose of human safety and for the lightning protection system. It can also benefit the insurance companies and weather forecast organizations. Step leaders propagate electromagnetic waves in the range of kHz-GHz within an electrical discharge [1]. There are several available methods to analyze and locate lightning signals such as the time of arrival [2], magnetic direction finding, and interferometry methods. One possible way to increase the accuracy of the location is to combine two or more locating methods as one measurement system [4]. A new method to determine the location of lightning strike with a better accuracy, based on the measurement of induced voltages due to lightning in the vicinity of an existing overhead telephone lines is proposed [5]. In this work, the TOA method is used for lightning locating due to its many advantages.

II. MATERIALS AND METHODS

The geometry of the installed antennas is shown in Figs. 1 and 2. The system consists of four circular plate antennas. Three of them are placed 14.5 meter apart to form two perpendicularly base lines, and the fourth one is diagonally located at 75.58 meter distance away. The antenna output signals were fed into a four-channel digital oscilloscope (Tektronix MSO4104) operating at 8-bit, 5Gs/s using three 50 m long coaxial cables (RG 59, 75 Ω), and one 100 m coaxial cable connected to the fourth antenna

The TOA method detects the electromagnetic waves arrival at the antennas and computes the time difference of arrival. To accomplish this, the detected signals should be properly captured and stored. Generally, the amount of data storage involved is huge and costly. The sequential triggering method had been used to overcome the problem [3]. Various methods can be used to analyze the captured waves. In this work, LabVIEW based cross correlation technique is used to determine the time delays. The LabVIEW software has the advantage of low cost and short processing time [6].

With the help of several geometric formulas, the azimuth and elevation angles of the radiation source can be determined. Together these angles specify the locus of the radiation source [7]. The 3D results can be further analyzed and examined to achieve more exact results [8]. This involves analyses of the 3D waves, application of mathematical formulas and non-linear equations [1].

The Newton-Raphson and Gauss-Seidel techniques can eb used to solve the non-linear equations. However, some problems may result, such as the existence of negative coordinates.
Genetic algorithm is another method to solve the non-linear equations [9]. Using this method, errors such as due to the interferences during wave propagation can be eliminated. Extinguished branches within a step leader can be a source of interference since their corresponding electromagnetic radiation signals will also be captured along the main lightning channel [10].

In the modeling work, significant errors for the azimuth and elevation angles determination based on the TOA method were found. These errors are also previously reported in the 3D lightning locating analyses [11-14].

Figure 1. The location of 1st, 2nd and 3rd antennas.

*Behnam Salimi, Institute of High Voltage and High Current (IVAT), Universiti Teknologi Malaysia 81310 UTM Skudai, Johor, Malaysia, Email: sbehnam3@live.utm.my ,cell: +60127704243

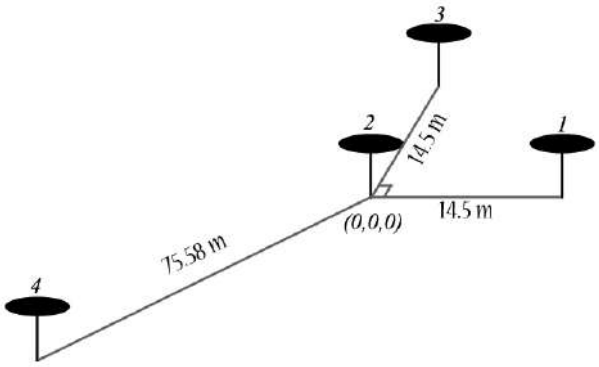

Figure 2. The baseline geometry for lightning locating using four antennas

III. RESULTS AND DISCUSSION

Detailed discussion on data analyses of experimental results using Matlab and LabView are given. An example of the calculated coordinates of a real lightning event is shown in Fig. 3. From the result, it can be seen that the calculated coordinates of lightning path are totally random. Most of the coordinates are distributed on the ground level and the pattern of the lightning path is kind of weird. The Matlab modeling of the whole detection system had already shown that the angles, especially the elevation angle, contain a significant error, and this error contributes to the error when it comes to calculate the x, y and z coordinates.

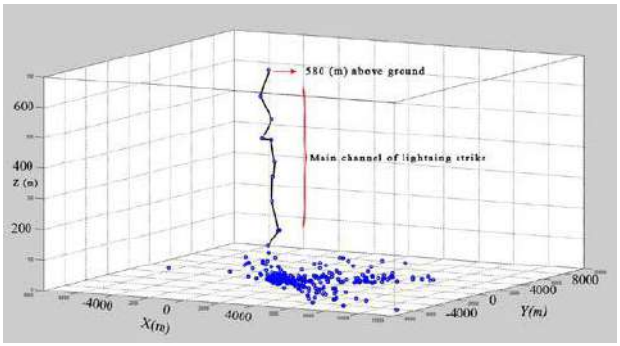

Figure 3. 3D plot of obtained points

REFERENCES

[1]Thanapol Tantisattayakul, Katsumi Masugata, Iwao Kitamura, Ken Kontani, "Broadband VHF sources locating system using arrival-time differences for mapping of lightning discharge process", 1364-6826/$, 2005 Elsevier Ltd.

[2]Rick Roberts, "TDOA Localization Techniques", IEEE P802.15 Working Group for Wireless Personal Area Networks (WPANs), October 2004.

[3]Redy Mardiana, Zen Kawasaki," Broadband Radio Interferometer Utilizing a Sequential Triggering Technique for Locating Fast-Moving Electromagnetic Sources Emitted from Lightning" IEEE Transactions on instrumentation and measurement, vol. 49, no. 2, April 2000.

[4]Paweł Kułakowski, Javier Vales-Alonso, Esteban Egea-López, Wiesław Ludwin, Joan García-Haro, "Angle-of-arrival localization based on antenna arrays for wireless sensor networks", journal Computers and Electrical Engineering, Elsevier, 2010.

[5]Aulia, Zulkurnain Abdul-Malek, Zuraimy Adzis, Novizon,"A New Localised Lightning Locating System Utilising Telecommunication Subscriber Lines", 2nd IEEE International Conference on Power and Energy (PECon 08), December 1-3, 2008, Johor Baharu, Malaysia.

[6]Kang Jianhua, Wang Baoqiang, Guo Jie, Wu Yanjie1"Research on Lightning Location Method Based on LabVIEW" The Eighth International Conference on Electronic Measurement and Instruments, ICEMI'2007.

[7]Saeed Vahabi Mashak, Hadi Nabipour Afrouzi, Zulkurnain Abdul-Malek."Simulation of Lightning Flash in Time of Arrival (TOA) Method by Using Three Broadband Antennas", 5th European Symposium on Computer Modeling and Simulation EMS 2011, IEEE.

[8]Saeed Vahabi Mashak, Hadi Nabipour Afrouzi, Zulkurnain Abdul-Malek." Simulation of Lightning Flash and Detection Using Time of Arrival Method Based on Four Broadband Antennas", First International Conference on Informatics and Computational Intelligence (ICI 2011), IEEE

[9]Daniel Aranguren, Andrés Delgadillo, Mauricio Vargas, Ernesto Pérez and Horacio Torres," Estimation of lightning electrostatic parameters based on atmospheric electric field measurements and genetic algorithms", 19th International Lightning Detection Conference 24-25 April • Tucson, Arizona, USA.

[10]Ray W. Klebesadel, W. Doyle Evans, Edward E. Fenimore, John G. Laros, and James Terrell, "time-of-arrival location technique", LOS ALAMOS SCIENCE, Sidebar 1: Time-of-Arrival Location Technique, Page 15, Summer 1982.

[11]Lothar H, Runhke, Boulder, Colo. "Determining Distance to Lightning Strokes from a Single Station", United Stated Patents 3715660, Feb.6, 1963

[12]Sao, K., and H. Jindoh, Real time location of atmospherics by single station techniques and preliminary results, J, Atmos. Terr. Phys., 36, 261-266,1974

[13]V.A. Rafalsky, A.P Nickolaenko, and A. V Scvets, "Location of Lightning Discharges from a Single-station", Journal of Geophysical Research, vol.100, p. 20829-20838,1995.

[14]W.Itano, I.Nagano, S. Yagitani, M.Ozoki, lightning location with single -station Of VLF sferics. 2nd Kanazawa Workshop. WAVE11- p22, March 2006.

A048

PRELIMINARY INVESTIGATION ON VERY LOW FREQUENCY METHOD FOR ELECTRICAL MACHINE INSULATION DIAGNOSTIC

Hadi Nabipour Afrouzi*, Kamyar Mehranzamir, Saeed Vahabi Mashak, Behnam Salimi, Zulkurnain Abdul-Malek
Institute of High Voltage and High Current (IVAT)
Universiti Teknologi Malaysia
81310 UTM Skudai, Johor, Malaysia
{nahadi4, mkamyar3, vmsaeed3, sbehnam3}@ live.utm.my, zulk@fke.utm.my

Keywords: Very Low Frequency, Insulator, Tan Delta, fault, on site testing

Abstract: Several methods exist for insulation testing, such as DC or AC testing method. Mostly, the users or companies are looking for method with less damaging on insulators and also light equipment is more suitable and interesting for their insulation testing. This paper describes a very low frequency method for insulation testing of machines. VLF can be best replaced for DC testing method because of several disadvantages of this method such as damaging the insulator. Since long time ago VLF is accepted for cable testing, however still it is not so common for testing insulators of machine. Actually, VLF is AC testing but, in very low frequency rate. Therefore, the equipment for testing is not heavy, large and expensive compare to AC testing. The article will discover the methodology to investigate the accuracy of very low frequency method by analyzing the data from experiment. The test will be done at voltage level from 11kv to 24kv and also the rate of frequency is 0.1 Hz. Partial discharge (PD), tan delta (TD), current and voltage are the parameters that will be measured and analyzed in this method.

I. INTRODUCTION

VLF method is not a new method for testing insulators; actually it is used since 70's for generator testing and cable testing. VLF is very low frequency in rate of 0.1 Hz or lower. Basically, the wave in this method is AC but with very low frequency output around 0.1Hz and 0.01Hz [1- 4]. This method is a diagnostic method for cable testing like DC method. VLF method is largely used after it is proven that DC method is destructive and will damage the solid deelectric cable and insulators. It is known that, there is three confirmed test voltage source for diagnostic testing, DC method, power frequency AC and very low frequency (VLF) [5]. The preferred method instead of DC methods is of course AC method, but there are several limitations for using AC method such as weight, size and cost [6-10]. Consider to basic physic, for capacitive load, required power decreases by reducing the frequency in a certain level voltage. On the other hand, the size and weight of power supply will increase when the frequency of voltage is decreased. So the problem of AC method will solve by VLF method. Therefore, VLF is the best replacement of DC method. However, it is primarily used for testing in cable for long time, and also it is suitable for testing transformers and rotating machines [4][12-16].

Figure 1. Winding of megawatt motor while the rotor removed.

REFERENCES

[1] Michael T. Paschal, "Needed Changes in Medium Voltage Cable Testing. Were you in on it? Welcome to the World of VLF", 978-1-4244-6301-5/10/2010 IEEE.
[2] Field Testing of HV Power Cables: Understanding VLF Testing. Hans Gnerlich DEIS Sept/Oct 1995 Vol. 11, No. 5.
[3] IEEE Recommended Practice for Insulation Testing of Large AC Rotating Machinery with High Voltage at Very Low Frequency ANSI/IEEE Std 433-1974 (reaffirmed 1979).
[4] IEC Standard, "Off-line partial discharge measurements on the stator winding insulation of rotating electrical machines" IEC/TS 60034-27, 2006.
[5] Experience With High Potential Testing Hydro Generator Multi Turn Stator Coils Using 60 Hz ac, dc, and VLF (0.1 Hz) Stefano Bomben, Howard Setting, John DiPaul, Rick Glowacki.
[6] G.S. Eager, C. Kat, B. Flyszczyn, J. Densley "High Voltage W Testing of Power Cables", IEEE Transactions on Power Delivery, Vol. 12, No. 2, April 1997.
[7] Junhua Luo, Zhuochun Zhou , Li Zhang,"Optimizing Validation of Voltage and Time for VLF(0.1Hz) Voltage Testing On-site", 978-1-4244-0448-9/07/ IEEE 2007.
[8] G. S. Eager, C. Katz, B. Fryszczyn, J. Densley and B. S. Bernstein, "High Voltage VLF Testing of Power Cables", IEEE Transactions on Power Delivery, Vol. 12, No. 2, April 1997, pp. 565-570.
[9] Srinivas. N.N. Bernstein. B.S. and Decker. R. "Effects of DC Testing on AC Breakdown Strength of XLPE Insulated Cables Subjected to Laboratory Accelerated Aging," IEEE Trans. Power Delivery. Vol. 5. No. 4. Oct. 1990, pp. 1643-1657.
[10] Henning Oetjen, "Principals and Field Experience with the O.1Hz VLF Method regarding the Test of Medium Voltage Distribution Cables", Conference Record of the 2004 IEEE International Symposium on Electrical Insulation, Indianapolis, IN USA, 19-22 September 2004.
[11] Ricliard Reid, "High Voltage Vlf Test Equipment with Sinusoidal Waveform", IEEE Transactions on Power Delivery, Vol. 12, No. 2, April 1999, pp. 565-570.
[12] Henning Oetjen, "Principals and Field Experience with the O.1Hz VLF Method regarding the Test of Medium Voltage Distribution Cables", Conference Record of the 2004 IEEE International Symposium on Electrical Insulation, Indianapolis, IN USA, 19-22 September 2004.
[13] IEEE Guide for Field Testing of Shielded PowerCable Systems Using Very Low Frequency (VLF) IEEE Std 400.2™-2004.
[14] Baur M, Mohaupt P, Schlick T, "New Results in Medium Voltage Cable Assessment using Very Low Frequency with Partial Discharge and Dissipation Factor Measurement " , CIGRE, 11h International Conference on Electrical Distribution, Barcelona, 12-15 May,2003.
[15] Junbua Luo, Liming Yang, Jikang Shi, "Review of Power Cable and Test Technology", High Voltage Engineering, Vol. 30, No.136, 2004.

A049

INVESTIGATION OF FERRORESONANCE MITIGATION TECHNIQUES IN 33 KV /110 V VOLTAGE TRANSFORMER USING ATP-EMTP SIMULATION

Zulkurnain Abdul-Malek, Kamyar Mehranzamir*, Behnam Salimi, Hadi Nabipour Afrouzi, Saeed Vahabi Mashak
Institute of High Voltage and High Current (IVAT), Universiti Teknologi Malaysia (UTM), Johor Bahru, Malaysia
zulk@fke.utm.my, k.mehranzamir@ieee.org, salimi.behnam@ieee.org{nahadi4, vmsaeed3} @ live.utm.my

Keywords: Ferroresonance, ATP/EMTP, Voltage Transformers, Over-voltages, Over-currents, Mitigation Techniques

Abstract: Ferroresonance is a complex non-linear electrical phenomenon that can cause dielectric and thermal problems to the electrical equipment. Electrical systems presenting ferroresonant behavior are nonlinear dynamical systems. The ferroresonance phenomenon may take place in the case when the core of an inductive device becomes saturated, and its current flux characteristic becomes non-linear. While in the case of the linear resonant circuit the resonant frequency is well defined, in the case of the non-linear circuit the oscillations may exist at various frequencies, depending on many factors characterizing the particular case. Customary linear mathematics has problems to construe the ferroresonance phenomenon so it is not fully appropriate for the study of ferroresonance. In this work, ferroresonance phenomena and mitigation techniques in 33kV/110V voltage transformers (VT) are studied using ATP-EMTP simulation. Some mitigation techniques are simulated to show the proficiency of the techniques.

I. INTRODUCTION

Ferroresonance is a complex non-linear electrical phenomenon that can cause dielectric and thermal problems to the electric power equipment. The term 'ferroresonance' has appeared in publications dating as far back as the 1920s, and it refers to all oscillating phenomena occurring in an electrical circuit which contains a non-linear inductor, a capacitor and a voltage source [1-3]. Ferroresonance does not occur customarily or predictably in response to a precise stimulus, hence it is troublesome to analyze it. The stable steady state responses are not unique in these systems which means more than one response can be gotten from the same initial circuit parameters. [2, 3].

The largest electricity utility company in Malaysia, TNB (Tenaga Nasional Berhad, Malaysia) has had several failures of 33kV voltage transformers (VT) in the system. This research has conducted physical investigations on the failed VTs which includes studies on the burn characteristics. The investigation was specifically carried out for the VT failure at PMU Kota Kemuning in Malaysia. The Electromagnetic Transients Program (EMTP) had been utilized to simulate this real system. The next step was to do the transient analyses in order to survey the effect of changes in the conditions of the system. After that the mitigation techniques were used to simulate the efficiency of using these techniques at the system.

II. POWER SYSTEM FERRORESONANCE

A. Ferroresonance Occurrence Conditions

Ferroresonance in a power system can result in any of the following conditions alone or in combination. High sustained overvoltages, both phase to phase and phase to ground, high sustained overcurrents, high sustained levels of distortion to the current and voltage waveforms, transformer heating and excessively loud noise, electrical equipment damage (thermal or due to insulation breakdown) and apparent mis-operation of protective devices.

B. Essential Ferroresonance Provisions

The following four elements are necessary for ferroresonance to occur. First, a sinusoidal voltage source which a power system generator will do quite nicely. Secondly, ferromagnetic inductances, these can be power transformers or voltage transformers. The third one is capacitance which this can come from installed power system capacitors, the capacitance to ground of transmission lines, the large capacitance of underground cable, or the capacitance to ground of an ungrounded system. Finally low resistance, this can be lightly loaded power system equipment, (unloaded transformer for example), low short circuit power source, or low circuit losses. [4, 5].

III. MITIGATION TECHNIQUES

Many studies have been done to identify possible ferroresonance mitigation methods. In this section, a number of ferroresonance mitigation techniques were analyzed. The simulation is being carried out to observe the effects of suggested techniques on the occurrence of ferroresonance.

A. Application of Load Resistance

Resistors can be connected at the secondary side of the voltage transformer to prevent or interrupt the ferroresonance phenomenon. This is a quite well known method of preventing ferroresonance whereby the resistor acts like a damping element to the resonant phenomenon.

B. Delta-Y Connection

This Simulation was done to show the effect of changing Y-Y connected voltage transformer to Delta-Y, and also Y-Delta. The output waveform of the Y-Y connected network will be simulated.

C. Application of Linear Elements on the Primary

Linear components such as resistors or inductors can be connected to the voltage transformer primary to prevent or interrupt the ferroresonancephenomenon. Simulation was carried out by placing linear components in parallel with the VT model. It was observed that placing the linear component in series to voltage transformer model did not help in preventing the ferroresonance.

1. Resistor

After connecting different resistors to the VT, the peak voltage dramatically decreases.

2. Inductor

Inductor was placed in parallel to the voltage transformer .From the results, it is clear that connecting an inductor in

*Kamyar Mehranzamir, Institute of High Voltage and High Current (IVAT), Universiti Teknologi Malaysia (UTM), 81310 Johor Bahru, Malaysia,k.mehranzamir@ieee.org

parallel to the voltage transformer can stop the ferroresonance from occurring

IV. CONCLUSION

Ferroresonance has been shown to be the result of specific circuit conditions, and can be induced predictably in the laboratory. Power system ferroresonance can lead to very dangerous and damaging overvoltages, but the condition can be mitigated or avoided by careful system design. Ferroresonance is triggered to happen due to system disturbances such as overvoltages due to lightning or switching surges, voltage transients, supply frequency variations and etcetera.

For the Kota Kemuning PMU in Malaysia, there was no record of lightning strikes nearby (from TNB Research LLS data), or reports of voltage transients immediately prior to the concerned VT failure. However, a complete data on system disturbances is not available and hence the possibility of ferroresonance occurring due to it cannot be totally eliminated.

REFERENCES

[1]Y K Tong ZE (2001) Ferroresonance experience in uk: Simulations and measurements.

[2]Zulkurnain Abdul Malek, Kamyar Mehranzamir ,Behnam Salimi , S. M. Investigation on the Probability of Ferroresonance Phenomenon Occurrence in Distribution Voltage Transformers Using ATP Simulation. Advances in Intelligent Systems and Computing. Chennai, India, Springer, Berlin Heidelberg. 171/2012.

[3]Zulkurnain Abdul Malek, S.J.Mirazimi, Kamyar Mehranzamir, Behnam Salimi, "Effect of Shunt Capacitance on Ferroresonance Model for Distribution Voltage Transformer," 2012 IEEE Symposium on Industrial Electronics & Applications (ISIEA2012), September 2012,Indonesia.

[4]Afshin Rezaei-Zare; Sanaye-Pasand, M.; Mohseni, H.; Farhangi, S.; Iravani, R.; , "Analysis of Ferroresonance Modes in Power Transformers Using Preisach-Type Hysteretic Magnetizing Inductance," *Power Delivery, IEEE Transactions on* , vol.22, no.2, pp.919-929, April 2007.

[5]B. A. Mork, "Five-legged wound-core transformer model: Derivation,parameters, implementation, and evaluation," *IEEE Trans. Power Del.*,vol. 14, no. 4, pp. 1519–1526, Oct. 1999.

A050

COST BENEFIT AND EMISSION ANALYSIS OF HYBRID ELECTRIC VEHICLE USING HOMER

Sajad A. Anbaran*, Amir Hesam Khavari, Jalal Tavalaei, Zulkurnain Abdul-Malek
Universiti Teknologi Malaysia (UTM)
Sajjad.abdollah@fkegraduate.utm.my*, hesamkhavari@fkegraduate.utm.my , jalal.tavalaei@fkegraduate.utm.my, zulk@fke.utm.my

Keywords: Plug-in Hybrid Electric Vehicle, Energy Cost, HOMER, Driveline

Abstract: Over the recent years hybrid electric vehicles (HEVs) has emerged as promising technology to reduce amount of the green house gases. This is due to the fact that significant amount of the imported petroleum both in developed and developing countries are consumed in transportation sector. However, the final price of the HEVs is one of the obstacles to gain solid foothold in automobile markets. Therefore, this paper studies the cost of hybrid electric vehicles (vehicle price and energy cost) and benefits (less fuel consumption and harmful emission). A detailed model is developed in HOMER to predict and analyze petroleum consumption and emitted tailpipe gas. Two driveline technologies are considered in this study namely, plug-in hybrid electric vehicle and parallel HEV. Finally, results are compared to a typical automobile with internal combustion engine.

I. INTRODUCTION

On the way to achieve green transportation system, only electric and low-emission hybrid vehicles are promising technology in automobile industry to meet regulations required for producing environmentally friendly and efficient vehicles. Despite of the fact that electric vehicles are more environmentally friendly and triple efficient than internal combustion engine (ICE) , but due to reasons they have not yet been able to gain a solid foothold in automobile market, including batteries limited amount of the stored energy, low life cycle owing to frequent charging and discharging and lower provided power intensity by electric motor, as well as, being costly and short range of the vehicle [1].The alternative solution is Hybrid Electric Vehicle (HEV) which offers higher energy efficiency and reduced emitted gas compared to conventional engine vehicles and long driving range, lessen dependency to battery energy sourced as well as higher performance compared to pure electric vehicle. Hybrid electric vehicles price is highly-influenced by varying in design topology, battery price and so on [2]. Hybrid vehicles, however, are greatly expensive than conventional cars and it mostly is due to high cost of the employed battery in the HEV configuration.

Many studies and researches have been carried out on hybrid electric vehicles. However, most of them used different simulation and modelling tool such as REV, PSAT, PSCAD, HEVSIM, MATLAB ,ADVISOR and etc to perform their study. However, few study have been observed used Homer as analytical tool.

II. HEV in HOMER

It is tried to simulate two different topology (SHEV and PHEV) of the HEV in HOMER and perform sensitivity analysis on effective factors on HEV cost. Then results are discussed and compared.

HOMER is a computer model that simplifies the task of evaluation of the design option for both grid-connected and off-grid system. It is developed specifically to meet needs of renewable energy industry's system analysis and optimization.

Table 1. Data for selected component

	Discription	Value
Battery	Type	Vision 6FM2000D
	Capital Cost	$11210
	Replacement	$11210
	Lifetime	$4000
Load(Electric Motor)	Peak Load	8-10yr
Converters(rectifier, inverter and power electronic elements)	Size	50 kW
	Capital Cost	30 kW
	Replacement	$1200
Generator	Size	$800
	Capital cost	30kW
	Replacement	$800
Grid	Two different electricity rate	$400
		Night rate 6 cent
Engine	Petrol	Day rate 15 cent
		$ 2.8-3.368

Three main tasks can be performed by HOMER: simulation, optimization and sensitivity analysis. In the simulation process, HOMER models a system and determines its technical feasibility and life cycle. In the optimization process, HOMER performs simulation on different system configuration to come out with optimal selection. In the sensitivity analysis process, HOMER performs multiple optimizations under a range of inputs to account for uncertainty in the model inputs [3].

This possibility is also predicted that vehicle might be utilized in 4 season countries. Hence, there would be two daily load profiles: one is for cold season that which is used only during noon time (11:00 am-3:00 pm) and one is for normal weather months. The selected component specifications are given in Table 3.

III. RESULTS AND DISCUSSION

In order to compare the benefit cost of the HEVs and amount of emitted harmful gases, two different configurations are modeled in HOMER. In the first modeling a series hybrid electric vehicle is simulated as off-grid system. Subsequently, plug-in HEV is modeled as grid-connected system that is able to charge its battery pack using grid during low electricity rate. In both case sensitivity analysis is performed for battery life time and fuel cost varying according to given data in Table 3. Following figures show simulation and sensitivity analysis result in HOMER.

By comparing two plots in Fig. 1, it can be easily notice that when system is grid-connected, certain amount of the needed electricity is provided from gird. Consequently, in the PHEV system the amount of the consumed fuel is less than SHEV system, therefore, in result, lessen GHG produced by PHEV.

*Sajjad A.Anbaran, 3-5-01 Desa skudai Apartment, skudai, Johor, Malaysia, +60177528057

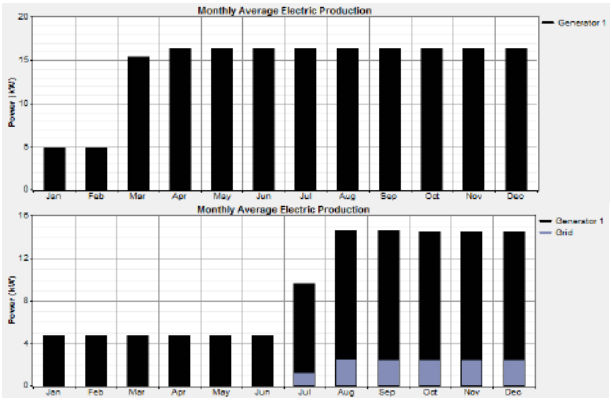

Figure 1. (a) Monthly average electricity production by SHEV, (b) Monthly average electricity production by PHEV

Table 2. Compares operating cost and COE between SHEV and PHEV. As demonstrated, operating cost of the series HEV is greater than PHEV while the COE is less. The reason is, in PHEV topology highly cost battery is operating whereas in SHEV due to less participation of battery in energy generation, it leads to low COE in off-grid (SHEV) system.

Table 2. Cost benefit comparison between SHEV and PHEV

Fuel Price	**Operating Cost $**		**COE**	
$/Lr	**PHEV**	**SHEV**	**PHEV**	**SHEV**
2.8	304,798	348,683	7,426	7,797
3.29	316,429	371,903	7,568	4,982
3.3	316,667	371,125	7,571	4,975
3.368	318,281	374,697	7,591	5,004

REFERENCES

[1] Gao, D.W., C. Mi, and A. Emadi, *Modeling and Simulation of Electric and Hybrid Vehicles.* Proceedings of the IEEE, 2007. 95(4): p. 729-745.

[2] A.simpson, Cost-Benefit Analysis of Plug-In Hybrid Electric Vehicle Technology, in 22nd international battery, fuel cell and hybrid car conferrence. 2008: Yokohama, Japan

[3] K.L. Lau, M.F.M.A., M. Anwari and A.H.M. Yatim, *performance analysis of hybrid photovoltaic/diesel energy system under Malaysian condition.* Energy Conversion and Management, 2010: p. 3245-3255.

A051

ANALYSIS OF HYBRID WIND/DIESEL ENERGY SYSTEM IN WIND BINALOOD WIND FARM

Amir Hesam Khavari*, Jalal Tavalaei, Sadjad Abdolahzadeh Anbaran, Zulkurnain Abdul-Malek, Nouradin Hashemi
Universiti Teknologi Malaysia (UTM)
hesamkhavari@fkegraduate.utm.my, jalal.tavalaei@fkegraduate.utm.my,
sajjad.abdollah@fkegraduate.utm.my,zulk@fke.utm.my, powerutm@gmail.com

Keywords: Diesel; Battery; HOMER, Binalood Wind Farm,

Abstract: This paper discusses a new analytical approach of reliability evaluation for wind-diesel hybrid power system with battery bank for power supply in remote areas. The diesel burns inside the engine and the combustion process causes rotational mechanical energy that turns the engine shaft and drives the alternator. The alternator in turn, converts mechanical energy into electrical energy. Due to highly fluctuating diesel price, such a system seems to be uneconomical and wasteful, especially in the long run if the supply of electricity for rural areas solely depends on such diesel generating system. This paper aims to analyze the potential use of hybrid wind/diesel energy system in remote locations. HOMER software was used to perform the techno-economic feasibility of wind/diesel energy system. The investigation demonstrated the impact of wind penetration, cost of energy and number of operational hours of diesel generators for the given hybrid configurations. Emphasis has also been placed on the percentage of fuel savings and reduction in carbon emissions of different hybrid systems.

I. INTRODUCTION

Renewable energy is the sort of energy which comes from natural resources such as sunlight, wind, rain, sea tides, and geothermal heat, which are naturally replaceable.Wind energy is the kinetic energy that is present in moving air; this kinetic energy in turn derives from the heating of the atmosphere, earth, and oceans by the sun.

A Diesel power station (also known as Stand-by power station) uses a diesel engine as prime mover for the generation of electrical energy.

In Iran these power stations are being used as emergency supply stations. The diesel burns inside the engine and the combustion process causes rotational mechanical energy that turns the engine shaft and drives the alternator. The alternator in turn, converts mechanical energy into electrical energy.Hybrid system is a combination of two or more alternative energy sources; solar power and wind power for instance.By combining two or more separate systems, you'll help to even out their characteristic peaks and valleys in power production. Solar panels only produce energy when they are exposed to sunlight.

At the present time, the designer of hybrid wind energy systems has the choice of a number of performance simulation models for such systems.

II. BATTERY BANK MODELING

In order to improve the system reliability, some of the wind-diesel hybrid systems have battery bank installed. Due to the fact that the wind energy fluctuates greatly with time, if the excess output power of turbine generator is stored in the battery, when the generation capacity is inadequate, the store energy in the battery can be used to offset the power loss.

The figure 1 shows that the battery details of battery banking in the Binalood wind farm.

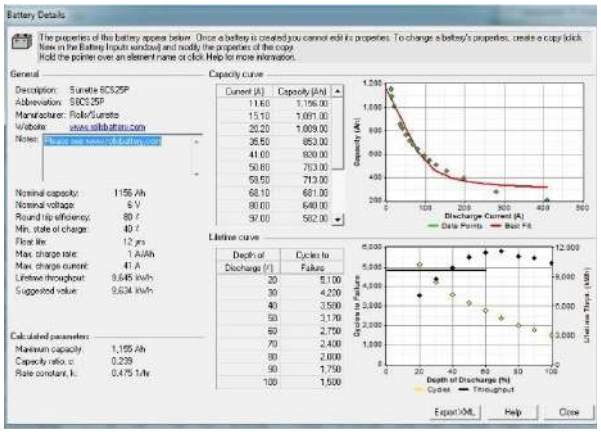

Figure 1. battery detail in the Binalood wind farm

III. RESULTS AND DISCUSSION

A typical hybrid system configuration is illustrated in Figure 2 which consists of wind turbines, diesel generators and battery bank. The approach proposed in this paper studies the performance of wind-diesel hybrid power system with battery bank in discrete wind speed frames on the wind speed distribution to obtain long term reliability indices. The battery charging and discharging scenario depends on the amount of excess wind energy while the system is in operation.

A series of case studies based on the methodology using the data of an operational wind-diesel power system in the "Binalood wind farm" which is located in north of Iran.

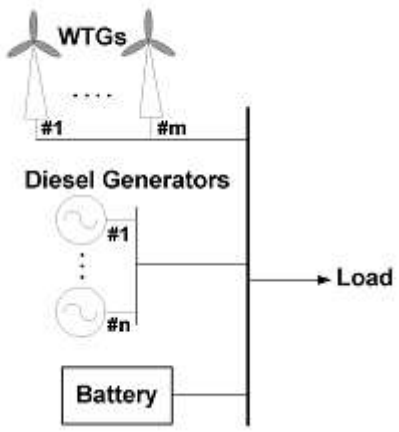

Figure 2. A typical wind diesel power system incorporating battery bank

The objective of this research is to present such a model, developed for the preliminary performance prediction of simple

*3/5-1, Desa Skusai Appartment,Jalan Sejahtera 15, johor bahro, Malaysia, +60127556239

wind diesel hybrid systems. Figure 3 shows that the modeled hybrid system consists of one wind turbines, two identical diesels, battery banking. Primary 1000 KWh for load. For load generation and wind speed modeling, this method results in a time series with a specified mean, standard deviation, autocorrelation and specified lag, and probability density function. Also, a diurnal sinusoidal variation, starting at a specific hour, may also be imposed.

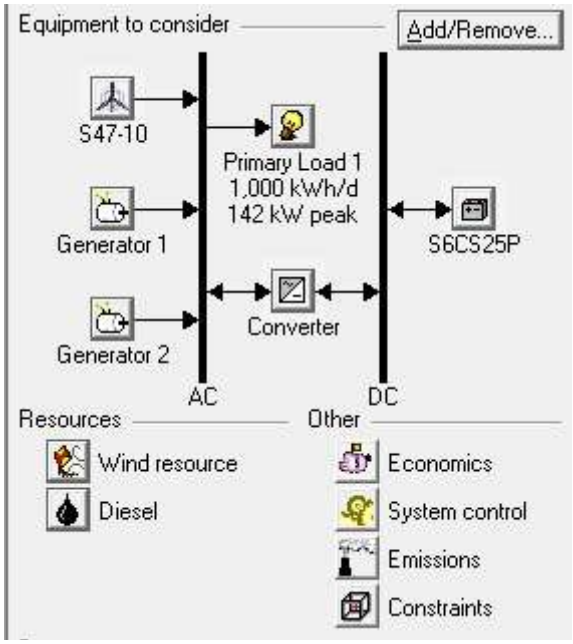

Figure 3. The modeled hybrid 1 wind generator and two Diesel generators with 82 KWH load.

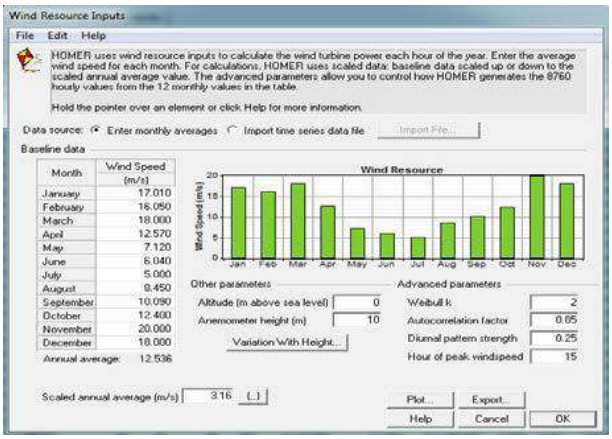

Figure 4. HOMER simulation for wind source input in Binalood wind farm in north of Iran.

This figure 4 shows that wind source input for a system with one wind generator and two diesel generators.the average of wind speed in the Binalood wind farm is 12.536 m/s. Also the speed of wind in each month, in the case of house load consumption of electrical is portrayed.In this novel about 150 house was choosen for case study. So electricity consumption 24 hourly in 12 month and inone year was ghathered.

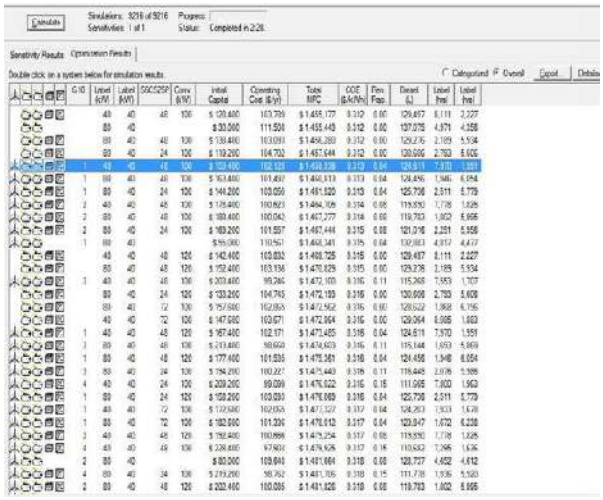

Figure 5. Comparison between different energy systems.

Optimization results was portrayed in figure 5. So, wind turbine is not applied into the system.. The initial capital was 128400 US $ and operation cost was about 103798 US $. in this system we have to pay 1455177 US $ As a total cost.

REFERENCES

[1] X. Liu and S. Islam, SMIEEE,"Reliability Evaluation of a Wind-Diesel Hybrid Power System with Battery Bank UsingDiscrete Wind Speed Frame Analysis" 9th International Conference on Probabilistic Methods Applied to Power Systems KTH, Stockholm, Sweden - June 11-15, 2006

[2] R. Billinton and G. Bai, "Generation capacity adequacy associated with wind energy," IEEE Transactions on Energy Conversion, vol. 19,pp.641-646, September 2004.

[3] R. Karki and R. Billinton, "Cost-effective wind energy utilization for reliable power supply," IEEE Transactions on Energy Conversion, vol. 19, pp.435-440, June 2004

A052

EFFECT OF WATER ON ELECTRICAL PROPERTIES OF REFINED, BLEACHED, AND DEODORIZED PALM OIL AS ELECTRICAL INSULATING MATERIAL

Nazera Ismail[1]* and Y. Z. Arief[1]
[1]Institute of High Voltage and High Current, Faculty of Electrical Engineering,
Universiti Teknologi Malaysia, 81310 Johor Bahru, Johor, Malaysia.

Keywords: palm oil, insulating liquid, electrical properties, chemical properties, physical properties.

Abstract: This paper describes properties of refined, bleached, deodorized palm oil (RBDPO) to be used as an insulating liquid. There are several important properties such as electrical breakdown, dielectric dissipation factor, specific gravity, flash point, viscosity and pour point of RBDPO was measured and compared to the mineral oil. Experimental results of electrical properties revealed the average breakdown voltage of the sample without adding water at room temperature is 13.368kV, however due to effect of water, the breakdown voltage decreased higher than that of commercial mineral oil (Hyrax). The flash point of RBDPO is very high compared to mineral oil which give possibility to be used safely as insulating material. However, the pour point of RBDPO is high compared to mineral oil. The study on the effect of water to RBDPO is still in progress of collecting and analyze of data.

I. INTRODUCTION

Insulation is one of the most important parts in a high voltage apparatus. Insulator described as a material that does not respond to an electrical field and completely resist the electrical charge flow through them. The valence electrons in insulating material are tightly bonded to their atoms. Therefore, it is very stable because the atom has tendency to stick at its valence shell. Practically, the true insulation does not exist. Therefore, the dielectric material with high dielectric constant can be considered as insulator. Liquid insulations are widely used in high voltage systems such as transformer where its function is to provide electrical insulation, suppress corona and arcing. This liquid insulator also acts as a coolant to prevent overheating of the transformer. The liquid insulating oil is widely used due to high dielectric strength, high thermal stability, low dielectric losses and it also can be found in low prices. Petroleum-based mineral oils are proposed for liquid insulator in power transformer because it met almost the specification to be a good insulator [5].

However, the used of mineral oil give negative impact to the environment. This is because it can contaminate the soil and water when serious spill takes place. Furthermore, this type of oil is non-renewable source where their existence in the world has been reduced as the time goes by and probably it will not occupy our needs for the next generation.

Therefore, due to the concern of community towards the environment, many researchers have been conducted to implement the problems.

Many type of oil samples have been examined such as CPKO (crude palm kernel oil), CPO (crude palm oil), CCO (crude coconut oil) and RBDPO (refined, bleached and deodorized palm oil) as electrical insulating material for such purpose [4]. Then, researchers found that the Refined, Bleached and Deodorized Palm Oil (RBDPO) has a potential to be an alternative insulating material because has a similar dielectric characteristics such as high dielectric strength.

II. EXPERIMENT

A. Sample

The sample of RBDPO and mineral oil are used along the experimental process conducted. In order to observe the effect of water to the insulating liquid, distilled water has been added into the sample for 0.2, 0.5, and 1.0 ml, respectively. The used of distilled water is to represent the water that have been condensed in power transformer.

B. Breakdown Voltage

Breakdown voltage test is a part of electrical characteristic insulating oil to measure the strength of the insulating material when a high voltage been injected. The electrode of the test cell is adjusted to 2.50 mm according to standard (IEC60156). The test cell is connected to high voltage up to 100kV and raises the voltage 2kV/s until sparks appear means that the breakdown occurs.

C. Dissipation Factor

The dissipation factor of each sample is tested based on British Standard BS 5737-Measurement of relative permittivity, dielectric dissipation factor and dc resistivity of insulating liquids. The test cell is injected with an increasing of 2.0kV voltage supply. The button at the bridge equipment is pushed to inject the voltage supply. The circuit will completely connect. The dissipation factor value is recorded.

III. RESULTS AND DISCUSSION

Table 1 shows the physical and chemical properties of RBDO compared with other commercial mineral oil, namely Hyrax, Shell Diala B and Silicon oil.

Table 1. Physical and Chemical Properties

Sample/Test	RBDPO	Hyrax	Shell Diala B	Silicon
SG@60/60^{0}F	0.9163	0.8815	0.9045	0.9652
Density@150^{0}C	915.5	880.5	903.5	955.4
API (^{0})	22.98	29.11	25.03	16.51
Viscosity (cSt) 40^{0}C	47.64	10.16	9.284	37.32
100^{0}C	12.59	3.287	2.676	20.13
Pour Point (^{0}C)	9	>-30	>-30	>-30
Flash Point (^{0}C)	320	170	160	330

Specific gravity of RBDPO is 0.9163 at 60^{0}F and it is higher compared to the sample of Hyrax. Lowest the specific gravity better the flow of oil in transformer and it facilitates convection. The pour point of RBDPO is 9^{0}C and much higher than the sample of mineral oil value of -30^{0}C. The pour point should be as lowest as possible to achieve a good flow of oil during cold environmental condition. The operation of transformer generates

*nazerai@yahoo.com, yzarief@fke.utm.my

heat which results the temperature increase in oil. However, when the power supply is disconnected for a long time and re-energizing the transformer in cold condition, RBDPO can solidify due to it high pour point. It may cause a failure in the transformer due to the creation of low creep age distance or voids [1].

Fig. 1 show the dissipation factor of RBDPO compared with other commercial mineral oil. The result shows that the sample of RBDPO has a lowest dissipation factor as compared to the sample of mineral oil. This shows that RBDPO is a good insulating liquid because of its low power losses.

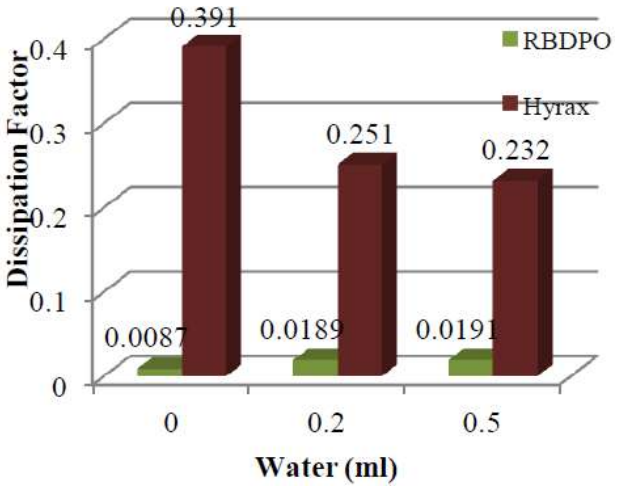

Figure 1. Dissipation factor of the samples

Fig. 2 shows the increasing amount of water injected, reduce the dielectric breakdown voltage of insulating liquid. The graph shows that although the increasing of water is small but it give a great impact on insulation condition.

According to the results obtained, RBDPO shows that it have their own better characteristics compared to mineral oil. However, RBDPO shows its weakness when their breakdown characteristic was greatly effected due to the water. Therefore, it is important to ensure that the insulating liquid is in good condition due to their physical, chemical and electrical standard.

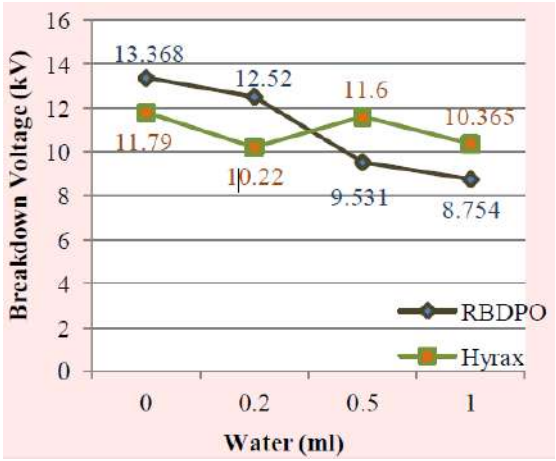

Figure 2. Breakdown Voltage (kV)

REFERENCES

[1] D.C. Abeysundara, C. Weerakoon, J R Lucas and K.C. Obadage K.A.I Gunatunga. "Coconut Oil as an Alternative to Transformer Oil."

[2] Abdul Rajab, Suwarno and Aminuddin S. "Properties of RBDPO Oleum as A Candidate of Palm Based- Transformer Insulating Liquid." 2009 International Conference on Electrical Engineering and Informatics: 548-552, 2009.

[3] Suwarno, F.Sitinjak, Ichwan Suhariadi and Luthfi Imsak. "Study on the Characteristics of Palm Oil and it's Derivatives as Liquid Insulating Materials." 7th International Conference on Properties and Application of Dielectric Materials. Nagoya: 495-498, 2003.

[4] Suwarno and Aditama. "Dielectric Properties of Palm Oils as Insulating Material: Effects of Fat Content." 2005 International Symposium on Electrical Insulating Material. Japan: 91-94, 2005.

[5] http://en.wikipedia.org/wiki/Insulator_(electrical).

A053

INFLUENCE OF ORGANO-MONTMORILLONITE ON ELECTRICAL TREE PARAMETERS IN EPOXY RESIN UNDER AC RAMP VOLTAGE

M. H. I. Saad*, Y. Z. Arief, M. H. Ahmad
Institute of High Voltage and High Current, Universiti Teknologi Malaysia, 81310, Johor Bahru, Johor, Malaysia

Keyword: Electrical Tree, Epoxy Resin, OMMT, Nanofiller

Abstracts: Nowadays, the uses of addictive filler in polymeric insulated cable are seldom in high voltage engineering for purpose of electrical treeing phenomena study. This paper describes the effects of nanofiller on electrical treeing phenomena in polymer nanocomposites. The polymer nanocomposites consist of epoxy resin as the base polymer and organic-montmorillonite (OMMT) as the nanofiller. The influence of these nanofiller on the electrical treeing breakdown resistance was investigated experimentally. The quantity of OMMT were added in epoxy resin (ER) based on weight percentage (wt %) where the weight percentage used in this experiment are 0 wt %, and 1 wt % respectively. All the samples were produced for electrical tree experiment in the form of leaf-like specimens which were categorized into two parts: non-filled sample (0 wt %) and filled sample (1 wt %). Sample of point-to-plane were made and tested under 0.5 kV/s HVAC ramp voltage. The data of tree inception voltage (TIV) and tree breakdown voltage (TBV) were collected and comparative results were made and presented. Electrical analysis shows that the existence of OMMT in ER can make significant improvement as an electrical tree retardant.

I. INTRODUCTION

Electrical treeing is one of the main factors for the long term degradation of polymeric insulation under continuously alternating current [1]. Electrical treeing is defined as a process of partial discharge electrical breakdown in a solid dielectric at very high electric field regions [2]. There are various type of electrical treeing such as bushed, branched, and bush-branched.
The usage of nanocomposites as an insulating medium are quite common because of its excellent in thermal, chemical, mechanical, and electrical properties. Currently, nanocomposites based on epoxy resin and nanofiller are drawn much attention to the researchers because they are expected to have improved over the pure polymer base epoxy resin.

II. RESULTS AND DISCUSSION

Table 1 shows tree inception voltage of base epoxy resin with the average value of TIV is 23.1 kV. While in Table 2 shows tree breakdown voltage of base epoxy resin with the average value of TBV is 28.15 kV.

Table 1. Tree Inception Voltage of base epoxy resin.

No. of Sample	Tree Inception Voltage, TIV (kV)
1	20
2	21
3	22
4	22
5	23
6	23
7	24
8	24
9	25
10	27

Table 2. Tree Breakdown Voltage of base epoxy resin.

No. of Sample	Tree Breakdown Voltage, TBV (kV)
1	24
2	27
3	27
4	27,5
5	28
6	28,5
7	28,5
8	30
9	30
10	31

III. REFERENCES

[1] S. Alapati, M.J. Thomas, "Electrical Treeing in Polymer Nanocomposites", Fifteenth National Power Systems Conference (NPSC), IIT Bombay, December 2008.
[2] L. A. Dissado and J. C. Fothergill, "Electrical Degradation and Breakdown in Polymers", ed. G. C. Stevens, Peter Peregrines, London, 1992.

*mhizzwan@gmail.com, yzarief@fke.utm.my

A054

FLASHOVER PHENOMENA ACROSS SOLID DIELECTRICS IN VACUUM: MECHANISM AND SUPPRESSION

Guan-Jun Zhang*, Hai-Bao Mu, Jun-Bo Deng, Jiang-Yang Zhan, Wen-Wei Shen
State Key Laboratory of Electrical Insulation and Power Equipment,
School of Electrical Engineering, Xi'an Jiaotong University,
28 Xianning West Road, Xi'an, Shaanxi 710049, P. R. China

Keywords : Surface flashover, vacuum, charge injection, secondary electron emission, machinable ceramics

Abstract: Based on the concurrent optical and electrical measurements and microscopic observations, surface flashover phenomena across solid dielectric in vacuum are investigated deeply. A pulsed high voltage is applied to probe the preflashover and flashover phenomana. A generalized model is proposed to explain the different experimental results. It is considered that there are two processed are closely related the flashover, i.e., a process occuring in the surface layer of a material, and a process occuring above the sample surface. Some effective methods are proposed to peomote the surface electric withstanding strength. Finally a kind of machinable ceramics is developed as a novel alternative with the both advantages of inorganic and organic materials.

I. INTRODUCTION

Surface flashover in vacuum is a great limitation of electrical and electronic system, since it typically takes place on the surface region of an insulating material at applied electric stress much lower than the bulk breakdown strength of the material, which is closely related to multiple factors such as the applied waveform, the included angle between electrode and the surface, the elements of desorbed gas, the kinds of material, the surface roughness, the temperature, the gas pressure, the electrical pre-stress and so on.

Essentially we consider it is a kind of complicated surface and interface physical phenomenon. In this paper, some recent research works in our group are reported.

II. MATERIALS AND METHODS

Alumina and polymers are used in our investigation. Each sample is placed on an organic glass substrate plate, and two circular stainless steel slices electrodes are butted on it with a gap spacing of 5 mm. Each electrode is fastened under an organic glass bar with a stainless steel cylinder. All samples are carefully cleaned with absolute acetone, alcohol and distilled water in ultrasonic cleaner before experiments.

Based on the concurrent optical and electrical measurements and microscopic observations, the research works of our group concentrate on the relationship between flashover and surface/interface condition of insulating materials.

III. RESULTS AND DISCUSSION

There are some different optical phenomena detected from the sample surface, and we attribute the preflashover phenomena to the differences between the surfaces of different insulating materials. The experimental results reveal that, under low electric field, prior to field electron emission from the cathode triple junction, electroluminescence phenomena occur due to the radiative recombination of electrons and holes injected into the surface states from the electrodes.

According to the results, the phenomena mentioned above are related to the trapping parameters in the surface layer of a material. This work is a contribution to the traditional secondary electron emission avalanche (SEEA) model, as shown in Fig. 1.

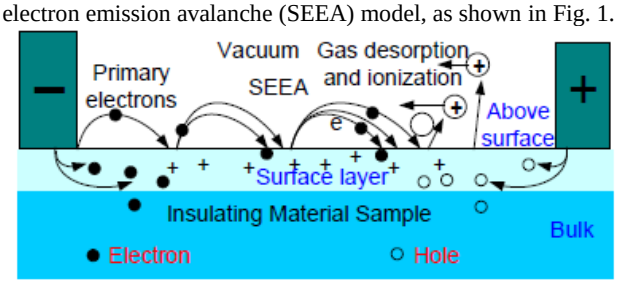

Figure 1. Developed model to describe flashover

A novel machinable ceramic is developed for vacuum insulation system, which has excellent machinable performance and good surface electrical capability. Moreover, different preparation technologies with doping and hydrofluoric acid (HF) etching treatment were investigated. The experimental results show that, the glass phase on the surface of machinable ceramics is an important factor for the largely existing shallow traps, and the shallow traps bring disadvantage in the flashover characteristics. By eroding off the glass phase in the sample with hydrofluoric acid treatment, the shallow traps can be reduced, thus its flashover stability can be greatly improved and its scattering phenomenon is significantly reduced.

REFERENCES

[1] H. C. Miller, "Flashover of Insulators in Vacuum: Review of the Phenomena and Techniques to Improve Holdoff Voltage", *IEEE Trans. EI.*, Vol. 28, pp. 512-527, 1993.
[2] H. Boersch, H. Harmish and W. Enlich, "Surface Discharges across Insulators in Vacuum", *Angew Phys.*, Vol. 15, pp. 518-525, 1963.
[3] Y. P. Raizer, *Gas Discharge Physics.* Berlin, Germany: Springer-Verlag, 1997, pp. 333–352.
[4] G. J. Zhang, X. R. Wang, Z. Yan, Y. S. Liu, M. Okada, K. Yasuoka and S. Ishii, "Optical Studies of Surface Discharge under dc Voltage in Vacuum", *IEEE Trans. DEI.*, Vol. 9, pp. 187-193, 2002.
[5] G. J. Zhang, Z. Yan and Y. S. Liu et al, "Preflashover and flashover phenomena of silicon- vacuum system under pulsed excitation", *Appl. Phys. Lett.* , vol. 80, pp. 3742-3744, 2002.
[6] K. K. Yu, G. J. Zhang, G. Q. Liu, X. P. Ma and G. X. Li, "Effect of surface shallow traps on flashover characteristics across machinable ceramic in vacuum", *IEEE Trans. Dielectr. Electr. Insul.*, Vol. 15, pp. 1464-1470, 2008.

*Guan-Jun Zhang, gjzhang@mail.xjtu.edu.cn, +86-29-8266-8172

A055

EFFECTS OF LOW-TEMPERATURE PLASMA ON BIOLOGICAL CELLS

Guan-Jun Zhang*[1], Zheng-Shi Chang[1], Xing-Min Shi[2], Zhuo-Yuan Dong[1], Wen-Long Liao[1]
[1]State Key Laboratory of Electrical Insulation and Power Equipment,
School of Electrical Engineering, Xi'an Jiaotong University,
28 Xianning West Road, Xi'an, Shaanxi 710049, P. R. China
[2]Environment and Genes Related to Diseases Key Laboratory of Education Ministry,
School of Medicine, Xi'an Jiaotong University,
76 Yanta West Road, Xi'an, Shaanxi 710061, P. R. China

Keywords: Low-temperature plasma, dielectric barrier discharge (DBD), biological cells, inactivation, proliferation, reactive oxygen species

Abstract: Low-temperature plasmas generated by dielectric barrier discharge (DBD) style at atmospheric-pressure are used to study the effects of plasma on biological cells. Different biological cells are chosen, such as the human lymphocytes, *Candida albicans*, Gram-positive S. *aureus* and Gram-negative E. *coli*, etc. Both the inactivation and proliferation effects of no-thermal plasma on the activity and function of different cells are revealed. It is concluded that reactive species inside plasmas play a major role in bacterial inactivation process. Some future prospects and potential uses of nonthermal atmospheric-pressure plasmas in the fields of biological and medical science are presented.

I. INTRODUCTION

Low-temperature plasma, or called non-thermal plasmas, can be easily generated with different gas discharges. Recently these kinds of plasmas at or near atmospheric pressures have received increased attention because of their emerging novel applications in the fields of biological and medical treatment, material modifications, food industry, waste gas and water purification and so on. Especially in micro-organisms treatment fields, some research results have shown very promising prospects in recent years.

In this paper, some recent research works in our group are reported.

II. MATERIALS AND METHODS

The low-temperature plasmas (LTPs) are generated with the dielectric barrier discharge (DBD) style at atmospheric-pressure. Different high-voltage power supplies are employed, e.g., the repetitive pulses, power frequency and medium frequency ac power sources, etc. Two kinds of typical DBD plasma reactors are presented, i.e., the parallel-plate electrode and the coaxial plasma jet. The electrical and optical characteristics of discharge and plasma generated under different conditions are reported, and the effects of power sources, electrode configurations and gas flow rate, etc., on plasma behaviors are discussed.

The different plasma reactors above are used to study the effects of plasma on biological cells. Different biological cells are chosen, such as *Candida albicans*, Gram-positive S. *aureus* and Gram-negative E. *coli*, human lymphocytes, etc.

III. RESULTS AND DISCUSSION

Based on the inactivation kinetics analysis, as well as the morphology images of the bacteria before and after plasma treatment, the effects and mechanisms of plasmas on the chosen bacteria are analyzed. Figure 1 shows the survival number of *S. aureus* cell via plasma exposure time tt different gap spacing (GS). The cells decrease continuously as the exposure time increasing, and 6 orders reduction of *S. aureus* is detected within 8 seconds. After 10s plasma treatment, the *S. aureus* cells are almost killed. The experimental results demonstrate that when the GS is at 3mm, the inactivation effect is better than the others.

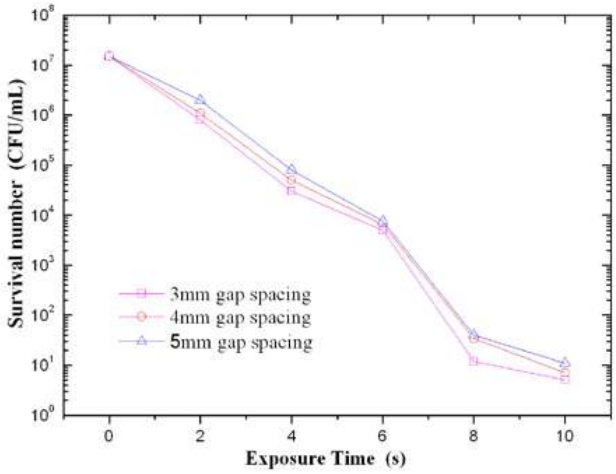

Figure 1. Survival of *S. aureus* with LTP exposure

Insights into the roles of UV radiation, electric field, active species, and charged particles, it is concluded that reactive species inside plasmas play a major role in bacterial inactivation process.

Remarkably, the experimental results about the effects of no-thermal plasma on the activity and function of human lymphocytes *in vitro* culture are exciting, and some possible activation phenomena are discovered, which provides a possible way to cure malignant tumors.

REFERENCES

[1] M. Laroussi, "Nonthermal decontamination of biological media by atmospheric-pressure plasma: Review, analysis and prospects," *IEEE Trans. Plasma Sci*., vol. 30, no. 4, pp. 1409–1415, Aug. 2002.
[2] K. Kelly-Wintenberg, D. M. Sherman, P. P.-Y. Tsai *et al*, "Air filter sterilization using a one atmosphere uniform glow discharge plasma," *IEEE Trans. Plasma Sci*., vol. 28, no.1, pp.64-71. Feb. 2000.
[3] X. Deng, J. Shi, G. Shama, andM. Kong, "Effect of microbial loading and sporulation temperature on atmospheric plasma inactivation of Bacillus subtilis spores," *Appl. Phys. Lett.*, vol. 87, no. 15, pp. 153901, Oct. 2005.
[4] Y. Ma, G. J. Zhang, X. M. Shi, G. M. Xu and Y. Yang, "Chemical mechanisms of bacterial inactivation using dielectric barrier discharge plasma at atmospheric air," *IEEE Trans. Plasma Sci*., vol. 36, no. 4, pp. 1615–1620, Aug. 2008.

*Guan-Jun Zhang, gjzhang@mail.xjtu.edu.cn, +86-29-8266-8172

A056

PROBABILITY OF FERRORESONANCE PHENOMENON OCCURRENCE IN DISTRIBUTION VOLTAGE TRANSFORMERS USING SERIES RLC EQUIVALENT CIRCUIT WITH ATP SIMULATION

Zulkurnain Abdul-Malek , Kamyar Mehranzamir*, Behnam Salimi
Institute of High Voltage and High Current (IVAT)
Universiti Teknologi Malaysia
81310 UTM Skudai, Johor, Malaysia
zulk@fke.utm.my, { mkamyar3, sbehnam3 } @ live.utm.my

Keywords :Ferroresonance, EMTP, Voltage Transformers, Over-voltages, Overcurrents

Abstract: Ferroresonance is a complex non-linear electrical phenomenon that can make thermal and dielectric problems to the electric power equipment. Ferroresonance causes overcurrents and overvoltages which is dangerous for electrical equipment.

I. INTRODUCTION

The first published work related to ferroresonance dates back to 1907 and it analyzed transformer resonances. The word ferroresonance was firstly used by Boucherot in 1920 to describe a complex resonance oscillation in a series RLCcircuit with nonlinear inductance . Nowadays, erroresonance is a widely investigated event in power systems including capacitors, saturable inductors and low losses. That is why it is a repeated event in electrical distribution systems, due to the transformers saturable inductance and the capacitive impact of the distribution lines. This capacitive effect is provided by several elements, such as protective elements (circuit breaker grading capacitance), power transmission elements (conductor to earth capacitance, cables capacitance, busbar capacitance, coupling between doublecircuit lines, capacitor banks), isolation elements (bushing capacitance) or measurement elements (capacitive voltage transformers)[1-4]

In this paper Transient analysis was chosen in order to the changes in the conditions purported ‹by the ferroresonance phenomenon can be simulated. For this purpose the Electromagnetic Transients Program (EMTP) had been utilized for all the simulation work carried out in this project.

II. PHENOMENA RELATIVE TO FERRORESONANCE

Although ferroresonance is a phenomenon with high prediction difficulties, some phenomena related to ferroresonance have been provided through the years. These phenomena can help to identify a ferroresonant situation. Some of them are[4-7] :

- Overvoltage and overcurrent
- Loud noise (magnetostriction)
- Misoperation of protective devices
- Overheating
- Electrical equipment damage
- Insulation breakdown
- Flicker

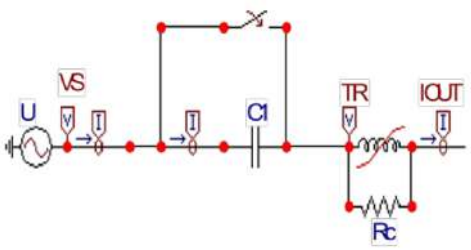

Figure 1. Simulation circuit to verify transformer model of series RLC circuit

III.SERIES RLC EQUIVALENT CIRCUIT

The simulation of series RLC circuit was shown in Figure 1. In this section the effect of the changing the value of resistance in magnetiing branch (Rc) is investigated. This circuit is supplied by AC source peak voltage of 26.94 KV with 50Hz frequency. Table 1 shows the output waveform for 10MΩ of Rc where ferroresonance has occurred. It is clear from the table 1 that Rc must be atleast 10MΩ for ferroresonance to occur.

IV. RESULTS AND DISCUSSION

Ferroresonance is triggered to happen due to system disturbances such as overvoltages due to lightning or switching surges, voltage transients, supply frequency variations and etcetera. Under normal operating conditions, no ferroresonance can occur since the preconditions for ferroresonance are not fully met.

Table 1. The effect of changing the value of resistance in magnetizing branch for series RLC circuit

Rc (MΩ)	Peak Voltage At Transformer (kV)		Peak Current At Transformer (mA)		Frequency Of System (Hz)		Ferro-Resonance
	Before	After	Before	After	Before	After	
0.001	26.943	0.0123	26944.0	8.464	50	50	No
0.1	26.944	0.988	269.45	8.462	50	50	No
1	26.943	8.391	27.327	8.0489	50	50	No
10	26.943	50.667	4.517	40.547	50	50	Yes
160	26.942	80.977	3.860	83.683	50	50	Yes
10000	26.942	112.28	3.859	125.39	50	50	Yes

However, when disturbances occur, there may be changes in the circuit configuration in terms of capacitance, inductance (non linear) and critical frequency, all of which acting together lead to ferroresonance.

REFERENCES

[1] Moses P, Masoum M, Toliyat H (2011) Impacts of hysteresis and magnetic couplings on the stability domain of ferroresonance in asymmetric three-phase three-leg transformers. Energy Conversion, IEEE Transactions on 26(2):581 –592.

[2] Santoso, S., Dugan, R. C., Grebe, T. E., Nedwick, P. “Modeling ferroresonance phenomena in an underground distribution system” IEEEIPST ’01 Rio de Janeiro, Brazil, June 2001, paper 34.

*Kamyar MehranZamir, Institute of High Voltage and High Current (IVAT), Universiti Teknologi Malaysia, 81310 Johor Bahru, Malaysia, mkamyar3@live.utm.my, 0060177428680

[3] Rezaei-Zare A, Mohseni H, Sanaye-Pasand M, Farhangi S, Iravani R (2006) Performance of various magnetic core models in comparison with the laboratory test results of a ferroresonance test on a 33 kv voltage transformer. In: Power Engineering Society General Meeting, 2006. IEEE, p 8.
[4] M.Val Escudero, I.Dudurych and M.A.Redfern, "Characterization of Ferroresonant Modes in HV Substation with CG Grading Capacitors", IPST '05 - Montréal, Canada, June 19-23, 2005, Paper 12a.
[5] B.Vahidi, R. Shariati Nasab, S. Ghaghaheh Zadeh and E. Abedi, "Ferroresonant Overvoltage Investigation in Wye-Wye Transformers on Transmission System by Using MATLAB", CHLIE 2005, 30th June to 2nd of July, Marbella, Spain.
[6] Martinez, J.A. and Mork, B.A., "Transformer modelling for simulation of low-frequency transients", CIRED 2003 Technical Programme, Round Table Discussions: Beta Day Sessions, 2003, Paper #91.
[7] Daniel W. Durbak, "Ferroresonance Damping Device Solves Amtrak's Problem", Shaw Power Technology Inc., Newsletter Issue 96, October 2004. N. Netravali and B. G. Haskell, *Digital Pictures*, 2nd ed., Plenum Press: New York, pp. 613-651, 1995.

A057

ANALYSIS OF DAMPING CIRCUIT OF SPARK GAP IN SERIES COMPENSATION EQUIPMENT

Bai-Peng Song[1]*, Wen-Wei Shen[1], Wei Song[1], Guan-Jun Zhang[1], Yu-Gan Niu[2], Jun-Liang Wang[2], Li-Miao Zhang[2], Yi-Qun Zhang[2]
[1]State Key Laboratory of Electrical Insulation and Power Equipment, Xi'an Jiaotong University. Xi'an, 710049, China
[2] Pingdingshan Power Supply Company, Pingdingshan, Henan 467001, China

Keywords: Damping circuit, Spark gap, Series capacitor, Simulation, Series compensation equipment.

Abstract: Series compensation is a means of improving the performance of power transmission. As the protective device, spark gap is installed on both sides of series capacitor. When the lines is struck by fault, the gap can strike the arc and discharge to protect series capacitors from being burned up. If the spark gap breakdowns, the damping circuit should limit discharging current. This paper discussed the influence of circuit parameters i.e. parallel resistance, inductance and arc resistance, on the discharging current. With the increasing of inductance, discharging current went down and the harmonic during the discharge oscillation decreased. Discharging current fell and then increased up if the parallel resistance contiued growing. Besides, the energy consumption of arc resistance was disscussed.

I. INTRODUCTION

As a means of improving the performance of transmission, series capacitors is widely used in the grid because of the positive effects provided by series compensation such as improving circuit voltage profile, reducing voltage fluctuations and higher circuit capacity. The series capacitor equipment typically includes the capacitors, overvoltage protection equipment, a bypass switch. MOA and self-sparking gap form the overvoltage protection of the capacitors. Self-sparking gap is widely used in many electric devices and experimental equipments, e.g. arresters and impulse voltage generators. When a fault occurs in the power system, the voltage across the series capacitors increases and the spark gap act, resulting in conducting the current to the parallel bypass switch or breaker interruptting the current. In this paper, we discuss the influence of damping circuit on spark gap discharging. It is helpful to choose the correct damping circuit parameters for reducing the damage and ablation of self-sparking gap device when designing the overvoltage protection of the capacitors.

II. MATERIALS AND METHODS

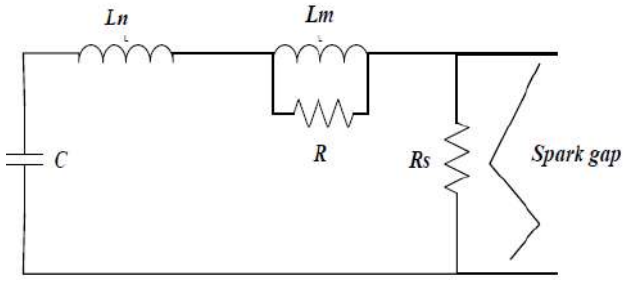

Figure 1. Schematic of damping circuit when spark gap discharging

When the spark gap discharges, the equivalent circuit model is built as Fig.1. Discharging gap channel is substituted by a small arc resistance. Eq.(1) presents the third order differential equation of the equivalent circuit. The paper studies the circuit and builds simulation model by using Matlab and ATP-EMTP.

$$\begin{aligned}\frac{dU_C}{dt} &= \frac{-I_C}{C} \\ \frac{dI_C}{dt} &= \frac{U_C - U_R - R_S \times I_C}{L_N} \\ \frac{dU_R}{dt} &= R \times \left(\frac{U_C - U_R - R_S \times I_C}{L_N} - \frac{R_S \times U_R}{L_M}\right)\end{aligned} \quad (1)$$

III. RESULTS AND DISCUSSION

The paper disscusses influence of circuit parameters on the discharging current and the consumption of resistance parallel and arc resistance, i.e. W_R and W_{RS}.

Table 1. Influence of inductance on the discharging current and the consumption

	C=200μF , R=5Ω					
μH	50	100	150	200	250	300
I_{m1}/A	22000	17525	14909	13151	11873	10899
I_{m1}/I_c	110	87.625	74.545	65.755	59.365	54.495
W_R/J	6201	11844	15390	17730	19370	20577
W_{RS}/J	22698	17055	13506	11170	9529	8322

With the inductance L_m growing and a cercain capacitor C and resistance, the first amplitude of currrent oscillation wave I_{m1} goes down. For reducing the damage and ablation of self-sparking gap device, I_{m1}/I_c should be limited below 100, I_c being the rated current. Consumption of arc resistance W_{RS} goes down while that of parallel resistance W_R rising. In this paper, influence of parallel resistance on the discharging current and the consumption is also been studied. If the parallel resistance increases, I_{m1}/I_c decreases and then goes up, indicating there being the minimum current value. Besides, oscillation of discharging currrent waves reducs with more inductance and less parallel resistance.

IV. CONCLUSION

The damping circuit parameters affects the the discharging current and the consumption of damping circuit. More inductance and less parallel resistance in a certain range can reduce the current and the damage or ablation of self-sparking gap.

*Song Baipeng, e-mail: songbaipeng.123@stu.xjtu.edu.cn

A059

ANALYSIS AND SIMULATION OF A FLYBACK CONVERTER FOR MICRO MACHINING BIOMEDICAL COMPONENT

Nazriah Mahmud*, Azli Yahya, Mohammed Rafiq Abdul Kadir
Faculty of Health Science and Biomedical Engineering
Universiti Teknologi Malaysia, 81310 Johor Bahru, Johor

Keywords: Electrical Discharge Machining, Flyback converter.

Abstract: Electrical Discharge Machining is a controlled process where pulsed electrical discharge is used to erode metal in workpiece. A number of EDM power supplies utilizing different topologies have been widely developed mainly for manufacturing micro components. Recently, a demand in micro machining has also extended into biomedical applications. In this paper a current mode flyback converter is implemented for micro machining biomedical component. A MATLAB/SIMULINK modeling technique of flyback converter is presented and the effectiveness of the flyback converter topology on machining performance is evaluated by changing the input voltage.

I. INTRODUCTION

Electrical Discharge Machining (EDM) is one of the earliest non-conventional material removal manufacturing processes. It is a controlled process where thermal energy is used to generate heat that melts and vaporizes the workpiece [1]. In EDM process, power supply is one of the important elements in providing thermal action between the electrode and the workpiece [2]. Since EDM has been accepted for manufacturing micro scale products, the important factor need to be considered is the level of discharge energy during machining. For good quality micro products produce, the discharge energy supplied must be reduced. It is suggested to limit the magnitude of the energy in order of 10^{-5} J to 10^{-9} J [3]. Previously, RC power supply unit is widely used in Micro EDM due to its capability of generating low discharge energy [4-5]. However, this power supply gives low material removal rate due to time to charge the capacitor. Thus, due to evolution in advanced power electronics system, a number of power supplies have been developed for better machining performance.

Machining products using micro machining not only become one of the important methods in manufacturing industrial part, but has also been introduced in biomedical field. A study by Tamaki et al. [6] shows that EDM able to produce sufficient surface roughness that help in improving implant lifespan. Therefore, in this study a new design of power supply will be explored in an attempt to develop a Pulse Power Generator (PPG) for machining the micro pits on hip implant which reduce the micro crack as well as eliminated the melted stray eroded material.

Now, flyback converter is the most commonly used circuit for low output power application. It's simple circuit topology and low cost makes it widely used for low output power range [7]. Thus, the power supply utilizes the flyback topology operated in current mode is implemented in this study for Micro-EDM application. Since EDM process requires a current source that can be switch on and off for very short time periods, a pulse is applied to the system. A MATLAB/SIMULINK modeling technique is employed and simulation results are provided to demonstrate the efficiency of the proposed flyback converter model.

II. METHODOLOGY

In this paper, the circuit design as shown in Figure 1 of Flyback converter topology is first described and the behavior model technique as presented in [8] is adopted. Then, a MATLAB/SIMULINK model of the system is implemented. The model is based on the mathematical representation as in Eq. (1)~(2) when switch Q is on and Eq. (3)~(4) when switch Q is off. The simulated waveform of primary side inductance current and output voltage were then observed by varying the input voltage. The input voltage is varied from 340 to 100 V. The simulated results are provided to demonstrated the validity of the proposed flyback converter model.

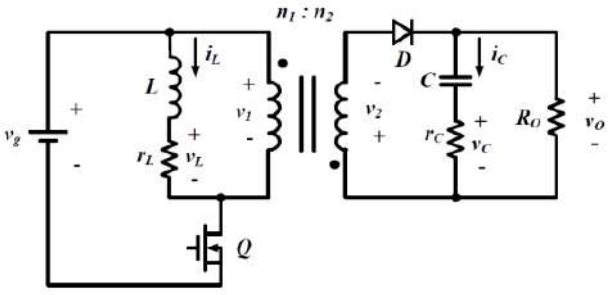

Figure 1. Flyback converter design with magnetizing inductance

$$\frac{di_L}{dt} = \frac{1}{L}\left(v_g - i_L r_L\right) \quad (1)$$

$$\frac{dv_c}{dt} = -\frac{1}{C}\frac{V_o}{R_o} \quad (2)$$

When switch Q is off, the state equation can be written as:

$$\frac{di_L}{dt} = \frac{1}{L}\left(-\frac{n_1}{n_2}v_o - i_L r_L\right) \quad (3)$$

$$\frac{dv_c}{dt} = \frac{1}{C}\left(\frac{n_1}{n_2}i_L - \frac{V_o}{R_o}\right) \quad (4)$$

III. RESULTS AND DISCUSSION

Figure 2 shows the MATLAB/SIMULINK block diagram. The switching frequency is 100 kHz with 30% duty cycle. The input voltage was varied as 340 V, 240 V and 100 V. Figures 3-5 show simulated results by varying the input voltage.

*Nazriah Mahmud, fkbsk, utm, nazriah2@yahoo.com

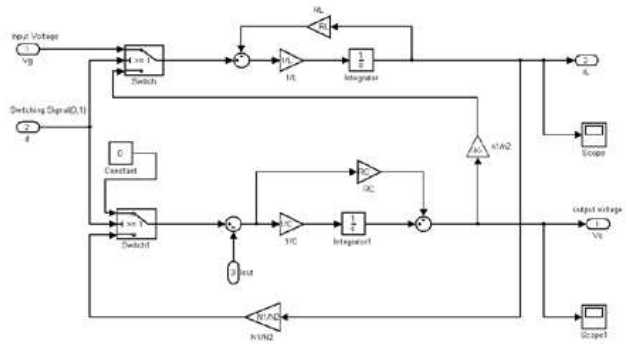

Figure 2. Sub-block diagram of the flyback converter

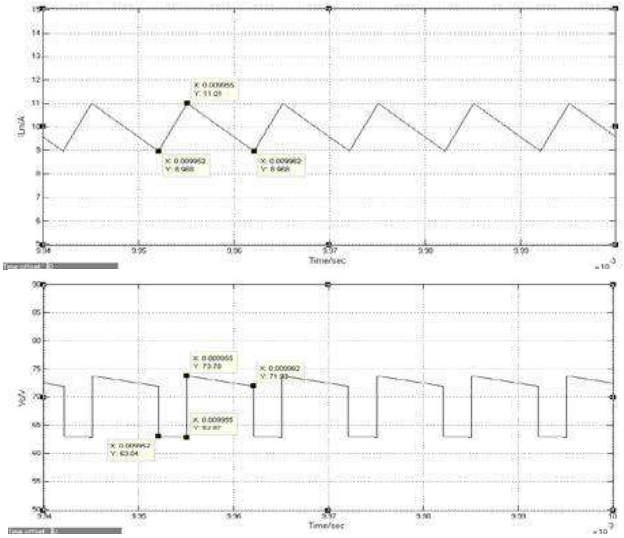

Figure 3. Primary inductance current, ILm and Vo with Vin =340V

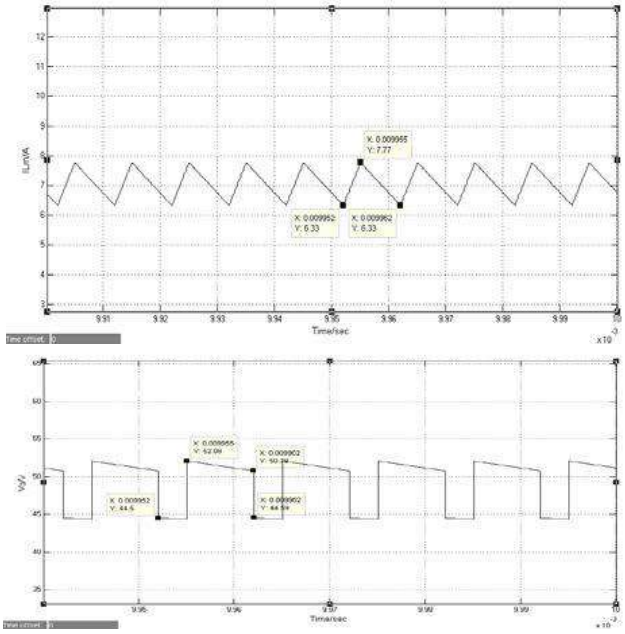

Figure 4. Primary inductance current, ILm and Vo with Vin =240V

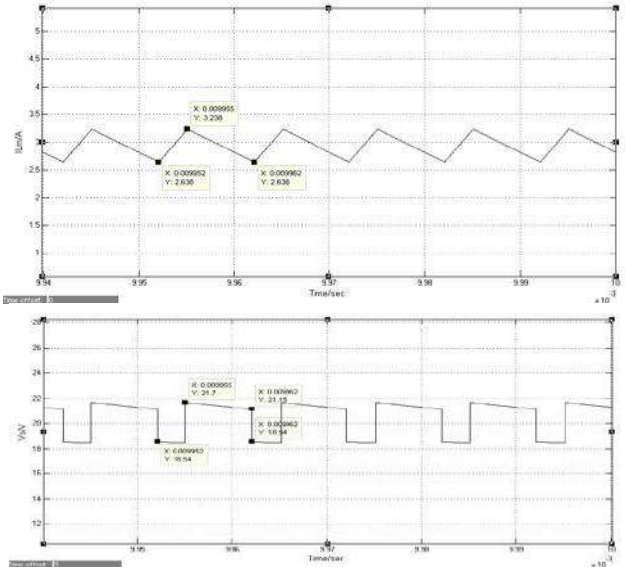

Figure 5 Primary inductance current, ILm and Vo with Vin =100V

The simulated results are compared between three different input voltage to verify the efficiency of machining performance towards changing input voltage. The waveform pattern is similar but the time for the system to achieve steady state is different.

REFERENCES

[1] M. Kiyak and O. Çakir, "Examination of machining parampeter on surface roughness in EDM of tool steel*"*, Journal of Material Processing Technology, Vol. 191, pp. 141-144, 2007.

[2] W. Mysinski, "Power supply unit for an electric discharge machine", Power Electronics and Motion Control Conference, EPE-PEMC 2008, 2008.

[3] C.M.F. Odulio, L.G.S., M.T. Escoto, "Energy-saving Flyback converter for EDM applications*"*. TENCON 2005 IEEE Region 10 2005: pp. 1-6, 2005.

[4] Y. S. Wong, M. R., H. S. Lim, H. Han and N. Ravi, "Investigation of micro-EDM material removal characteristic using single RC-pulse discharge ",Journal of Materials Processing Technology, Vol. 140, pp. 303-307, 2003.

[5] H.S. Tak, C.S.H., D.H. Kim, H.J. Lee, H.J. Lee, M.C. Kang, "Comparative study on discharge conditions in micro-hole electrical discharge machining of tungsten carbide (WC-Co) material". Transactions of Nonferrous Metals Society of China, 19(Supplement 1): pp. s114-s118, 2009.

[6] Y. Tamaki, Y.K., I.K. Jang and T. Miyazaki, "Bone Regenerative Potential of Mesenchymal Stem Cells on a MicroStructured Titanium Processed by Wire-Type Electric Discharge Machining". The Open Materials Science Journal, Vol. 4: pp. 113-116, 2010.

[7] B.Nagaraju, K.S., "A Novel Active Clamped Dual Switch Flyback Converter*"*. International Journal of Engineering Research and Applications (IJERA), 2(1): pp. 195-206,2012.

[8] L. W. Hsin, W. S. Chung and L. Y. Hua, "Learning switched mode power supply design using MATLAB/SIMULINK", IEEE Region 10 Conference, 2009.

A060

IMPLEMENTATION OF REAL TIME LIGHTNING DATA FOR PEKAN AND VALIDATION DATA WITH LIGHTNING TNBR

Nurul Fazirah binti Ghazali, Wan Ismail bin Ibrahim
Faculty of Electric and Electronic Engineering, Universiti Malaysia Pahang
nurulfazirah@hotmail.com, wismail@ump.edu.my

Abstract: Pekan are located at east of peninsular Malaysia which that like other tropical countries which experience very high cloud to ground (CG) density. Many members of public has lack information about lightning, therefore the website are responsible to publish the lightning real time data at this area. This thesis presents the real time lightning data for Pekan which detected by using LD-250 Boltex lightning detection hardware that connected to the computer and analyze the data using Lightning/2000 software. LD-250 is sensor that detect lightning using magnetic direction finder (MDF). Data collected by Lightning/2000 are compared with Tenaga Nasional Berhad Research Sdn.Bhd (TNBR) to avoid from forecast error before it can be publish to the website.

I. INTRODUCTION

Lightning is a common phenomenon in Pekan region which located at coast of Laut China Selatan. The populations in this area consist of fishermen who make a livelihood from the sea and industrial park which exposed to damage that cause by lightning. A few information about lightning occurrences at this region might help these people to buckle up during lightning. It is important to understand the phenomena and characteristic of the lightning because lightning cannot be prevented.

This project is to develop a website for real time lightning data in Pekan region. The purpose of developing this website is to publish real time lightning data in 50km radius from the sensor coordinate which is located on the rooftop of UMP FKEE building. This website can contribute in safety and knowledge in lightning to people in this region as the purpose of this project.

Malaysia meteorological department can broadcast the weather information to people around, but they are not focusing on lightning occurrence. Even in their website not mentioning the location of real time lightning data which is very important for some factory or organization for safety purpose. By implementing the real time lightning data for Pekan in the website, people will start take a serious precaution during storm which might bring lightning along.

This project is collaboration with Tenaga Nasional Berhad Research (TNBR) to validate the data collected by LD-250 with data collected by TNBR using IMPACT ESP sensor which is located at eight difference location in Malaysia. TNBR also tracking the real time lightning data and estimating fault location. [1]

II. METHODOLOGY

1. Software and hardware installation

Lightning/2000 is a software tool that cans be used to Replay "canned" lightning archive files created by Lightning/2000, or when used on a system that has the Boltek lightning detection hardware and antenna, detect and analyze real-time lightning data and can be displayed both textually and graphically. It is able to process all available sensor information in real time, and thus can compute a separate location for each individual stroke in the flash.

Do the backgrounds map installations for Pekan after finished installed the software in the computer. This software can display more than 300km radius of lightning in that area, but only 30km radius were selected as limitation area of the forecasting station project.

2. Validation data with TNBR

Data validation is very important to make sure all the collected data is accurate. The LDN has made possible detection of lightning in the Peninsular Malaysia in real-time. Quantitative data on stroke locations, time and parameters have enabled accurate estimation of lightning severity in Malaysia. This information which never has been available before has provided TNB the opportunities to be more scientific and quantitative in their approach when dealing with lightning [2]. The LDN has become an invaluable resource for TNB to facilitate lightning mitigation actions.

Historical data obtained from Tenaga Nasional Berhad (TNB) Research, Peak discharge current, location and time. After several weeks of collecting data, all the collected data must be validate with lightning TNBR before proceeding to the next step. Once the data had been validate, analyze on comparison between data and find the error percentage. Only accurate data will be publishing in the website.

3. Data publishing

Publishing data into the website include the process of:

i. Domain registration - Register the domain name using lightningpekan.com which is the address and foundation of the website.
ii. Web development scripts - The purpose of the scripts is to grab the Lightning/2000 data and display it and graph it on the web browser. Use Ajax tools for JavaScript to updates the data every minute so we don't need to refresh the page to get new data.
iii. Write custom summary language scripts - Write the custom summary scripts that control the behavior of system programs. In Lightning/2000, the scripting language is already provided during the installation but can be edited depends on what condition we want to display on the website. The custom summary script must be save in text file and give it a place to store the outputted data.
iv. Data uploading - This is the process of sending data from a local system to a remote system which is a server. Use file manager in control panel to upload data from Lightning/2000 into the website. The entire database uploaded must be in the required file format so that it can be generate properly in the website.

III. RESULT AND ANALYSIS

1. Data validated with TNBR

Data collected by Lightning/2000 are validate with TNBR lightning data by comparing the lightning amplitude and time occurrences of each lightning. Since LD-250 sensor cannot identify the type of stroke, all collected data in Lightning/2000 for the amplitude are positive. Table 1 shows the validation data for March 2012.

Date	Lightning/2000		TNBR	
	Time	Lightning amplitude	Time	Lightning amplitude
2/3/2012	17:36:26	26.8	17:37:13	-19
6/3/2012	17:35:34	24.1	17:35:34	-22
6/3/2012	17:53:55	29	17:52:10	-46
6/3/2012	18:02:04	28.4	18:02:58	-23
6/3/2012	18:34:31	40.2	18:34:29	-42
7/3/2012	17:53:21	32.4	17:52:46	-33
8/3/2012	4:01:45	42.1	4:01:57	-42
8/3/2012	4:18:54	14.4	4:17:39	-14
8/3/2012	5:06:40	63.9	5:17:44	64
8/3/2012	5:29:28	76.9	5:28:39	-79
21/3/2012	14:09:09	38.9	14:09:09	-31
21/3/2012	14:16:51	15.1	14:15:35	-14
21/3/2012	17:07:35	25.5	17:08:01	-36
27/3/2012	17:25:27	20.6	17:25:56	-28
27/3/2012	17:33:42	22.5	17:33:46	-21
27/3/2012	17:45:41	21.4	17:45:08	-22
29/3/2012	17:01:19	36.7	17:01:29	-33
29/3/2012	18:42:38	23.6	18:40:46	-28

Table 1. Validation data with lightning TNBR

2. Website (http://lightningpekan.com/aninoquisi/wxl2k.php)

Data was successfully uploaded to the website through file transfer protocol from Lightning/2000. Real time lightning display will automatically update every 60 second. Lightning map information is also provided for more detail information about the lightning occurrences.

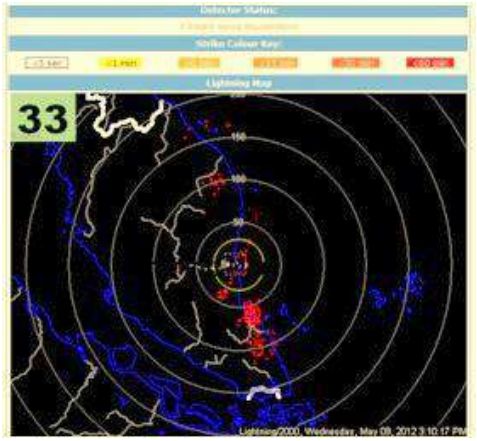

Figure 1. Real time lightning display on website

Daily strokes data are also publish in the website with flash, stroke and noise rating. The graph at the bottom of the page indicates the total flash in last 60 minutes.

CONCLUSION

The lightning website enable the reader to estimate the lightning occurred for their particular locations. Factories and building around Pekan will be more aware of the lightning strikes. It is important to understand the phenomena and characteristic of the lightning for mitigation of lightning related problems.

REFERENCES:

[1] NoradlinaA;MohdP.Y;Dr.NadiahS.A;,"Implementation and use of lightning detection network in Malaysia," IEEE international conference on power and energy (PECon 08),2008.

[2] M.P.Yahya; "lightning phenomena in Malaysia", seminar for ARSEPE, 2007.

A061

POTENTIAL DISTRIBUTION MEASUREMENT ON STRESS GRADING SYSTEM OF INVERTER-FED FORM WOUND MOTOR COIL

K. Kiuchi*, S. Matsuoka, A. Kumada, H. Ikeda, K. Hidaka,
The University of Tokyo, 7-3-1 Hongo, Bunkyo-ku, Tokyo, 113-8656, Japan
Y. Tsuboi, K. Ushiwata, Y. Ishikawa, S. Yamada, T. Yoshimitsu
Toshiba Mitsubishi-Electric Industrial Systems Corporation

Keywords : Inverter, Surge, Hot spot, Pockels effect, Coil end, Stress grading system

Abstract: A surface potential measuring system was developed by utilizing Pockels sensor for measuring the potential distribution on the stress grading (SG) system of form wound motor coils. The spatial resolution of the system is 5 mm, and the system has a broad frequency response up to GHz-range. With this system, the surface potential distributions on a model bar coil were measured under the applications of 50 Hz-sinusoidal, 1 kHz-sinusoidal and 1 kHz-rectangular AC voltages of 10 kVp. The The maximum potential gradient on the model bars under each cinditon were 0.34 kV/mm, 0.41 kV/mm and 0.48 kV/mm, respectively. The surface temperature of the model bar was also observed by an infrared camera and it turns out that the temperature on the end of the CAT, where the electric field tends to concentrate, increases under higher frequency field.

I. INTRODUCTION

The importance of inverter fed drives to control high voltage motors has been increasing for energy saving and high efficiency recently. However, these drives using pulse width modulation (PWM) whose voltage waveform contains high frequency components, so the SG system to be less effective in linearizing the voltage along the coil surface. In such a case, the concentration of capacitive currents creates local heating of the insulation material, resulting in the acceleration of the thermal aging [1].

The experimental information on the potential distribution of such SG system under the application of PWM voltage is essential for advanced designing of end-winding insulation system. However, it is difficult to apply a conventional electrostatic probe to the surface potential distribution measurement of such SG system due to the limitation of the response time.

In this study, a surface potential measuring system is developed utilizing Pockels sensor in longitudinal mode and applied it to the potential distribution measurement on the SG system of a model bar-coil.

II. MEASUREMENT METHOD

One model bar-coil was designed and fabricated in reference to a form wound actual motor coil. The test voltages were applied between the strand conductors and the mock stator core. The BGO Pockels crystal was set 1mm away from the model coil and the induced potential on the BGO was monitored by moving the model coil along a longitudinal direction. Then, from the sensor output, the surface potential on the measuring object is inversely calculated. For the detailed test principle, see Ref [2].

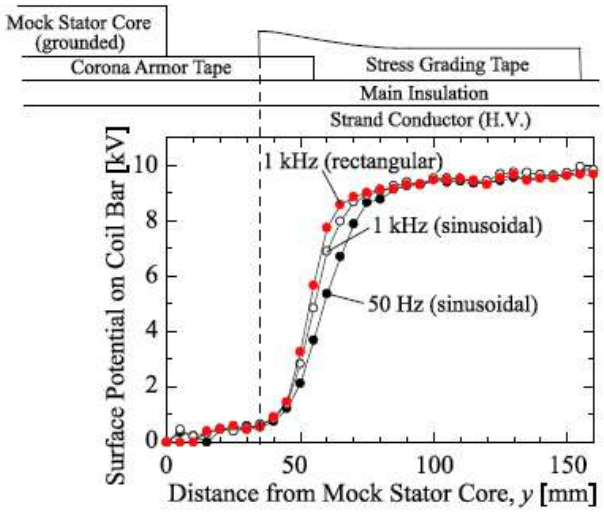

Figure 1. Potential distribution on model coil

III. RESULTS AND DISCUSSION

Figure 1 shows the potential distribution of the model coil under each condition when the values of the electric field maximize. The potential starts to increase sharply from the grounded level around at y = 45 mm, which is the center of the region where SGT and CAT are overlapped. The maximum potential gradient were 0.34 kV/mm, 0.41 kV/mm, and 0.48 kV/mm under 50 Hz-sinusoidal, 1 kHz-sinusoidal and 1 kHz-rectangular AC voltages, respectively. In addition, the surface temperature of the model bar was also monitored by a infrared camera. It was confirmed that the SG system becomes less effective and electric field tends to concentrate on the end of the CAT under higher frequency field, resulting in the surface temperature increase.

REFERENCES

[1] Qualification and Acceptance Tests for Type II Electrical Insulation Systems used in Rotating Electrical Machines Fed from Voltage Converters, IEC/TC 60034-18-42, 2008.
[2] A. Kumada, S. Okabe, and K. Hidaka, IEEE Trans. Dielectr. Electr. Insul., Vol. 11, pp. 122 - 129, 2004.

*Kento Kiuchi Department of Electrical Engineering, The University of Tokyo 7-3-1 Hongo, Bunkyo-ku, Tokyo, 113-8656, JAPAN TEL: 81-3-5841-6759; FAX: 81-3-5841-6725 Email: kiuchi@hvg.t.u-tokyo.ac.jp

A062

PARTIAL DISCHARGE CHARACTERISTICS IN INSULATION SYSTEM FOR HTS CABLE

Yuto.Kikuchi*, Shigeyasu Matsuoka, Akiko Kumada, Kunihiko Hidaka
Department of Electrical Engineering and Information Systems, The University of Tokyo, Japan
Mailing Adress: 3-1, Hongo, 7-chome Bunkyo-ku, Tokyo, Japan
kikuchi@hvg.t.u-tokyo.ac.jp
Kazuaki.Tatamidani, Takato.Masuda
Sumitomo Electric Industries Ltd., Osaka Japan

Keywords: High-temperature superconducting cable, partial discharge, polypropylene laminated paper, insulation system.

Abstract: High-temperature Superconducting (HTS) cable systems are expected to be a solution for improving the power grid. For insulation testing it is necessary to consider a partial discharge (PD) which is generated in butt gaps of the insulation layers. The electrical insulation system of HTS cables consists of liquid nitrogen (N2(l)) and polypropylene laminated paper (PPLP). N2(l) cooling system is installed in the power system and N2(l) will flow through the cables after their installation in the system. Filling the HTS cable with N2(l) in order to perform pre-shipment inspection is costly for cable manufacturers. Therefore, they are trying to find a cost effective method for pre-shipment inspections. One alternative is to use high pressure gaseous nitrogen (N2(g)) instead of N2(l) for pre-shipment inspections. This article discusses PD characteristics such as partial discharge inception field (PDIE) and partial discharge elimination field (PDEE) in a butt gap of HTS cables in high pressure N2(g) composite insulation. The results are compared with PD characteristics in N2(l)/PPLP to find the difference between insulation material in PD characteristics.

I. INTRODUCTION

N2(l)/PPLP composite is adopted in the electrical insulation system of HTS cable because of their high insulation strength and low dielectric loss. N2(l) coolant will flow through cable after its installation in power system.[1] Before the shipment of cables, pre-shipment insulation test is usually performed in the manufacturer. For the HTS cable, inserting N2(l) through HTS cable by intention to perform pre-shipment inspection is not economically efficient and it is necessary to use more cost effective method for pre-shipment inspection.

From the above background, the authors have focused on the alternatives such as inspection method in N2(g) instead of in N2(l).[2] In this paper, therefore, the PD characteristics not only of N2(l)/PPLP insulation system but also in N2(g)/PPLP isulation system are investigated.

II. MATERIALS AND METHODS

Q-V characteristics are measured under 0.1MPa to 0.3Mpa N2(l) and 0.1MPa to 1.0MPa N2(g) environment with not only cable models but also sheet models, where three PPLP papers are piled and a hole simulating a butt gap is puctured on the middle paper. PDIE and PDEE for each sample were obtained from Q-V characteristic with increasing the application voltage and from that with decreasing the application voltage, respectively.

II. RESULTS AND DISCUSSION

Figure 1 shows the relation between PDIE and PDEE in N2(g) and those under 0.3MPa-N2(l). For any gas pressure, PDIE and PDEE in N2(g) are linearly correlated with those in N2(l), that is, PD characteristics in N2(l) can be estimated from the values in N2(g). In Fig. 1, regression line for each gas-pressure also plotted and its slope increases with the pressure of N2(g). PDIE and PDEE in 1.0MPa N2(g) are approximately half of those in 0.3MPa N2(l). It indicates that if the inspection test is conducted in 1.0MPa N2(g) with the same applied voltage with that in 0.3MPa N2(l), it is roughly twice as severe as that in N2(l).

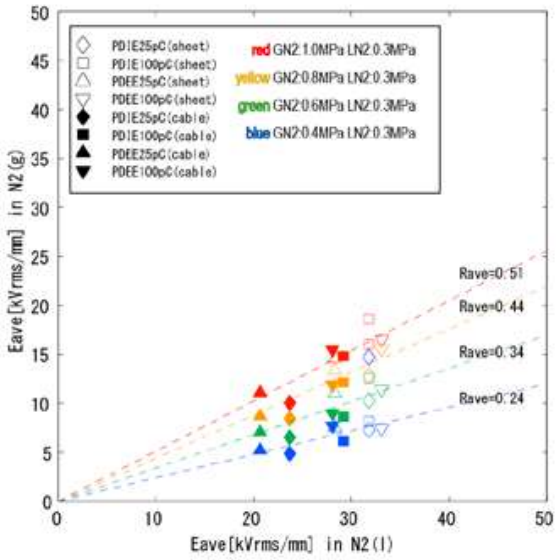

Figure 1. Comparison of PDIE, PDEE under N2(l) and N2(g)

REFERENCES

[1] Alexander Bulinski and John Densley, "High Voltage Insulation for Power Cables Utilizing High Temperature Superconductivity",IEEE Electrical Insulation Magazine,Vol.15,Issue2,Part2,2005,pp.14.

[2] 22F.Rezifar,et al "Characterization of Partial Discharge in HTS cable" IEEE Trans. on Dielectrics and Electrical Insulation vol.17 , No6 , pp.1747-1753 (2010).

*YutoKikuchi Department of Electrical Engineering, The University of Tokyo 7-3-1 Hongo, Bunkyo-ku, Tokyo, 113-8656 JAPAN TEL: 81-3-5841-6759; FAX: 81-3-5841-6725 Email: kikuchi@hvg.t.u-tokyo.ac.jp

A063

DATA TRANSMISSION SYSTEM OF REFM NETWORK USING MICROCONTROLLER AND GSM MODULE

Mook Boon Kean, Muhammad Abu Bakar Sidik
Institute of High Voltage and High Current, Faculty of Electrical Engineer,
Universiti Teknologi Malaysia, 81310, Skudai, Malaysia
Email: bkmook8@gmail.com, abubakar@fke.utm.my

Keywords: REFM, data transmission, microcontroller, GSM, GPRS, wireless.

Abstract: This paper presents a research on the data transmission sytem of the REFM sensors. The main function of the proposed system is to transmit data from sensors and a computer wirelessly. For this purpose, microcontrollers and GSM modules are used to send the information from REFM sensors using GPRS technology. The information will be stored in a computer in data centre building for observation and analysing purpose.

I. INTRODUCTION

Lightning strike represented as one of the most important causes of deaths, injuries and property damage from environmental phenomena. Malaysia, a country with high atmospheric humidity and solar heating, result in higher lightning strike density. Kuala Lumpur, the country capital city is ranked fifth in the world with its high lightning strike density [1]. In addition, a typical lightning strike is able to last more than 1 (one) second, and plenty of discharges occurred within the second. Therefore, both electrical and magnetic induction will occur even in significant distance from the strike location [2]. Magnetic coupling from lightning strike can induce high voltage surge to conductors and cause damages to devices. While the electric fields generated before lightning strike can go up to approximately 500 kV/m within 100 m range of strike [3].

Thus, a specialized device for instance Rotating Electric Field Mill, (REFM) is needed to measure the atmospheric electric field and to predict time of lightning storm. REFM is electro-mechanical device which measures the relative strength of an electric static field.

The REFM sensor, normally, will be installed in open area which is far from the data centre building. For that reason, in order to collect, record, and analyse the magnitude of atmospheric electric field from REFM sensor, a transmission system is required to send the data.

There are mainly two types of data transmission methods, which are wired and wireless. For this work, wireless had been selected over wired technology due to the coverage range and mobility. Since most of the sensors located far apart in remote areas, global system for mobile communication (GSM) is the most suitable technology to be applied.

GSM network is on the market for a long time and it is offering varieties of features and having users of more than 5 billion people, more than 80% of earth population [5][6]. In addition, GSM is offering low cost ownership and worldwide coverage as this technology has been existed for more than 20 years [6]. However, GSM has several shortcomings, which it is unable to perform transmitting and receiving data concurrently and the unsatisfactory real-time ability [7].

With the shortcoming of the 2G network, then it further develop into 2.5G, which is the GPRS network. GPRS is a packet data technology based on GSM that support both Point-to-Point Protocol, PPP and Internet Protocol, IP, it provide a shorter time for internet service provider connections and the charging will be based on amount of data sent instead of connection time. With the added packet-switching protocols, it will break the voice or data information into packets which only few kilobytes each. Then based on addressing data within packet, the information will be routed by network between different destinations. As compare to GSM, GPRS has high transmission rate, ability to transfer real-time data, supporting internet protocol, IP and having the ability to access the internet [15].

Therefore, in this paper a wireless network data acquisition system using GPRS is advances. GPRS is a packet data technology based on GSM that support both Point-to-Point Protocol (PPP) and Internet Protocol (IP). In addition, GPRS has high transmission rate,ability to transfer real-time data [7]. By uisng this technology data collected from remote sensors could be transmitted a computer in data centre that is connected internet with a fix IP address.

The objectives of this research are to develop an interface between REFM sensor and GSM module as well as to develop database system and an observation website.

II. HARDWARE AND SOFTWARE DESIGN

a. Hardware design and development

The hardware arrangment for data transmission is shown in Fig. 2. The analogue output of REFM sensor is connected to a Analogue to Digital (A/D) converter input of the microcontroller (PIC 16F877A) [8]. Afterwards, between the microcontroller and GSM module (SIM300) a voltage driver (IC MAX232) should be located since the working voltage of the two hardwares are different [9]. The microcontroller working voltage is 5 V (CMOS signal) meanwhile the GSM module working voltage is 12 V (RS232 signal). The connection of the MAX232 voltage driver is showned in Fig. 3 [10].

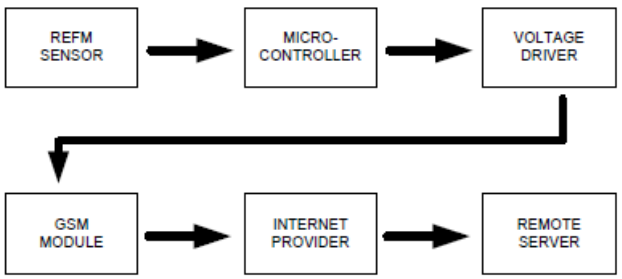

Fig. 2 Block diagram of the system.

Finally, through the internet provider system the data will be transmitted to a PC (remote server) in data centre building. In here, the range of the wireless transmission system will be within the coverage of GSM signal provider−it is able to go up to few hundred or thousand of kilometres−all around the globe.

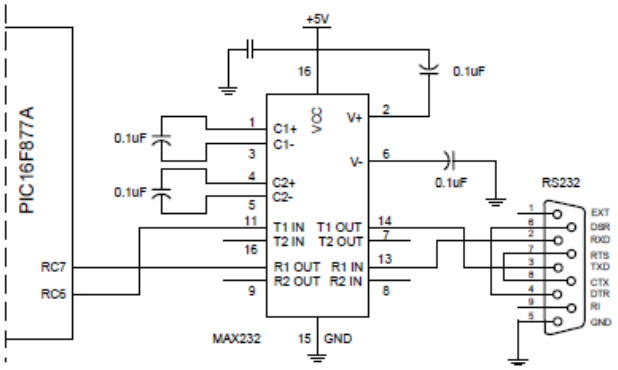

Fig 3. Connection between microcontroller and serial lines.

In this work four units REFM data transmission system (REFM Datsys) have been developed to collect data of atmospheric electric field from four stations. Each stations will have their own set of hardware−consist of REFM sensor, microcontroller, IC MAX232 and GSM module.

All the microcontrollers used in this work are incorporated with a LCD screen display. The main function of the LCD display is to show the status of the GSM module whether the connection is successful or fail. The complete connection of the 4 (four) REFM Datsys(s) is shown is Fig. 4.

b. Software development

The project software is mainly on the programming of the hardware, which is putting instruction to the PIC microcontroller and the GSM module so that the hardwares able to execute the system automatically.

At early stage of software development, MPLAB IDE will be familiarised by running with some C programming language. By using C language, the needed resources that are I/O ports, timers, USART module, and initialization of LCD will be configured [8][11][12]. Further programming will be done by sending the AT commands to the GSM module, as AT commands are the standardized coding used to control a modem [13].

The program flow chart of the microcontroller to the GSM module is as shown in Fig 5. Initially, when the programs start to run, each module has to be initialised, the microcontroller and GSM module, by sending AT commands to the GSM module and the GSM module will reply its status to the PIC microcontroller. It is about transmitting and receiving progress whic is occurred in between these two hardware. Figure 5 below shows the programme code of the initialisation process.

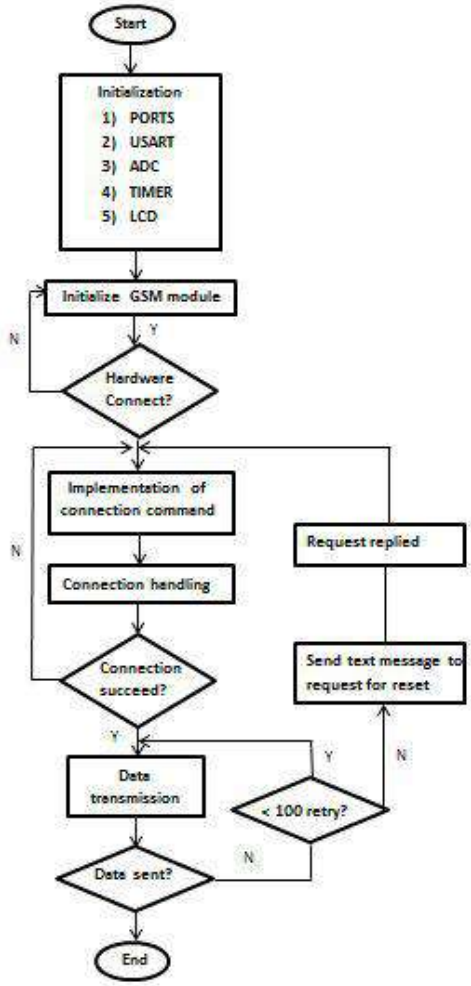

Fig 5. Process flow chart

Besides of hardware programming, there will be programming for the webserver which offer the user to access to data collected from the sensor located at remote area. MySql, a relational database management system will be configure so that data sent from the GSM module will be stored at the database. Then programming language Hypertext Preprocessor, PHP will be used to generate web contents in the the web server. As shown in Fig 6., PHP will be in between of the MySql and the web browser, when there are page request from web browser, it will function to fetch the data stored from the MySql database [14]. Then it will send out the data dynamically as an HTML page for the web browser so that the user can read the data collected.

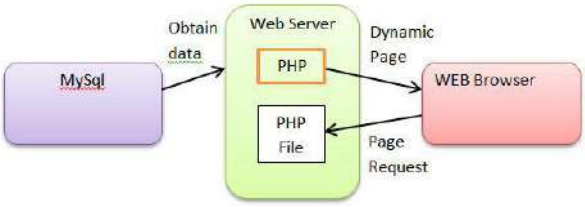

Fig 6. Access diagram using PHP.

III. RESULTS AND DISCUSSION

The baud rate of the microcontroller can be obtained using the following equation[8]:

Baud Rate = Fosc/ (16(X+1)), X= value in SPBRG (1)

After calculated the X value, it will be included in the C program, so that the proper baud rate is set to the microcontroller. By setting the correct baud rate for the microcontroller and GSM module interface, the data transmission able to progressed at the most optimum rate and the maximum communication speed set is 115,200 bps. Throughout the whole implementation of the project, the main concern is to establish the access to the internet by using the GPRS network, so that the data can be transmitted from the EFM sensor to the remote server wirelessly. A GSM module with GPRS function and a SIM card that have applied the GPRS services are essential. Then the communication protocol in betweem will be AT command, part of the AT commands that used to permit the connection are shown in Table 1, the other AT commands can be found in [13].

Table 1. AT commands

AT+CGATT=1	This command indicated the state of GPRS attachment, where the value '1' result in the activation of GPRS function. Once it response 'OK', the GPRS connection is established, else response 'ERROR' received showed that connection failed.
AT+CDNSORIP=1	Sets the connection with IP address server or domain name server. By selecting value '1', indicates as selecting the remote server as domain name.
AT+CIPSTART='TCP','domain name', '80'starts up the 'TCP' or 'UDP' connection.	By setting 'TCP' is to establish a TCP connection and the 'domain name' is user's remote server domain name. The value '80' is the remote server port selected, and this port value, is the server port for Hypertext Transfer Protocol, HTTP.
AT+IPR=115200	This command is to set the baudrate of the GSM module manually.

Then the experimental results collected from the EFM sensor that stored in the MySql database will be displayed as PHP page as shown in Fig 7. This allow the users to check and analyze the real time important information from the EFM sensor.

Fig 7. Webpage to observe data transmitted from REFM network .

IV. CONCLUSION

This paper has been presented a development process of wireless data tranmission system that will be used for REFM sensor network. The wireless transmission system device has materialised a real-time data acquisiton for remote REFM sensor locations. All information about the atmospheric electricl field condition sensed by the REFM sensors will be stored in a database system that could be monitored online through the developed website.

REFERENCES

[1]National Lightning Safety Institute (NLSI). http://www.lightningsafety.com/nlsi_info/world-lightning-activity.html. Access on May 2012.

[2] John Wiley & son, "Reliability Technology: Principles and Practice of Failure Prevention in Electronic System", Wiley 1 edition, pp. 5-44- 5-45, 2011.

[3] Mark I. Montrose, Edward M. Nakauchi, "Testing for EMC Compliance: Approaches and Techniques", pp. 175-176, 2004.

[4] Albert Edward Green, Alfred John Bourne, "Reliable Technology", Wiley-Interscience, 1972, Digitized Dec, 2007.

[5] GSM Association, "GSM World statistics", retrieved 8 June 2010.

[6] Eugen Horatiu Gurban and Gheorghe-Daniel Andreescu, "SCADA Element Solutions using Ethernet and Mobile Phone Network" IEEE 9th International Symposium, September 2011.

[7] Hong Cai, "A Remote Wireless Data Acquisition System Based on Ad Hoc Network and GPRS", 2009Second International Workshop on Computer Science and Engineering, IEEE, 2009.

[8] Microchip Technology Inc., "PIC16F87XA Data Sheet", 2003.

[9] Nobbert Stuban, "Wireless Data Transmission between Personal Computers", IEEE 27th Int'l Spring Seminar, 2004.

[10] Maxim integrated products, "+5V-Powered, Multichannel RS-232 Drivers/Receivers", 2010.

[11] Microchip Technology Inc., "MPLAB C Compiler For PIC32 MCUs User's Guide", 2009..

[12] Jivan S. Parab, Vinod G. Shelake, Rajanish K. Kamat and Gourish M. Naik, "Exploring C for Microcontrollers", Springer, 2007.

[13] SIMCOM Limited, "SIM300 AT Commands Set", version01.03,2004.

[14] Marcelo Sylvio M. dos Santos, Raimundo Carlos S. Freire, Jose Felicio da Silva, "Wireless Data Acquisition System for Remote Care of Newly Born Premature", MeMeA 2006 – International Workshop on Medical Measurement and Applications, 20-21April 2006

[15] Xiang-Yang Li, "Wireless Ad Hoc and Sensor Networks theory and Applications", Cambridge book online, Cambridge university press, 2011.

A064

DEVELOPMENT AND STUDY ON TRANSFORMER CHARACTERISTICS OF A HIGH REPETITION PULSE GENERATOR

Muhammad Abu Bakar Sidik[1,3], Hamizah Shahroom[1], Hussein Ahmad[1], Zolkafle Buntat[1], Zafar Iqbal[1], A. S. Samosir[2], Zainuddin NawawI[3], Muhammad 'Irfan Jambak[3]
[1]Insitute of High Voltage and Current (IVAT), Faculty of Electrical Enginnering, Universiti Teknologi Malaysia, 81310 Skudai, Johor, Malaysia
[2]Department of Energy Conversion, Faculty of Electrical Engineering, Universiti Teknologi Malaysia
[3]Department of Electrical Engineering, Faculty of Engineering, Universitas Sriwijaya
30662 Indralaya, Ogan Ilir, South Sumatera, Indonesia
Email: abubakar@fke.utm.my

High repetition pulse/ high frequency generators are of great interest for scientific and technological applications, including high voltage devices. The industrial environment for the application of high pulse generators to produce high voltage is currently expanding. Two different technologies have been developed in the past, in which the pulse is obtained directly through high voltage or the pulses are generated at the low medium link and then amplified for the pulse transformer [1]. The technique can be used to generate high voltages by implementing a combination of the microcontroller and semiconductor switching devices with the use of step up transformers such as a neon transformer, flyback transformer, ignition coil transformer, and others. Secondly, the transformer is used to further increase the voltage pulses which are limited due to the existence of parasitic elements that worsen the pulse shape [2].

In this paper the design and development of an automatic high repetition pulse generator using a PIC microcontroller (PIC 16F877A) is presented. The PIC microcontroller was used to generate two PWM pulses to drive the IGBTs through the optocouplers, which can perform fast switching in high voltage devices with low switching losses. A Matlab Simulink model was also developed to simulate the system ,in which two types of transformer were introduced to predict its validity in real operation with high voltage devices. Details of the software and hardware of its design and operation have been discussed.

The circuit was designed on a double layer printed circuit board (PCB) using Protel Advanced PCB software. The design must be precisely placed so that the components fit well. On the multiple layer board, the holes are plated internally with copper so that the bottom and top of the board are electrically connected at every hole. Most of the holes are for the fitted components but some holes exist just to connect the copper line known as the track or trace. These special holes are known as vias. Figure 5 shows the project prototype.

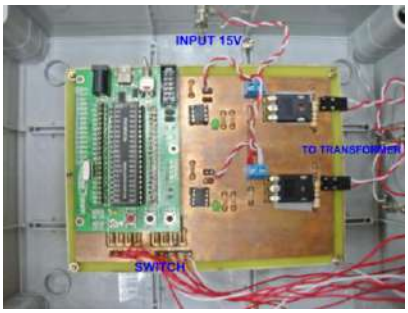

(a)

(b)

Figure 5. Project prototype

The experimental results of the oscillograph for PWM1is shown in Figure 6.

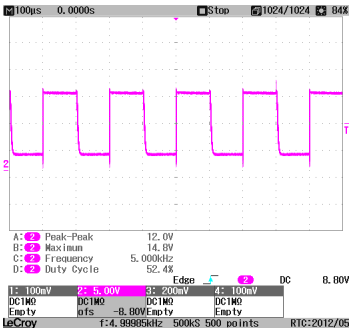

(a)

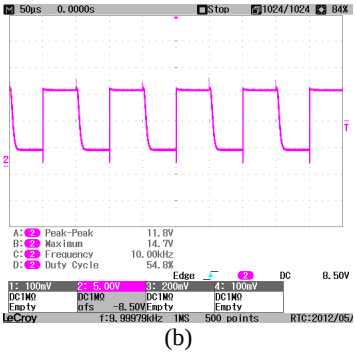

(b)

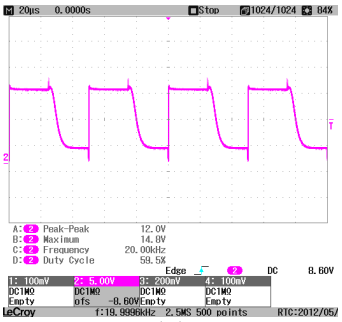

(c)

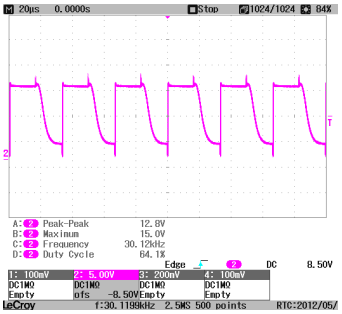

(d)

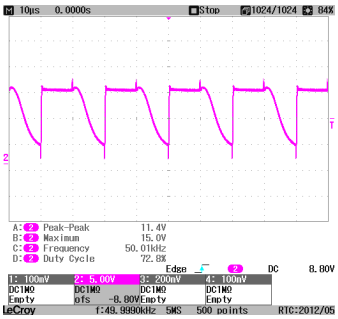

e)

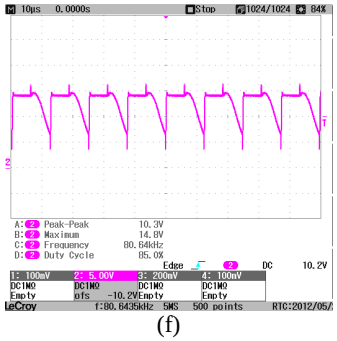

(f)

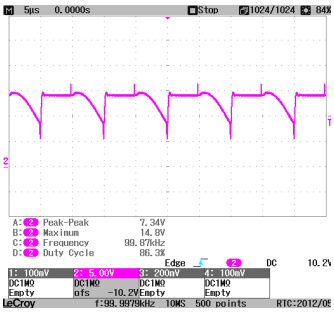

(g)

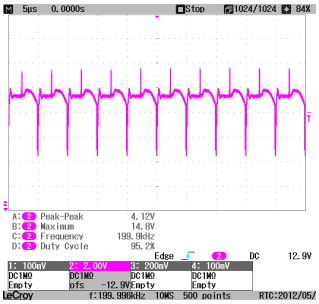

(h)

Figure 6. Waveform observed in PWM1 oscillograph with a frequency of (a) 5kHz (b) 10kHz (c) 20kHz (d) 30kHz (e) 50kHz (f) 80kHz (g) 100kHz (h) 200kHz

The development of a high repetition pulse generator was successfully achieved. The effect of changing the frequency and duty cycle was observed in the waveform on the oscilloscope. The high voltage characteristic of the transformer of different iron core transformers was verified through simulation results, in which the ignition coil transformer is found to be a suitable transformer that can be used in this high frequency range. On the basis of the analysis of the test data it can be concluded that the applicable frequency range for this system is 2kHz< f <200kHz. This system is applicable for high voltage applications such as switching purposes.

REFERENCES

[1] L. Heinemann, Kjell Porle, Per Ranstad, "Design of a high pulse voltage generator for electrostatic precipitators using magnetic switching technique," in *Proc. 12th Ann. Applied Power Electronics Conf. Expo. (APEC '97)*, pp. 948–952, 1997.

[2] D.M Goebel, "Chapter 8: Pulse technology," in A. Anders (ed.), *Handbook of Plasma Immersion Ion Implantation and Deposition*, 1st edition, New York: John Wiley & Son, 2000, p. 760, ISBN 0-471-24698-0.

A065

ATMOSPHERIC ELECTRIC FIELD DATA LOGGER SYSTEM

Muhammad Abu Bakar Sidik[1, 2], Che Nuru Saniyyati Che Mohd Shukri[1], Hussein Ahmad[1],
Zolkafle Buntat[1], Nouruddeen Bashir Umar[1], Y. Z. Arief[1], Zainuddin Nawawi[2]
[1]Insitute of High Voltage and Current (IVAT), Faculty of Electrical EngineeringUniversiti Teknologi Malaysia,
81310 UTM Skudai Johor, Malaysia
[2]Department of Electrical Engineering, Faculty of Engineering, Universitas Sriwijaya,
30662 Indralaya, Ogan Ilir, South Sumatera, Indonesia
Email: abubakar@fke.utm.my

Weather can be unpredictable as there are a lot of uncertainties in predicting thunderstorms. Most of our navigation systems, including those on air, land and water, as well as broadcasting systems, are directly affected by weather on a daily basis. The inconsistent and unreliable nature of storms brings out the importance of research in atmospheric electric field data logging systems.

In investigations of electric fields using weather field instruments, the field in the clouds and the field gradients were recorded at the earth's surface [1]. Changes in the electric field strength and polarity were detected using a real-time monitor for the local thunder cloud and an early warning was sent when there was a change in the atmospheric electric field [2].

This paper presents a study to develop a virtual instrument with the capability to analyse and store the magnitude (data) of atmospheric electric fields. In this research, three stages will be implemented. The first stage is to develop a programme flowchart to collect data and a Read File data logger system. The next stage is to programme the virtual instrument using LabVIEW. The last stage is to test the data logger system. This is important to verify the result obtained from the simulation. The investigation consists of several phases to achieve the objective of the research. The first phase is the study of the physics of cloud profiles, followed by the visualization and simulation of cloud profiles using LabVIEW programming and the DAQ instrument. The last phase is result validation through a simulation using LabVIEW programming.

Figure 1 shows the programme flowchart for collecting and saving data using the LabVIEW software package. Initially, the analog input obtained from the DAQ USB-6216 or the simulation signal must be changed from AC to DC. A few tests were done to obtain the correct signal and thus the waveform. The waveform must be checked to get the most accurate one before the data is tabulated. Tabulation stops once all the data are carefully saved. The flowchart for data reading is shown in Figure 2. This data reading can be done using a specific front panel created in LabVIEW and it is important for future analysis.

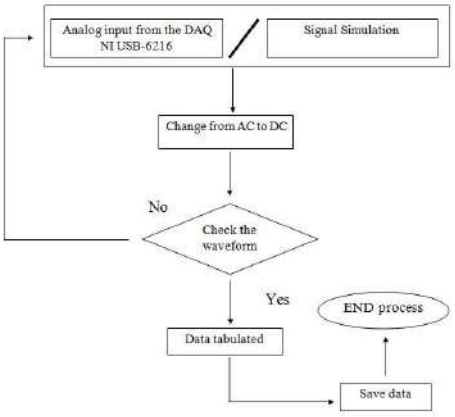

Figure 1. Programme flowchart for collecting and saving data

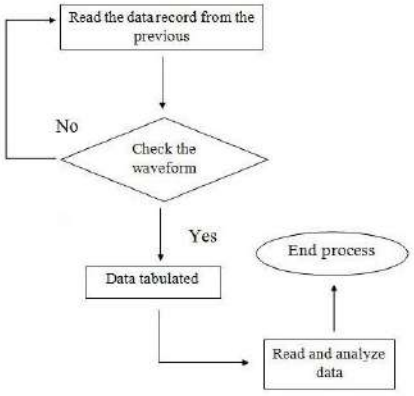

Figure 2. Program flowchart for reading data

The developed virtual instrument consists of waveform chart, tabulated data, and histogram for real time observation. Moreover, it has feature to save and recall data for further analysis.

The data in Figure 3 is tabulated every second and saved every minute. The files are saved in a TDMS file and can only be called back using read file programming by LabVIEW. The programme is set to have a time interval of 100 ms or 0.1 s. All the sensors (Sensors 1 to 6) are set to run the programme. Figure 4 shows the "select signal" front panel, which can be selected as preferred by the user. The data is visualized using a waveform chart in terms of voltage (kV/cm) and time (s) in two different charts; all signals and select signal chart. The "all signals" waveform chart displays all the waveforms obtained,

while the "select signal" waveform chart only displays the preferred signals.

Figure 5 shows the histogram of the data. The histogram obtained from the simulation shows the information where the x-axis represents the measurement scale of results for the ambient electric field strength and the y-axis describes the frequency of the electric field strength, showing how often the results occur. After all the data are saved, the data will be recalled using the Read File programme, as shown in Figure 6, and can be displayed.

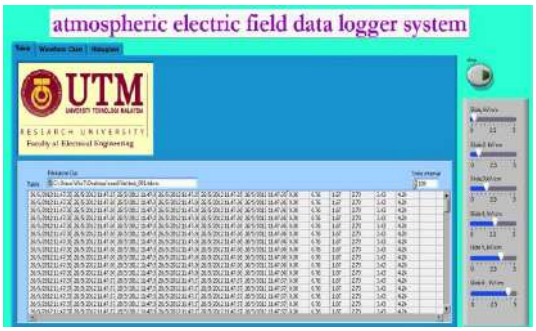

Figure 3. Data tabulated

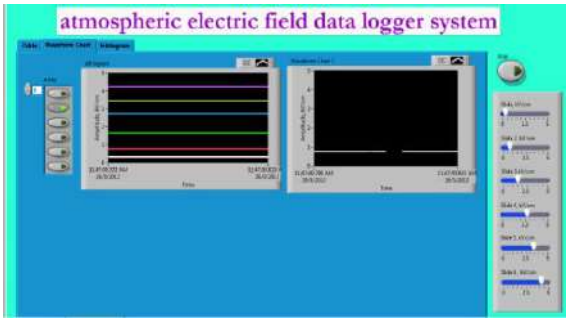

Figure 4. Front panel of the waveform chart and "select signal"

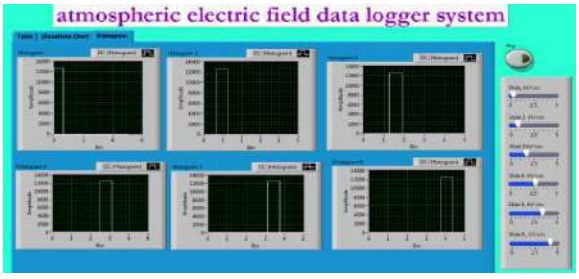

Figure 5. Histogram of the data

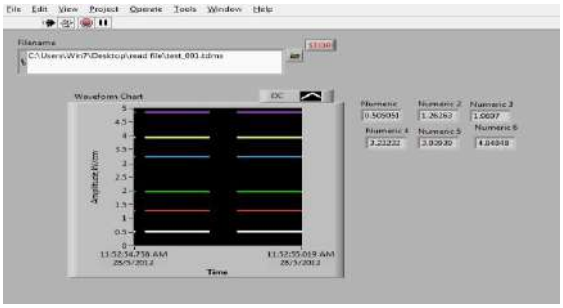

Figure 6. Read file as data logger

The LabVIEW programme that has been developed will give a notification in the form of a waveform chart to show the condition of the atmospheric electric field strength.

REFERENCES

[1] Edward Beck, Harold R. McNutt, Jr., Derrill F. Shankle, and Charles J. Tirk (1969). Electric fields in the vicinity of lightning strokes. *IEEE Trans on Power Apparatus and Systems.* 88(6), (904-910).

[2] Chen Xiyang, Long Yan, Xu Bin, and Liu Gang (2011). Simulation of the relations between the height of thunder cloud base and the electric field around the tip protrusion. *2011 7th Asia Pacific International Conference on Lightning.* 1-4 November. Chengdu,China: IEEE, 98-102.

A066

STUDY THE AGEING OF 132KV SURGE ARRESTER BY USING LEAKAGE CURRENT MEASUREMENT

N. Asilah[1], Zulkurnain Abdul-Malek[1], Novizon[1, 2], Wooi Chin Leong[1]
[1]High Voltage and High Current Institute, Faculty of Electrical Engineering, Universiti Teknologi Malaysia
[2]Department of Electrical Engineering, University of Andalas, Padang, Indonesia
nasilah4@gmail.com, zulk@fke.utm.my, novizon@gmail.com, wcl51952@hotmail.com

Keywords: Resistive leakage current, degradation, surge arrester, harmonic analysis, temperature

Abstract: Arrester is widely used to protect high voltage equipment or electric power lines from lightning strike or temporary overvoltage and is specially used in the power station. During lightning strike or overvoltage, there is a leakage current flows out and this leakage current can cause degradation or ageing to the arrester. The level of degradation and ageing of arrester can be measured by separating the third harmonic resistive leakage current. Nowadays, there is a method that separate resistive leakage current from total leakage current. This method has been used to detect the performance of zinc oxide (ZnO) surge arrester either it is in a good condition or in a bad condition. The increased in leakage current and power loss indicate the bad condition or the degradation of ZnO surge arrester. The aim of this paper is to find out the leakage currents at laboratory temperature on six samples of 132kV surge arrester with differents insulating house structure. The results are analyzed using compensation method and shifted current method (SCM).

I. INTRODUCTION

Surge arrester is a device that is used to protect the insulation on the power systems from lightning strike or temporary overvoltage. The arrester can limit overvoltage that occur across the terminals of the equipment below its withstand voltage to protect the equipment [1,8]. Its highly non linear voltage current characteristic is caused by electrical potential barriers involving thick grain boundary region between the successive ZnO grains [2,7]. The grain boundaries are highly resistive which show a non ohmic property. The arrester act as an insulator during normal operating voltage which shows it has very high resistance and it conduct current during overvoltage which shows it has relatively low resistance [3].

During lightning strike or overvoltage, there is a leakage current flows out and this leakage current can cause degradation or ageing to the arrester. Total leakage current consists of capacitive and resistive component where it is the summation of both capacitive and resistive current.

$$it = ic + ir \quad (1)$$

Nowadays, the resistive component, in particular, the third harmonic resistive current component is used to measure the level of degradation or ageing of zinc oxide surge arrester as the resistive component varies with the degradation of arrester [4]. There are few methods to separate the resistive leakage current from the total leakage current in order to monitor the performance of arrester such as compensation method, point of wave technique, compensation circuit technique and shifted current method (SCM) [5].

The most common method used to separate resistive leakage current from total leakage current is the compensation method. However, this method requires the value of voltage across the arrester terminal to obtain resistive leakage current and is difficult to measure applied voltage outside the laboratory especially in the substation. Another method used to separate resistive leakage current from total leakage current is shifted current method (SCM). This method does not require the knowledge of applied voltage and is basically using waveform manipulation to obtain resistive leakage current [1,4-6]. It makes this method suitable for both online and offline measurements. This paper present a few measurement of leakage current on six samples of 132kV surge arrester at laboratory temperature. Sample 1, sample 2 and sample 3 are polymeric arresters while sample 4, sample 5 and sample 6 are porcelain arresters. The experiment was conducted by using voltage divider measurement with 1kΩ resistance. The results are then analyzed by using compensation method and shifted current method (SCM) and verified if these methods are suitable to identify the level of degradation of arrester.

III. RESULTS AND DISCUSSION

The laboratory temperature while conducting the experiment is 30°C and the results from all six samples are plotted to show total resistive leakage current and 3rd harmonic resistive leakage

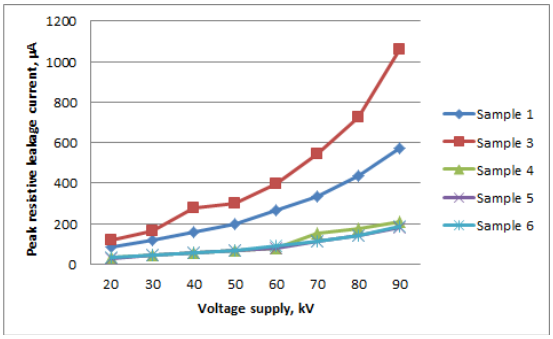

Figure 1. Measurement of total resistive leakage current by using Compensation Method

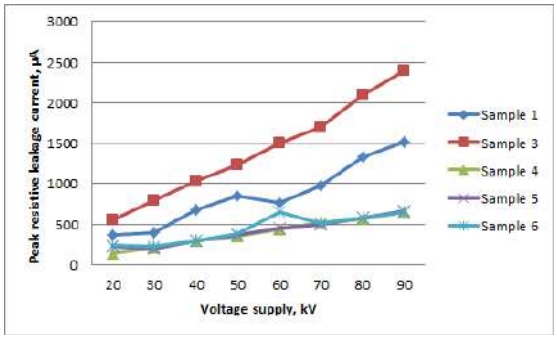

Figure 2. Measurement of total resistive leakage current by using Shifted Current Method

*N.Asilah, UTM, nasilah4@gmail.com

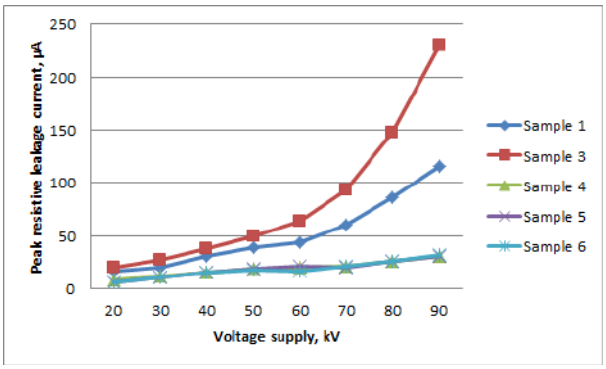

Figure 3. Measurement of third harmonic resistive leakage current by using shifted current method

Figure 1 and Figure 2 show the measurement of total resistive leakage current on five samples by using compensation method and shifted current method. Figure 3 shows the measurement of third harmonic resistive leakage current on five samples by using shifted current method. For all figures, the values of leakage current of sample 1 and sample 3 are close by at voltage supply of 20kV. As the voltage supply increases, the leakage current for both sample become more different. The values of leakage current for sample 4, sample 5 and sample 6, are intercepting to each other at voltage supply from 20kV to 90kV. Samples of polymeric arresters also have higher value of leakage current compared to samples of porcelain arresters. From this result, it shows that condition for porcelain arresters are better than polymeric arresters which indicate polymeric arresters are more ageing.

REFERENCES

[1] Novizon, Zulkurnain Abdul-Malek, Nouruddeen Bashir, and Aulia, "Condition Monitoring of Zinc Oxide Surge Arresters, Practical Applications and Solutions Using LabVIEW™ Software",FoleaSilviu (Ed.), ISBN: 978-953-307-650-8, InTech, 2011

[2] H. Andoh, S. Nishiwaki, H. Suzuki, S. Boggs, and J. Kuang, "Failure Mechanisms and Recent Improvements in ZnO Arrester Elements", EI Magazine, 1999

[3] Daniel W. Durbak, "Surge Arrester Modeling", IEEE Power Engineering Society Winter Meeting, Vol. 2, pp. 728-730, 2001.

[4] Zulkurnain Abdul-Malek,NovizonYusoff, and Fairouz, "Field Experience on Surge Arrester Condition Monitoring – Modified Shifted Current Method", International Conference on High Voltage Engineering and Application, New Orleans, 2010

[5] Zulkurnain Abdul-Malek, Novizon, and Aulia, " A New Method to Separate Resistive Leakage Current of ZnO Surge Arrester", JurnalTeknika, FakultasTeknikUniversitasAndalas, Padang, Indonesia, No. 29, Vol. 2, pp. 67- , 2008

[6] Zulkurnain Abdul-Malek, NovizonYusoff, and Fairouz, "Performance Analysis of Modified Shifted Current Method for Surge Arrester Condition Monitoring", 45th International Universities' Power Engineering Conference, Cardiff, 2010

[7] Kazuo Eda, "Zinc Oxide Varistors", IEEE Electrical Insulation Magazine, Vol. 5, No. 6, 1989

[8] Kai Steinfeld, Reinhard Göhler, and Daniel Pepper, "High Voltage Surge Arresters for Protection of Series Compensation and HVDC Converter Stations", The 4th International Conference on Power Transmission and Distribution Technology, Berlin, 2003

A067

STREAMER-TO-LEADER TRANSITION ACROSS SURFACE/GASEOUS GAP IN SF_6/N_2 GAS MIXTURE

Hiroshi Moriyama*, Shigeyasu Matsuoka, Akiko Kumada, Kunihiko Hidaka
Department of Electrical Engineering and Information Systems, The University of Tokyo, Japan
Mailing Adress: 3-1, Hongo, 7-chome Bunkyo-ku, Tokyo, Japan
moriyama@hvg.t.u-tokyo.ac.jp

Keywords: surface discharge, streamer-to-leader transition, SF6/N2 gas mixture, precursor model, high time-resolved measurement, pockels effect

Abstract: This study shows the experimental analysis of streamer-to-leader transition in SF6/N2 gas mixture. The streamer to leader transition process were observed with a streak camera and a framing camera. In the gas mixture, a 'leader precursor' was clearly observed in the transition from a streamer to leader. The transient change in the potential distribution along a surface leader propagating in the gas mixture was also measured with a pockels measuring system. The electric field and charge distributions were calculated from the measured potential profile. The electric field and charge distributions were compared with ICCD images. These results indicate that streamer-to-leader transition can be explained by the precursor model.

I. INTRODUCTION

Surface discharge on a dielectric material has a great influence on the insulating performance of electrical apparatuses and electronic devices. The phenomena of leader inception and propagation have been studied extensively. Precursor and stem models have been proposed to explain the leader transition process in gaseous gaps, but there still remains many things to be clarified for quantitative discussion.

This paper describes the experimental analysis of streamer-to-leader transition of positive discharge in SF6/N2 gas mixture with high time resolution. The streamer to leader transition process were observed with a streak camera and a framing camera (Specialized Imaging : SIM) .

II. RESULTS AND DISCUSSION

Figure 1 shows streamer-to-leader transition in SF6/N2 gas mixture taken with a streak camera and a digital camera. A pin-to-plate electrode was installed in a chamber filled with SF6/N2 gas mixture, whose mixture ratio was 1 to 4. The impulse voltage of 94 kV was applied. Figure 1(a) is a picture of overview image by a dijital camera. Figure 1(b) is its streak images (sweep speed is 1.46μs/9.2mm). In Figure 1 (b), streamer occured around at t = 150 ns, and light-emitting chanel corresponding "precursor" occurred at t = 600 ns, and then leader occurred at t = 1.2 μs.

A surface discharge in SF6/N2 gas mixture was also observed. A chamber was filled with SF6/N2 gas mixture, whose mixture ratio was 1 to 4. The impulse voltage of 15 kV was applied. Figure 2(a) timing of a framing camera. Figure 2(b) shows framing images of streamer to leader transition taken by a ultra-high-speed camera (Specialized Imaging : SIM). A streamer propagated radially from the electrode (Frame 1), and two weak light-emitting channels corresponding precursors appeared in the streamer (Frame 2 and 3), and then subsequent streamers were formed at the tips of right emitting chanel (Frame 4), respectively. These results indicate that streamer-to-leader transition can be explained by precursor model.

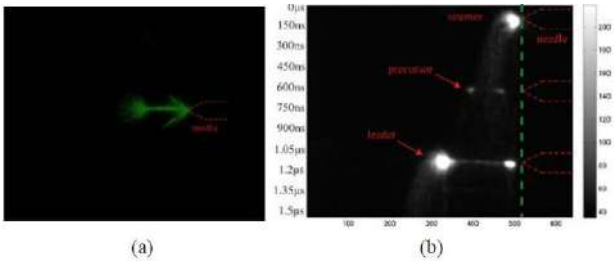

(a) Digital camera image (b) Streak camera image

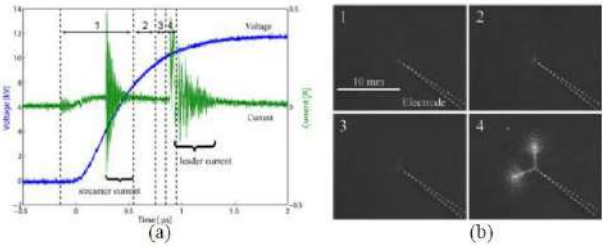

Figure 2. Surface discharge in SF6/N2 gas mixture
(a)Voltage waveform, current waveform and capturing timing (1: 700 ns, 2: 200 ns, 3: 100 ns, 4:100 ns) (b) SIM pictures

REFERENCES

[1] Gallimberti and N. Wiegart, "Streamer and leader formation in SF6 and SF6 mixtures under positive impulse conditions : II. Streamer to leader transition ", J. Phys. D: Appl. Phys.19,pp.2363-2379, 1986

*Hiroshi Moriyama Department of Electrical Engineering, The University of Tokyo 7-3-1 Hongo, Bunkyo-ku, Tokyo, 113-8656 JAPAN TEL: 81-3-5841-6759; FAX: 81-3-5841-6725 Email: moriyama@hvg.t.u-tokyo.ac.jp

A068

ELECTRICAL PERFORMANCE OF INSULATORS POLYMERIC, CERAMIC AND GLASS UNDER ARTIFICIAL TROPICAL CLIMATE AGEING

Salama Manjang, Mustamin
Departemet of Electrical Engineering, Hasanuddin University
Jl. Perintis Kemerdekaan Km 10, Makassar 90245, INDONESIA
Email: salamamanjang@unhas.ac.id, salama.m@lycos.com

Keywords: Silicone Rubber, Ceramic, Glass, Aging, Leakage Current
Abstract: This paper describes the effects and the accelerated aging of polymer, ceramic and glas insulators under artificial tropical climate. A comparison of the surface leakage current of the polymer insulator with a ceramic and a glass insulator can be known if operated in tropical climatic environment.The methods used were making design concept of the chamber construction and its accessories, so it could be well functioned and useful.
The tests carried out in several stages in the chamber. The exprimental results showed that the characteristic of the surface leakage current of silicone rubber polymer insulators is much smaller and more stable than ceramic insulator and glass insulator. The test under various artificial tropical climate stresses indicates that the surface leakage current of the silicone rubber polymer is very small. It showed that all types of the tropical climate impacts and the smallest comparison occurs when it is blown by the pollution of salty fog in which the average comparison achieves 1: 3.14 : 4.26 towards ceramic and glass insulator. The difference of the lowest leakage current reaches the average of 72.03 % towards the ceramic insulator and 58.21% towards the glass insulator. work.

I. INTRODUCTION

Polymeric insulators have been increasingly accepted by industry and utilities to replace porcelain and gelass insulators because of the well-known advantages that polymeric insulators, sucs as light weight, ase of handling, reduced installtion and maintaenance costs, vandalism resisance, and improved contaminations performance. Although polymer insulators have some advantages over porcelain and glass insulators, they showed degradation due to climate stresses such as UV in sunlight, moisture, temperature, pollutants, etc., and the degradation may reduce the performance. This reduction is actually a result of leakage current leading to dry-band arcing is one of the main causes of aging in polymer insulators. [1,2].

In tropical regions, like Indonesia that consists of thousands islands, has a complex contamination and high rate of contamination-triggered insulators failure. External polymer insulators are subjected to extremely simultaneous severe tropical climate conditions such as the UV irradiation is always 12 hours a day. As equatorial region solar radiation level in Indonesia can reach 1.250 W/m2 and contributes to warm air throughout the year, humidity approach 100% during the night and early morning, and temperature is always higher than 16^{o}C. Annual rainfall is relatively large, of which parts of lrian Jaya prove to be the area with the highest rainfall (mean annual up to 3185 mm), while Java-Madura regions (the most populated regions) have the mean annual rainfall of 2571 mm [3,4].

High voltage electrical insulator which being used in Indonesia until now are insulators made of ceramic and glass because its aging resitance. Investigation on how to find polymeric insulating material which is suitable for high voltage outdoor application under the influence of natural tropical climate needs a long time research is needed. Therefore, this paper describes electrical characteristics of the insulator of silicone rubber polymer and porcelain/glass under multi stress condition in the aging test chamber.

II. MATERIALS AND METHODS

The materials test used are polymer insulator of silicone rubber (SIR), ceramics (CR) and glass (GL) insulator. The materials test were installed into the test chamber room, and then tested according to standard procedures and quality tests are non-ceramic insulators IEC1109 [3].

The methods used were making design concept of aging chamber construction and it accessories, designing it, so it could be well functioned and useful. The aging test chamber was made of stainless steel sheets. The size of the chamber is size 1.8x1.8x1.8 m^3. In the chamber, the samples are subjected to ambient conditions (relative humidity 50%-100%, temperature 20^{o}C-47^{o}C, UV-B radiation 59.6–159.2 lux, rain 0.05-1.0 mm/min), salt pollution 1-19 mS, and ac high voltage 20 kV.

Electrical characteristics that we test in the research of polymer insulators SIR is to know the characteristics of leakage current on polymer insulators SIR under the artificial tropical weather. Also aging test performed on ceramic and glass insulators to be used as a comparison. Period and the schedule that used in this research follow standard quality test non-ceramic material is used by the IEC 1109.

Instruments is used in the research of polymer insulators (SIR) is humidification, heating, demineralization rain, salt fog 7 kg/m3, solar radiation simulation and high voltage 20 kV by taking samples of ceramic and glass insulators new which has been applied in tropical area for comparison. Constraints experienced in the use of ceramic insulators, especially in areas of high pollution become a factor in finding the best solution. Testing of polymer insulators with pollution, artificial weather and climate on the high voltage laboratory to test it conductivity and other electrical characteristics.

III. RESULTS AND DISCUSSION

In Figure 1. below we can see the recording pulse of the polymer insulator leakage current at the time of UV radiation are given 56.9 to 159.2 lux at 20 kV AC voltage, a frequency of 50 Hz with a humidity of 80%, temperature 29 °C, with test duration of 120 minutes for each level of UV radiation are used.

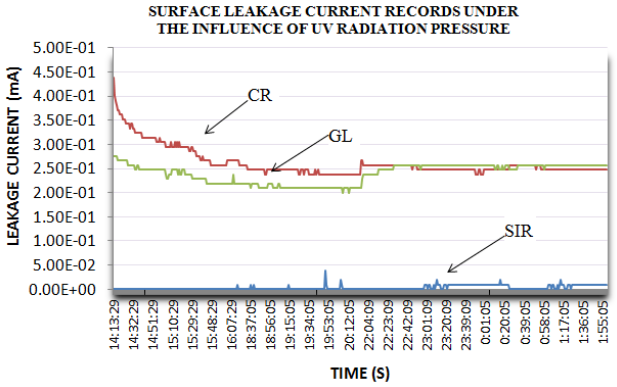

Figure 1. Characteristic of the surface leakage current records under the influence of UV radiation

These results indicate that the polymer insulator surface leakage current SIR with exposure to ultra violet radiation 56.9 up to 159.2 lux was very small (excellent) in comparison with ceramic insulators and insulating glass. Aging in the ultra violet radiation level equal to the ratio of the average leakage current average 1:120.66:109.6. Percentage difference of surface leakage current on polymer insulator of ceramic insulators average is 98.91% and for glass insulators average is 98.91%.

The polymer insulator surface leakage current SIR with exposure to thermal stress of 20 °C up to 47 °C is very small (excellent) in comparison with ceramic insulators and insulating glass in the ultra violet radiation level equal to the ratio of the average leakage current 1: 2.45: 4.44. Percentage difference of surface leakage current on polymer insulator of ceramic insulators average is 59.30% and for glass insulators average is 76.55%.

The surface leakage current of silicone rubber with exposure to humidity 50% up to 100% is very small (excellent) in comparison with ceramic insulators and insulating glass in the ultra violet radiation level equal to the ratio of the average leakage current is 1: 2.81: 4.92. Percentage difference of surface leakage current on polymer insulator of ceramic insulators average is 63.65% and for glass insulators average is 79.07%.

Aging under exposure to rainfall intensity 0.05 mm/min up to 1.00 mm/min (simulated rain from drizzle to rain cats and dogs) showed the leakage current of insulator SIR are very small (excellent) in comparison with ceramic insulator comparison of leakage current with an average of 1: 4.11. Percentage difference of surface leakage current on polymer insulator of ceramic insulators average is 73.35%.

The recording pulse of the polymer insulator leakage current when exposed to salt fog pollution conductivity of 1 mS/cm until the conductivity of 17 mS /cm at 20 kV AC voltage, frequency 50Hz, temperature 28 °C, with a test duration of 60 minutes at each level of the conductivity of salt fog pollution. These results indicate that the surface leakage current of polymer insulator SIR pollution exposure to salt fog with conductivity 1 mS /cm up to of 17 mS / cm is very small (excellent) in comparison with ceramic insulators and insulating glass with a comparison of the average leakage current is 1: 3.45: 4.68. Percentage difference of surface leakage current on polymer insulator of ceramic insulators average is 56.86% and for glass insulators average is 54.03%.

When the fog conductivity of salt (NaCl) to be increased greater than 12.58 mS/cm or 7 kg/m^3, insulators SIR showed increased surface leakage current exceeds the surface of ceramic insulators and glass insulators, even seen a slight discoloration on the surface of the insulator SIR. But after testing was stopped for a week, then testing continued discoloration and leakage current SIR insulator surface normal. This indicates that the insulator SIR does not cause permanent aging due to exposure to salt pollution

Based on the characteristics of the surface leakage current under artificial accelerated multi stress is known that the leakage current is very small polymer insulator SIR for all kinds of the tropical climate influences compared with ceramic and glass insulators.

REFERENCES

[1] Salama, Suwarno, K. T. Sirait, H.C. Kaerner, "The dielectric properties and surface hydrophobicity of silicone rubber under the influence of the artificial tropical climate", *Proc, 1998 International Symposium on Electrical Insulating Materials*, Toyohashi, Japan, P2-3, 607-610, 1998.

[2] Manjang. S, Mustamin, *Kajian Karakteristik Isolator Polimer Tegangan Tinggi Oleh Penuaan Berbagai Tekanan Buatan pada Daerah Tropis*, Proc, National Conference on Industrial Electrical and Electronic, UNTIRTA, Cilegon, Indonesia, 15-16 Desember 2010.

[3] Marsudi, D., PLN Experience in the Field of Design & Operation of The Indonesian Electric System, Conference of Electropic '96, Jakrta, Indonesia, 22-26 September 1996.

[4] Composite Insulators for a.c.Overhead Lines With a Nominal Voltage Greater than 1000 V – Definitions, Test Methods and Accceptance Criteria" Publication IEC 1109.

[5] Gorur, R.S., Cherney, E.A., Burnham, J.T. *Outdoor Insulators.* Arizona: USA, 1999.

[6] Ayman H. El-Hag, Shesha H. Jayaram and Edward A. Cherney, "Fundamental and Low Frequency Harmonic Components of Leakage Current as a Diignosiic Tool to Study Aging of RTV and HTV Silicone Rubber in Salt-Fog, IEEE Trans. EI. Vol. 10, pp. 128-136, 2003.

[7] *IEC 60-1, High Voltege Test Technique.*

[8] *R.S. Gorur, E.A. Cherney, R. Hackam and T. Orbeck, "The Electrical* Performance pf Polymeric Insulating Materials Under Accelerated Aging in Fog chamber", IEEE Trans. PD, Vol. 3, pp. 1157-1164, 1988.

A069

A FILTER-BANK APPROACH FOR EXTRACTING FEATURES FOR THE CLASSIFICATION OF PARTIAL DISCHARGE SIGNALS IN HIGH VOLTAGE XLPE CABLES

R. Ambikairajah*, B. T. Phung, J. Ravishankar
School of Electrical Engineering & Telecommunications, University of New South Wales

Keywords: Partial Discharge, Fast Fourier Transform, Classification, Features

Abstract: The classification of partial discharge (PD) signals is a key criterion in the evaluation and diagnosis of the performance of insulation systems in power equipment, as it is a good indicator of the severity of the partial discharge. Either time or frequency domain features can be extracted from a PD signal for PD classification. This paper investigates a filter-bank based approach to extract frequency domain based features to represent a PD signal. The filter-bank comprises N band-pass filters, and the energy corresponding to each band-pass filter is calculated in order to obtain N dimensional features to represent the PD signal. These filters can be organized in either equal or octave frequency sub-bands, and in this paper, both are analyzed with the use of a Support Vector Machine (SVM) classifier. Results show that the proposed features are robust and provide a strong classification accuracy of PD signals that can be used in online condition monitoring systems.

I. INTRODUCTION

The insulation systems of power equipment are susceptible to the occurrence of voids, cavities and other defects that are a result of factors as flaws in the initial manufacturing process or subsequent ageing/deterioration due to electrical, mechanical and thermal stress, and environmental impact. These defects give rise to the occurrence of partial discharge (PD) and if unaddressed, they can propagate through the insulation and cause a breakdown of the power equipment, which has safety and economic implications. The monitoring of PD is therefore a vital part of the asset management of power equipment [1]. In general, there are 3 key types of PD including corona discharge, which occurs at sharp points that protrude from electrodes in gases or liquids, surface discharge that can occur along the interface between a solid and either gas or liquid dielectric and internal discharge which occurs in gas or oil filled cavities.

One of the challenges in condition monitoring of PD signals is that they are often corrupted by noise from the environment in a substation and surrounding areas, and this results in the recorded PD signal being completely buried in noise. De-noising algorithms have been developed in both the time [2] and frequency domains [3] for use prior to extracting features from the PD signal for classification. Methods of extracting these features are an ongoing area of interest. The discriminatory qualities of the features that are chosen determine the dimension of the features required for successful classification of the PD signal.

This paper looks at a filter-bank approach, consisting of *N* sub-bands (band-pass filters), to extract these features in the frequency domain. These features are used as an input to a Support Vector Machine (SVM) classifier and the results are analyzed in this paper.

II. FEATURE EXTRACTION

Discrete Fourier Transform

The PD signal is sampled at a frequency of 100MHz over an AC cycle of 20ms, resulting in 2 million time samples. After the Fast Fourier Transform (FFT) processing, there are 2 million frequency bins, and the frequency resolution, Δf = 50 Hz. In the FFT processing, the analysis window length used was 20ms, which implies that the window shift does not occur, as the AC cycle is also 20ms.

The frequency bins in the FFT domain need to be grouped such that they form *N* sub-bands (filter-bank). Once the filter-bank is formed, the next step is to de-noise the signal in each sub-band.

Frequency domain based features

The log average energy corresponding to each sub-band is calculated, producing an energy vector (E1, E2, …., EN) which can be used as a feature. Smoothing these energy vectors using the Discrete Cosine Transform (DCT) to obtain transformed coefficients (C0, C1, C2,….CN-1) can also be used as features [5]. However, this paper will only look at energy vector based features.

A PD based classification system is shown in Figure 3 and there are two distinct stages. The training phase in this system has 3 steps: de-noising the signal, extracting features from the de-noised signal and then using these features to train a classifier.

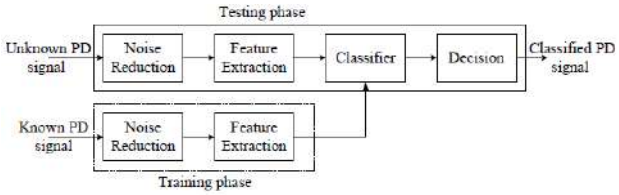

Figure 3. PD classification system - outlining the training and testing phases

The testing phase for the system also has 3 steps: the signal is de-noised, features are extracted and based on the classifier input, a decision is made. There are a variety of classifiers that could be used, including Probability Neural Network (PNN), Support Vector Machine (SVM) and the Sparse Representation Classifier (SRC), however this paper will focus on the SVM alone [6].

PD Data collection

A PD measurement circuit that complied with the IEC 60270 standard [8] was set-up and comprised a PD-free high voltage transformer, that could step up to 50kV, was connected to the various laboratory models created for corona, surface and internal discharges. When the partial discharge was produced by the test object, *Cx*, a small current flowed through the blocking capacitor, *Cb*, and this current was sensed by a High Frequency Current Transformer (HFCT) with upper cut-off frequency of ~50MHz. The output of the HFCT was sent to the digital oscilloscope for recording of the PD data at that instant. In

*R. Ambikairajah, School of Electrical Engineering & Telecommunications, University of New South Wales, r.ambikairajah@student.unsw.edu.au

parallel, the PD magnitude and activity was also monitored via a quadripole measuring impedance *Z* and a commercial PD measurement system. Figure 7 shows the circuit for measuring PD signals.

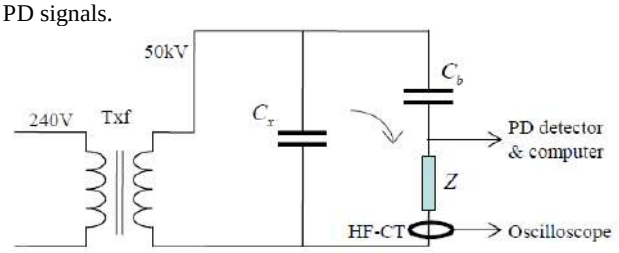

Figure 7. Partial discharge measurement circuit

For each type of PD, the applied voltage was steadily increased; this data recorded was used as training data for the classifier. The applied voltage was also steadily decreased for each PD type and this recorded data was used as classifier test data. The applied voltage ranged between 2.5kV to 8kV. Table 1 shows the details of the training and test data collected for the experiments in this paper.

Table 1. Details of test and training data for corona, surface and internal partial discharge for 3 classes

Class Type	Training data	Test data
Class 1: Surface discharge	22	16
Class 2: Corona discharge	19	13
Class 3: Internal discharge	13	9
Class 4: Corona discharge with polarity reversed	13	5
Class 5: Surface discharge with polarity reversed	21	13

IV. RESULTS AND EVALUATION

In order to train a Support Vector Machine (SVM) classifier, the energy features discussed in Section 2.3 of this paper, were extracted for both training and test data, as in Table 1. For each feature, both equal and octave frequency sub-bands were used, to determine which of the two had robust feature extraction. Classification accuracy results of the 5 class problem using energy features are presented in Table 2.

Table 2. Classification results for a 5 class problem using energy features

Class Type		Equal sub-bands	Octave frequency sub-bands
Classification accuracy	7 bands	100	100
	5 bands	98.2	100
	3 bands	91.07	96.42

V. CONCLUSION

This paper investigated a filter-bank based approach for extracting frequency domain based features to represent a PD signal. The filters can be organized in either in equal or octave frequency sub-bands. Three types of partial discharge were analyzed and tested. A Support Vector Machine classifier is trained and the preliminary results shows that the octave frequency sub-bands performed better than equal sub-bands when energy vectors are used as features.

Future research will look at collecting more data to create a larger data set and to further analyze the differences and robustness of the octave and equal frequency sub-bands. Other methods of dimensionality reduction can also be investigated.

REFERENCES

[1] R. Bartnikas, "Partial Discharges: Their mechanism, detection and measurement", IEEE Trans. Dielectr. Electr. Insul, Vol. 9, No.5, pp. 763-808, October 2002

[2] D. Evagorou, A. Kyprianou, P. L. Lewin, A. Stavrou, V. Efthymiou, G. E. Georghiou: "Evaluation of Partial Discharge Denoising using the Wavelet Packets Transform as a Pre-processing Step for Classification," Annual Conf. on Electrical Insulation and Dielectric Phenomena, Quebec, Canada, 26 - 29 Oct 2008, pp.387-390.

[3] R. Ambikairajah, B.T. Phung, J. Ravishankar, T.R. Blackburn: "A Comparison of Noise Reduction Techniques for Online Monitoring of Partial Discharge in High Voltage Power Cables," Int. Conf. on Condition Monitoring and Diagnosis (CMD), Tokyo, Japan, Sept. 6-11, 2010, Paper B1-5.

[4] X. Ma, C. Zhou and I.J. Kemp, "Interpretation of wavelet analysis and its application in partial discharge detection" IEEE Trans. Dielectr. Electr. Insul, Vol. 9, No.3, pp. 446-457, 2002

[5] R. Ambikairajah, B. T. Phung, J. Ravishankar, T. R. Blackburn and Z. Liu, "Novel Frequency Domain Features for the Pattern Classification of Partial Discharge Signals", Int. Symp. on High Voltage Engineering, Hannover, Germany, August 22-26, 2011, Paper F-044.

[6] N. F. Ab Aziz, L. Hao and P. L. Lewin, "Analysis of Partial Discharge Measurement Data using a Support Vector Machine", Conference on Research and Development, SCOReD, pp. 1-6, 12-11 Dec. 2007

[7] K. X. Lai, "Application of Data Mining Techniques for Characterisation and Recognition of Partial Discharge", University of New South Wales, Australia, PhD Thesis, 2010

[8] IEC60270 Ed. 3.0, High-Voltage Test Techniques - Partial Discharge Measurements, 2001

A070

PHENOL REMOVAL FROM WATER BY PULSED POWER DISCHARGE: A REVIEW

Hashem Ahmadi[1], Muhammad Abu Bakar Sidik[1, 3], Zolkafle Buntat[1], Mehrdad Khamooshi[2]
[1]Insitute of High Voltage and Current (IVAT), Faculty of Electrical Enginnering, Universiti Teknologi Malaysia, 81310 Skudai, Johor, Malaysia
[2] Faculty of Mechanical Engineering, Eastern Mediterranean University, Famagusta, Gazimagusa, North cyprus
3Department of Electrical Engineering, Faculty of Engineering, Universitas Sriwijaya
30662 Indralaya, Ogan Ilir, South Sumatera, Indonesia
Email: abubakar@fke.utm.my

EXTENDED ABSTRACT

Abstract: In the last three decades, pulsed high voltage discharge technology has offered promising techniques possible to be used to treat wastewaters, which are supposed to be released to the environment by industries. A significant effort has been directed to understand the processes, which occur during the discharge of solution for variety of reactor configurations. This review presents the disadvantages and advantages of different reactors based on discharge phase. Detailed information is also provided on the principals used in each technique, advantages and disadvantages associated with each method. Finally a discussion on the different discharge areas is proposed.

I. INTRODUCTION

Polluted water with phenol has concerned a lot of scientists due to its harmful impacts on human life as they easily can penetrate through natural membranes, cause a broad spectrum of genotoxic, mutagenic, and hepatotoxic effects [1]. Conventional methods of wastewater treatment, which are based on chemical, physical and biological processes posses some defects such as dissipation of cost and time, difficulty in decomposition of some pollutant and need for large facilities, which makes the need for more advance technologies unavoidable. Research began from 1980s [2] showing unique characteristics of pulse discharge plasma as one of the advanced oxidation process (AOP) compare to conventional methods. Advantages of this technology such as removal of several pollutants at the same time, operation at ambient pressure and temperature, high efficient destruction and no selection for contamination made it high potentially suitable as a new method to meet the needs of a more efficient and complete water purification system. The non-thermal plasma produced in water and aqueous solutions by pulsed high voltage discharge efficiently causes a variety of effects like ultraviolet radiation, shock waves, high electric field, and generation of chemically active species. Decomposition of phenol in aqueous solutions was studied by Sharma et al. [3] using pulsed streamer discharge. Highly active species formed in the solution to be treated completely oxidize the organic and oxidizable inorganic materials to water and carbon [4]. Degradation of phenol in water using electrical discharge has been studied in a lot of works [5-8] demonstrating different abilities of purification for variety of reactors. However, a review on the effectiveness and efficiency of different types of discharging area for contaminant removal has never been done. Generally discharging area can be expressed into three categories based on different configuration of reactors and electrodes arrangement, which are: The gas-phase electrical discharge [9], the liquid-phase electrical discharge [10] and gas-liquid electrical discharge [11]. This review presents the disadvantages and advantages of different reactors based on discharge phase. Detailed information is also provided on the principals used in each technique, advantages and disadvantages associated with each method. Finally a discussion on the different discharge areas is proposed.

Electrical discharge in liquid or gas-liquid phases has higher efficiency due to direct contact with the solution to be treated but the amount of generated plasma is affected by conductivity and uniformity level of gas-liquid phase [12,15]. Conductivity of industrial wastewaters is very high, leading to reduction in discharge current and energy efficiency and increment in conduct current. Hence, liquid-phase reactors could not decompose contaminant effectively [15]. Unlike Wang and Quan [12] and Chen et al. [15], Solution conductivity variation has little effect on the decomposition rate in gas and gas-liquid phase electrical discharges.

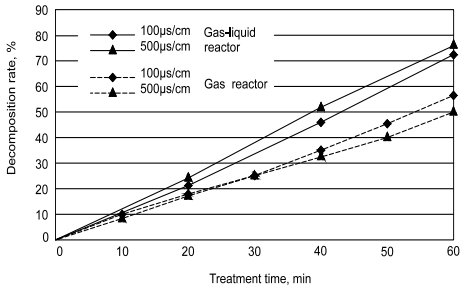

Figure 1. Effect of solution conductivity on decompostion rate of gas and gas-liguid reactors [13, 14].

Figure 1. shows a comparison between decomposition rates of gas and gas-liquid phase reactors. It can be seen that variation in solution conductivity has a little effect on decomposition rate of both gas and gas-liquid phase reactors but it can be found that decomposition rate of gas-liquid phase reactor is much higher than gas-phase reactor.

Figure 2. depicts the change of decomposition rate for both gas and gas-liquid reactors under different pH values. It can be deduced from the plot that decomposition rate was lower in the acidic condition than in the basic condition with pulse discharge [16]. The reason for such this result is that in basic condition the ozone produced in the solution can be easily transformed into

•OH, which possess stronger oxidation capability than ozone leading to higher decomposition efficiency [17].

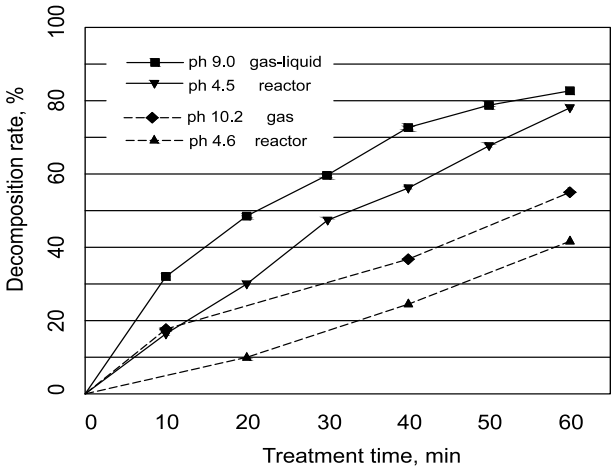

Figure 2. Effect of solution conductivity on decompostion rate of gas and gas-liguid reactors [13,14].

Increasing population and consequently increment in production of wastewater by different human activities caused clean water to be critically important for our planet survival. Drawbacks in current water purification systems demand more cost effective, compact and efficient technologies. The present study reviewed the development of previous and current reactor electrode configuration that can be used to decompose phenol within the aqueous solutions.

New technologies effectively replace traditional concepts. Gas-liquid phase electrical discharge produces hydrogen peroxide in water and ozone in the gas phase. Generated ozone in gas phase results in higher concentration of reactive species in the liquid phase. Comparison of data show higher efficiency for hybrid gas-liquid phase discharge than was seen previously for gas and liquid phase electrical discharge. Various key issues and challenges need to be addressed for better understanding of mechanism in such reactors.

REFERENCES

[1] J. W. Yager, D. A. Eastmond, M. L. Robertson, W. M. Paradisin, and M. T. Smith, "Characterization of Micronuclei Induced in Human Lymphocytes by Benzene Metabolites," *Cancer Res.*, vol. 50, pp. 393–399, 1990.

[2] L. R. Grabowski, E. M. van Veldhuizen, A. J. M. Pemen, and W. R. Rutgers, "Breakdown of Methylene Blue and Methyl Orange by Pulsed Corona Discharge," *Plasma Sources Sci. Technol.* , vol. 16, pp. 226–232, 2007.

[3] A. K. Sharma, B. R. Locke, P. Arce, and W. C. Finney, "A Preliminary Study of Pulsed Streamer Corona Discharge for the Degradation of Phenol in Aqueous Solutions," *Hazard. Waste Hazard. Mater.*, vol. 10, p. 209, 1993.

[4] H.-j. Wang and X.-y. Chen, "Kinetic analysis and energy efficiency of phenol degradation in a plasma-photocatalysis system," *Journal of Hazardous Materials*, vol. 186, pp. 1888-1892, 2011.

[5] R. Xie, C. Chen, W. Li, and X. He, "Phenol Degradation by a Hybrid Gas-liquid Discharge Reactor with Digital-analog Mixed Control," in *Proceedings of the 29th Chinese Control Conference*, Beijing, China, 2010, pp. 5013-5016.

[6] M. Sato, T. Tokutake, T. Oshima, and S. Anto Tri, "Aqueous Phenol Decomposition by Pulsed Discharges on the Water Surface," *IEEE Transactions on Industry Applications*, vol. 44, pp. 1397-1402, 2007.

[7] L. Xiaoyong, C. Jierong, and G. Li, "Enhanced Degradation of Phenol by Carbonate Ions With Dielectric Barrier Discharge," *IEEE Transactions on Plasma Science*, vol. 40, pp. 112-117, 2012.

[8] S. Mayank and R. L. Bruce, "Degradation of chemical warfare agent simulants using gas–liquid pulsed streamer discharges," *Journal of Hazardous Materials*, vol. B137, pp. 1025-1034, 2006.

[9] J. S. Clements, M. Sato, and R. H. Davis, "Preliminary Investigation of Prebreakdown Phenomena and Chemical Reactions Using a Pulsed High-Voltage Discharge in Water," *Industry Applications, IEEE Transactions on*, vol. IA-23, pp. 224-235, 1987.

[10] M. Muhammad Arif, R. Ubaid ur, G. Abdul, and A. Kurshid, "Synergistic effect of pulsed corona discharges and ozonation on decolourization of methylene blue in water," *Plasma Sources Science and Technology*, vol. 11, p. 236, 2002.

[11] L. R. Grabowski, E. van Veldhuizen, A. J. M. Pemen, and A. Fabregat, "Corona Above Water Reactor for Systematic Study of Aqueous Phenol Degradation," *Plasma Chemistry and Plasma Processing*, vol. 26, p. 3, 2006.

[12] H. Wang, J. Li, and X. Quan, "Decoloration of azo dye by a multi-needle-to-plate high-voltage pulsed corona discharge system in water," *Journal of Electrostatics*, vol. 64, pp. 416-421, 2006.

[13] J. Li, M. Sato, and T. Oshima, "Degradation of Phenol in Water Using a Gas–liquid Phase Pulsed Discharge Plasma Reactor," *Thin Solid Films*, vol. 515, pp. 4283-4288, 2007.

[14] W. Yan, L. Jie, L. Guo-Feng, L. Nan, Q. Guang-Zhou, S. Chang-Hai, and M. Sato, "Decomposition of Phenol in Water by Gas Phase Pulse Discharge Plasma," in *Industry Applications Society Annual Meeting, 2009. IAS 2009. IEEE*, 2009, pp. 1-4.

[15] Y. S. Chen, X. S. Zhang, Y. C. Dai, and W. K. Yuan, "Pulsed High-voltage Discharge Plasma for Degeradation of Phenol in Aqueous Solution," *Separation and Purification Technology*, vol. 34, pp. 5-12, 2004.

[16] P. S. Lang, W. K. Ching, D. M. Willberg, and M. R. Hoffmann, "Oxidative Degradation of 2,4,6-Trinitrotoluene by Ozone in an Electrohydraulic Discharge Reactor," *Environmental Science & Technology*, vol. 32, pp. 3142-3148, 1998/10/01 1998.

[17] A. T. Sugiarto, T. Ito, T. Oshima, m. sato, and D. S. jan, "Oxidative decoloration of dyes by pulsed discharge plasma in water," *Journal of Electrostatics*, vol. 58, 2003.

A071

INACTIVATION OF MELANOMA CELLS USING DBD PLASMA JET IN ATMOSPHERIC PRESSURE ARGON

Xing-Min Shi[1]*, Guan-Jun Zhang[2], Zheng-Shi Chang[2], Zhao-Yu Peng[2], Xian-Jun Shao[2]
[1]Environment and Genes Related to Diseases Key Laboratory of Education Ministry, Xi'an Jiaotong University College of Medicine, 76 Yanta West Road, Xi'an, Shaanxi 710061, China
[2]State Key Laboratory of Electrical Insulation and Power Equipment, Xi'an Jiaotong University, 28 Xianning West Road, Xi'an, Shaanxi 710049, China
Contact address:
Mailbox 87#, Xi'an Jiaotong University College of Medicine,
No.76 Yanta West Road, Xi'an 710-061, China
E-mail: shixingmin142@163.com

Keywords: Low-temperature plasma, Melanoma Cells, Cell viability

Abstract: An argon atmospheric pressure plasma jet (APPJ) is used to generate low-temperature plasma (LTP) for the treatment of B16 murine melanoma cells cultured *in vitro*. Experimental results reveal that, the LTP significantly decrease the cell viability, melanin synthesis and tyrosinase activity of melanoma cells in a time/dose-dependent manner. Based on the detection of emission spectroscopy of LTP, it is found there are NO, OH radical and excited-state oxygen atom existing in Ar APPJ. Examination of cell apoptosis shows that LTP can induce cell apoptosis and cell necrosis of melanoma cells. Our results suggest that, NO, OH radicals and excited-state oxygen atoms generated in LTP might decrease cell viability, melanin content and tyrosinase activity of melanoma cells via inducing cell apoptosis and cell necrosis.

I. INTRODUCTION

In recent years atmospheric pressure plasmas have been used to treat live cells and tissues, including cell proliferation, cell detachment，cell attachment, cell apoptosis, cell necrosis, blood coagulation ,wound healing and tumor therapy[1][2].LTP is an alternative method for tumor treatment, which has been proven to have less side effects and high efficiency [3]. LTP treatments offer the possibility of removaling tumor cells without inflammation and excessive damage to the body.

In this paper, a sinusoidal alternating voltage was applied to the electrodes to generate Low-temperature plasma jet in atmospheric pressure argon. Mouse Melanoma Cells were chosen as model and were treated by the low-temperature plasma jet. The purpose of this study is to investigate the effect and mechanism of low-temperature plasma on inactivation of mouse melanoma Cells cultured *in vitro*.

II. MATERIALS AND METHODS

A Generation of low-temperature plasma jet

An experimental setup of coaxial DBD plasma jet was designed to operate at atmospheric pressure in Ar, as illustrated in Fig. 1. The coaxial DBD reactor consisted of a central copper wire of 0.94 mm in diameter covered with polytetrafluoroethylene (PTFE) of 1.03 mm in thickness as the high voltage electrode, a quartz glass tube of 6 mm in inner diameter and 1 mm in thickness, a copper strip of 10 mm in width wrapped around the surface of the tube as the ground electrode. And the argon at a controllable rate flowed through the glass tube from the inlet.

The two electrodes is applied with a 37 kHz AC sinusoidal power supply. The applied voltage was measured by a high voltage probe (Tektronix Tek6015A, with a band width of 75 MHz and a dividing ratio of 1000), and the discharge current was measured by an inductance-free resistor of 100 Ω connected in series into the circuit. And the waveforms are recorded by a digital oscilloscope (Tektronix TDS 4034, with a band width of 350 MHz, a sampling rate of 2.5 GSa/s). In all the experiments, the flow rate of Argon is fixed at 11.80 m/s, and the voltage at a peak value of 3 kV. Then an atmospheric plasma jet is generated around the outlet of the glass tube.

The components of plasma jet were determined by detecting its emission spectra.

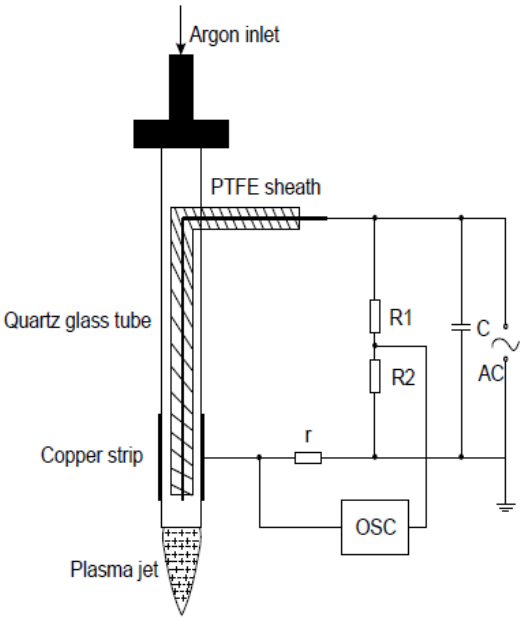

Figure 1. Experimental setup of DBD plasma jet

B Plasma Treatment and related medical detection

Before plasma treatment, cells are suspended in 200 μL culture media(1×10^5/mL) in a 96-well plate. When the experiment is conducted, the lid of 96-well plate is opened and the cells are treated for 2, 4, 6 and 8 s with plasma jet, which is just in contact with the liquid surface. After plasma treatment, the plate is covered and immediately placed in CO_2 incubator at 37 °C for 72 h.Then cell viability, melanin content, tyrosinase activity were respectively measured. And transmission electron microscopic (TEM) observation, examination of cell apoptosis were performed to explore the inactivation mechanisms of plasma jet on mouse melanoma cells.

III. RESULTS AND DISCUSSION

Detection of emission spectroscopy of plasma jet found NO, OH radical and excited-state oxygen atom exist in plasma jet. And it found that plasma inhibited the cell proliferation, melanin synthesis and tyrosinase activity of mouse melanoma cells in a time/dose-dependent manner. When the treatment time is more than 8s, there are even no cells alive.

TEM examination found that plasma treatment resulted in melanin particles decreased, endocytoplasmic reticulum and and swollen mitochondria destroyed, cell membranes broken and cytoplasm leakage. Examination of cell apoptosis shows that LTP can induce cell apoptosis and cell necrosis of melanoma cells.

IV. CONCLUSION

The inactivation effects of DBD plasma jet in atmospheric pressure argon on the B16 murine melanoma cell *in vitro* culture are investigated. Results indicate that LTP treatment can decrease the cell viability, melanin content and tyrosinase activity of melanoma cells. Analysis of emission spectra of the argon plasma jet and examination of cell apoptosis revealed that, NO, OH radical and excited-state oxygen atom generated in LTP might play a dominant role in the process of decreasing the cell viability, melanin content and tyrosinase activity of melanoma cells. It suggests that low-temperature atmospheric pressure plasma jet may provide a novel approach that can be used to treat melanoma.

REFERENCES

[1] I. E. Kieft, M. Kurdi, and E. Stoffels, "Reattachment and apoptosis after plasma-needle treatment of cultured cells", IEEE Trans. Plasma Sci, Vol.34, PP.1331–1336, 2006.

[2] S.U. Kalghatgi, A.Fridman, G.Friedman and A. M. Clyne,. "Endothelial cell proliferation is enhanced by low dose non-thermal plasma through fibroblast growth factor-2 release", Ann. Biomed. Eng., Vol.38, PP.748–757, 2010.

[3] J. Heinlin, G. Isbary, W. Stolz, G. Morfill, M. Landthaler, T. Shimizu, B. Steffes, T. Nosenko,J.L. Zimmermann, S. Karrer, "Plasma applications in medicine with a special focus on dermatology", Journal of the European Academy of Dermatology and Venereology, Vol.25, PP.1-11,2011.

A072

MAKING PERMANENT MAGNET USING HIGH IMPULSE CURRENT

Haryono T.*, Denny Rinaldo*, Prasetyohadi* and Daryadi*
*Electrical Engineering and Information Technology Department Universitas Gadjah Mada, Indonesia
2 Grafica St, Yogyakarta, Indonesia, thrharyono@gmail.com, Phone 0811250611

Keywords: B-H curve, saturation, impulse current

Abstract: A strong magnet permanent may cause damage to some electronic instrument placed close to it. That is why usually a permanent magnet is not transported, but it is magnetized at the place where it will be used. In this research, it was an impulse current generator that was used to do the job. The impulse current generator has five high voltage capacitors, which can be connected in parallel in order to provide higher peak impulse current. To obtain longer value of the impulse current front time, an inductor was inserted to the impulse current circuit. The inductance of it could be varied according to the value of impulse current front time that was going to be created. The impulse current successfully changed a concrete nail to be a permanent magnet

I. INTRODUCTION

When an electric current flows through an electrical power lines, around the lines it will be created electromagnetic field. When the line is in the form of a coil, the electromagnetic field will also exist in the core of the coil. In the case of an iron core, the coil produces higher value of the electromagnetic field strength due to that the iron core has higher permeability value than an air core. Futher, the air core inductor has smaller inductance compared to that of an iron core one.

Fossil fuel energy based on oil and coal, which are used as the main fuel nowadays for electrical generation, will be more and more decrease in number and finally no more can be found. Oil will be quickly end as it is being used for air, sea, and land transportation system and other purposes. Therefore, it is suggested to also use renewable energy sources, forinstance hydro power, wind power, geothermal energy, sea wave energy, ocean thermal different energy and solar energy for electrical power generation. Most of renewable energy usage is in small capacity resulting in the use of small electrical generation. Small electrical generation, commonly, can be found in the form of small electrical generation capacity, which operates based on permanent magnet.

In the current condition, at least in Indonesia, electrical generator are imported from other countries, so that local country industry contributes only in the assembling process of the electrical generator.

To support the growing program of small scale electrical power industry in the usage of renewable energy, it is important to make permanent magnet. If strong permanent magnet is able to be self made, then the industry of small scale permanent magnet generator will fastly grow. Therefore, the cost for producing renewable energy based for electrical power generators can be much reduced. So, a research to find a simple method for producing permanent magnet is needed.

The following research result was the effect of magnetic material variation to magnetic quality. This needed relevance knowledge related to chemical one.

When a curent flows through a coil having metal or non metal core, magnetic fields is produced in the core. The higher the current makes the bigger value of the magnetic field strength.. However, there is a limit in magnitude of the current flowing, above which the magnetic field strength cannot be increased anymore as the saturation condition has been reached. For Neodymium-Iron-Boron material. If Hs > 40000 Oersteidt, Br cannot been futther increased. After reaching this point, if Hs is reduced, the return path will not use the same path. Instead, the path that is used, is the upper path resulting in the Br ≠ 0 for Hs = 0. Then the value of Br is called residual magnetic. This shows that permanent magnet is produced.

II. MATERIALS AND METHODS (when applicable)

An impulse current generator being able to produce a peak current of 8663.79 A with front time of 5.37 μS and tail time of 24 μS was used to make permanent magnet.

A NYA cable having the diameter of 1.5 mm wound surrounding a PVC pipe having inner diameter of 17 mm with it's length of 100 mm was used as magnetizer's coil. Several number of turn coils were produced, each of which has 5, 10, 20, 35, 46, and 86 turns.

In order to produce longer front time and tail time of the impulse current obtained, two different inductors consisting of 86 turns and 100 turns surrounding E-I core was made and was connected in series to the magnetizer's coil.

Material to be magnetized was in the form of 7 concrete nails, Fig.1, that were inserted in the PVC pipe performing as the coil core.

Figure 1. Concrete nails.

III. RESULTS AND DISCUSSION

Using 7 concrete nails as the core of the coils, each of which having 5, 10, 20, 35, 46, and 86 turns, with the implementation of impulse current produced by 7 kV capacitor voltage charging, it could be obtained permanent magnets. The permanent magnet strength produced by the central of the nails up to 10 days measurement can be seen in Figure 2, and the permanent magnet strength produced by concrete nails surrounding the central ones for 10 days are easily seen in Figure 3.

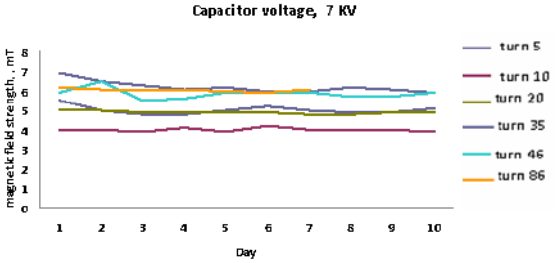

Figure 2. Magnetic field strength of central concrete nail under the capasitor voltage of 7 kV

A074

STUDY ON PARTIAL DISCHARGE CHARACTERISTICS OF GENERATORS: CASE STUDY AT TANJUNG BIN POWER PLANT, JOHOR, MALAYSIA

A. H. Muhamad[1], Y. Z. Arief[2]*, and Z. Adzis[2]
[1]Tanjung Bin Power Plant, Jalan Tanjung Bin, 82300 Kukup, Johor, Malaysia.
[2]Institute of High Voltage and High Current, Faculty of Electrical Engineering, Universiti Teknologi Malaysia, 81310 Johor Bahru, Johor, Malaysia.

Keywords: generator, partial discharge, PDViewsoftware, generator stator winding.

Abstract: Power generation is a business that both satisfy industrial and consumer needs. Power generation technologies had emerged from conventional power plant which is denoted by conventional steam plant and evolved all the way to nuclear plant. While mechanical arrangements are usually unique and differ from a type of power plant compared to another, electrical assemblies are almost the same. Much anticipating factor is sizing of the electrical equipment. Among fundamental equipment that is a must have in a power plant is an electrical generator. In principle, generator is crucial equipment that needs a proper maintenance in order to produce a steady output stream. The objective of this study is to investigate partial discharge characteristics of 3 unit generators stator winding at Tanjung Bin Power Plant, Johor, Malaysia. We will compare the partial discharge characteristics of unit 10, 20 and 30 generators stator winding, respectively. Software designed by *Iris LP* will be used throughout these processes. The software-*PDView* will demonstrate graphical view of the partial discharge occurrence in the generator stator winding. Compiled data will be analyzed using *Microsoft Excel* in order to establish an evaluation of the generator stator winding. The analyzed results showed that all generators are in good condition.

I.INTRODUCTION

The rule of thumb when a conductor is moved across a magnetic field or vice versa, current is generated inside the conductor. A generator produces electricity. In a generator, whenever something initiates the shaft or armature to spin, electricity is generated. Generator is the heart of electricity production where pure electrical reactions occurr and effectively produce massive amount of currents that is beneficial for the industrial and home uses.

Competent electricians are aware of the role played by a generator in the power generation business. A generator must be well kept, maintained and monitored. Among maintenance activities that should be carried out are carbon brush measurement, slip ring cleaning and shaft voltage cleaning. These activities are normally carried out on monthly basis or during shutdown.

Failure to do a proper maintenance will result in devastating event. All maintenance histories are documented and audited periodically. While all these kind of maintenances are performed on generator, there is one more maintenance action that should be taken into consideration. Partial discharge in stator winding is a kind of slow deterioration process occuring on winding insulation. Measurements of the partial discharge in stator winding could be done on-line or off-line.

Studies show that most stator windings are very reliable (about 95%) at any given time [4]. Knowing this, it is important for users of large machines to know or at least have an idea if their machine is one of the 5%. There are advantages to knowing that there are no problems. Some machines are known to be more reliable than others because of their design and how they are operated. However, eventually these machines will fail, if for no other reason, due to gradual thermal aging of the stator winding insulation. Users of the partial discharge test will be able to find problems while on line and also identify machines that are in good condition enabling them to extend the time between major outages.

II. MATERIALS AND METHODS

Partial discharge data can be collected using many different techniques, the important criteria for any measurement made during normal generator operation is the ability to deal with electrical interference or noise. With the machine in operation and connected to the power system, many sources of noise are present including power system corona, slip ring sparking, poor electrical connections external to the stator winding, local power tool or arc welding equipment operation, and many more. All of these can generate pulses with characteristics similar to partial discharge, which can often be orders of magnitude larger than the actual partial discharge levels in the winding[5].

This study will focus on the predominant on-line partial discharge measurement technique in use today, which detects the voltage pulse that is created when a partial discharge occurs via either a high voltage capacitor connected to the machines stator winding; or a *stator slot coupler* (SSC) which is a type of antenna installed in stator slots. Fig. 1 is a sample of SSC installed in on line partial discharge system.

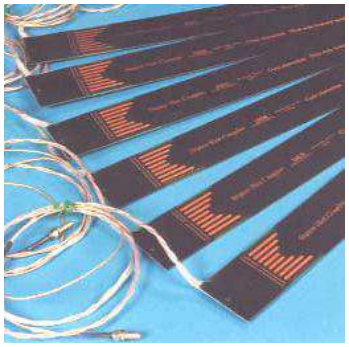

Figure 1. Stator Slot Couplers (SSC)[5]

Each generator monitored requires a *data acquisition unit*(DAU) to be installed nearby and within 30cm of the PD termination box. Size appropriatecoaxial cables connect the PD termination box to the DAU[5]. The DAU measures the partial dischargesactivity from all of the partial discharge sensors installed on the machine, separates the partial discharge from noise, and counts the number, magnitudeand phase position of

*yzarief@fke.utm.my

the partial discharge. The DAU contains a computer and memory to temporarily store the data, and to enable communications with a *system controller* via a number of communication methods. The DAU also accepts analog inputs to measure the generator operating information such as active power, reactive power, temperature, voltage, and hydrogen pressure.

III. RESULTS AND DISCUSSION

Partial dischargesplots were obtained from *system controller*. Graphs were generated using *PDView*Software provided by *IrisPower*. Each graph will consist of *bipolar slot total*and *bipolar endwinding*. Generator Unit 10, 20 and 30 are equipped with six sensors per unit. They are named RS40, YS8, BS24, RS9, YS25 and BS4, respectively. Every sensor is positioned at 30, 150, and 270degree according to the respective phases. For the ease of analysis, we group the sensors into two groups. The first group is denoted by RS40-YS8-BS24 and the latter would be RS9-YS25-BS41. Examples of *bipolar slot total*and *bipolar endwinding*wereshown in Fig.2.

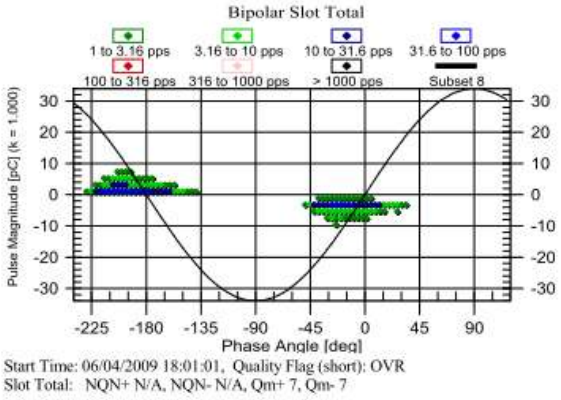

Figure 2. Bipolar Slot Total

In order to establish a 5-year trending for respective unit, we took three measurements per year for every unit. We decided to take measurement in January, June and December each year for every unit for five consecutive years. All measurements taken were from 2007 until 2011. Somehow, not all months are available within the data range. Unavailable data that is missing due to anonymous problem was replaced with nearest month available. Clarification will be made in the affected unit. From graphs generated by *PDView*software, we tabulatedthe maximum PD occurrence of each graph. The trending wasplotted using *Microsoft Excel*and illustrated further in the respective section.

In order to establish a 5-year trending for respective unit, we took three measurements per year for every unit. We decided to take measurement in January, June and December each year for every unit for five consecutive years. All measurements taken were from 2007 until 2011. Somehow, not all months are available within the data range. Unavailable data that is missing due to anonymous problem was replaced with nearest month available. Clarification will be made in the affected unit. From graphs generated by *PDView*software, we tabulatedthe maximum PD occurrence of each graph. The trending wasplotted using *Microsoft Excel*and illustrated further in the respective section.

Throughout five years, we obtained eighty-percent measurements that followed our default time of measurement namely January, June and December for each year. Slight of changes were done on measurement on June 2010, June 2011 and December 2011. The data were replaced with July 2010, May 2011 and November 2011, respectively. However, the plotted graphs denoted default date as January, June and December. For example, red phase graph for Generator Unit 10 were illustrated in Fig. 3.

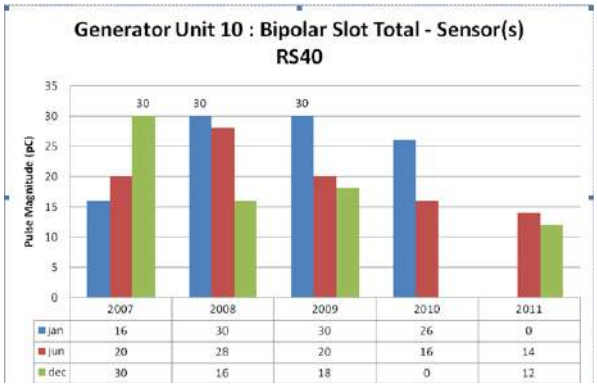

Figure 3. Sensors RS40 Bipolar Slot Total

Fig. 4showsthe maximumPD pulse magnitude for generator Unit 20. Thisindicates the RS40-YS8-BS24 sensors.

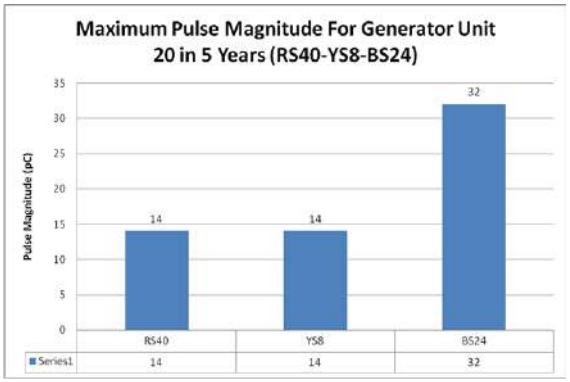

Figure 4. Maximum PD Pulse Magnitude for Generator Unit 20 (RS40-YS8-BS24)

REFERENCES

[1] IEEE Power Engineering Society, "*IEEE Trial-Use Guide to the Measurement of Partial Discharges in Rotating Machinery*" , 2000, IEEE.

[2] Iris Power LP, "*On-Line Partial Discharge Testing for Motors & Generators* ".

[3] Iris Power LP, "*Interpretation of PD Results : On-line Testing Using Capacitive or Stator Slot Couplers*".

[4] G.C Stone and Vicki Warren, "*Practical Experience with On-Line Partial Discharge Condition Monitoring of Stator Windings*", Iris Power, 1 Westside Drive, Unit 2, Toronto, M9C 1B2 Canada.

[5] TgBin-TSB-B7-B-09710_O&M Manual 7-10 Partial Discharge Monitoring

A075

DISTINCTIVE FEATURES OF INITIAL BREAKDOWN PROCESS BETWEEN GROUND AND CLOUD DISCHARGES

M. R. Mohd Esa*[,a,b], M. R. Ahmada,[c], V. Cooray[a]
[a] Ångström Laboratory, Division for Electricity
Department of Engineering Sciences,
Box 534, S-751 21, Uppsala University, Sweden
[b] Universiti Teknologi Malaysia
81310 Skudai, Johor Bahru
Johor, Malaysia
[c] Universiti Teknikal Malaysia Melaka
Hang Tuah Jaya, 76100 Durian Tunggal
Malacca, Malaysia

Keywords: Initial breakdown, Ground discharge, Cloud discharge

Abstract: This paper investigates the existence of distinctive features of initial breakdown process between ground (CG) and cloud (IC) discharges. 10 ground discharge and 10 cloud discharge waveforms have been selected from a collection of waveforms measured using fast broadband antenna system. The measurements were carried out in Uppsala, Sweden from June to August 2010. Major distinctive features are discovered between the initial breakdown process of ground and cloud discharges. Within the first 1 ms duration, the initial breakdown process of CG has more than twice number of pulses, more bipolar pulses than unipolar pulses, and shorter inter-pulse duration when compared to IC.

I. INTRODUCTION

Any lightning discharge must start with an electrical breakdown process. Such breakdown process is known as initial or preliminary breakdown (PB) process. However information regarding the initiation of the breakdown process is still not really well understood. Two famous hypothetical mechanisms have been proposed to explain the inception of breakdown process namely conventional breakdown mechanism and runaway breakdown mechanism [1]. The initial breakdown process could be grouped into 2 categories. Initial breakdown process associated with ground and cloud discharges is the most common and well-studied category. The second category is an isolated breakdown process that doesn't lead to any subsequent activity. Such breakdown process has both polarities as explained in details in [2]. In this paper we focus only on the first category of initial breakdown process. In this paper, more distinctive features are investigated with the aim to observe any difference that may exist between ground and cloud discharges. The investigated distinctive features are the total number of pulses, total number of unipolar and bipolar pulses, average of normalized amplitudes, and average of interpulse duration (IPD).

II. MATERIALS AND METHODS

The measurements were done in the shielded mobile lightning research station in the premise of Ångstrom Laboratory, Uppsala University, Sweden (59.8ºN and 17.6ºE) during summer thunderstorm between June and August 2010. A broadband antenna system equipped with parallel flat-plate and whip antennas was used to capture fast and slow vertical electric field changes respectively. Zero-to-peak rise time of the broadband antenna system was less than 30 ns for the step input pulse. The decay time constant values were fixed at 15 ms and 1 s for fast and slow field measurements respectively. The data presented in this paper were recorded at 20 MS/s (50 ns time resolution) with 300 ms delay.

III. RESULTS AND DISCUSSION

Ten waveforms each were chosen from ground and cloud discharges. The analysis focuses on the pulses found in the initial breakdown process for the first 0.5 ms and 1 ms durations. The maximum number of pulses in ground discharge is more than twice higher than in cloud discharge with 79 ground discharge pulses compared to 29 cloud discharge pulses. Following the same characteristic, the minimum number of pulses recorded 30 ground discharge pulses, more than twice higher in comparison to 11 cloud discharge pulses. We observe that the same characteristic also true for the 0.5 ms duration. We observe that the number of bipolar pulses is always higher than unipolar pulses in 8 waveforms from the total of 10 observed waveforms for ground discharge. However the cloud discharge shows different feature where in 0.5 ms duration case, the number of unipolar pulses is almost equal to the number of bipolar pulses. Since it is insignificant to compare the amplitudes between waveforms (strength is relative to the distance from the discharge source), we adopted a categorization method used in [3] to level the amplitudes to the same reference level. Then, we introduced a normalization method by selecting the largest intensity from the large pulse group and labelled as the main pulse and the other pulses amplitudes were normalized to the main pulse.

We observe that the average of the normalized electric field intensity for both ground and cloud discharges is almost the same. The variations are between 0.2 to 0.4 and 0.3 to 0.6 for 1 ms and 0.5 ms respectively. We observe that the inter-pulse duration of cloud discharge is longer compared to ground discharge.

REFERENCES

[1] V. A, Rakov and M. A. Uman, *Lightning: Physics and Effects*, Cambridge University Press, pp. 121-122 , 2003.
[2] S. R. Sharma, V. Cooray and M. Fernando, "Isolated breakdown activity in Swedish lightning", Journal of Atmospheric and Solar-Terrestrial Physics, Vol. 70, pp. 1213-1221, 2008.
[3] N. A. Ahmad, M. Fernando, Z. A. Baharudin, M. Rahman, V. Cooray, Z. Saleh, J. R. Dwyer, H. K. Rassoul, "The first electric field pulse of cloud and cloud-to-ground lightning discharges", Journal of Atmospheric and Solar-Terrestrial Physics, Vol. 72, pp. 143-150, 2010.

*Tel: +460760812053. E-mail address:monariza.esa@angstrom.uu.se

A076

MITIGATION OF FERRORESONANCE IN POWER SYSTEM BY USING FACTS DEVICES

Jalal Tavalaei*, Zulkurnain Abdul-Malek
Universiti Teknologi Malaysia, 81300 Johor Bahru
Jalal.Tavalaei@fkegraduate.utm.my, zulk@fke.utm.my

Keywords: Ferroresonance, Switching, Preisach-type hysteretic, Transformer, Damping, Coupling capacitance.

Abstract: Ferroresonance as one of EMI phenomena in power system often causes severe damage to power system equipment. Although it usually occurs for duration of several seconds which is much shorter than the duration of current faults, yet explosion of instrument transformers and melting of power transformer lamination can occur due to the ferroresonance effect. Most of previous researches focus on power system stability aspect and magnetizing characteristics of the iron cores. There is minimal study on the ferroresonance damping solution for power system. In this paper, mitigation of ferroresonance is carried out by applying FACTS devices which can change the power system topology at ferroresonance point. While voltage and current waveform are between normal value before switching and maximum point after in ferroresonance time, this phenomenon can be mitigated. The simulation results prove that if FACTS devices are applied before the ferroresonance threshold, the overvoltage and overcurrent values significantly reduce and become tolerable for equipments.

I. INTRODUCTION

Ferroresonance is a resonance situation with nonlinear inductance, so the inductive reactance not only depends on frequency, but also on the magnetic flux density of the iron core (such as the transformer iron core). The inductive reactance is represented by the saturation curve of a magnetic iron core. Theoretically, this nonlinear inductance could be represented by two inductive reactances, according to the situation on the saturation curve.

- Linear zone → XL−linear = ωLlinear
- Saturation zone → XL−sat = ωLsat

Like resonance, depending on the connection between the capacitance and the nonlinear inductance, the ferroresonance equivalent circuit may be in series or parallel [1].

$$E = V_C + V_L \quad (1)$$

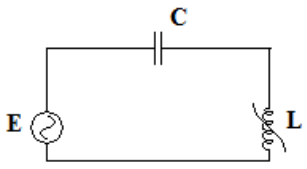

Figure1. Series Ferroresonance circuit

The magnetizing branch of transformer is modeled by Preisach type model as a nonlinear inductance in parallel with a nonlinear resistance and these represent the nonlinear saturation characteristic:

$$(\varphi - i_{Lm}) \quad (2)$$

and nonlinear hysteresis and Eddy current Characteristics [2]:

$$(V_m - i_{Rm}) \quad (3)$$

For Analysis the iron core saturation characteristic is giving by:

$$i_{Lm} = s_1\phi + s_2\phi^2 \quad (4)$$

Where depends on degree of saturation.
The core loss is described by a third order power series whose coefficients are fitted to match the hysteresis and eddy current nonlinear characteristic as:

$$i_{Rm} = h_0 + h_1 V_m + h_2 {V_m}^2 + h_3 {V_m}^3 \quad (5)$$

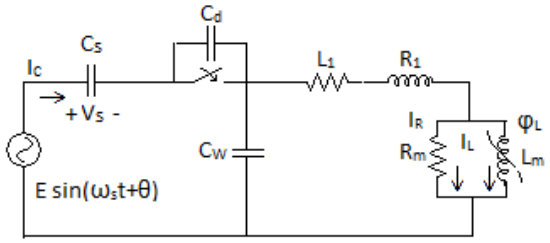

Figure 2. Equivalent circuit for modeling Ferroresonance

II. SIMPLIFIED FACTS DEVICES AND EFFECT ON TRANSIENTS STABILITY

FACTS devices are equipments used in power transmission network to overcome power quality problems. As the FACTS device is switch off, the VSC source is in the charging process and its effect on the settled line is minimum. Yet, when the device senses any power quality problem, switch on and inject or absorb power to mitigate this problem. It is clear that, by switching on any FACTS devices, system topology at connection node will change [3]. FACTS devices are sensitive to any change in current or voltage; moreover, these devices are connecting to the network in the partial of time, so we expected that these devices can mitigate Ferroresonance. In this novel the effect of STATCOM and UPFC is considered. The Unified Power Flow Controller is the most versatile FACTS controller for the regulation of voltage and power flow in a transmission line. It consists of two voltage source converters (VSC) one shunt connected and the other series connected. The DC capacitors of the two converters are connected in parallel. Yet, the STATCOM is just the shunt part of figure 3.1, while the interconnection switches areoff. Although STATCOM ability to mitigate transients is less than UPFC, this FACTS device has faster response.

Table 1. Yield of Applying FACTS on Peak of voltage

FACTS	UPFC -1	Ferro.	UPFC-2	Ferro.	STATCOM	Ferro.
ON	1.57 *p.u*	2.42 *p.u*	0.96 *p.u*	2.2 *p.u*	1.3 *p.u*	1.9 *p.u*

*Jalal Tavalaei, Department of Electrical Engineering, Universiti Teknologi Malaysia, E-mail address: jalal.tavallaei@gmali.com, Tel: +6-010 7059825.

Yield	35%		56%		31.6%	
OFF	1.22 *p.u*	2.1 *p.u*	1.16 *p.u*	1.78 *p.u*	1.25 *p.u*	1.81 *p.u*
Yield	41.9%		34.8%		30.9%	

III. RESULT AND DICUSSION

In Figure 3 portrays the different between ferroresonance and 3 FACTS devices that applied to mitigate ferro-resonance. It is shown that circuit breaker switch off at 0.15 sec, and entire network back fed by coupling capacitance. When ferroresonance occur the voltage peak rises to 3.5 times more than normal condition. Yet by applying UPFC in mode-1 at 0.18 sec, after a transient, it shows good damping during UPFC in mode-1 is switch on. Switching off the UPFC in mode-1 at 0.38 sec slightly distort the voltage waveform. In the third subplot, effect of UPFC in mode-2 is shown. When the circuit breaker switches off, the ferroresonance voltage peak is more than normal condition of ferroresonance. Moreover, switching on the UPFC in mode-2 reduced the voltage to half of normal condition (after a transient). Furthermore, after switching the UPFC in mode-2 off, the voltage increase, yet it's containing upper harmonics which are dominant and distort the waveform considerably. The last subplot portrays the STATCOM yield of ferroresonance. When the STATCOM switch on, by a transient it reduce the ferroresonance. Furthermore, turn off the STATCOM slightly changes the voltage waveform.

From the work carried out in this research, the following conclusions can be made:

- The THD during ferroresonance increases significantly. When the FACTS devices switch on, UPFC in mode-1 portrays better mitigation compared to STATCOM. The UPFC in mode-2 increases the THD. Furthermore, while FACTS are switched off, the STATCOM illustrates better damping compared to UPFC in both mode-1 and mode-2.
- The 1st harmonic falls down by using FACTS devices. When FACTS are switched on, although UPFC in mode-1 and STATCOM reduce 1st harmonic, yet 1st harmonics is more than 1 p.u after damping. But, The UPFC in mode-2 over damps the 1st harmonic. Moreover, while the FACTS switched off, all FACTS have close range in damping to each others.
- The mitigation of UPFC in mode-1 on the 2nd harmonic is better than STATCOM and UPFC in mode-2 when they are switched on. Furthermore, while switching the FACTS off, the effect of UPFC in mode 1 is better than UPFC in mode-2 and STATCOM.
- When FACTS are switched on, the effective device is UPFC in mode-1, UPFC in mode-2 and STATCOM, in order of merit. But, while the FACTS are switched off, the UPFC in mode-1 and STATCOM portrays better damping than UPFC in mode-2.
- When FACTS devices are switched on, UPFC2 reduces ferroresonance better than others, yet when they become switched off UPFC in mode-1 has better damping than others.
- Generally, when the FACTS are switched on, the UPFC in mode-1 has the best mitigation effect. But, when FACTS are in off mode, the best device can be STATCOM and UPFC in mode-1. Moreover, the UPFC in mode-2 illustrates the uncontrollable and unreasonable damping compared to others.
- Table 1 portray that, when FACTS devices are switch on, UPFC2 reduces ferroresonance better than others. Its effectiveness is 56%, yet UPFC1 and STATCOM are 35% and 31.6%, respectively. When the FACTS are turn off, UPFC1 shows better mitigation by around 42% effective damp. Yet UPFC2 and STATCOM mitigation effect is 35% and 31%, respectively.

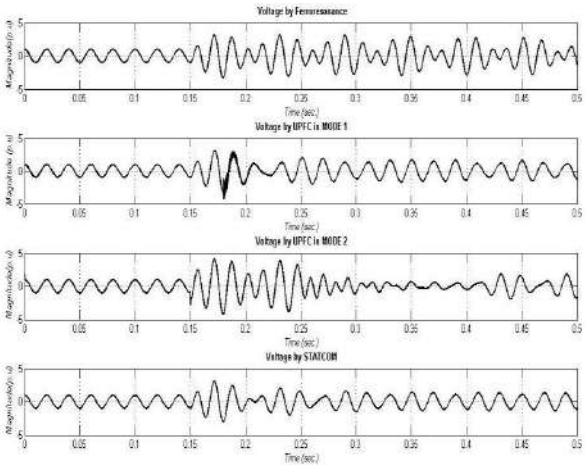

Figure 3. Compare between voltages

REFERENCES

[1] V. Valverde, A.J. Mazón, I. Zamora, G. Buigues, "Ferroresonance in Voltage Transformers: Analysis and Simulations" , pp:1-7.

[2] FACTS Modeling and Simulation in Power Network, Enrique Acha, Claudio R. Fuerte-Esquivel, Hugo Ambriz-Pe'rez, Ce'sar Angeles-Camacho, John Wiley & Sons Ltd, The Atrium, Southern Gate, Chichester, West Sussex PO19 8SQ, England, Copyright 2004, ISBN:0-470-85271-4.

[3] Mork, B.A.S., D.L., Application of nonlinear dynamics and chaos to ferroresonance in distribution systems. Power Delivery, IEEE Transactions, April 1994 **9**(2): p. 1009 - 1017.

A077

CHARGE DISTRIBUTION MEASUREMENT ON GIS DOWNSIZED MODEL SPACER WITH LOW-RESISTANCE COATING

Hiroyuki Iwabuchi[1]*, Shigeyasu Matsuoka[1], Akiko Kumada[1], Kunihiko Hidaka[1],
Yoshikazu Hoshina[2], Takanori Yasuoka[2], and Masafumi Takei[2]
[1]The University of Tokyo, Tokyo, Japan [2]Toshiba Corporation, Kanagawa, Japan
iwabuchi@hvg.t.u-tokyo.ac.jp

Keywords: GIS, spacer, dc electric field, charge accumulation, low-resistance coating, numerical electric field computation

Abstract: When a dc voltage is applied to an insulating spacer, the electric field distribution around it is determined by the resistivity of the material. Consequently, charges are accumulated on the surface of the insulator, and the breakdown voltage of it can become low. For designing a highly reliable electric power apparatus, it is indispensable to get information on such accumulated charge distribution. In this paper, the charge density distribution of the downsized model spacer was measured. Charge measurement was conducted with the spacer, on which low-resistance coating was applied and surface resistivity was changed. The results indicate that the surface resistivity nonuniformity is the main factor of charge accmulation in this experiment.

I. INTRODUCTION

In this paper, the charge density distribution of the downsized GIS disc spacer made of epoxy resin, the relative permittivity of which is 5.93, was measured. A dc voltage was applied to the spacer, and after the removal of a dc voltage, the charge density on the surface was measured using an electrostatic probe. Voltage application and charge measurement were conducted in an experimental chamber filled with 0.1-MPa SF6 continuously without opening the chamber. The applied voltage was set at 30kV and the spatial resolution of the measurement system is 5.4 mm. As pointed out in the preveous research[1], the charge accumulation is affected by the surface resistivity nonuniformity on the spacer. Therefore, the charge measurement was conducted with the spacer, on which low-resistance coating was applied. With the low-resistance coating, the surface conductivity changed. The experiment was conducted with two spacers, the one of which was concentrically coated with low-resistance coating shown in figure 1(a). The other one was full-coated on the spacer shown in figure 1(b).

II. RESULTS AND DISCUSSION

The charge distribution of the concentrically-coated spacer after 100 hours voltage application is shown in figure 2(a). Charges were accumulated along the boundary of the coated region concentrically and no radial charge patterns were appeared. The maximum charge density was over 160pC/mm2. On the contrary, the maximum charge density was below 40pC/mm2 on the full-coated spacer, shown in figure2(b), which is much lower than that in the case of the concentrically-coated spacer. This is because the resistivity of the spacer was uniformized by the low-resistance coating. The experimental results verify the assumption that the surface resistivity distribution is the main factor of the charge accumulation.

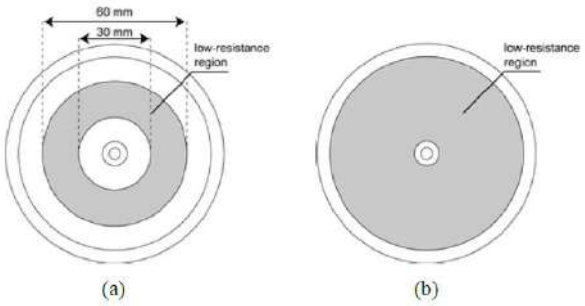

Figure 1. Coating region of disc spacer
(a) Concentrically coating (b) Full coating

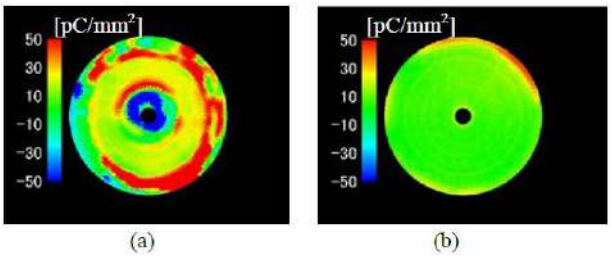

Figure 2. Charge density distribution after 100 hours of voltage application (a) Concentrically coating (b) Full coating

REFERENCES

[1] T. Donen et al., "Influence of Surface-conductivity Nonuniformity on Charge Accumulation Phenomena of GIS Insulator under DC Electric Field", IEEJ Trans. PE, Vol. 131, pp. 584-590, 2011.

*Hiroyuki Iwabuchi Department of Electrical Engineering, The University of Tokyo 7-3-1 Hongo, Bunkyo-ku, Tokyo, 113-8656 JAPAN TEL: 81-3-5841-6759; FAX: 81-3-5841-6725 Email: iwabuchi@hvg.t.u-tokyo.ac.jp

A078

AN EXPERIMENTAL STUDY ON SURFACE DISCHARGE CHARACTERISTICS OF DIFFERENT TYPES OF POLYMERIC MATERIAL UNDER AC VOLTAGE

N. Baharin[1], Y. Z. Arief*[1], W. A. Izzati[1], M. Z. H. Makmud[2], Z. Adzis[2]
[1]Institute of High Voltage and High Current, Faculty of Electrical Engineering, Universiti Teknologi Malaysia, 81310 Johor Bahru, Johor, Malaysia.
[2]School of Science and Technology, Universiti Malaysia Sabah, Kota Kinabalu, Malaysia

Keywords: Surface discharge, High-density polyethylene, Ethylene-vinyl acetate, Polystyrene, Surface morphology.

Abstract: Surface discharge is a common electrical discharge that normally occurs on the surface of outdoor insulators and also causes the failure in the electrical insulation system. One of the causes of surface discharge was the presence of high voltage stress. The experimental work was carried out to examine the surface discharge characteristics on polymers as an insulation material. The IEC (b) electrode configuration had been used to investigate the surface discharge phenomenon of different types of polymeric materials with controlled of relative humidity. In this experimental work, there are three types of polymer that have been selected which are high-density polyethylene (HDPE), ethylene-vinyl acetate (EVA), and polystyrene (PS). The characteristics of the discharge are critically depending on the types of polymer. The surface discharge characteristics observed through surface morphology which is examined by stereo microscope (SZM Series). Moreover, surface discharges intensity and occurrence of each polymeric material are investigated. The data analysis was done to compare the surface discharge characteristics between those samples. From the results, it is discovered that EVA have the severe degradation on its surface compared to HDPE and PS.

I.INTRODUCTION

Surface discharges can occur in a gas, liquid, or a vacuum in close to a solid dielectric surface. Even though the magnitude of such discharges is usually small, they can cause progressive deterioration and leads to failure. Therefore, it is important to investigate these surface discharge characteristics to find the solutions for the problem occurs in application of the solid dielectrics. Solid dielectric materials are used in all kinds of electrical apparatus and devices to insulate one current carrying part from another when they operate at different voltages. A good dielectric should have low dielectric loss, high mechanical strength, should be free from gaseous inclusions, and moisture, and be resistant to thermal and chemical deterioration. Solid dielectrics have higher breakdown strength compared to liquids and gases. Solid insulating materials, which are generally used in practice, are of two types, namely the organic materials, such as paper, wood, rubber, etc and the inorganic materials, such as mica, porcelain, etc, and synthetic polymers such as perspex, high-density polyethylene (HDPE), polypropylene (PP), polyvinyl chloride (PVC), ethylene-vinyl acetate (EVA) and polystyrene (PS).

The objective of this study is to examine the surface discharge characteristics on such polymers as an insulation material. The IEC (b) electrode configuration had been used to investigate the surface discharge phenomenon of different types of polymeric materials with controlled of relative humidity.

The surface morphology due to partial discharge activities are also examined in order to confirm the correlation of ageing time and degradation on polymers surface.

II. MATERIALS AND METHODS

2.1 Sample

In this experimental study, three types of polymeric materials used was high-density polyethylene (HDPE), polystyrene (PS) and ethylene-vinyl acetate (EVA). Each material has its own characteristics. EVA is copolymer of ethylene and vinyl acetate. It's an extremely elastic material that can be sintered to form a porous material similar to rubber, yet with excellent toughness. It is three times as flexible as LDPE. PS is a vinyl polymer. Structurally, it is a long hydrocarbon chain, with a phenyl group attached to every other carbon atom. HDPE is the high density version of polyethylene (PE) plastic. It is harder, stronger and a little heavier than LDPE, but less ductile.

2.2 IEC(b) Electrode Configuration

IEC(b) electrode configuration (IEC 60343:1991) is a recommended standard test method for determining the relative resistance of insulating materials to breakdown by surface discharges. According to this method, we can also observe the discharge intensity as an electrical parameter for this experiment.

In this experiment, the IEC (b) electrode configuration will be a closed condition. This experiment will be conducted to control the relative humidity of the air inside the IEC (b) electrode configuration during the experiment.

2.3 Experimental Procedure

The experiment done used HVAC supply to test the polymeric material samples. The test was used the closed condition IEC (b) configuration and the relative humidity in the closed chamber of IEC (b) was fixed at medium range of 25-49%. The relative humidity in the chamber was controlled by using the silica gels. The percentage reading of relative humidity was taken used hygrometer. The tests are made using 8kVrms AC voltage and frequency of 50Hz. The samples were tested with constant ageing time, 1 hour.

Three test samples have been used in this experimental study. They are from polymeric materials group which are high-density polyethylene (HDPE), ethylene-vinyl acetate (EVA), and polystyrene (PS) .

III. RESULTS AND DISCUSSION

Figure 1 shows the picture of each sample for unaged and aged images.

*yzarief@fke.utm.my

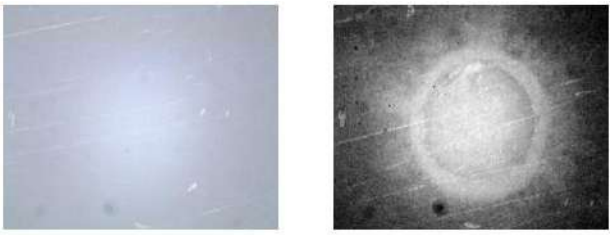

(a) (b)

Figure 1. Picture of HDPE sample; (a) before and (b) after 1h of ageing time

Figure 2 showsthe average peak voltage of surface discharge for each sample during 1h ageing time.As can beseen clearly from the figure, EVA sample hashighest average surface discharge voltage compared to HDPE and PS. It alsoobserved that there is a trend of discharged voltages which rise and fall within minute 0 to minute 50.

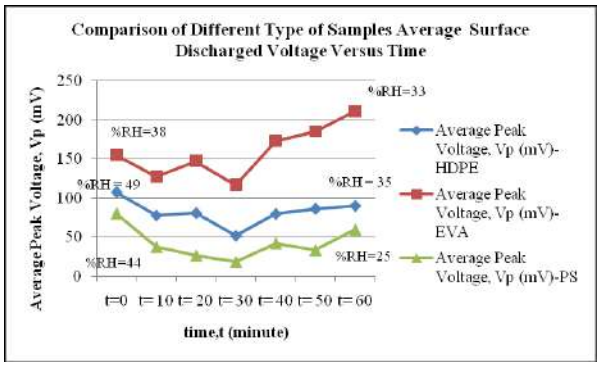

Figure 2. Average peak voltage onsurface dischargesfor HDPE, EVA and PS during ageing time.

Each of polymers has their own characteristics and properties. The arrangement of the electron and molecule bonding greatly influences chemical and physical properties of the polymer. The stronger the chemical bonding, the harder the surface degradation to occurs. So when a high voltage stress applied on the surface of polymer, it will be affected the arrangements of its electron and some chemical process occur.

It is observed that there is a trend of discharged voltages which rise and fall during 1 hour experiment. This might be due to the discharge voltages have become source of energy used in breaking the covalent bond within the polymeric molecular structure that causes electrochemical degradation of polymeric structure. Later, energy is releasedin form of heat and this heat will roughen the surface and cause erosion to form surface cavities.

Degradation occurs when the electrons in a polymeric bond are so strongly attracted to another atom or molecule (called a "foreign" atom or molecule) outside the bond that the polymer bond breaks. The foreign molecules are often part of the environment surrounding the polymeric material and for this experimental study it being effected through source of high voltage. The most common foreign molecule that has significant effects on polymer is oxygen. The process of reaction with oxygen is called oxidation [5].

As time passes, these cavities eventually lead to treeing and possible of insulation failure. High humidity and contamination such as dirt will speed up the process of breakdown. Dirt contamination and moisture film foamed on the insulation surface due to high humidity in an open-air arrangement cause increased electrical conductivity which might be increasing the frequency of the partial discharges. So that, dry and clean surface may help to minimize or eliminate the ageing time effect of partial discharge on polymeric insulator.

In summary, surface discharges of polymeric material under high voltage ac causes severe polymeric sample's surface deterioration as time passes. The prolonged operation under high voltage stress cause tracking and treeing as two of the ageing time effects which gradually lead to permanent insulation failure or breakdown.

REFERENCES

[1] Dr F.H Kreuger (1964). *Discharge Detection in HV Equipment*, Butterworth & Co.

[2] Chai Pei Keon, Nur Akmal Bt Mohd Zin, Mohd Faiz Bin Mohd Jailani, Muhd Hazrul B. Mustapha (2009). *Effect of Ageing Time on Surface Discharge Characteristics of Polymeric Materials under AC Voltage*. UTM Skudai.

[3] Mohamad Zul Hilmey Bin Makmud (2009), "*An Experimental Study Surface Discharge Characteristic on the Polymeric Materials under AC Voltage*", Universiti Teknologi Malaysia, PSM Thesis.

[4] British Standard (BS EN 60343:1993/IEC 343:1991): *Recommended test methods for determining the relative resistance of insulating materials to breakdown by surface discharges*.

[5] Yanuar Z. Arief, "*Study On Partial Discharge Degradation Mechanism of Polymeric Power Cable Insulating Material*",Ph.D. Thesis.

[6] R.A .Fouracre, S.J.MacGregor and F.Teuma (1998). *Some Properties of Surface Discharges*. The Institution of Electrical Engineers.

[7] M. A. Elborki, P. A. Crossley, Z. D. Wang, A. Darwin, G. Edwards (2002). *Detection and Characterisation of Partial Discharges in Transformer Defect Models*. MIEEE.

[8] C. Chang and Q. Su (2000). *Partial Discharge Distribution Pattern Analysis Using Combined Statistical Parameters*. Department of Electrical & Computer Systems Engineerin. Monash University, Australia.

[9] M.S Naidu, V Kamaraju(2004). *High Voltage Engineering*, Third Edition McGraw Hill. Singapore.

A079

ARCING FAULT CONDITION ANALYSIS OF MINERAL INSULATING TRANSFORMER OIL BY POLARIZATION DEPOLARIZATION CURRENT (PDC) MEASUREMENTS

Mohd Aizam Talib*, N. A. Muhamad[1], Zulkurnain Abdul-Malek[1]
TNB Research Sdn Bhd*
No 1 Jalan Air Itam
43000 Kajang, Selangor
Faculty of Electrical Engineering[1]
University of Technology Malaysia
81310 Skudai
Malaysia Johor, Malaysia

Keywords: Polarization Current, Depolarization Current, Mineral Insulating Oil, Transformer Diagnostic, Arcing Fault

Abstract: Reliability of power transformers is most important for a safe and economic operation of electrical networks. Condition monitoring of the transformers is an important issues since many transformers in electrical industries and utilities around the world are approaching the end of their design life. Many testing and monitoring techniques have been used by power utilities to detect failures occur in power transformers as a results of the degradation of the liquid and solid insulation due to various stresses. In the last decade, several dielectric diagnostic methods in time and frequency domain were widely discussed and occasional used to assess the condition of the insulation systems of power transformers. This paper presents the pattern and analysis results of dielectric response in time domain known as polarization and depolarization current (PDC) on mineral insulating transformer oil under arcing fault conditions.

I. INTRODUCTION

Power transformer is one of the most important and expensive components in electrical transmission and distribution system. Faults in transformers can cause interruption of power supply and results to revenue losses to power utilities. The minimization of the time needed for transformer fault diagnosis and repair is an important task for electric utilities, especially in cases where the continuity of supply is crucial. Thus, preventive tests and diagnosis are of benefit to predict fault in the transformer, optimize maintenance and increase reliability of this strategic units.

Many testing and monitoring techniques have been used by power utilities to detect failures occur in power transformers. They can be separated into traditional diagnostic methods such as dissolved gases analysis, oil quality analysis, dielectric loss angle, insulation resistance, turn ratio and winding resistance that have seen widespread use for many year and non-traditional methods such as frequency response analysis and dielectric response measurement. Some of these non-traditional methods are starting to be used and some methods are still in the research stage [1-3].

Dielectric response measurement in frequency and time domain are one of the modern electrical testing techniques. Dielectric characteristics of material are related to the molecular properties of the material. Different faults and ageing in the power transformer will influence the material properties like conduction and polarization and identified easily on dielectric response. The breaking of hydrocarbon chain of mineral insulating oil under arcing fault in power transformer was found influence the conductivity of the oil and observed at the initial of time domain response [4-6].

In this paper, the dielectric response in time domain known as polarization depolarization current (PDC) was used to analyse faults occur in power transformer. The dielectric response of mineral insulating transformer oil with known faults was measured and finally analysed.

II. EXPECTED RESULT

PDC pattern of mineral insulating oil after experince arcing fault is expected to have sligtly different response from mineral oil in healty condition. It will be proven by the result of the statictical analysis run on the PDC measurement data and pattern that will be plot.

REFERENCES

[1] M. Darveniza, D. J. T. Hill, T. T. Le and T. K. Saha, ‘‘Investigations into Effective Methods for Assessing the Condition of Insulation in Aged Power Transformers’’,IEEE Trans. Power Del., Vol, 13, pp. 1214_1223, 1998.

[2] T.K. Saha, P.Purkait, “Investigation of Polarization and Depolarization Current Measurements for the Assessment of Oil-paper Insulation of Aged Transformers”IEEE Trans. on Dielectrics and Electrical Insulation, Vol. 11, No.1, pp 144-154

[3] Vahe Der. Houhanessian and W. S. Zaengl, ‘‘Time Domain Measurements of Dielectric Response in Oil-Paper Insulation Systems’’, IEEE Intern. Sympos. Electr. Insul., Canada, Vol. 1, pp. 47_52, 1996.

[4] U. Gafvert, L. Adeen, M. Tapper, P. Ghasemi and B. Jonsson, ‘‘Dielectric Spectroscopy in Time and Frequency Domain Applied to Diagnostics of Power Transformers’’, IEEE 6th Intern. Conf. Properties and Applications of Dielectric Materials ICPADM., China, Vol. 2, pp. 825_830, 2000.

[5] A. A. Shayegani , O. Hassan , H. Borsi , E. Gockenbach and H. Mohseni , ‘‘PDC Measurement Evaluation On Oil-Pressboard Samples’’, IEEE International Conference on Solid Dielectrics, Toulouse, France, July 5-9, 2004

[6] N.A Muhamad, B.T Phung , T.R Blackburn, “Polarization And Depolarization Current (PDC) Tests On Biodegradable And Mineral Transformer Oils”, 16th International Symposium on High Voltage Engineering, 24 - 28 August 2009, Cape Town, South Africa.

*Mohd Aizam Talib is affiliated with TNB Research Sdn Bhd, Malaysia (e-mail: mohdaizam@tnbr.com.my)

A080

POLARIZATION AND DEPOLARIZATION CURRENT MEASUREMENT OF POLYMER ADDED WITH NANO-PARTICLES OF SILICON OXIDE FOR HV INSULATION

N. A. M. Jamail[1, 2]*, M. A. M. Piah[2], N. A. Muhamad[2], R. A. Zainir[2], N. F. Kasri[2]
[1]Faculty of Electrical and Electronic, University of Tun Hussein Onn Malaysia (UTHM), Batu Pahat, Johor, Malaysia
[2]Faculty of Electrical Engineering, Universiti Teknologi Malaysia (UTM), Skudai, Johor, Malaysia
norakmal@uthm.edu.my, fendi@fke.utm.my, norasiah@fke.utm.my, rabiadza@gmail.com, akta1988@live.com

Keywords: LLDPE nanocomposite, polarization current, depolarization current, DC conductivity

Abstract: Polymer nanocomposites materials have recently emerged as dielectric and electrical insulation. Polyethylene has long been used as extruded cable and HV insulation. Currently, this material has received significant attention because of its ability to enhance electrical insulation properties by addition of nano-filler. Polarization and Depolarization Current (PDC) measurement is an efficient and effective diagnostic technique based on time domain measurement for evaluating and condition monitoring of polymer nanocomopsite for HV insulation. Electrical conduction for polymer nanocomposites has been used widely as a tool to monitor the dielectric behaviour. This paper focuses on application of Polarization and Depolarization Current (PDC) testing method to evaluate and determine the performance of LLDPE nanocomposite for high voltage insulating material. The experiment was conducted to find PDC pattern of the material when added with nano-filler (silicon oxide) as well as to find its conductivity values at different percentage of nano- filler. PDC values and DC conductivity exhibits significant reduction with addition of nano-filler at different %wt of concentration. This was due to the decreasing of initiation probability of short circuit treeing in the insulation. The result shows that the addition with certain percentage of nano-filler into the LLDPE based material could improve HV insulation properties of the material by using PDC method.

I. INTRODUCTION

The oriented structure of polymers has been extensively investigated owing to its enhancement in many properties. Polymer composites are important commercial materials with various applications. As known, polymers filled with nanoscale fillers are recognized as polymer nanocomposites. Apparently, with addition of nanoscale fillers into polymers, robust materials can potentially be produced due to the synergistic effects (cooperating for enhanced effects) arising from the blending process[1]. Nano-silicone oxide (SiO2) with huge surface area is widely used in polyolefin composites. Its application is now mainly focused on the improvement of mechanical and electrical properties [2-4]. Among all non-destructive monitoring techniques, the Polarization and Depolarization Current (PDC) measurement is gaining popular due to its ability to assess the conductivity of HV insulations within the initial periods after a DC step voltage application. PDC Analysis can easily identify whether the cause of insulation trouble is due to conduction such as free water or ageing process caused by temperature effects. The dielectric properties of an insulating material change with moisture, ageing and contamination[5]. In this paper, PDC technique is used to monitor the conductivity variations due to its polarization and depolarization current values. Different types of nano-filler can give different variations.

II SAMPLE AND MATERIAL PREPARATION

LLDPE used in this study is a commercial linear low density polyethylene from Titan Chemical, Malaysia. It has a density of 0.918 g/cm3, a melt index of 25g/10 min. Nanoparticle of silicon oxide is made from China with a particle size of about <50nm was used as filler. This nano scale filler has a nearly spherical shape with a specific surface area of about 100 m2/g. The filler was dried before use. Natural rubber grade SMR CV 60 supplied by Taiko Plantations Sdn Bhd was used for blending and mixing with LLDPE and nanofiller. Polyethylene nanocomposites were prepared by melt mixing at 1650C using a Brabender type model 835201.041 mixer with chamber size of 50 cm3. The mixer has a high shear force and the screw speed was controlled at 35 rpm with the mixing time of 2 min. The polymer nanocomposites were finally prepared into square shape of 10cm x 10cm with the thickness of 3 mm by hot melt pressing at 1 tone pressure at 170 0C for 10 min. Four types of polyethylene nanocomposite square shaped with a diamension of 10 cm x 10 cm were prepared with concentrations of nanofiller of 0, 1, 3, 5 and 7 wt %, respectively.

III PDC MEASUREMENT FOR LLDPE NANOCOMPOSITE INSULATION

The polarization currents measurement was performed by applying a DC voltage step on the dielectric materials and depolarization current is measured by removing the dc voltage source incorporating with a switch which turn on to short circuit the tested objects. The dc voltage applied was 1000V for about 10,000 seconds for polarization and depolarization time. Figure. 1 shows the polarization and depolarization current measurement. The test cell that has been used is three terminal electrode types.

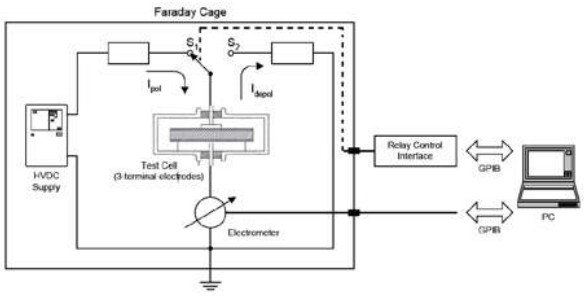

Figure. 1. PDC measurement setup for solid insulation.

IV EXPECTED RESULTS

Diffferent types of nano-filler and percentage of concentration will give different values of polarization and depolarization current values. It can be observed, changes in insulation polarization and depolarization current values tend to

*Nor Akmal Mohd Jamail , Faculty of Electrical Engineering, Universiti Teknologi Malaysia(UTM), Skudai, Johor, Malaysia, norakmal@uthm.edu.my, +60124613382

affect the value of conductivity. From the results, it can be concluded that adding nano particles into LLDPE nanocomposite can reduce the PDC values. However, different amount of nano-fillers will give different results. By reducing the conductivity to the lowest value, it can be known that a small amount of nano-fillers is separated inside the dielectric with a certain wide distance, which can be known as 'extra traps' for the dielectric, and therefore improve the insulation property. However, if more nano particles adding into the LLDPE, for example 5% wt has showed a better insulation property than the pure samplewith the conductivity is higher compared to the samples of 1% and 3% wt. This is because that some of the nano-fillers are too closed to each other, and each nano particle has an interaction zone around it that resulting some overlap of interaction zones. For higher contents of nanofiller, the probability of interaction zones overlap is getting higher, and therefore, the nano particles may aligned together which helps the charges moving across the dielectric. The results from PDC measurements can be used to determine the insulating condition properties of LLDPE nanocomposite..Higher values of polarization and depolarization currents contribute to higher conductivity of the materials. The trends of the conductivity variation were found to be dependent on the polarization and depolarization currents values.

REFERENCES

[1] B. Jongsomjit, *et al.*, "Effect of nanoscale SiO2 and ZrO2 as the fillers on the microstructure of LLDPE nanocomposites synthesized via in situ polymerization with zirconocene," *Materials Letters*, vol. 61, pp. 1376-1379, 2007.

[2] D. Xiaobing, *et al.*, "Space Charge in Low-density Polyethylene /micro-SiO2 composite and Low-density Polyethylene/ nano-SiOx composite with different metal electrode pairs," in *Solid Dielectrics, 2007. ICSD '07. IEEE International Conference on*, 2007, pp. 377-380.

[3] Y. Huang, *et al.*, "Characterization of LLDPE/nano-SiO2 composites by solid-state dynamic mechanical spectroscopy," *Polymer Testing*, vol. 23, pp. 9-15, 2004.

[4] J.-S. Jang, *et al.*, "Experimental and analytical investigation of mechanical damping and CTE of both SiO2 particle and carbon nanofiber reinforced hybrid epoxy composites," *Composites Part A: Applied Science and Manufacturing*, vol. 42, pp. 98-103.

[5] N. A. Muhamad, *et al.*, "Polarization and Depolarization Current (PDC) tests on biodegradable and mineral transformer oils at different moisture levels," in *Power Engineering Conference, 2009. AUPEC 2009. Australasian Universities*, 2009, pp. 1-6.

A081

DC CONDUCTIVITY OF POLYMER NANOCOMPOSITES FOR DIFFERENT TYPES AND AMOUNT OF NANO-FILLER

N. A. M. Jamail[1, 2]*, M. A. M. Piah[2], N. A. Muhamad[2], R. A. Zainir[2], N. F. Kasri[2]
[1]Faculty of Electrical and Electronic, University of Tun Hussein Onn Malaysia (UTHM), Batu Pahat, Johor, Malaysia
[2]Faculty of Electrical Engineering, Universiti Teknologi Malaysia (UTM), Skudai, Johor, Malaysia
norakmal@uthm.edu.my, fendi@fke.utm.my, norasiah@fke.utm.my, rabiadza@gmail.com, akta1988@live.com

Keywords: Polymer nanocomposite, DC conductivity, dielectric

Abstract: Polymer nanocomposites for HV insulation have been extensively researched in recent years because of the unique properties and the ability to enhance electrical performance. Electrical conduction for polymer nanocomposites have been used widely as a tool to monitor the dielectric behaviour. This paper reviewed, analyzed and compared DC conductivity patterns of polymer at various nano-filler concentration percentage. Results from previous researches studies and experiments have been compiled and analyzed to find the patterns and trends of DC conductivity. DC conductivity exhibits significant reduction with addition of any types of nano-filler at right amount, however the right percentage added is different from one to another. This was due to decreasing of initiation probability of short circuit treeing in the insulation. The results found that addition of nano-filler into the polymer nanocomposites material will improve electrical insulation properties of the material.

I INTRODUCTION

Recently, nano-composite material had attracting many researchers' attention in the field of dielectric and electrical insulation. Polymer nanocomposite materials have been given much attention as a new insulation material because the properties of the original material can be drastically improved by adding a few percent of nano-sized filler. Polymer nanocomposite insulating materials are widely applied to power apparatuses and cables. Traditionally, additive agents and fillers are often used for improving insulating and mechanical properties[1]. A nanocomposite polymer is composed of nano-filler, of which diameter is as small as a few tens to a few hundreds of nanometers, and a polymer as a matrix. Polyethylene or epoxy resin are widely used as insulators in industrial applications and are the object of many recent studies, while SiO2, Al2O3, MgO, TiO2 or layer silicates (LS) and nano clay are typical nanofillers. Many researchers have been conducted to determine the electrical properties such as dielectric breakdown strength, partial discharge resistance, space charge and conduction current measurement of polymer nanocomposite insulator[1-6].

It is well known that the two phenomena which determine the response of a dielectric to an electric field are the electric conduction and the electric polarisation. Even though the two phenomena coexist in a dielectric, they are essentially separate and, for the most part, independent processes: the polarisation is the result of a finite displacement of charges in a steady electric field, while the conduction is the result of a finite average velocity of motion of charges in a steady electric field[7].

A lot of research had been done on electrical properties of polymer nanocomposite as insulating material. This paper shows the comprehensive reviewed and analysis based on the studied done by previous researchers to identify and compared the DC conductivity patterns and trends for different types of nano-filler of the polymer nanocomposite insulating materials.

II METHODOLOGY

Figure 1 shows the electrode configuration and the experimental setup for the conduction current measurement [5, 6]. A gold electrode of 40 mm in diameter was formed by vacuum evaporation on one side of the film. On the other side, a gold electrode of 26 mm in diameter was formed as the main electrode and a gold electrode of 32 mm in inner diameter and 40 mm in outer diameter was formed as the guard electrode. The conduction current measurement was performed at 303 K. The conduction current at 10 min after the DC voltage application was employed to determine the volume resistivity.

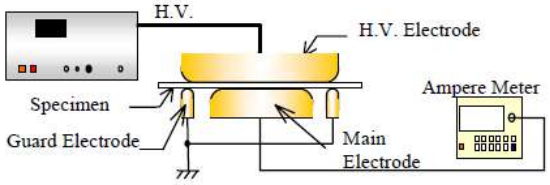

Figure 1.Conduction current measurement system [5, 6]

The DC conductivity test was done in the oven, with a 20 mm diameter gold electrodes on both sides at 6.5 kV for 1 hour. The testing temperature was fixed at 30°C to avoid the influence of small temperature fluctuation in the room on measured current[8].

III RESULTS AND ANALYSIS

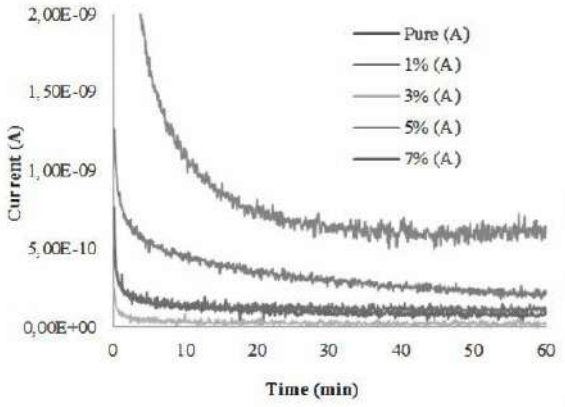

Figure 2. Current for TiO2 based polyimide nanocomposite at different % amount added [8]

*Nor Akmal Mohd Jamail , Faculty of Electrical Engineering, Universiti Teknologi Malaysia(UTM), Skudai, Johor, Malaysia, norakmal@uthm.edu.my, +60124613382

From the results above, it can be concluded that adding nano particles into dielectrics can improve its electrical properties. However, different amount of nano-fillers will give different results. As 1 % and 3% samples reduce the conductivity to the lowest point, it can be known that a small amount of nano-fillers is separated inside the dielectric with a certain wide distance, which can be known as 'extra traps' for the dielectric, and therefore improve the insulation property.

However, if more nano particles adding into the dielectrics, for example, 5% sample has a better insulation property than the pure sample, but its conductivity is higher than 1% and 3% samples. This is because that some of the nano-fillers are too closed to each other, and each nano particle has an interaction zone around it, which results some overlap of interaction zones. For 7% sample or higher amount nano dielectrics, the probability of interaction zones overlap is getting higher and higher, and therefore, the nano particles may align together, which helps the charges moving across the dielectric.

REFERENCES

[1] T. Tanaka, "Dielectric nanocomposites with insulating properties," *Dielectrics and Electrical Insulation, IEEE Transactions on,* vol. 12, pp. 914-928, 2005.

[2] T. Okazaki, *et al.*, "Electric characteristics of MgO/LDPE nanocomposite up to breakdown under DC ramp voltage," in *Electrical Insulation and Dielectric Phenomena, 2009. CEIDP '09. IEEE Conference on*, 2009, pp. 654-657.

[3] Y. Murata, *et al.*, "Effects of nano-sized MgO-filler on electrical phenomena under DC voltage application in LDPE," in *Electrical Insulation and Dielectric Phenomena, 2005. CEIDP '05. 2005 Annual Report Conference on*, 2005, pp. 158-161.

[4] G. Chen, *et al.*, "Conduction in linear low density polyethylene nanodielectric materials," in *Properties and Applications of Dielectric Materials, 2009. ICPADM 2009. IEEE 9th International Conference on the*, 2009, pp. 845-848.

[5] Y. Murakami, *et al.*, "DC conduction and electrical breakdown of MgO/LDPE nanocomposite," *Dielectrics and Electrical Insulation, IEEE Transactions on,* vol. 15, pp. 33-39, 2008.

[6] S. Masuda, *et al.*, "DC conduction and electrical breakdown of MgO/LDPE nanocomposite," in *Electrical Insulation and Dielectric Phenomena, 2007. CEIDP 2007. Annual Report - Conference on*, 2007, pp. 290-293.

[7] F. Ciuprina and I. Plesa, "DC and AC conductivity of LDPE nanocomposites," in *Advanced Topics in Electrical Engineering (ATEE), 2011 7th International Symposium on*, 2011, pp. 1-6.

[8] Y. Zhuang, *et al.*, "Surface potential decay and dc conductivity of TiO<inf>2</inf>-based polyimide nanocomposite films," in *Electrets (ISE), 2011 14th International Symposium on*, 2011, pp. 155-156.

A083

AN EXPERIENCE OF AGEING ON XLPE INSULATION

W. G. Ariastina*[1], A. I. Weking[1], I N. S. Kumara[1], I. A. D. Giriantari[1], I N. Sugiarta[2]
[1]Department of Electrical Engineering, Udayana University, Bali-80362, Indonesia
[2]PT PLN (Persero) Distribution of Bali, South Bali Network Area, Bali-80113, Indonesia

Keywords: XLPE insulation, ageing, partial discharges

Abstract: A case study of ageing on XLPE conductor insulation of 20kV primary distribution feeder is presented in this paper. The insulation degradation mainly occurred around conductor tie where the conductor is attached to the post insulator. A section of distribution feeder with defects on the conductor insulation has been examined for this study. Potential losses due to presence of discharges have been investigated by measuring the difference current at locations of the affected conductor. Temperature measurements of the insulation surface have also been carried out. Provisional maintenance procedures were introduced to eliminate the discharges. Measurements of current and surface temperature were repeated nine months after completion of the maintenance work. Results indicated that the discharges have been completely disappeared.

I. INTRODUCTION

Recently, the utilisation of AAAC-S (all aluminium alloy conductor – sheathed) for distribution network has been broadened, particularly in South and East part of Bali. In these parts of the island, most of the distribution networks are supplying consumers at tourism areas near beaches. It is well known that the utilisation of the AAAC-S has a number of advantages compared to that of the bare conductors. The AAAC-S has an ability to protect the distribution network from temporary disturbances which are mainly caused by falling kite and nearby tree contacts. Direct contact of airborne pollutants with the conductor strands may also be avoided.

Nevertheless, after a few years of utilisation, problems began to appear on the insulation of the AAAC-S. It was found that the XLPE sheath degrade rapidly, particularly near the insulator tie. Tiny sparks at the degraded sheath section can be observed clearly at night, indicating the occurrence of discharges. Visual observation of the conductor insulation during day time showed burnt sections around the conductor tie. At some sections, the XLPE sheath has been completely disappeared. This situation obviously requires immediate attention and appropriate maintenance measures.

The occurrence of discharges on the distribution network absolutely causes energy losses. The amount of energy loss very much depends on the characteristics of discharges occurred on the conductor. This paper discusses the potential losses due to degradation of the AAAC-S conductor insulation applied to distribution network. Investigation was carried out on a section of 20kV primary distribution feeder. The section consists of 12 poles at which insulation defects were preliminary identified. Flowing current and surface temperature of the conductor were measured around the conductor tie for each pole. The measurements of current and surface temperature were carried out during dry season to reduce risk of being electrified. A comparison of measurement results before and after planned maintenance operation is also discussed in this paper.

II. MEASUREMENT OF CURRENT AND TEMPERATURE

The effects of the insulation defects on potential power losses have been investigated on a series of twelve poles with impaired conductor sheath. The poles support conductors that are part of a 20kV primary distribution feeder. The feeder lied adjacent to a main road and is approximately 500m from coast line. There are no electrical loads within the twelve poles.

Two medium voltage clamp meters were used to measure potential loss due to the presence of defects. One clamp meter wasplaced before the conductor tie, while the other was placed after the tie, in referred to the current flow. The difference of current measured between the two is considered as the difference current. The difference current indicates potential power losses at the defect location. Measurements of the difference current were carried out for the three phases and for the twelve poles.

Following the identification of the insulation damage, a life maintenance procedure was carried out. This work was aimed to prevent further defect on the conductor strand due to high energy discharges. The work includes tie changed and removal of the affected conductor sheath. Consequently there are some parts of the lines became completely bared at the tie points.

An infrared thermo vision camera was utilised to examine the conductor surface temperature before and after maintenance process. For each location of the degraded insulation, images were taken before and after maintenance works were completed. Results of the two measurements then can be compared and analysed. A reduction of surface temperature is expected when the sparks at the degraded insulation are diminished.

III. RESULTS AND DISCUSSIONS

1. Current Measurement

The current measurement results of the red phase for the twelve poles before maintenance are presented in Figure 1. Bars with darker colour indicate incoming current (I0), while those with lighter colour indicate outgoing current (I1). It is clear that the difference current exists which is indicating the potential power loss at most of damaged insulation sections.

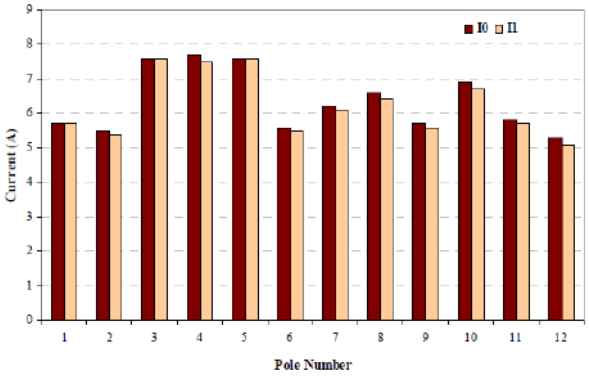

Figure 1. Measured current of red phase

The measured quantity of flowing current on the conductor depends on the load of the remaining part of the feeder at the time of measurement. The magnitude of difference current

*W. G. Ariastina, Department of Electrical Engineering, UdayanaUniversity, Kampus Bukit Jimbaran, Bali-80362, Indonesia.
Email: w.ariastina@unud.ac.id.

varies from point to point of measurements, with an average value of 0.108A for the red phase and of 0.117A for the yellow and the blue phases.

Potential power loss at all phases was identified at seven out of twelve explored poles, while potential power loss at only one phase was discovered for one pole. This fact indicates that the insulation damage occurred around conductor tie at all the investigated twelve poles. The results also designate that at 91% of the total number of poles, the insulation ageing involves two or more phases.

Following the identification of defects on the XLPE insulation, immediate life maintenance works were carried out to prevent further defects on the conductor. Measurements of the flowing current were repeated after completion of the maintenance. There was no indication of difference current during the second measurement.

2. Temperature Measurement

As complement of current detection, measurements of surface temperature of the XLPE sheath were also carried out. The temperature of the insulation surface may provide information of existence of discharges. Note that the measured temperature does not indicate the temperature of sparks appeared on some locations of the insulation defects. The indicated values are the average temperature of insulation surface near damaged points. Similar to that of current measurement, the temperature measurement was also carried out before and after the completion of the maintenance works.

The average temperature of the XLPE sheath surface near defect locations (before maintenance) is slightly above 30°C. In contrast, after completion of the maintenance works, the approximate average XLPE sheath surface temperature became 26.5°C. There was a reduction of about 3.5°C in surface temperature of the XLPE sheath after maintenance process was completed.

IV. CONCLUSIONS

Investigation of ageing on XLPE insulation of a 20kV primary distribution feeder has been carried out. Initial measurement results indicated that there are high potential losses due to the presence of discharges. Measurements of the XLPE sheath surface temperature confirmed the situation.

It is not clear however; whether the fast ageing process of the XLPE insulation was caused by production imperfection of the conductor or due to improper installation and application of the conductor. The fact that most discharges that promote ageing on the XLPE sheath were located on the conductor tie exhibit that advanced explorations are required. Further investigation has been planned to look at this issue in the future.

REFERENCES

[1] PT. PLN (Persero), "PLN Standard 41-8-1981: All Aluminium Alloy Conductor" (in Indonesian).

[2] PT. PLN (Persero), "PLN Standard 41-10-1991: All Aluminium Alloy Conductor-Sheathed" (in Indonesian).

[3] PT. PLN (Persero), "PLN Standard 39-1-1981: Power Cable Tests" (in Indonesian).

[4] I N Sugiarta, "A Study of Partial Discharge Phenomena on AAAC-S Conductor Ties in East Bali 20kV Distribution Network", Udayana University, 2011 (in Indonesian).

[5] A. Garton, S. Bamji, A. Bulinski and J. Densley, "Oxidation and Water Tree Formation in Service-Aged XLPE Cable Insulation", IEEE Trans. Electr. Insul., Vol. EI-22, No. 4, pp. 405-412, 1987.

[6] J. L. Parpal, J. P. Crine and C. Dang, "Electrical Aging of Extruded Dielectric Cables: A Physical Model", IEEE Trans. Dielectr. Electr. Insul., Vol. 4, No. 2, pp. 197-209, 1997.

[7] G. C. Montanari, C. Laurent, G. Teyssedre, A. Campus and U. H. Nilsson, "From LDPE to XLPE: Investigating the Change of Electrical Properties. Part I: Space Charge, Conduction and Lifetime", IEEE Trans. Dielectr. Electr. Insul., Vol. 12, No. 3, pp. 438-446, 2005.

[8] E. S. Cooper, L. A. Dissado and J. C. Fothergill, "Application of Thermoelectric Aging Models to Polymeric Insulation in Cable Geometry", IEEE Trans. Dielectr. Electr. Insul., Vol. 12, No. 1, pp. 1-10, Feb. 2005.

[9] M. S. Mashikian and A. Szatkowski, "Medium Voltage Cable Defects Revealed by Off-Line Partial Discharge Testing at Power Frequency", IEEE Electr. Insul. Mag, Vol. 22, No. 4, pp. 24-32, 2006.

[10] G. C. Montanari, A. Cavallini, F. Puletti, "A New Approach to Partial Discharge Testing of HV Cable Systems", IEEE Electr. Insul. Mag,Vol. 22, No. 1, pp. 14-23, 2006.

[11] W. Li at. al., "Frequency Dependence of Breakdown Performance of XLPE with Different Artificial Defects", IEEE Trans. Dielectr. Electr. Insul., Vol. 19, No. 4, pp. 1351-1359, 2012.

A084

EFFECT OF DESIGN PARAMETERS ON INDUCED VOLTAGE EVALUATION OF 33kV DISTRIBUTION LINE

N. Rameli*, M. Z. A. Ab Kadir, M. Izadi, C. Gomes and J. Jasni
Centre for Electromagnetic and Lightning Protection Research (CELP)
Universiti Putra Malaysia, 43400 Serdang, Selangor, MALAYSIA.
email: ayumie46@yahoo.com

Keywords: Lightning; induced overvoltage, striking distance; vertical lightning channel; inclined lightning channel.

Abstract: This paper investigates the effect of design parameters on the induced voltages on a distribution power line. This investigation is based on perfect ground conductivity, single stroke lightning and lightning without branches. The design of the parameters includes, d, the striking distance of the lightning, h, the height of the conductor, and r, the diameter of the conductor, all of which are elements that produce the variation in the induced voltage on a distribution power line with respect to a vertical or an inclined lightning channel. Thus, the outcomes of this investigation can act as a guide for the utility companies or other power engineers in order to plan an appropriate protection scheme for a distribution power line.

I.INTRODUCTION

Lightning is a discharge phenomenon. The discharging of lightning from cloud to ground with a negative discharge occurs more frequently than positive discharges and accounts for 90 % of the lightning strikes. The negative discharge contributes to the most damage, injuries and death [1-4].This is because the negative discharge gives rise to a higher peak current for the first stroke as compared to the subsequent lightning strokes [5-6]. Moreover, backflashover, shielding failure and induced overvoltage in power lines are the main result when lightning strikes to the ground [7-8]. However, the induced overvoltage in the power lines is more due to an indirect strike (striking to the ground or a nearby object) which has a greater effect on a distribution power line [9-10].

Apart from that, the induced voltages on distribution power lines are affecting by the parameter designs [11-15].Its includes the lightning parameters such as the velocity of the lightning, the height of the lightning channel, crest, front time, maximum current steepness, and duration. Further, the line parameters also have to be considered when determining the affecting factors that give rise to induced voltages on a power line. The line parameters include the height of the conductor line, the diameter size of the conductor, the gap distance between the three-phase conductor and the associated matching impedance. The other design parameters such the substation parameters, tower parameters and lightning protection parameters are the main parameters which should be considered when studying induced voltages. However, most of parameter designs evaluate the induced voltage with respect to a vertical lightning channel only [9-15]. It should be noted that in reality, the lightning channels are not vertical but strike at a certain inclined angle at the surface of the ground [16-19]. Therefore, for the evaluation of the lightning induced overvoltage (LIOV) it should be evaluated using an inclined lightning channel with specific inclined angle. These inclined angles have a few percentage differences on the effect of the parameters on the induced voltage as compared to a vertical lightning channel [16-21]. Thus, this paper will provide information concerning induced voltages which are affected by the parameter designs with respect to vertical and inclined lightning channels by using a fast and simple determination method.

II. METHODS

In order to investigate the effect of parameter design on the induced voltage on distribution power lines in Malaysia, the work is divided into two parts, namely the determination of the parameter design and the determination of induced voltages on the distribution lines. Both of these determinations are implemented through programming. Injected lightning current of 10 kA with an inclined angle set at 10 degree is used in this work.

Evaluating the induced voltages on a distribution power line involves several steps as depicted in Fig 1.This figure shows that there are two types of lightning channel, which are the vertical and the inclined lightning channel. The phenomena of a lightning channel is referred to as 'neutralization' which occurs when the negative charges inside a cloud are travelling down and at the same time positive charges from the ground are trying to attach to these negative charges. This phenomenon is completed in around 20 ms [1]. Therefore, the step of evaluating induced voltages begins when the lightning channel strikes the surface of the ground.

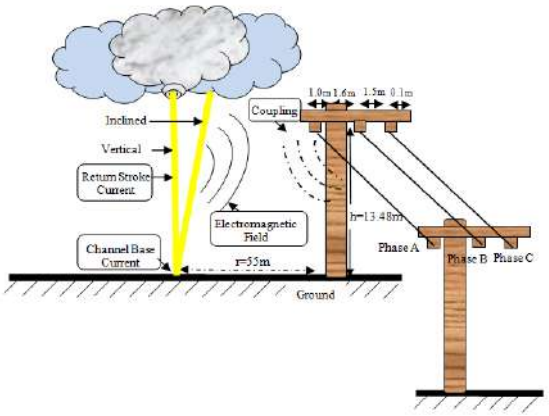

Figure 1. Voltage induced on power lines due to vertical and inclined lightning channel [22]

In this paper, the channel base current is selected to be the step current and the TL model as a return stroke current. The Hybrid method is selected to serve as the numerical evaluation of the electromagnetic field and the Agrawal model for the coupling model evaluation. The selection of these models should provide for a fast calculation of the induced voltage.

IV. CONCLUSION

In this paper, the effects of parameter designs will be investigated. Based on the result, full consideration should be

*N. Rameli, M. Z. A. Ab Kadir, M. Izadi, C. Gomes, J. Jasni, Centre for Electromagnetic and Lightning Protection Research (CELP), Universiti Putra Malaysia, 43400 Serdang, Selangor, MALAYSIA. email: ayumie46@yahoo.com

given when setting up an appropriate protection scheme for the distribution line, particularly related to the BIL and the Critical Flashover voltage (CFO) of the line, where the striking distance may influence the induced overvoltage of the line. In this case, perhaps the Lightning System Detection Network (LSDN) can be used to map the lightning occurrence with respect to the distribution line which can help the utility to plan for a proper protection scheme of the line.

V. ACKNOWLEDGEMENT

The authors gratefully acknowledge the financial support from Universiti Putra Malaysia under Research University Grant Scheme (Project No: 05-02-12-2016RU).

REFERENCES

[1] V. Cooray, ''The lightning Flash'', The Institution of Engineering and Technology, London, United Kingdom, 2010

[2] J. Kuffel., ''High Voltage Engineering Fundamental'', Second Edition, Butterworth-Heimann,2000

[3] P. Chowdhuri, J.G. Anderson, W.A. Chisholm, T.E. Field, M. Ishii, J.A. Martinez, M.B. Marz, J. McDaniel, T.R. McDermott, A.M. Mousa, T. Narita, D.K. Nichols, T.A. Short, ''Parameters of Lightning Strokes: A Review'', IEEE Transactions On Power Delivery, Vol. 20, No. 1, January, 2005

[4] Interim Report on the Performance of the Electricity Supply Services in Malaysia for the First Half Year of 2010.

[5] V.A. Rakov , ''Lightning Parameters for Engineering Applications (Keynote Speech)'', Asia Pacific International Symposium on Electromagnetic Compatibility, Beijing-China, April 12, 2010

[6] V.A. Rakov, ''Lightning: Phenomenology and Parameters Important for EMC '' CEEM'2006/Dalian 3A1-01 283.

[7] H.M. Ariff, ''Insulation Coordiantion Studies on HV Substations'', MSc thesis, Oct, 2009.

[8] N.A. Abd Rahman, ''Study on Lightning Performance Improvement of the 33kV Tanjung Batu-Rompin Overhead Distribution Line'', TNB Research, 2008.

[9] C.A. Nucci, ''Lightning-Induced Voltages on Distribution Systems:Influence of Ground Resistivity and System Topology'', Journal of Lightning Research, Volume 1, pp 148-157, 2007

[10] P.D. Kannu, M.J. Thomas, "Lightning Induced Voltages on Multiconductor Power Distribution Line ''IEEE Proc.-Gener. Transm. Distrib., Vol. 152, No. 6, November 2005

[11] M.Z.A Ab Kadir, H. M. Ariff. A.M. Azmi, ''Modelling 132 kV Substation for Surge Arrester Studies'', International Journal of Emerging Electric Power Systems, Volume 9, Issue 5, 2008

[12] P.P. Barker, T. A. Short, A.R. E-Berard and J.P. Berlandis ''Induced Voltage Measurements on An Experimental Distribution Line During Nearby Rocket Triggered Lightning Flashes'', IEEE Transactions On Power Delivery, Vol. 11, No. 2, April 1996

[13] M.Z.A. Ab Kadir, M. H. Mohamad Ariff, R. Mesron, M. T. Salahuddin, ''Substation System Simulation Models for Transformer Risk Assessment Analysis'', European Journal of Scientific Research, , Vol.23 , No.1, pp.141-148 ,2008

[14] S.M.A. Razzak, M.M. Ali, M.Z.I. Sarkar, H. Ahmad, ''Lightning Induced Over Voltages on Overhead Distribution Lines Including Lossy Ground Effects'', 3rd International Conference on Electrical & Computer Engineering (ICECE), 2004

[15] P. Durai Kannu, M. Joy Thomas, ''Lightning Induced Voltages on Overhead Conductors At Different Heights'', IEEE Bologna PowerTech Conference, 2003

[16] J. Schoene, ''Analysis of Parameters of Rocket-Triggered Lightning Measured During the 1999 and 2000 Camp Blanding Experiment and Modeling of Electric and Magnetic Field Derivatives Using the Transmission Line Model'', MSC, University of Florida, 2002.

[17] R. Hill, ''Analysis of Irregular Paths of Lightning Channels'', Journal of Geophysical Research, vol.73, pp 1897-1906, 1968.

[18] R. Hill, ''Electromagnetic Radiation from Erratic Paths of Lightning Strokes'', Journal of Geophysical Research, vol.74, pp 1922-1929, 1969.

[19] A.Sakakibra, ''Calculation of Induced Voltages on Overhead Lines Caused by Inclined Lightning Strokes'', IEEE Transactions on Power Delivery, Vol.4, No.1, January 1989.

[20] R. Moini, S.H.H. Sadeghi,B. Kordi, F. Rachidi, ''An Antenna-Theory Approach for Modelling Inclined Lightning Return Stroke Channels'', Electric Power System Research, pp 945-952, 2006

[21] A. Andreotti, U. D. Martinis, C. Petrarc, V. A. Rakov, L.Verolino, ''Lightning Electromagnetic Fields and Induced Voltages: Influence of Channel Tortuosity '', General Assembly and Scientific Symposium, 2011 XXXth URSI, pp 1-4, 13-20August 2011

[22] N.A. Abd. Rahman, N. Abdullah, M.F. Ariffin, ''Influence of Earthing Resistance on the Performance of Distribution Line Lightning Arrester'' Asia-Pacific International Symposium on Electromagnetic Compatibility, Beijing, China, April 12 - 16, 2010

A085

EARLY PREVENTION SYSTEM FOR ELECTRICAL FLASHOVER DISCHARGE IN GAS INSULATED SWITCHGEAR

M. F. Agos & N. A. Muhamad*
Institute of High Voltage & High Current,
Universiti Teknologi Malaysia, 81310 Skudai, Johor, Malaysia

Keywords: Flashover, Gas Insulated Switchgear, Particle, Computer Vision, SF_6 Gas.

Abstract: The phenomenon of metallic particle contamination in gas insulated switchgear is a major problem for triggering electrical flashover discharge. The breakdown chances can be reduced by improving better quality checks on the cleanliness of the enclosure from foreign metallic particle during assembly. By introducing computer-aided particle detection system, it is expected to improve the deficiency caused by human fatigue during the construction of the switchgear. The particle detector prototype is consists of borescope and program with image processing algorithms. The scope of the detection is particle size range from 1mm and above, coaxial and round shape. This paper will present the assessment on accuracy of the prototype in detecting the particles and analysis on the efficiency of the system.

I. INTRODUCTION

Gas insulated switchgear (GIS) has been widely used in power electrical system in Malaysia. The perks that GIS offered are much superior compared to other type of insulation of switchgear. However, practical GIS suffer from metallic particles contamination. Long metallic particles can affect the performance of gaseous insulated because they can migrate to critical regions. For example, a horizontal switchgear arrangement. A particle lying on the surface of the enclosure will obtain a charge which is proportional to the local field, will experiences an electrostatic force. The particle will lift off and float in the gas space when applied voltage is sufficiently high. Under 60Hz ac excitation, a particle does not fall down when the voltage is near its zero crossings, but will, due to inertia, respond in a time-averaged manner. It will acquire a slow (compared to 60 Hz) bouncing movement. The bounce height increases with the applied voltage. At a sufficiently high voltage, the particle is able to cross the gap between the conductor and the grounded enclosure and initiate breakdown.

The existence of metallic particle contaminations inside GIS enclosure is usually caused by the construction works during the first assembly process of the switchgear. Poor quality control can be caused by human fatigue and other human limitation factor.

This paper aims to develop a new approach on controlling the quality control to minimize the existence of metallic particle during the assembling works by using computer-aided system. This system used a computer vision technique in order to achieve the desired objective. The accuracy and the efficiency of the system are also presented.

II. MATERIALS AND METHODS

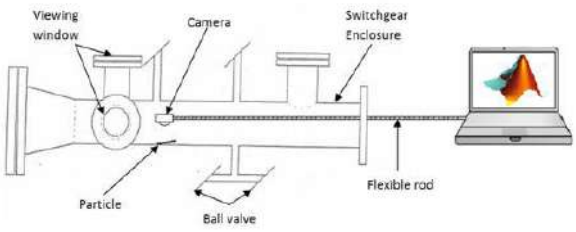

Figure 1. Experimental arrangement

Figure 1 shows the experimental arrangements. Simulated GIS was used for the experiments. The conductor rod are taken out to simulate the condition of GIS during assembly before the enclosure is seal off and fill with SF_6 gas. The particle detector system consists of borescope and a program made using MATLAB. Various length of size wire particles range from 1mm to 10mm are put on the inner surface of the GIS enclosure. The borescope is inserted into the enclosure to test the particle detector system efficiency. The experiments will be conducted few times using different quantity and different particle size.

III. RESULTS AND DISCUSSION

The particle detection system will detect and highlight the particle inside the enclosure in real-time mode. The accuracy and the efficiency of the system will be presented by comparing the data from the experiments.

REFERENCES

[1] T. K. Huan, A. B. Darus, Pattern Recognition of Partial Discharge Signal in Gas Insulated Switchgear Apparatus using Visual and Cluster Analysis, *IEEE*, 2002, pp. 1842 – 1846.
[2] B. Mazurek, The Effect of a Metallic Particle near a Spacer Flashover Phenomena in SF_6, *IEEE Transactions on Electrical Insulation, vol. 28 n. 2*, April 1993, pp. 219 – 229.
[3] L. S. Loong, *Image Processing Using MATLAB – Learning Tool*, Bachelor Degree dissertation, Dept. Elect. Eng., Universiti Teknologi Malaysia, Johor, Malaysia, 2010.
[4] M. V. Shirvaikar, *Trends in Automated Visual Inspection* (Springer DOI Link, 2006).
[5] T. I. Hentea, Algorithm for Automatic Threshold Determination for Image Segmentation, *IEEE Electrical and Computer Engineering*, 1993.
[6] S. T. Bow, *Pattern Recognition and Image Preprocessing* (Marcel Dekker, Inc., 2002).
[7] M. F. Agos, N. A. Muhamad, Particle Detection in Gas Insulated Switchgear Using Image Processing, *The 2nd International Senior Project Conference (ISPC)*, March 23-26, 2011, Bangkok, Thailand.
[8] A. A. Sewisy, Detection of Lines in Images by Curve Fitting Using Hough Transform, *International Review on Computers and Software, vol. 2 n. 4*, July 2007, pp. 342 - 349.
[9] M. Benkiniouar, M. Benmohammad, Real Time Implementation of the Face Detection Algorithm Based Adaboost on VLIW Processor, *International Review on Computers and Software, vol. 5 n. 1*, January 2010, pp. 106 - 112.

*Nor Asiah Muhamad, Fakulti Kejuruteraan Elektrik, Universiti Teknologi Malaysia, 81310 Skudai, Johor Malaysia, norasiah@fke.utm.my, +607-5535263

[10] J. Liu, C. Huang, Y. Qian, . Jiang, Analysis on Partial Discharge Localization using UHF Combined with Acoustic Method in GIS, *International Review on Electrical Engineering, vol. 5 n. 3*, June 2010, pp. 1266 - 1270.
[11] T. Y. S. Okabe, "Voltage-Time Characteristics For Steep-Front Impulse Voltages Of Particle-Contaminated Spacers in SF6 Gas-Insulated Switchgear," *IEEE Transactions on Power Delivery*, vol. 7, 1992.
[12] L. Ming, "Influence Of Impulse Voltage Waveshape On The Flashover Of Clean And Particle-Contaminated Spacers In A SF6 Gas-Insulated System," *IEEE Transactions on Power Delivery*, vol. 4, 1989.
[13] M. Hikita, *et al.*, "Cross-equipment Evaluation of Partial Discharge Measurement and Diagnosis Techniques in Electric Power Apparatus for Transmission and Distribution," *IEEE Transactions on Dielectrics and Electrical Insulation*, vol. 15, p. 505, April 2008 2008.
[14] R. Schurer and K. Feser, "PD Behaviour and Surface Charging of a Particle Contaminated Spacer in SF6-Gas Insulated Switchgear," *IEEE Conference on Electrical Insulation and Dielectric Phenomena*, 1998.
[15] B. T. P. K.X Lai, TR Blackburn, N.A Muhamad, "Separation and Identification of Multiple PD Sources using Independent Component Analysis," presented at the International Conference for Condition Monitoring and Diagnosis (CMD 2008), Beijing, China, 2008.

A086

IMPACT OF LIGHTNING STRIKE ON PHOTOVOLTAIC SYSTEM

A. Z. Abidin*[1], A. H. A. Bakar[2], H. Mokhlis[1], H. A. Illias[1]
*[1]Department of Electrical Engineering,
Faculty of Engineering University of Malaya, 50603 Kuala Lumpur, Malaysia
[2] University of Malaya Power Energy Dedicated Advanced Center (UMPEDAC),
Level 4, Wisma R&D University of Malaya, 50603 Kuala Lumpur, Malaysia.
a.halim@um.edu.my

Keywords: Photovoltaic system, lightning, inverter

Abstract: Nowadays, photovoltaic (PV) system is one of the popular green technologies. PV arrays are usually installed on the roof-top of houses in residential areas, which enables the electrical energy to be generated. However, these arrays are risking from direct lightning strikes and can be affected by the nearby flashes. The lightning strikes may damage the electrical equipment connected to the PV arrays and can cause power outage. In this paper, the effect of lightning strikes on photovoltaic system was studied through simulation model using PSCAD software. The relationship of the lightning current and the voltage magnitude produced by the photovoltaic module and inverter were studied. From the results obtained, further investigation can be done to solve the problem caused by the lightning strike such as the lightning protection for photovoltaic system in order to reduce the impact on the photovoltaic system.

I. INTRODUCTION

Nowadays, green technologies are very popular and having high demand from consumers. One of the green technologies that is very promising as a future energy technology is the Photovoltaic (PV) system [1]. PV system converts sunlight directly into electricity in a quiet, clean and reliable way. PV cells are wired together in modules or panels with a specific power output. The most widely used PV cells are single-crystal silicon, multi-crystal silicon and amorphous silicon. However, the most efficient cell at converting sunlight to electricity is single-crystalline. PV cell technologies have operating lives of over twenty years [2].

PV system can be divided into two categories; stand-alone and grid-connected PV systems. These two systems can be classified as Building Integrated Photovoltaic (BIPV) if the PV is integrated into the building [3]. The grid-connected system is mostly used in urban areas. The number of BIPV installations in home systems is increasing in the world, including in Malaysia [1]. The PV system at the residential area enables the electrical energy to be generated from home. The house is also connected to the utility. Therefore, when the energy produced by the PV system is less than the demand, the house can draw extra energy from the utility. A conventional PV system is shown in Fig. 1. The PV array produces a DC voltage and the voltage passes through an inverter, which converts it into an AC voltage.

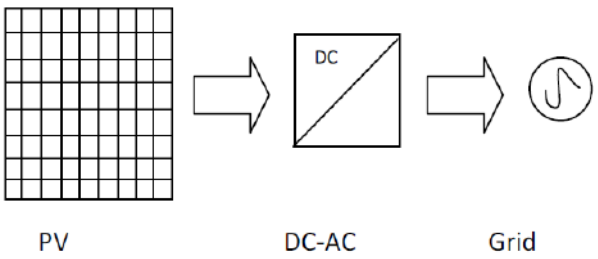

Figure 1. Grid-connected PV system topology

A photovoltaic system consists of PV generator (solar module), inverter, meter, grid connection and DC and AC cablings. This system is installed on the roof-top of buildings for BIPV [4-5]. However, the PV arrays located outdoor are risking from direct lightning strikes and can be affected by the nearby flashes. This may cause damage to the electrical equipment connected to the PV arrays. Consequently, this results in a power outage, production losses and the whole component needs to be repaired and replaced. In this paper, the impact of the lightning strike on the photovoltaic system was studied through simulation using PSCAD software. The results obtained may increase an understanding of relationship between the lightning current with the voltage produced by the photovoltaic module and inverter.

II. SIMULATION RESULTS

A. Photovoltaic System Before Lightning Strike

A photovoltaic system has been implemented in PSCAD software. PV array is connected to the grid through the five-level inverter and the filter. The grid system is set to 240 V since this system is a single phase photovoltaic grid-connected. The inverter produces an AC voltage after converting the DC voltage from the photovoltaic output.

B. Photovoltaic System After Lightning Strike

A lightning current was injected into the photovoltaic system to observe the effect of the photovoltaic module after a lightning strike. Since the peak current amplitude related to the lightning stroke in Malaysia is between 2 kA and 200 kA, the lightning current amplitude in the simulation was varied between these values [6]. A complete diagram of the whole model is shown in Fig. 2.

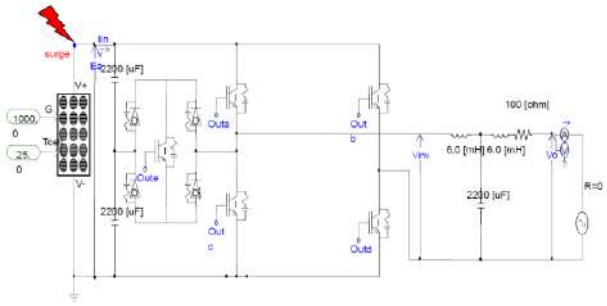

Figure 2. Complete simualtion model including lightning current model

The lightning current was varied from 2kA to 200 kA and the output voltage from photovoltaic module and inverter were observed. The waveform of the output voltage is similar when different values of lightning current were injected, except that the magnitude of the output voltage is different. Table 1 shows the value of the output voltages for different lightning current

injected in the simulation model. When the magnitude of the lightning current is increased, the output voltage is higher.

Table 1. Lightning strike effect

Lightning current (kA)	Photovoltaic output voltage, V_{dc} (V)	Inverter output voltage, V_{ac} (V)
0	450.0	337.8
8	462.7	349.6
20	491.3	367.6
80	655.6	484.9
120	769.2	588.3
150	854.4	667.0
200	1016.9	795.3

REFERENCES

[1] R. Muhida, M. Ali, P. S. J. Kassim, M. A. Eusuf, A. G. E. Sutjipto, and Afzeri, "A simulation method to find the optimal design of photovoltaic home system in Malaysia, Case Study: A building integrated photovoltaic in Putra Jaya," International Journal of Human and Social Sciences, vol. 5, no. 2, 2010.

[2] R. E. I. Schropp, M. Zeman, "Amorphous and microcrystalline silicon solar cells: Modeling, Materials and Device Technology"

[3] Ir. Ahmad Hadri Haris, "Grid-connected and building integrated photovoltaic" : Application status & prospect for Malaysia , 2006.

[4] N. Phanthuna, N. Thongchompoo, B. Plangklang, K. Bhumkittipich, "Model and experiment for study and analysis of
photovoltaic lightning effects," in Power System Technology (POWERCON), International Conference, October 2010.

[5] J. C. Hernandez, P. G. Vidal, F. Jurado, "Lightning and surge protection in photovoltaic installations," IEEE Trans.Power Delivery, vol. 23, October 2008, pp. 1961 – 1971.

[6] A. H. A. Bakar , N. A. Rahim, M. K. M. Zambri, "Analysis of lightning-caused ferroresonance in Capacitor Voltage Transformer (CVT)," Electrical Power and Energy Systems, vol. 33, 2011, pp.1536-1541.

A087

EFFECT OF TEMPERATURE TO LEAKAGE CURRENT OF GAPLESS METAL OXIDE SURGE ARRESTER

C. L. Wooi[1], Saeed Vahabi Mashak[2], Zulkurnain Abdul-Malek[3]
[1,2,3] Institut Voltan dan Arus Tinggi, Universiti Teknologi Malaysia
IVAT, Fakulti Kejuruteraan Elektrik, UTM, 81310, Skudai, Johor Bahru, Malaysia.
Phone: +60-7-5535432; Fax: +60-7-5578150
wcl5195@gmail.com[1],vmsaeed3@live.utm.my[2], zulk@fke.utm.my3

Keywords: ZnO surge arrester, ageing level, ambient temperature, leakage current.

Abstract: Zinc oxide(ZnO) gapless surge arrester are a protective device of an electric power system. Various methods have been applied to determine the aging level of surge arrester using leakage current of a surge arrester. However, leakage current of a surge arrester is found to be dependence on ambient temperature. In this study, leakage currents three 120kv metal oxide arrester with polymeric housings were evaluated in different ambient temperature. In severe condition the results shown difference effects the leakage current up to 20.69%. Therefore, based on the results, ambient temperature should be closely observed while taking the reading of leakage current of surge arrester. This paper will explain the effect of surrounding temperature on surge arrester.

I. INTRODUCTION

Surge arresters have been playing an important rule on power systems since the beginning of ac transmission. Overvoltages usually occur in a power system due to lightning, fault and switching operation. Surge arresters are often used to protect power and electronic from the destructive transient overvoltage. In order to protect power system equipments and guarantee an economic and reliable operation, surge arresters are applied in almost all types of electrical network[1].These devices are used to limit the overvoltage to a level which is sufficiently safe for the equipment being protected by diverting the large current to be ground [2].

The impedance of metal oxide arresters at voltages below the rated voltage is so high that the resulting current is in the milliampere range. During over voltage events the metal oxide surge arrester limits the voltage to an almost constant value, even if the discharge current increases extremely. The direct consequence of this low current consumption was the possibility of constructing surge arresters with no series gaps [3, 4].

However, because these arresters contain no gaps, a leakage current flows through the material at working voltages, which causes power losses and heating of the ZnO elements. This can be dangerous to the stability of the arrester, particularly in the low conduction regime (0-0.001A) where the voltage-current characteristic of ZnO material is very sensitive to temperature [4]. The thermal stability of ZnO surge arresters is affected by ambient temperature and and heat dissipation capability, impulse degradation and ageing [5, 6].

If the temperature exceeds the certain temperature of particular arrester, the arrester will break down. Therefore, surge arrester must operate properly in both normal operating voltage and fast transient condition [7]. In the case of ambient temperature, although ambient temperature cannot exceed the temperature limit which will cause the arrester to break down, but it has affected the measurement of leakage current.

There were some experiments has been done to show the thermal characteristic of a complete surge arrester and zinc oxide element, but the correlation between the temperature and total leakage current is not yet developed[8, 9]. Therefore, this research aims shows that the correlation between the temperature and total leakage current is determined.

II. MATERIALS AND METHODS

The gapless metal oxide surge arrester will be installed inside a canvas with controlled environment, and their thermal and electric properties will be analyzed. Canvas is specially design for temperature insulation, and the volume is 3x3x3m with surge arrester in the middle of the canvas. Canvas was designed in such a way that big enough to make clearance for high voltage to connect to surge arrester without any unnecessary discharge happen.

In order to measure the leakage current of the metal oxide surge arrester, a digital oscilloscope, a current probe, and a designed signal amplified was used.The minimum value that current probe of this experiment manages to get is 100mA. Therefore, we need an amplified and filter circuit to amplify the signal and at the same time filter all the noise, which is not necessary to get the measured data. In order to avoid the electric field interference to the signal amplifier, a completed grounded seal steel box has been used.

Before the real measurement is determined, the current probe and the signal amplifier need to be caliberated. Therefore, the caliberation experiment is carried out with three signal generators and two ammeters, and two digital oscilloscopes were needed to make the caliberation possible.

Finally, the temperature will be recorded together with amplified total leakage current. The measurements recorded was analyzed to compare the effect of temperature on total leakage current.

III. RESULTS AND DISCUSSION

This experiment is carried out in johor bahru, Malaysia, the ambient temperature of malaysia usually range from 30°C to 40°C. Therefore it is important to focus on these temperature if we need to measure the ageing of ZnO arrester with leakage current method.

For sample 1, the temperature increase around 5°C, the leakage will change around 16-84μA. This will definitely affect the result of determining whether the arrester already aged or still can provide its service.

*C.L.Wooi, Saeed Vahabi Mashak vmsaeed3@live.utm.my,zulk@fke.utm.my) Phone: +60-7-5535432; Fax: +60-7-5578150 Zulkurnain Abdul-Malek are with Institut Voltan dan Arus Tinggi, Universiti Teknologi Malaysia, IVAT, Fakulti Kejuruteraan Elektrik, UTM, 81310, Skudai, Johor Bahru,Malaysia.(email:wcl5195@gmail.com,

Table 1. Sample 1: Percentage difference of leakage current for each temperature compared with 30°C

Voltage (kV)	**Ambient Temperature (°C)**			
	30-35°C	30-40°C	30-45°C	30-50°C
20	9.31%	10.30%	13.07%	16.97%
30	9.15%	8.94%	11.69%	15.75%
40	9.05%	10.70%	14.11%	16.34%
50	10.08%	10.84%	12.74%	16.36%
60	9.94%	11.38%	13.47%	15.55%
70	10.81%	11.36%	13.72%	17.46%
80	10.00%	12.29%	14.94%	19.16%
90	11.17%	12.12%	16.86%	19.50%

From this table, it can be conclude that the leakage current of surge arrester is highly affected by ambient temperature which can be as high as 19.50% difference. In Malaysia ambient temperature cannot goes up to 50°C, however comparing 30°C to 40°C, we can see there is leakage current difference up to 12%. This definitely can affect our analysis regarding the degradation of ZnO arrester especially leakage current is measure in μA which is a small unit. If the amient temperature affect the leakage current, our analysis on degradation of surge arrester will not be accurate.

In conclusion, any leakage current measurement techniques will need to take into account of temperaturre effect before determining the surge arrester aging level.

REFERENCES

[1] Z. A.-M. Novizon, Nouruddeen Bashir and Aulia, *Condition Monitoring of Zinc Oxide Surge Arresters*, 2011.

[2] Z. Abdul-Malek, *et al.*, "A new method to extract the resistive component of the metal oxide surge arrester leakage current," in *Power and Energy Conference, 2008. PECon 2008. IEEE 2nd International*, 2008, pp. 399-402.

[3] E. C. Sakshaug, *et al.*, "A new concept in station arrester design," *Power Apparatus and Systems, IEEE Transactions on*, vol. 96, pp. 647-656, 1977.

[4] M. Kobayashi, *et al.*, "Development of Zinc-Oxide Non-Linear Resistors and Their Applications to Gapless Surge Arresters," *Power Apparatus and Systems, IEEE Transactions on*, vol. PAS-97, pp. 1149-1158, 1978.

[5] A. Vicaud, "A. C. Voltage Ageing of Zinc - Oxide Ceramics," *Power Delivery, IEEE Transactions on*, vol. 1, pp. 49-58, 1986.

[6] P. Kirkby, *et al.*, "Long-term stability and energy discharge capacity of metal oxide valve elements," *Power Delivery, IEEE Transactions on*, vol. 3, pp. 1656-1665, 1988.

[7] E. T. W. Neto, *et al.*, "Artificial Neural Networks Used for ZnO Arresters Diagnosis," *Power Delivery, IEEE Transactions on*, vol. 24, pp. 1390-1395, 2009.

[8] Y. Miyakawa, *et al.*, "Influence of temperature variation on characteristics of ZnO elements," in *Electrical Insulating Materials, 2008. (ISEIM 2008). International Symposium on*, 2008, pp. 119-122.

[9] H. Jinliang, *et al.*, "Thermal characteristics of high voltage whole-solid-insulated polymeric ZnO surge arrester," *Power Delivery, IEEE Transactions on*, vol. 18, pp. 1221-1227, 2003.

Author Index